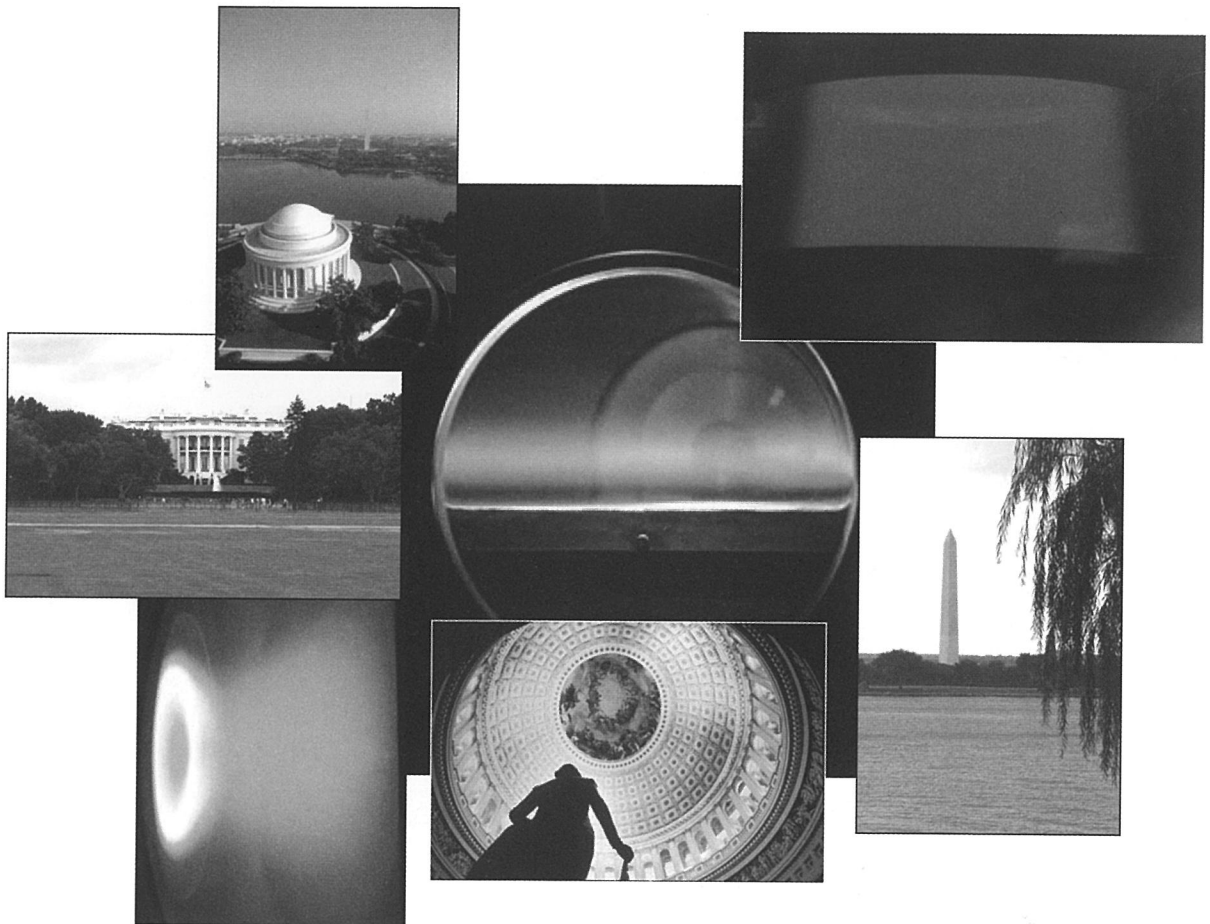


BULLETIN

OF THE **AMERICAN PHYSICAL SOCIETY**

**PROGRAM OF THE 60th ANNUAL
GASEOUS ELECTRONICS CONFERENCE**

**October 2–5, 2007
Arlington, Virginia**



October 2007
Volume 52, No. 8

APS
physics

BULLETIN

OF THE AMERICAN PHYSICAL SOCIETY

Coden BAPSA6

Series II, Vol. 52, No. 8

Copyright 2007 by the American Physical Society

ISSN: 0003-0503

October 2007

APS COUNCIL 2007

President

Leo P. Kadanoff,* *University of Chicago*

President-Elect

Arthur Bienenstock,* *Stanford University*

Vice President

Cherry Murray,* *Lawrence Livermore National Laboratory*

Executive Officer

Judy R. Franz,* *University of Alabama, Huntsville*
(on leave)

Treasurer

Joseph Serene,* *Georgetown University (Emeritus)*

Editor-in-Chief

Gene Sprouse,* *State University of New York at Stony Brook* (on leave)

Past-President

John J. Hopfield,* *Princeton University*

General Councillors

Robert Austin, Christina Back, Elizabeth Beise, Wendell Hill, Evelyn Hu,* Ann Orel,* Arthur Ramirez, Richard Slusher*

Division, Forum and Section Councillors

Charles Dermer (*Astrophysics*), P. Julienne (*Atomic, Molecular & Optical Physics*), Robert Eisenberg (*Biological*), Charles S. Parmenter (*Chemical*), Moses H. Chan (*Condensed Matter Physics*), Richard M. Martin (*Computational*), James Brassuer (*Fluid Dynamics*), Peter Zimmerman* (*Forum on Education*), Roger Stuewer (*Forum on History of Physics*), Patricia Mooney* (*Forum on Industrial and Applied Physics*), David Ernst (*Forum on International Physics*), Philip "Bo" Hammer* (*Forum on Physics and Society*), Steven Rolston (*Laser Science*), Leonard Feldman* (*Materials*), Akif Balantekin (*Nuclear*), John Jaros* (*Particles & Fields*), Ron Ruth (*Physics of Beams*), David Hammer (*Plasma*), Scott Milner (*Polymer Physics*), Paul Wolf (*Ohio Section*), Heather Galloway (*Texas Section*)

*Members of the APS Executive Board

Meetings Abstracts Coordinator:

Vinaya K. Sathyasheelappa

APS MEETINGS DEPARTMENT

One Physics Ellipse

College Park, MD 20740-3844

Telephone: (301) 209-3286

Fax: (301) 209-0866

Email: meetings@aps.org

Donna Baudrau, *Director of Meetings & Conventions*

Terri Gaier, *Assistant Director of Meetings & Conventions*

Don Wise, *Registrar*

Christine Parvez, *Meetings Program Coordinator*

International Councillor

Albrecht Wagner

Chair, Nominating Committee

Margaret Murnane

Chair, Panel on Public Affairs

Robert Eisenstein

ADVISORS

Representatives from other Societies

Harvey Leff, *AAPT*; Fred Dylla, *AIP*

International Advisors

Francisco Ramos Gómez, *Mexican Physical Society*;

Louis Marchildon, *Canadian Association of Physicists*

Staff Representatives

Alan Chodos, *Associate Executive Officer*; Amy Flatten, *Director of International Affairs*; Ted Hodapp, *Director of Education and Outreach*; Michael Lubell, *Director, Public Affairs*; Daniel Kulp, *Editorial Director*; Christine Giaccone, *Director, Journal Operations*; Michael Stephens, *Controller and Assistant Treasurer*

Administrator for Governing Committees

Ken Cole

Please Note: APS has made every effort to provide accurate and complete information in this *Bulletin*. However, changes or corrections may occasionally be necessary and may be made without notice after the date of publication. To ensure that you receive the most up-to-date information, please check the meeting Corrigenda distributed with this *Bulletin*.

BULLETIN

OF THE AMERICAN PHYSICAL SOCIETY

Vol. 52, No. 8, October 2007

GEC Meeting 2007

TABLE OF CONTENTS

General Information	3
Special Sessions and Events	3
<i>Sessions</i>	3
Presentation Formats	3
GEC Student Award for Excellence	4
Registration	4
Banquet and Reception	4
E-mail and Other Business Services	4
Audio-Visual Equipment	4
Dining Options	4
Guest Program	5
Call for Nominations for GEC General and Executive Committees	5
<i>GEC Executive Committee</i>	5
<i>Conference Secretary</i>	6
Epitome	7
Main Text	10
<i>Monday, October 1</i>	10
<i>Tuesday, October 2</i>	11

<i>Wednesday, October 3</i>	31
<i>Thursday, October 4</i>	47
<i>Friday October 5</i>	66
Author Index	73
Restaurants	85
Floor Plan	At End of Issue

TABLE OF CONTENTS

General Information 31

Special Sessions and Events 47

Registration 66

Presentation Formats 73

CEC Student Award for Excellence 85

Handout and Reception 85

E-mail and Other Business Services 85

Audio-Visual Equipment 85

Dining Options 85

Guest Program 85

Call for Nominations for CEC General and Executive Committee 85

CEC Executive Committee 85

Conference Secretary 85

Epitome 85

Main Text 85

Monday, October 1 85

Tuesday, October 2 85

60th Annual Gaseous Electronics Conference

October 2-5, 2007

Arlington, VA

GENERAL INFORMATION

Welcome to Arlington for the 60th Annual Gaseous Electronics Conference (GEC) of the American Physical Society. The GEC 2007 will address a broad range of topics at the forefront of gaseous electronics. The program includes the GEC Foundation Talk, Student Award for Excellence Talks, 26 invited talks and over 230 contributed papers presented in oral and poster sessions. The conference is held in the Doubletree Hotel Crystal City, Arlington, VA.

SPECIAL SESSIONS AND EVENTS

The GEC Executive Committee is pleased to announce that the GEC Foundation Talk for 2007 will be presented by Professor Don Madison from University of Missouri, Rolla. His talk, "*Why would anyone be interested in charged particle ionization of atoms or molecules?*" will be given Wednesday morning at 10 AM in the combined Crystal Ballrooms. The GEC Foundation talk, alternating each year with the Allis Prize Lecture, provides a keen insight and individualized perspective into the principles of gaseous electronics.

SESSIONS

- Session AS Opening Reception
- Session BT1 Plasma Combustion and Chemistry
- Session BT2 Electron Impact Ionization
- Session CT1 Capacitively Coupled Plasmas
- Session CT2 High Pressure Arcs
- Session DT1 Materials Processing in Low Pressure Plasmas I
- Session ET1 Plasma-Surface Interactions
- Session ET2 Electronegative Plasmas
- Session FPT1 Poster Session I
- Session GW1 Lighting Plasmas

- Session GW2 Electrons and Positrons: Transport and Annihilation
- Session HW GEC Foundation Talk
- Session LW1 Plasma Applications for Nanotechnology
- Session LW2 Plasma Propulsion
- Session MPW1 Posters Session II
- Session PR1 Laser and Air Plasmas
- Session PR2 Electron Attachment and Recombination
- Session QR1 Plasma Sources
- Session QR2 Electron-Atom Collisions
- Session RR1 Micro and Dielectric Barrier Discharges
- Session RR2 Electron-molecule Collisions
- Session SRP1 Poster Session III
- Session TR1 Reception and Banquet
- Session VF1 Materials Processing in Low Pressure Plasmas II
- Session VF2 Plasma Diagnostics I
- Session WF1 Biological and Emerging Applications of Plasmas
- Session WF2 Plasma Diagnostics II

PRESENTATION FORMATS

Papers that have been accepted for presentation are listed in the technical program. Invited papers are allotted 25 minutes, with 5 additional minutes for questions and discussion. Oral contributed presentations are allotted 12 minutes, with 3 additional minutes for questions. Poster sessions will be provided with 48 in. by 96 in. poster boards. Presenters may mount their posters anytime in the day upon which their presentation is scheduled. Poster materials must be removed at the close of the poster session.

GEC STUDENT AWARD FOR EXCELLENCE

In order to recognize the outstanding contribution students of GEC student members, the GEC Executive Committee will award a \$1000 prize for the best paper presentation by a student. Students must be nominated by a professional member before being selected to present and compete for the award. Students competing for the award, in the order of their appearance in the program, are:

Julian Schulze, Ruhr-University Bochum, "Electron heating in asymmetric capacitively coupled RF discharges at low pressures," Tuesday, October 2, 10:45 AM.

Juan Trelles, University of Minnesota, "Comparison between non-equilibrium and equilibrium modeling results of an arc plasma torch," Tuesday, October 2, 11:45 AM.

Fukutaro Hamaoka, Keio University, "Modeling of deep reactive ion etching of Si under plasma molding in 2f-CCP in SF₆/O₂," Tuesday, October 2, 2:00 PM.

Corinne Duluard, GREMI, Orleans, "Neutral production in SF₆/SiCl₄ inductively coupled plasmas," Tuesday, October 2, 2:15 PM.

Ali Baby, University of Ulster, "Ion flux and energy measurement at a pulsed biased electrode in a C₂H₂:Argon inductively coupled plasma during DLC growth," Tuesday, October 2, 3:15 PM.

Joydeep Guha, University of Houston, "Surface recombination study in near real time in Cl₂ plasmas," Tuesday, October 2, 4:00 PM.

Amanda Rider, The University of Sydney, "Binary quantum dot arrays: A plasma-based deterministic approach," Wednesday, October 3, 3:15 PM.

Scott Baalrud, University of Wisconsin-Madison, "Double layers at anode spots in low-pressure plasma," Thursday, October 4, 11:30 AM.

Katia Allegraud, LPTP, Ecole Polytechnique, "Self organization of streamers in a surface DBD: evidence of collective breakdowns," Thursday, October 4, 3:00 PM.

REGISTRATION

The registration desk will be located outside the Crystal Ballrooms in the Doubletree Hotel. Registration will be available Monday afternoon from 4:00 – 6:00 PM and throughout most of the week, starting at 7:30 AM. The on-site conference registration fee is \$400 for regular registrations and \$200 for students and retirees.

BANQUET AND RECEPTION

An opening reception will be held on the evening of Monday, October 1, 2007, in the Windows Over Washington restaurant starting at 18:00. Windows Over Washington is on the 14th floor of the Doubletree Hotel and has floor to ceiling windows that offer breathtaking views of the DC sky line.

The conference banquet will be held in the Crystal Ballrooms of the Doubletree Hotel on Thursday evening, October 4, starting with a reception in the lobby at 6 pm. Banquet tickets are \$65 and are available upon registration. Conference participants and guests are encouraged to attend the reception and the banquet.

E-MAIL AND OTHER BUSINESS SERVICES

Wireless internet access will be available throughout the conference hotel, including all guest rooms and public areas. A group logon and password will be provided with registration materials. Other business services (fax, photocopy services, etc.) will be available from the hotel business center.

AUDIO-VISUAL EQUIPMENT

Each conference room will be equipped with an LCD projector. If additional equipment is required, please contact the conference secretary.

DINING OPTIONS

A list with dining options in the vicinity of the Doubletree Hotel is included in the registration packet provided to each conference participant.

GEC STUDENT AWARD FOR EXCELLENCE

In order to recognize the outstanding contribution students of GEC student members, the GEC Executive Committee will award a \$1000 prize for the best paper presentation by a student. Students must be nominated by a professional member before being selected to present and compete for the award. Students competing for the award, in the order of their appearance in the program, are:

Julian Schulze, Ruhr-University Bochum, "Electron heating in asymmetric capacitively coupled RF discharges at low pressures," Tuesday, October 2, 10:45 AM.

Juan Trelles, University of Minnesota, "Comparison between non-equilibrium and equilibrium modeling results of an arc plasma torch," Tuesday, October 2, 11:45 AM.

Fukutaro Hamaoka, Keio University, "Modeling of deep reactive ion etching of Si under plasma molding in 2f-CCP in SF₆/O₂," Tuesday, October 2, 2:00 PM.

Corinne Duluard, GREMI, Orleans, "Neutral production in SF₆/SiCl₄ inductively coupled plasmas," Tuesday, October 2, 2:15 PM.

Ali Baby, University of Ulster, "Ion flux and energy measurement at a pulsed biased electrode in a C₂H₂:Argon inductively coupled plasma during DLC growth," Tuesday, October 2, 3:15 PM.

Joydeep Guha, University of Houston, "Surface recombination study in near real time in Cl₂ plasmas," Tuesday, October 2, 4:00 PM.

Amanda Rider, The University of Sydney, "Binary quantum dot arrays: A plasma-based deterministic approach," Wednesday, October 3, 3:15 PM.

Scott Baalrud, University of Wisconsin-Madison, "Double layers at anode spots in low-pressure plasma," Thursday, October 4, 11:30 AM.

Katia Allegraud, LPTP, Ecole Polytechnique, "Self organization of streamers in a surface DBD: evidence of collective breakdowns," Thursday, October 4, 3:00 PM.

REGISTRATION

The registration desk will be located outside the Crystal Ballrooms in the Doubletree Hotel. Registration will be available Monday afternoon from 4:00 – 6:00 PM and throughout most of the week, starting at 7:30 AM. The on-site conference registration fee is \$400 for regular registrations and \$200 for students and retirees.

BANQUET AND RECEPTION

An opening reception will be held on the evening of Monday, October 1, 2007, in the Windows Over Washington restaurant starting at 18:00. Windows Over Washington is on the 14th floor of the Doubletree Hotel and has floor to ceiling windows that offer breathtaking views of the DC sky line.

The conference banquet will be held in the Crystal Ballrooms of the Doubletree Hotel on Thursday evening, October 4, starting with a reception in the lobby at 6 pm. Banquet tickets are \$65 and are available upon registration. Conference participants and guests are encouraged to attend the reception and the banquet.

E-MAIL AND OTHER BUSINESS SERVICES

Wireless internet access will be available throughout the conference hotel, including all guest rooms and public areas. A group logon and password will be provided with registration materials. Other business services (fax, photocopy services, etc.) will be available from the hotel business center.

AUDIO-VISUAL EQUIPMENT

Each conference room will be equipped with an LCD projector. If additional equipment is required, please contact the conference secretary.

DINING OPTIONS

A list with dining options in the vicinity of the Doubletree Hotel is included in the registration packet provided to each conference participant.

GUEST PROGRAM

Welcome to the greater metropolitan area of our nation's capital. Crystal City is a business and meeting place strategically placed between Reagan National Airport and downtown Washington, DC. Crystal City bustles with activity based in the military, commercial and civilian government sectors. A short taxi or metro ride places you in the middle of the National Mall, flanked by the Washington Monument, the US Capitol and numerous Smithsonian Museums.

The Doubletree Crystal City is located in the northern portion of Crystal City, next to the Pentagon and Pentagon City Mall. The Mall provides locals and visitors with convenient access to shopping and dining and is short walk from the hotel. Downtown Washington, DC is a tourist's paradise, between the numerous Smithsonian Museums (Natural History, American History, National Gallery of Art, Air and Space, Holocaust, Hirshorn, to name a few), national monuments (Washington, Jefferson, Lincoln, WWII, Korean War, Viet Nam, Iwo Jima,...) performing arts (Kennedy Center) the US Capitol, White House and Arlington National Cemetery. Guided and bus tours are available all day, every day and arrangements can be made in advance or on site at the Doubletree hotel. The fall in Washington, DC is pleasantly warm, and a tour of the monuments at night is particularly breathtaking.

For more information on the wide variety of activities and places of interest in Washington, DC, please visit www.washington.org.

CALL FOR NOMINATIONS FOR GEC GENERAL AND EXECUTIVE COMMITTEES

The GEC Executive Committee (ExComm) is the governing body of the GEC. It is the responsibility of the ExComm to oversee all aspects of the conference. This includes selection of meeting sites, budgetary decisions, selection of special topics and invited speakers, accepting and rejecting abstracts, and arranging of the program. The General Committee and the ExComm meet during the GEC, and the ExComm meets again during the summer to plan the program of the next GEC. There are numerous communications between members of the ExComm (usually e-mail) during the year to ensure the successful completion of their duties. We have been fortunate over the years to have a dedi-

cated group of volunteers who have been willing to take on these very necessary roles.

The bylaws of the Gaseous Electronics Conference describe the process whereby members of the ExComm are elected. At the GEC Business Meeting (to be held on Wednesday, October 3, at 11:00 in the Crystal Ballroom), nominations are accepted for members of the GEC General Committee (GenComm).

The GenComm consists of the ExComm and six at-large members elected at the Business Meeting. The eligible voting membership of the GEC (defined as those attending the Business Meeting) elects six at-large members. The GenComm then meets to fulfill its only duty: to elect new members of the ExComm.

The ExComm membership consists of the Chair, Treasurer, Past-Secretary, Secretary, Secretary-elect, past or incoming Chair, and four at-large members. The Chair is a 4 year term (1 year incoming, 2 years Chair, and 1 year past-Chair), the Secretary is a 3 year term (1 year incoming, 1 year Secretary, 1 year past-Secretary), and all other ExComm members serve 2 years. The Secretary is the person who manages the local arrangements for the meeting and is usually "recruited" and appointed to the ExComm.

The ExComm welcomes nominations, including self-nomination, for both the GenComm and the ExComm. Becoming a GenComm and/or ExComm member provides a unique opportunity to see both how the GEC is run and to influence its future direction by helping to define the programs and choosing future sites.

Please submit your nominations to the GEC Chair or any member of the ExComm. The ExComm also welcomes inquiries on hosting future GECs.

GEC 2007 EXECUTIVE COMMITTEE

- *Peter Ventzek*, Chair, Tokyo Electron
- *Greg Hebner*, Past-Chair, Sandia National Laboratory
- *Klaus Bartschat*, Treasurer, Drake University
- *Darrin Leonhardt*, Secretary, Fusion UV Systems
- *Scott Walton*, Co-Secretary, Naval Research Laboratory
- *Walter Lempert*, Past-Secretary, Ohio State University
- *Larry Overzet*, Secretary-Elect, University of Texas, Dallas
- *Stephen Buckman*, Australia National University
- *Michael Schulz*, University of Missouri, Rolla

Rainer Johnson, University of Pittsburgh
Svetlana Radovanov, Varian Semiconductor
Pascal Chabery, LTPT, Ecole Polytechnique
Kouichi Ono, Kyoto University

CONFERENCE SECRETARY

Darrin Leonhardt
 Fusion UV Systems
 910 Clopper Road
 Gaithersburg, MD 20878
 Voice: 301/990-8700 X8751
 Fax: 301/527-2661
 E-mail: dleonhardt@fusionuv.com

Scott Walton
 Naval Research Lab – Code 6752
 4555 Overlook Ave, SW
 Washington, DC 20375
 Voice: 202/767-7531
 Fax: 202/767-3553
 E-mail: Scott.Waltonnrl.navy.mil

GEC07 SPONSORS AND EXHIBITORS

Sponsors and exhibitors allow the GEC Executive Committee to provide many benefits to attendees, including travel assistance and decreased registration fees for junior attendees.

The GEC07 has been fortunate to receive support from the following organizations:

Applied Materials
 LAM
 GE
 NSF
 DoE
 Sandia
 AFOSR
 AE
 Tech X Corp
 IOP
 Hiden Analytical
 Nor-Cal

Epitome of the 60th Gaseous Electronics Conference of the American Physical Society

18:00 MONDAY EVENING
1 OCTOBER 2007

AS **Reception**
Windows Over Washington
Doubletree Crystal City

8:00 TUESDAY MORNING
2 OCTOBER 2007

BT1 **Plasma Combustion and Chemistry**
Christophe Laux
Crystal Ballroom A,
Doubletree Crystal City

BT2 **Electron Impact Ionization**
Philip Bartlett, John B. Boffard
Crystal Ballroom B,
Doubletree Crystal City

10:00 TUESDAY MORNING
2 OCTOBER 2007

CT1 **Capacitively Coupled Plasmas**
Miles Turner
Crystal Ballroom A,
Doubletree Crystal City

CT2 **High Pressure Arcs**
Crystal Ballroom B,
Doubletree Crystal City

13:30 TUESDAY AFTERNOON
2 OCTOBER 2007

DT1 **Materials Processing in Low Pressure Plasmas I: Etching, Deposition, New Materials**
Remi Dussart
Crystal Ballroom A,
Doubletree Crystal City

16:00 TUESDAY AFTERNOON
2 OCTOBER 2007

ET1 **Plasma-Surface Interactions**
Gottlieb Oehrlein
Crystal Ballroom A,
Doubletree Crystal City

ET2 **Electronegative Plasmas**
Ludovic Godet
Crystal Ballroom B,
Doubletree Crystal City

19:30 TUESDAY EVENING
2 OCTOBER 2007

FTP1 **Poster Session I**
Crystal Ballroom C,
Doubletree Crystal City

8:00 WEDNESDAY MORNING
3 OCTOBER 2007

GW1 **Lighting Plasmas**
Crystal Ballroom A,
Doubletree Crystal City

GW2 **Electrons and Positrons: Transport and Annihilation**
Robert Robson, C.M. Surko, Gleb Gribakin
Crystal Ballroom B,
Doubletree Crystal City

10:00 WEDNESDAY MORNING
3 OCTOBER 2007

HW **GEC Foundation Talk**
Don Madison
Crystal Ballrooms A/B,
Doubletree Crystal City

11:00 WEDNESDAY MORNING
3 OCTOBER 2007

JW **Business Meeting**
Crystal Ballroom A,
Doubletree Crystal City

12:00 WEDNESDAY NOON
3 OCTOBER 2007

KW **General Committee Meeting**
Crystal Ballroom A,
Doubletree Crystal City

13:30 WEDNESDAY AFTERNOON
3 OCTOBER 2007

LW1 **Plasma Applications for
Nanotechnology**
Masaru Hori
Crystal Ballroom A,
Doubletree Crystal City

LW2 **Plasma Propulsion**
Edgar Choueir
Crystal Ballroom B,
Doubletree Crystal City

16:00 WEDNESDAY AFTERNOON
3 OCTOBER 2007

MWP1 **Poster Session II**
Crystal Ballroom C,
Doubletree Crystal City

8:00 THURSDAY MORNING
4 OCTOBER 2007

PR1 **Laser and Air Plasmas**
Martin Lampe
Crystal Ballroom A,
Doubletree Crystal City

PR2 **Electron Attachment and
Recombination**
Crystal Ballroom B,
Doubletree Crystal City

10:00 THURSDAY MORNING
4 OCTOBER 2007

QR1 **Plasma Sources**
Crystal Ballroom A,
Doubletree Crystal City

QR2 **Electron-Atom Collisions**
Alexander Dorn, Arati Dasgupta
Crystal Ballroom B,
Doubletree Crystal City

13:30 THURSDAY AFTERNOON
4 OCTOBER 2007

RR1 **Micro and Dielectric Barrier
Discharges**
*Leanne Pitchford, Antoine
Rousseau*
Crystal Ballroom A,
Doubletree Crystal City

RR2 **Electron-Molecule Collisions**
*Kurt Becker, Murtadha A. Khakoo,
Marco Lima*
Crystal Ballroom B,
Doubletree Crystal City

16:00 THURSDAY AFTERNOON
4 OCTOBER 2007

SRP1 **Poster Session III**
Crystal Ballroom C,
Doubletree Crystal City

19:00 THURSDAY EVENING
4 OCTOBER 2007

TR **Banquet**
Crystal Ballroom,
Doubletree Crystal City

8:00 FRIDAY MORNING
5 OCTOBER 2007

- VF1 **Materials Processing in Low Pressure Plasmas II: Etching, Deposition, New Materials**
Hirotaaka Toyoda
Crystal Ballroom A,
Doubletree Crystal City
- VF2 **Plasma Diagnostics I**
Nicholas Braithwaite
Crystal Ballroom B,
Doubletree Crystal City

10:30 FRIDAY MORNING
5 OCTOBER 2007

- WF1 **Biological and Emerging Applications of Plasmas**
Thomas M. Orlando, Eva Stoffels, David Graves
Crystal Ballroom A,
Doubletree Crystal City
- WF2 **Plasma Diagnostics II**
Koichi Sasaki
Crystal Ballroom B,
Doubletree Crystal City

SESSION AS: RECEPTION

Monday evening, 1 October 2007 at 18:00

Windows Over Washington

Doubletree Crystal City

**18:00
AS 1 Reception**

Doubletree Crystal City
 1700 S. Crystal Drive
 Arlington, VA 22202
 Phone: 703.556.1234
 Fax: 703.556.1235
 Website: www.doubletree.com

SESSION BT1: PLASMA COMBUSTION AND CHEMISTRY

Tuesday morning, 2 October 2007; Crystal Ballroom A, Doubletree Crystal City at 8:00

Leanne Pitchford, LAPLACE, presiding

Invited Papers

8:00

BT1 1 Plasma-Assisted Flame Ignition and Stabilization using Nanosecond Repetitively Pulsed Discharges.*CHRISTOPHE LAUX,[†] *Ecole Centrale Paris*

Ever more stringent environmental regulations are providing impetus for reducing pollutant emissions, in particular nitric oxides and soot, in internal combustion and aircraft engines. Lean or diluted combustible mixtures are of particular interest because they burn at lower flame temperatures than stoichiometric mixtures and thus produce lesser amounts of thermal nitric oxides. Over the past decade, high voltage nanosecond pulsed discharges have been demonstrated as energy efficient way to ignite such mixtures. However, the practical application of these discharges for ignition purposes is limited by the very high electric fields required, especially in high pressure combustion chambers. Moreover, stabilization requires a steady-state addition of energy that cannot be achieved with single or low repetition frequency pulses. In the present work, we investigate the applicability and effectiveness of high voltage nanosecond discharges with high pulse repetition frequencies, typically up to 100 kHz. The high repetition frequencies are chosen to exceed the recombination rate of chemically active species. In this way, the concentration of active species can build up between consecutive pulses, thus yielding significantly higher concentrations than with low frequency pulses. These discharges are investigated for two applications, the ignition of diluted air/propane mixtures, at pressures up to several bars in a constant volume chamber, and the stabilization of atmospheric pressure lean premixed air/propane flames. Time-resolved electric and spectroscopic measurements are presented to analyze the discharge regimes, the energy deposition, the gas temperature evolution, the electron number density, and the production of excited species. The results show that nanosecond repetitive pulses produce ultrafast gas heating and atomic oxygen generation, both on nanosecond time scales, via excitation of molecular nitrogen followed by dissociative quenching of molecular oxygen. These effects result in a significant reduction of the lower flammability limit and in the subsequent extension of the domain of flame stability, for a power consumption typically less than 1% of the heat released by the flame.

*This work has been supported by Safran, CNRS, and DGA under the INCA program (Initiative sur la Combustion Avancée) directed by Dr. M. Cazalens

[†]Laboratoire EM2C, CNRS and Ecole Centrale Paris

Contributed Papers

8:30

BT1 2 Spatially and Temporally Resolved Atomic Oxygen Measurements in Short Pulse Discharges by Two Photon Laser Induced Fluorescence* WALTER LEMPERT, MRUTHUNJAYA UDDI, EUGENE MINTUSOV, NAIBO JIANG, IGOR ADAMOVICH, *Ohio State University* Two Photon Laser Induced Fluorescence (TALIF) is used to measure time-dependent absolute oxygen atom concentrations in O₂/He, O₂/N₂, and CH₄/air plasmas produced with a 20 nanosecond duration, 20 kV pulsed discharge at 10 Hz repetition rate. Xenon calibrated spectra show that a single discharge pulse creates initial oxygen dissociation fraction of ~ 0.0005 for air like mixtures at 40-60 torr total pressure. Peak O atom concentration is a factor of approximately two lower in fuel lean ($\phi=0.5$) methane/air mixtures. In helium buffer, the initially formed atomic oxygen decays monotonically, with decay time consistent with formation of ozone. In all nitrogen containing mixtures, atomic oxygen concentrations are found to initially increase, for time scales on the order of 10-100 microseconds, due presumably to additional O₂ dissociation caused by collisions with electronically excited nitrogen. Further evidence of the role of metastable N₂ is demonstrated from time-dependent N₂ 2nd Positive and NO Gamma band emission spectroscopy. Comparisons with modeling predictions show qualitative, but not quantitative, agreement with the experimental data.

*Work supported by NASA and Air Force Office of Scientific Research.

8:45

BT1 3 Mechanisms of iodine atoms production by pulse discharge* ANATOLY NAPARTOVICH, IGOR KOCHETOV, SRC RF TRINITI NIKOLAY VAGIN, NIKOLAY YURYSHEV, P. N. Lebedev Physics Institute Pulsed electric discharge is most effective to turn COIL operation into pulse mode by instant production of iodine atoms. Numerical model is developed for simulations of an electric discharge in a mixture of gas flow outgoing from the singlet oxygen generator (SOG) with CF₃I. Electron scattering cross sections from CF₃I molecules are analyzed to reproduce recently published swarm data for CF₃I and N₂ mixtures. The model comprises a system of kinetic equations for neutral and charged species, electric circuit equation, gas thermal balance equation, and the photon balance equation. Reaction rate coefficients for processes involving electrons are found by solving the electron Boltzmann equation, which is re-calculated in a course of computations when plasma parameters changed. The processes accounted for in the Boltzmann equation include excitation, dissociation and ionization of atoms and molecules, electron-ion recombination, electron-electron collisions, second-kind collisions, and stepwise excitation of molecules. The last processes are particularly important because of a high singlet oxygen concentration in gas flow from the SOG. Results of numerical simulations for conditions of the experiments are compared with results of measurements.

*The partial support of the ISTC Project #3253 is acknowledged.

9:00

BT1 4 Pulsed Nanosecond Discharge Development and Production of Active Particles EVGENY MINTOUSSOV, AINAN BAO, WALTER R. LEMPERT, IGOR V. ADAMOVICH, *Department of Mechanical Engineering, The Ohio State University* Pulsed nanosecond discharges are being actively used for different engineering applications such as plasma-assisted ignition, plasma flow control, and gas dynamics lasers. The main advantages of using of this type of discharge are (i) efficient production of active particles, and (ii) sustaining uniform, volume filling plasmas at high pressures and power loadings. In the present work, development of a nanosecond pulse discharge (pulse amplitude up to 40 kV, pulse repetition rate up to 100 kHz, pulse duration of 4 ns) was studied at different pressures. Discharge parameters, such as fast ionization wave amplitude and velocity have been measured. Energy input into the flow was also determined. Active particle production in high-speed combustible flows (up to 100 m/s) was estimated by comparing heating of air-fuel flow and air flow in the discharge. The results suggest that additional heat release in air-fuel flows is due to plasma chemical fuel oxidation reactions, which at certain conditions leads to ignition. Kinetic model describing production of active particles in the discharge, subsequent plasma chemical reactions, and ignition process is developed.

9:15

BT1 5 An improved description of the vibrational energy transfers in nitrogen discharges VASCO GUERRA, M. LINO DA SILVA, *Centro de Física dos Plasmas, Instituto Superior Técnico, 1049-001 Lisboa, Portugal* S. GOCIC, *Department of Physics, University of Nis, 18001 Nis, Serbia* J. LOUREIRO, *Centro de Física dos Plasmas, Instituto Superior Técnico, 1049-001 Lisboa, Portugal* The vibrational levels of ground-state $N_2(X)$ molecules are often the main energy reservoirs in nitrogen discharges and their post-discharges. As a consequence, they have a direct and crucial importance in the understanding of several fundamental phenomena occurring in nitrogen, such as dissociation, ionization, gas heating and the nitrogen pink afterglow. In recent years, nitrogen discharges have been modeled assuming the vibrational levels to be described by a Morse oscillator. Accordingly, the resulting number of bound vibrational states is 45. In this work we investigate how the vibrational energy distribution function of $N_2(X)$ molecules and the relaxation of vibrational energy are modified when a more realistic intra-molecular potential is used. To this purpose, the ground-state potential curve has been reconstructed with the RKR method and a total of 59 vibrational bound levels were obtained. The discharge and the afterglow were modeled by solving the electron Boltzmann equation, coupled with a system of rate-balance equations for the creation of the most important heavy-particles. The relevant rate coefficients for vibrational exchanges were obtained using the Forced Harmonic Oscillator theory.

SESSION BT2: ELECTRON IMPACT IONIZATION

Tuesday morning, 2 October 2007; Crystal Ballroom B, Doubletree Crystal City at 8:00

Klaus Bartschat, Drake University, presiding

Invited Papers

8:00

BT2 1 Electron-Atom Ionization Calculations using Propagating Exterior Complex Scaling.PHILIP BARTLETT, *Centre for Antimatter-Matter Studies, Murdoch University, Perth 6150, Australia*

The exterior complex scaling method (*Science* **286** (1999) 2474), pioneered by Rescigno, McCurdy and coworkers, provided highly accurate *ab initio* solutions for electron-hydrogen collisions by directly solving the time-independent Schrödinger equation in coordinate space. An extension of this method, propagating exterior complex scaling (PECS), was developed by Bartlett and Stelbovics (*J. Phys. B* **37** (2004) L69, *J. Phys. B* **39** (2006) R379) and has been demonstrated to provide computationally efficient and accurate calculations of ionization and scattering cross sections over a large range of energies below, above and near the ionization threshold. An overview of the PECS method for three-body collisions and the computational advantages of its propagation and iterative coupling techniques will be presented along with results of: (1) near-threshold ionization of electron-hydrogen collisions and the Wannier threshold laws, (2) scattering cross section resonances below the ionization threshold, and (3) total and differential cross sections for electron collisions with excited targets and hydrogenic ions from low through to high energies. Recently, the PECS method has been extended to solve four-body collisions using time-independent methods in coordinate space and has initially been applied to the *s*-wave model for electron-helium collisions. A description of the extensions made to the PECS method to facilitate these significantly more computationally demanding calculations will be given, and results will be presented for elastic, single-excitation, double-excitation, single-ionization and double-ionization collisions.

8:30

BT2 2 Electron-Impact Excitation Out of the Metastable Levels of Argon and Other Rare Gas Atoms.*JOHN B. BOFFARD, *University of Wisconsin-Madison*

In a typical low-temperature plasma, the primary mechanism for populating excited levels is electron-atom collisions. While the vast majority of atoms are typically in their ground state, the few atoms in long-lived metastable levels can also serve as targets of the incident electrons. Indeed, in a typical plasma the excitation rate out of the metastable levels into select upper levels can surpass the excitation rate from the ground state. I will review our group's measurements of the excitation cross sections out of the metastable levels of neon, argon, krypton, and xenon. In addition to their applications in plasma modeling, the study of these cross sections has also been interesting from a fundamental collision-physics perspective.

*Work supported by the National Science Foundation.

Contributed Papers

9:00

BT2 3 Single Ionization of He and H by 75 keV Proton Impact

JASON ALEXANDER, AARON LAFORGE, MICHAEL SCHULZ, *Department of Physics and the Laboratory for Atomic, Molecular, and Optical Research, University of Missouri-Rolla, Rolla, Missouri 65401* Recoil-ion momentum spectroscopy and projectile momentum spectroscopy have been applied to the study of single ionization of He and H by 75keV proton impact. Doubly differential cross sections as a function of the projectile energy loss (or equivalently electron energy) and the scattering angle will be discussed. The results will be compared to earlier doubly differential data for ionization of helium [1]. There, qualitative discrepancies to various theories were observed. Here, we will discuss to what extent these discrepancies can be attributed to an insufficient description of the initial target state. Analyzing the recoil-ion momenta will eventually enable us to obtain fully differential cross sections. [1] Vajnai, T. et al. Phys. Rev. Lett. 74 3588 (1995)

9:15

BT2 4 Out-of-Plane Cross Sections for Electron Impact Ionization of He and H₂*

OLA AL-HAGAN, DON MADISON, CHRISTIAN KAISER, ANDREW MURRAY, *University of Manchester* We have seen in recent years a sharp disagreement between the theory and experiment for heavy particle ionization of He for electrons ejected out of the scattering plane while good agreement was found in the scattering plane. The lack of agreement between experiment and theory for out-of-plane has been attributed to a double scattering mechanism where the projectile first 'hits' the electron and then scatters off the nucleus. If these effects are important for a He nucleus, they should be even more important for a H₂ ion. We will report theoretical and experimental cross sections for in and out of the scattering plane for electron impact ionization for both He and H₂. We will show that the orientation of the molecular axis can produce very different results outside the scattering plane for molecules as compared to atoms.

*Work Supported by NSF grant PHY-0456528

SESSION CT1: CAPACITIVELY COUPLED PLASMAS

Tuesday morning, 2 October 2007; Crystal Ballroom A, Doubletree Crystal City at 10:00

Zoran Petrovic, Institute of Physics, Belgrade, presiding

Invited Papers

10:00

CT1 1 Electron heating in dual-frequency capacitive discharges.MILES TURNER, *Dublin City University*

Capacitive discharges excited by a superposition of two frequencies are important tools in applications where precise control of the plasma conditions is important, as when the energy and flux of ions leaving the plasma must be controlled independently. Elementary discussion of these discharges assumes that the two frequencies control the ion flux and energy practically independently, but more detailed investigation shows that that this is true only to a limited extent. In this paper, we focus on electron heating in dual frequency discharges. Such heating can be attributed to three mechanisms: Stochastic heating, Ohmic heating and secondary emission from plasma facing surfaces. We consider the processes contributing to these three mechanisms and their relative importance. We will discuss recent work on collisionless or stochastic heating in dual-frequency discharges, the relative importance of Ohmic and collisionless heating, and the effect of secondary electron emission. We will show that stochastic and Ohmic heating typically depend on both the low- and high-frequency current densities, so that the net heating depends strongly on both. We will also show that recent phase-resolved optical emission spectroscopy measurements are difficult to understand without the assumption that secondary electron emission is an important process. These results show that the two-frequencies coupled in a complex fashion, which does not however necessarily preclude effective independent control of ion flux, ion energy, and other important process parameters

Contributed Papers

10:30

CT1 2 Ionisation dynamics and frequency coupling in dual frequency capacitively coupled plasmas D. O'CONNELL, *Centre for Plasma Science and Technology, Ruhr University Bochum, Germany* T. GANS, *Centre for Plasma Physics, Queen's University Belfast, Northern Ireland* E. SEMMLER, P. AWAKOWICZ, *Centre for Plasma Science and Technology, Ruhr University Bochum, Germany* A.R. ELLINGBOE, M.M. TURNER, *National Centre for Plasma Science and Technology, Dublin City University, Ireland* Multi-frequency discharges can provide additional process control for technological applications. Plasma ionization and sustaining mechanisms are investigated in an asymmetric capacitively coupled radio-frequency (rf) discharge operated with 2 MHz and 14 MHz applied simultaneously to the same electrode. Energetic electrons, key to ionization mechanisms, are probed using phase resolved optical emission spectroscopy (PROES) resolving both the low and high frequency rf cycles. The electron dynamics exhibits a complex spatio-temporal structure. The observed dynamics is compared to particle-in-cell (PIC) simulations. Pronounced coupling effects of the two frequencies can be observed, in particular, when they are phase locked. The relative phase between the two frequencies and the ratio of the applied voltages determines details of the electron dynamics. Plasma ionization mechanisms can be controlled and tailored through variations of the relative phase and the voltage ratio. Funding: SFB 591, ProInno II, GRK 1051, EPSRC.

10:45 Student Excellence Award Finalist

CT1 3 Electron heating in asymmetric capacitively coupled RF discharges at low pressures JULIAN SCHULZE, BRIAN HEIL, DIRK LUGGENHOELSCHER, UWE CZARNETZKI, *Ruhr-University Bochum* Electron dynamics in asymmetric capacitively coupled discharges is investigated by applying a combination of various diagnostics: Laser electric field measurements for the sheath, phase resolved optical emission spectroscopy for the excitation, Langmuir probe measurements for the EEDF and electron density in the bulk, a SEERS sensor for current measurements and a high voltage probe for the determination of the applied voltage. During the sheath expansion beams of high energetic electrons are observed. At low pressures the RF current is not sinusoidal, but strong high frequency oscillations caused by the Plasma Series Resonance (PSR) effect are observed. These current oscillations increase the sheath velocity and enhance stochastic heating. The current is compared to emission measurements showing a direct correlation. The electric field measurements are compared to a fluid sheath model. The measured RF current is compared to an analytical PSR model. Another analytical model demonstrates the influence of electron beams on the time averaged isotropic EEDF as it is measured by probes. It clearly demonstrates, that high energetic electron beams lead to an enhanced high energy tail, that is usually attributed to stochastic heating.

11:00

CT1 4 Electron heating and ionization mechanisms in capacitively coupled dual frequency plasmas EGMONT SEMMLER, DEBORAH O'CONNELL, *Ruhr-University Bochum* TIMO GANS, *Queens University Belfast* PETER AWAKOWICZ, ACHIM VON KEUDELL, *Ruhr-University Bochum* Capacitively coupled dual-frequency plasmas are increasingly used in various technological applications. They have been motivated for their

separate control of plasma density and ion bombardment energy. It is known that the plasma density is mainly controlled by the high frequency component in the plasma current, whereas the ion bombardment energy can be tuned by the low frequency component. However the nonlinear nature of the plasma boundary sheath is the cause for critical frequency coupling effects that occur in these devices. Recent measurements by Langmuir probe, VI-probe and a rf-current sensor reveal strong resonant behavior at integer driving frequency ratios capable of enhancing the plasma production by a factor of two compared to non-integer ratios. This can be explained by indirectly heating the electrons at the plasma series resonance frequency. Additional measurements of ionization mechanisms through energetic electrons by means of phase resolved optical emission spectroscopy (PROES) have unveiled complex coupling effects between the low and high frequency component.

11:15

CT1 5 Numerical modelling of electron beams accelerated by the RF plasma boundary sheath* B.G. HEIL, J. SCHULZE, D. LUGGENHÖLSCHER, U. CZARNETZKI, *Institute for Plasma and Atomic Physics, Ruhr-University Bochum* T. MUSSEN-BROCK, R.P. BRINKMANN, *Institute for Theoretical Electrical Engineering, Ruhr-University Bochum* The exact mechanism of electron heating by the RF plasma boundary sheath is a current research topic. Electron beams accelerated by the RF sheath and travelling through the plasma bulk have been observed using phase resolved measurements of plasma emissions and also with a Monte-Carlo simulation. In this work the acceleration of electron beams by the RF sheath is numerically investigated. At lower pressures, the RF current and also the expansion and contraction of the sheath are modulated by the plasma series resonance (PSR) effect. This modulation can lead to multiple electron beams being accelerated per RF cycle. It can also temporarily cause larger sheath velocities than would be the case if the current is sinusoidal as is commonly assumed, leading to a larger acceleration of the electron beams. The hypothesis is that at least a part of what is called stochastic heating is due to these electron beams.

*Supported by the DFG through: SFB591 and GK1051, and Andor Technology.

11:30

CT1 6 Discharge Electrode Impedance Effect on Nonlinear Wave Generation in Dual-Frequency Capacitively Coupled Plasma YOHEI YAMAZAWA, *Tokyo Electron AT LTD.* Resonantly growth of the wave originated from the plasma nonlinearity was observed in a capacitively coupled plasma reactor. We experimentally demonstrated the growth of the harmonics of the bias frequency by tuning a variable capacitor attached to the bottom electrode. We also observed the amplification of the wave having the frequency corresponding to the difference of the source and the bias frequency. A simple nonlinear equivalent circuit model can reproduce the experimental results. The results indicate that the electrode impedance should be taking into account in considering the resonance condition that dominates the amplification of the nonlinear wave.

11:45

CT1 7 Analogy between electron heating mechanisms in symmetric dual and asymmetric single frequency capacitive RF discharges JULIAN SCHULZE, BRIAN HEIL, DIRK LUGGENHOELSCHER, UWE CZARNETZKI, *Ruhr-University Bochum* BERT ELLINGBOE, *Dublin City University* Electron heating mechanisms in single and dual frequency capacitively coupled RF discharges are a current research topic. Many theoretical, but only few experimental investigations on this topic exist. In this work electron heating is investigated experimentally in dual and single frequency discharges by Phase Resolved Optical Emission Spectroscopy. In both cases, the generation of beams of high energetic electrons during sheath expansion is identified to be the dominant cause of heating. In an asymmetric single frequency discharge the Plasma Series Resonance effect leads to high frequency modulations of RF current and sheath width similar to the sheath oscillation using two frequencies, which are caused by a second externally applied high frequency voltage. These modulations can be observed in terms of excitation in both cases. The reflection of electron beams at the opposite plasma boundary as well as a localised field reversal during the phases of sheath collapse is observed applying one and two frequencies. Electron heating is generally related to the sheath motion, which can be similar in dual and single frequency discharges under certain conditions. The physics of the beams and related excitation seems to be similar, although the rapid sheath oscillations have quite different causes.

SESSION CT2: HIGH PRESSURE Arcs

Tuesday morning, 2 October 2007

Crystal Ballroom B, Doubletree Crystal City at 10:00
Joachim Heberlein, University of Minnesota, presiding

10:00

CT2 1 Generation and Properties of Plasmas in Contact with Ionic Liquids RIKIZO HATAKEYAMA, KAZUHIKO BABA, TOSHIRO KANEKO, *Department of Electronic Engineering, Tohoku University* Recently, much attention is paid to the plasmas in contact with liquids for potential applications in the material synthesis fields. We have focused on sheath electric fields in gas-liquid interfacial regions because the electric fields are effective for the control of ion behavior in both gaseous and liquid phases on the synthesis process. Here, ionic liquids are regarded as the liquids introduced into the plasma because of their greatly interesting characteristics such as their composition consisting of only positive and negative ions and extremely low vapor pressure. In this work, a plasma in contact with ionic liquids is generated in the range of low gas and atmospheric pressures. The plasma ion irradiation to ionic liquids is realized through the formation of the sheath electric field. As a result, the ion irradiation causes a remarkable change of the ionic liquid color and has effects on the plasma parameters in gas phase such as an increase in the electron density. The chemical and physical reactions induced by irradiating the plasma ion are expected to contribute to the novel material synthesis.

10:15

CT2 2 Spatiotemporal behavior of a dielectric capillary atmospheric pressure plasma jet BRIAN SANDS, BISWA GANGULY, *Air Force Research Laboratory* KUNIHIDE TACHIBANA, *Kyoto University* We have studied an atmospheric pressure plasma jet utilizing time- and space-resolved emission spectroscopy by flowing helium/argon gas mixtures through a cylindrical glass capillary energized using a $\Delta t_{rise} \sim 15$ ns high voltage pulse. Emission measurements from Ar $2p_1-1s_2$ were acquired from both the inner capillary DBD and the outer plasma jet. Just outside the capillary, the jet emission was found to occur up to 20 ns before the emission from the DBD and also exhibited a temporal variation with axial distance of 10^5 m/s. These observations preclude both direct photo-excitation and heavy particle collisional excitation from the DBD as the primary mechanism for external plasma jet formation as the former is expected to be nearly instantaneous and the latter is too slow to account for our measurements. This suggests that the outer plasma jet is not directly coupled to the interior DBD and is more likely the result of a corona discharge set up by surface charging at the capillary edge. Additional results from varying discharge conditions such as driving voltage, repetition rate, and gas mixture ratios will be presented.

10:30

CT2 3 Microwave Plasma Torches Driven by Surface Waves JULIO HENRIQUES, ELENA TATAROVA, EDGAR FELIZARDO, FRANCISCO DIAS, CARLOS FERREIRA, CENTRO DE FISICA DOS PLASMAS, INSTITUTO SUPERIOR TECNICO, 1049-001 LISBOA CODEX. TEAM, Plasma torches driven by surface waves at atmospheric pressure were studied by optical emission spectroscopy. The relative intensity of OH rotational bands and the broadening of H Balmer lines were measured. The microwave (2.45 GHz) plasma torches were created in a cylindrical fused silica tube ($R = 7.5$ mm) in air and N_2 -Ar, with powers in the range 200-2000 W and flows of 500-10000 sccm. Due to the axial gas flow an afterglow is formed beyond the discharge zone. The measured SW wave number and attenuation coefficient axial changes follow the SW dispersion law. The small variation of the gas temperature along the main part of the plasma column (4000-3000 K) is followed by a sharp drop (down to 1000 K) in the afterglow. The large difference between the gas and the wall temperatures ($T_w \sim 500$ K) is indicative of strong radial variations in the plasma quantities. "Hot" O atoms (with ~ 1.7 eV) were detected in the air torch. Acknowledgment: This study was funded by FCT/FEDER in the framework of the project "Ecological Plasma Engineering Laboratory" POCI/FIS/61679/2004.

10:45

CT2 4 Atmospheric Pressure Plasma Jet (APPJ) and Dielectric Barrier Atmospheric Pressure Glow Discharge (DB-APGD) in Comparison S. REUTER, *University of Duisburg-Essen* V. SCHULZ-VON DER GATHEN, *Ruhr-University Bochum* H.F. DÖBELE, *University of Duisburg-Essen* In this work two prominent types of low temperature atmospheric pressure plasma sources are compared. First, a plane-parallel 13.56 MHz RF-excited atmospheric pressure plasma jet (APPJ) operated with 2 m³/h helium feed gas containing 0.5 % molecular oxygen is investigated. Its stainless steel electrodes' area measures 8 x 4 cm² and the discharge gap is 1.1 mm. The effluent leaving the discharge through the jet's nozzle contains very few charged particles and a high oxygen radical density in the order of 10¹⁶ cm⁻³.

By covering both electrodes with a dielectric, the APPJ is then modified to a dielectric barrier atmospheric pressure glow discharge (DB-APGD). The homogeneity of the respective discharges is investigated by phase-resolved optical emission intensity measurements as well as by voltage and current signal measurements. The atomic oxygen generation efficiency of both plasma sources is determined (according to [1, 2]) by measuring the absolute atomic oxygen ground state density in the effluent by two-photon absorption laser induced fluorescence (TALIF) measurements. [1] K. Niemi, V. Schulz-von der Gathen, H.F. Döbele, *Plasma Sources Sci. Tech.* 14 (2005), 375; [2] K. Niemi, S. Reuter, V. Schulz-von der Gathen, H.F. Döbele, *Proceedings of the 17th ESCAMPIG* (2004), 157.

11:00

CT2 5 Investigation of a gas discharge switch based on a Lorentz drift M. IBERLER, A. FEDJUSCHENKO, J. JACOBY, J. OTTO, T. RIENECKER, CH. TESKE, *University of Frankfurt, Institute for Applied Physics* Fast switches are very important tools for pulsed power applications. Basically, there are two complete different principles used to realise a high power switch. One is based on the use of semiconductors, where as the other is based on a triggered breakdown in gases or in vacuum. This contribution gives an introduction in a new kind of gas discharge switch, which consists of a coaxial electrode geometry. The insulated electrode acts initially as an anode, whereas the coaxially arranged electrode is used as cathode. This switch device is called, based on its underlying effect, as Lorentz Drift Switch (LDS). The Lorentz Drift Switch discharge is a low low pressure gas discharge, which is positioned on the left branch of a breakdown voltage curve, similarly to the Paschen curve. Using an external triggering the gas breakdown is initiated and forms a conductive plasma sheath which closes the external electric circuit. The main circuit consists of a capacity as an energy storage system in connections with the switch. To determine the working point of the switch the Paschen break down voltage of the electrode systems was determined. Further investigations were accomplished to improve the understanding of the voltage and current behaviour depending on the loading parameter like the maximum voltage and the external capacity.

11:15

CT2 6 Instability Analysis of Formation of Multiple Arc Anode Attachments GUANG YANG, JOACHIM HEBERLEIN, *University of Minnesota* To understand the origin of the multiple arc-anode attachments and the origin of the restrike behavior in the anode region of high intensity arcs, linear stability analyses of a non-uniform singly-ionized argon plasma and of the arc-anode interface are performed. The short characteristic times of such anode phenomena allow significant simplification and linearization of the governing equations, from which dispersion relations of the plasma are obtained. According to the calculations, we propose that the electron overheating instability and the anode evaporation-ionization instability are responsible for the formation of these anode phenomena. The electron overheating instability, which generates an electron temperature run-away situation, is excited by small-amplitude fluctuations in the plasma with specific combination of current flow, electric field, electron temperature and electron density. The vaporization-ionization instability, which leads to

current run-away in a small area, is encouraged by large electric fields accelerating electrons towards the anode. The regions of these instabilities are identified with our experimental measurements. The results show that the multiple arc-anode attachments form in the fringes of the arc, and that the restrike behavior starts from flow instabilities, which bring high electron temperature cloud to the anode surface. Observations to the anode surface confirm the analysis results.

11:30

CT2 7 Discharge dynamics in a micro-plasma jet* T. GANS, *Centre for Plasma Physics, Queen's University Belfast, Northern Ireland* L. SCHAPER, N. KNAKE, K. NIEMI, V. SCHULZ-VON DER GATHEN, J. WINTER, *Center for Plasma Science and Technology, Ruhr-University Bochum, Germany* Micro-plasmas operated at ambient pressure with dimensions of the confining geometry in the order of a few ten micrometers to a millimetre bear enormous potential for technological applications. However, fundamental discharge phenomena and energy transport mechanisms in these discharges are only rudimentary understood. The atmospheric pressure plasma jet (APPJ) is a homogeneous non-equilibrium discharge. A specially designed radio-frequency (rf) μ -APPJ provides excellent optical diagnostic access to the discharge volume and the interface to the effluent region. The discharge dynamics and energy transport mechanisms from the discharge core to the effluent region are investigated using phase resolved optical emission spectroscopy (PROES) and two-photon laser induced fluorescence spectroscopy (TALIF). PROES measurements give detailed insight into the dynamics of electrons sustaining the discharge. The TALIF measurements provide spatial profiles of absolutely calibrated atomic oxygen densities.

*Funding: SFB 591, GRK 1051, EPSRC.

11:45 Student Excellence Award Finalist

CT2 8 Comparison between Non-Equilibrium and Equilibrium Modeling Results of an Arc Plasma Torch JUAN TRELLES, JOACHIM HEBERLEIN, EMIL PFENDER, *University of Minnesota* The strong plasma – cold-flow interaction, added to the intense cooling of the electrodes, suggests that thermal non-equilibrium effects could be important inside arc plasma torches. These effects can modify significantly the energy balance within the torch and subsequently affect the arc dynamics. In this research, a two-temperature non-equilibrium and a local thermodynamic equilibrium model are developed and applied to the three-dimensional and time-dependent simulation of the flow inside a plasma torch. The equations in both models are approximated numerically by a multi-scale finite element method. The results show large non-equilibrium regions near the plasma – cold-flow interaction region and close to the anode surface. Furthermore, marked differences between the non-equilibrium and equilibrium results in the arc dynamics, and in the magnitudes of the voltage drop, and outlet temperatures and velocities are observed. The non-equilibrium results show improved agreement with experimental observations, and clearly indicate the necessity for considering non-equilibrium effects in the description of plasma processing systems where strong plasma – cold-flow interactions are present.

SESSION DT1: MATERIALS PROCESSING IN LOW PRESSURE PLASMAS I: ETCHING, DEPOSITION, NEW MATERIALS

Tuesday afternoon, 2 October 2007; Crystal Ballroom A, Doubletree Crystal City at 13:30
 Shahid Rauf, Applied Materials, presiding

Invited Papers
13:30
DT1 1 A new generation of cryogenic processes for silicon deep etching.

REMI DUSSART, GREMI - University of Orleans

Deep etching of silicon is intensively used in microtechnology for MEMS and power microelectronic components. At GREMI, we study and develop the cryoetching process, which is a good alternative in terms of rapidity and cleanliness compared to other processes (e.g. Bosch process). The reactor is an ICP where the wafer is cooled down to a very low temperature (about -100[°C]). SF₆ and O₂ are the basic gases involved in the process. O₂ (10 %) is used to form an SiO_xF_y passivation layer, which grows on vertical sidewalls not submitted to ion bombardment. This oxidation occurs very efficiently at very low temperature of the substrate. The perfect control of this passivation layer formation is a key issue in the cryogenic process. Mass spectrometry measurements give the evolution of the oxidation threshold (necessary oxygen proportion to form the passivation layer) as a function of temperature, RF power and bias. The role of the etch by-products (SiF₄) in the formation of the SiO_xF_y layer was investigated using ellipsometry and mass spectrometry. With this study, we were able to develop new processes based on steps of SiF₄/O₂ plasmas to enhance the passivation layer deposition and efficiency.

Contributed Papers
14:00 Student Excellence Award Finalist
DT1 2 Modeling of Deep Reactive Ion Etching of Si under plasma molding in 2f-CCP in SF₆/O₂

FUKUTARO HAMAOKA, TAKASHI YAGISAWA, TOSHIKI MAKABE, Keio University In large-scale etching used in MEMS fabrication, plasma molding is one of the important issues. In our previous study, the effect of plasma molding on the etch profile was numerically investigated without neutral reaction [1]. In this study, we numerically investigate the feature profile evolution of deep Si etching under plasma molding in 2f-CCP in SF₆/O₂, including RIE by ions and F radicals and passivation layer formation by O radicals. In SF₆(83%)/O₂ at 300 mTorr, the removal of the passivation layer at the bottom corner is strengthened by the distorted SF₅⁺ ion incidence under plasma molding. The chemical etching rate of Si layer for F radicals is much higher than that of passivation layer. Thus, when the passivation layer is removed by ion impact, the Si etching is enhanced by addition of F radicals. As a result, this indicates that anisotropy of the etching profile is not achieved especially at the bottom in this condition [2]. In addition, we will discuss the influence of the percentage of the oxygen on anisotropic etch profile. [1] F. Hamaoka et al., Jpn. J. Appl. Phys., vol. 46, no. 5A, pp. 3059-3065, 2007. [2] -, IEEE Trans. Plasma Sci., (accepted for publication), Oct 2007.

14:15 Student Excellence Award Finalist
DT1 3 Neutral production in SF₆/SiCl₄ inductively coupled plasmas

C. DULUARD, R. DUSSART, L.E. PICHON, E.H. OUBENSAID, P. LEFAUCHEUX, P. RANSON, GREMI, Orleans M. PUECH, Alcatel Micro Machining Systems In this study we investigate the mechanisms involved during silicon etching by SF₆/SiCl₄ mixtures in an industrial inductively coupled plasma reactor. To that purpose, the plasma is analysed by mass spectrometry and optical emission spectroscopy. Relative concentrations of reactive neutrals such as F and Cl are determined using the actinometry technique. Neutral species are also monitored in the diffusion chamber by a quadrupole mass spectrometer whose ionisa-

tion energy is set to 70 eV. At this energy, the ionisation of molecules is mostly dissociative and produces several ions of lower mass. Therefore, a detected ion can stem from various molecules. Knowledge of the fragmentation spectra for different molecules is thus crucial to deduce the contribution of all the species, either being the primary gas molecules (e.g. SF₆, SiCl₄) or the resultant radicals (e.g. SF₄, SiCl₂). The study focuses on the influence of the gas flow rate on the evolution of neutral concentrations. Other parameters such as pressure and source power are fixed in the 1-10 Pa range and 800-3000 W range respectively. All these experiments are compared between the case of a bare and an oxidised silicon wafer, so as to distinguish silicon-enhanced reactions from plasma-phase and other surface reactions.

14:30
DT1 4 Atomic-scale model analysis of the feature profile evolution during Si etching in chlorine- and bromine-containing plasmas

SHOKI IRIE, YUGO OSANO, MASAHITO MORI, KOJI ERIGUCHI, KOUICHI ONO, Kyoto University Profile simulations are indispensable for understanding the influences of complex reaction processes in plasma etching, to achieve the nanometer-scale control of etched profiles and critical dimensions. This paper presents an atomic-scale model for the feature profile evolution during Si etching in chlorine- and bromine-containing plasmas. The model incorporated an atomic-scale cellular model of surface reaction layers and the Monte Carlo calculation for the trajectory of ions on feature surfaces, including their reflection on and penetration into surfaces, where the potential function for Cl-Si and Br-Si systems was determined from quantum chemical calculations. The model also took into account the formation of surface reaction layers caused by adsorption of neutrals and penetration of ions, chemical etching, ion-enhanced etching, deposition of etch products and by-products, and surface oxidation. The simulation was performed to reproduce experimental observations in Si etching with Cl₂/O₂ and HBr/O₂ chemistries: profile anomalies near the feature bottom such as footing and microtrenching,

sidewall tapering and etched depth depending on feature width, and surface roughness or residues. The mechanisms concerned are discussed in terms of competition between etching and passivation, along with ion reflection on feature surfaces.

14:45

DT1 5 Effect of VUV Radiation on Fluorination of Polypropylene in Low Pressure Plasmas* YANG YANG, *Iowa State University* MARK STROBEL, SETH KIRK, *3M, Inc.* MARK J. KUSHNER, *Iowa State University* Affixing fluorine to the surface of polypropylene (PP) lowers surface energy and increases hydrophobicity. One such fluorination process is the immersion of PP sheets in a low pressure, F_2 containing plasma wherein F atoms both abstract H atoms from and adhere to the surface. The vacuum ultraviolet (VUV) radiation these plasmas produce affect surface properties by reactions such as cross-linking, bond scission and removal of molecular group (e.g., CH_3). In this talk, the consequences of VUV radiation during low-pressure plasma fluorination of PP will be discussed with results from a computational investigation. The capacitively coupled discharge is sustained in He/F_2 mixtures. The reactor is patterned after industrial plasma sources for polymer fluorination. Plasma and surface processes on the moving web were simulated using a 2-dimensional plasma hydrodynamics and surface chemistry model. To properly address radiation trapping, a Monte Carlo radiation transport module is used to generate the photon fluxes incident on the PP film. Assessment of the roles of various photon activated processes in the fluorination process will be made.

*Work supported by 3M, Inc. and NSF.

15:00

DT1 6 Effect of gas mixture ratio on atomic oxygen density in an inductively coupled plasma in O_2/Ar mixture TOSHIKAZU SATO, TOSHIKI MAKABE, *Keio Univ.* Oxygen plasmas are extensively used in material processing such as ashing of photoresist, surface modification and oxidation. It is well known that dilution of oxygen by rare gas increases the plasma density and enhances the processing speed. Kitajima et al experimentally investigated argon diluted oxygen plasma and showed that the metastable argon efficiently produces metastable atomic oxygen in capacitively coupled discharge [1]. In this work, we perform a two-dimensional modeling of an inductively coupled plasma (ICP) in O_2/Ar mixture and investigate the effect of Ar dilution on the mechanism of the atomic oxygen production. A steady state plasma structure and the spatial distribution of neutral species are calculated by using the relaxation continuum model. Atomic oxygen is produced mainly through the dissociation of oxygen molecule by electron impact and the recombination on the reactor surface is the most dominant loss mechanism of atomic oxygen in highly diluted O_2/Ar ICP at 100 mTorr. Ground state atomic oxygen increases monotonically with increasing O_2 fraction (less than 10%), on the other hand, metastable atomic oxygen steeply increases under the O_2 fraction less than 3%. [1] T. Kitajima, T. Nakano, and T. Makabe, *Appl. Phys. Lett.* 88, 091501 (2006).

15:15 Student Excellence Award Finalist

DT1 7 Ion Flux and Energy Measurement at a Pulsed Biased Electrode in a C_2H_2 :Argon Inductively Coupled Plasma During DLC Growth. A. BABY, C.M.O. MAHONY, P.D. MAGUIRE, *Nanotechnology and Integrated BioEngineering Centre, University of Ulster* Diamond-like carbon is an important material for biomedical and mechanical applications. Knowledge of growth mechanisms is severely limited by lack of basic hydrocarbon

plasma data since measurement is extremely challenging due mainly to probe deposits. Plasma models suffer from a lack of basic information e.g. T_e , n_e . We measured ion energy distributions and neutral fluxes for six dominant species directly at the growing substrate in a C_2H_2 :Argon ICP (≤ 10 mTorr) for the first time. By RF pulse biasing the substrate electrode we have also determined the absolute values of positive ion flux^[1]. From analysis of bimodal IEDs and 1D modelling of multi-species ion transport across the sheath, we intend to extract plasma density. This requires internal probe measurement to confirm model estimates of n_e and T_e . Pulsed bias generates a central peaked trimodal IED from which we can better isolate the impact of ion energy during our DLC growth. We estimate dissociation kinetics from infrared TDLAS and neutral flux measurement. Correlation of film properties with growing substrate fluxes will be a first for this important material and will be an critical input to current rudimentary growth models. [1] Braithwaite et.al. *Plasma Source Sci Technol.* 5 (1996) 6

SESSION ET1: PLASMA-SURFACE INTERACTIONS

Tuesday afternoon, 2 October 2007

Crystal Ballroom A, Doubletree Crystal City at 16:00

Antoine Rousseau, LPTP, presiding

Contributed Papers

16:00 Student Excellence Award Finalist

ET1 1 Surface recombination study in near real time in Cl_2 plasmas* JOYDEEP GUHA, VINCENT M. DONNELLY, *University of Houston* We have started a new approach of studying surface reactions in near real time, in which a hollow section of the reactor wall is rotated at high frequencies between the plasma and differentially pumped diagnostic chambers, thereby periodically exposing the surface to the plasma and diagnostic probes. Surface recombination reactions of Cl atoms on anodized aluminum have been investigated by this technique in chlorine plasmas. Cl_2 desorption following surface recombination was monitored over a time scale of 0.8 to 38 ms after the surface was exposed to the plasma. Cl recombination probabilities were measured over a wide range of Cl atom flux by varying the plasma pressure and absorbed power. Langmuir-Hinshelwood Cl recombination coefficients (γ_{Cl}) were measured by extrapolating the desorption flux to $t = 0$. For 5mTorr 600W Cl_2 plasma, the desorption flux was $2.7 \times 10^{15} \text{ cm}^{-2}\text{s}^{-1}$ at $t = 0$. γ_{Cl} values ranged from 0.01 to 0.08 and were found to increase with increasing power and decrease with increasing total pressure. With plasma on, adsorption of undissociated Cl_2 competes with Cl adsorption particularly at high pressure and low power. Weakly bound Cl_2 appears to block adsorption sites on the surface, thereby reducing the recombination probability, as observed. Auger analysis of the surface at different plasma conditions suggests that less than 10% of adsorbed Cl atoms actually participates in surface recombination.

*Supported by Lam Research Corp., ACS/PRF, NSF, and the University of Houston GEAR.

16:15

ET1 2 Analysis of plasma-surface interactions during plasma etching by in-situ diagnostics of reactants and reaction products YOSHINORI UEDA, MASAHIRO YOSHIDA, KOJI ERIGUCHI, KOUICHI ONO, *Kyoto University* The incoming ions and neutrals onto substrate surfaces govern the etching characteristics achieved; moreover, the product species, desorbed from the substrate being etched, also play an important role in processing. This paper presents a mechanistic study of plasma etching processes, using in-situ plasma and surface diagnostics of reactants and reaction products, to gain a better understanding of competitive mechanisms that occur during etching. Experiments were performed primarily in an inductively coupled plasma reactor, with emphasis being placed on Si etching with Cl_2/O_2 chemistries and on HfO_2 etching with $\text{BCl}_3/\text{Cl}_2/\text{O}_2$ chemistries. Optical emission spectroscopy, laser-induced fluorescence spectroscopy, and quadrupole mass spectrometry were employed to observe reactant and product species in the gas phase. Fourier transform infrared absorption spectroscopy was also employed, to observe triatomic and larger molecules of reactants and reaction products in the gas phase and on surfaces; in practice, the gas-phase species was observed by transmission absorption spectroscopy, and the product species such as SiCl_x and HfCl_x on the surface by reflection absorption spectroscopy. The mechanisms responsible for selective etching of Si over SiO_2 and of HfO_2 over Si are discussed based on these observations.

16:30

ET1 3 Experimental study and modeling of plasma-polymer interactions* ANATOLY NAPARTOVICH, YURI AKISHEV, MIKHAIL GRUSHIN, NIKOLAY DYATKO, IGOR KOCHETOV, NIKOLAY TRUSHKIN, *SRC RF TRINITY TRAN DUC, FRANCOISE SOMMER, Biophy Research S.A.* Atmospheric pressure discharges producing high non-thermal plasma were employed for polypropylene (PP) film surface. Two types of discharges were examined: pulse periodic streamer-like discharge in air flow and glow discharge in nitrogen. Water/surface contact angles before and after plasma treatment were measured. A pronounced improvement of surface wettability is observed, and its

Invited Papers

17:00

ET1 5 Plasma-Surface Interactions With Advanced Polymers For Nanoscale Patterning Of Materials.* GOTTLIEB OEHRLEIN, *University of Maryland, College Park, MD 20742-2115*

Photolithography and plasma-based transfer of resist patterns to produce devices are the basis of the information technology, and other technologies where patterned films or substrates are needed. The most highly developed is the silicon integrated circuit industry, which employs plasmabased etching to produce device features with precisely controlled nanoscale dimensions. Given the tremendous success of this technology, it is surprising that one of the least understood elements of this approach remains the interaction of the plasma species with the organic molecules arranged either as a blanket film or a nanoscale pattern, and the chemical, morphological and topographic changes induced by these interactions in the macromolecules themselves and the macromolecule defined nanoscale features. In this talk we review recent work aimed at improving our understanding and control of plasma-surface interactions with advanced polymers for nanoscale patterning of materials. Based on collaborations with S. Engelmann, R. L. Bruce, T. Kwon, R. Phaneuf, Y. C. Bae, C. Andes, D. Graves, D. Nest, J. Vegh, E. A. Hudson, B. Long, G. Willson, P. Lazzeri, E. Iacob and M. Anderle.

*We gratefully acknowledge financial support of this work by the National Science Foundation under awards Nos. DMR-0406120 and NIRT CTS-0506988.

dependence on plasma exposer is found. This effect is stronger for nitrogen glow discharge processing. Ageing of surface properties proceeds slower after nitrogen plasma treatment. XPS method was implemented to characterize changes in functional groups on polymer interface. The theoretical models were developed for plasma chemistry induced in air by streamer-like discharge and for plasma-surface interactions governed by chemical radicals. Processes of hydrogen abstraction from the surface, secondary reactions with formed active sites, and finally backbone scission are considered. Satisfactory agreement with respect to after treatment composition of functional groups on the surface is achieved between results of XPS measurements and theoretical model predictions. The plasma-surface interaction model provides a solid basis for attacking the ageing problem.

*State contract 02.513.11.3023

16:45

ET1 4 Hydrogen plasma interaction with graphite surface GILLES CARRY, CEDRIC THOMAS, JEAN-MARC LAYET, THIERRY ANGOT, *CNRS-Universite de Provence* Interaction of hydrogen with graphite surfaces is of great interest for controlled fusion, where carbon material erosion by hydrogen is a key issue. Indeed, tritium retention resulting from carbon redeposition is a safety problem. In this perspective, we study interaction between hydrogen plasma and graphite. We aim to understand erosion mechanisms and identify the role of ions and neutrals. In order to unravel all plasma-surface interaction mechanisms, we associated on a same ultra-high vacuum set-up, an ICP plasma source, an atomic hydrogen source and a hydrogen ion gun. Surface properties were probed with *in-situ* high-resolution electron-energy-loss spectroscopy (HREELS) and with *in-situ* scanning tunneling microscopy (STM). Comparison with DFT calculations leads us to establish the model of H adsorption process. Surface exposition to atomic hydrogen leads to relatively weak adsorption of H atoms. Surface exposition to 300eV H_2^+ ions leads to formation of defects without H adsorption. Subsequent H exposition shows the presence of strongly bonded H atoms. Plasma expositions reveal the presence of strongly bonded H atoms.

Contributed Papers

17:30

ET1 6 Comparison of gas-phase chemistry during deposition of amorphous carbon films using capacitive and inductive discharges. S. RAMACHANDRAN, L. OVERZET, W. HU, L.S.N. TAO, *UT Dallas* G.-S. LEE, C. NELSON, M. GOECKNER, *UT Dallas* Diamond like carbon films (amorphous carbons) are just beginning to find applications as protective coatings in nano-imprint lithography. These films have appropriate hardness, inertness and surface free energy. They can be deposited using a variety of plasma tools. We compare the capacitive and inductive

methane plasmas for depositing films to be used as mold material in nano-imprint lithography. Gas-phase chemistry studies of the deposition process were made using Fourier transform infrared (FTIR) spectroscopy and emission spectroscopy. It was observed that the methane broke down into CH₃, CH₂, CH and H. In addition, larger species were found in the gas, including acetylene and ethylene. Vibrational and rotational temperatures of several species were determined. Concurrent studies of the resulting films, shows that the capacitive discharge had a larger processing window for the production of suitable quality films. We believe that this is tied to the degree of dissociation of the methane, as well as the presence of the larger species found in the gas phase.

SESSION ET2: ELECTRONEGATIVE PLASMAS

Tuesday afternoon, 2 October 2007; Crystal Ballroom B, Doubletree Crystal City at 16:00

Matt Goeckner, University of Texas at Dallas, presiding

Invited Papers

16:00

ET2 1 Plasma-Based Low Energy Ion Implantation.*

LUDOVIC GODET, *Varian Semiconductor Equipment Associates*

After intense research and development of plasma doping systems, successful application of pulsed glow discharge in low energy ion implantation has been demonstrated. This approach offers great potential for both economic benefit, as a much higher throughput process than traditional beam line implantation, as well as enabling new fabrication options for advanced CMOS or non-planar implant. Understanding the discharge physics - collisions, ion energy distributions, plasma composition, secondary electron emission in the sheath of the dc pulsed plasma is indispensable for controlling the low energy ion implantation process. In this paper, ion energy distribution is directly measured from the high voltage sheath in a pulsed dc glow discharge using BF₃ or BF₃ mixed with inert gases as a gas feedstock. The impact of the ratio of BF₃ mixed with inert gases on the ion energy distribution of the different ions and plasma parameters in the bulk and in the sheath is studied. The effects of elastic and inelastic collisions in the sheath on the ion energy distributions were experimentally and theoretically determined. It was found in several experiments that molecular ion such as BF₂⁺ dominates the BF₃ glow discharge. A possibility of negative ion formation is discussed with the recent experimental results taken into account. The analysis of the ion energy distribution and plasma parameters enabled a better understanding of the key parameters that control the nature, the concentration and the depth distribution of the implanted species. Based on the ion energy distributions measured with the mass spectrometer, the dopant depth profile is predicted and the plasma parameters are optimized in order to obtain shallow dopant depth distribution in the silicon after plasma doping implantation. This review of pulsed plasma-based implantation for semiconductor applications will focus on plasma diagnostics results thus far and the prospects for low energy implant applications.

*Acknowledge Dr Svetlana Radovanov for participating in this research

Contributed Papers

16:30

ET2 2 Theory and particle-in-cell simulation of ion-ion plasmas GARY LERAY, ALBERT MEIGE, JEAN-LUC RAIMBAULT, PASCAL CHABERT, Ion-ion plasmas have many potential applications such as in material processing (to minimize charging in the fabrication of microelectronic devices), in negative ion sources etc. In all these applications, the design of extracting grids implies a good knowledge of the sheath and the presheath in such plasmas. A full particle-in-cell simulation and a kinetic theory are developed to investigate ion-ion plasmas under the influence of a DC bias voltage. It is shown that high-voltage sheaths following the classical Child-law sheaths form within a few μ s after the DC voltage is applied. It is also shown that there exists the equivalent of a Bohm criterion with the corresponding presheath accelerating ions collected at one of the electrodes to the sound speed before entering the sheath.

16:45

ET2 3 Propagating double layers in electronegative plasmas

ALBERT MEIGE, NICOLAS PLIHON, GERJAN HAGELAAR, JEAN-PIERRE BOEUF, PASCAL CHABERT, ROD BOSWELL, *LPTP, Ecole Polytechnique* Double layers have been observed to propagate from the source region to the diffusion chamber of a helicon-type reactor filled up with a low-pressure mixture of Ar/SF₆ [N. Plihon et al., *J. Appl. Phys.*, **98**(023306), 2005]. In the present paper the most significant and new experimental results are reported. A full self-consistent hybrid model where the electron energy distribution function, the electron temperature and the various source terms are calculated is developed to investigate these propagating double layers. The spontaneous formation of propagating double layers is only observed in the simulation for system where the localized inductive heating is combined with small diameter chambers. The conditions of for-

mation and the properties of the propagating double layers observed in the simulation are in good agreement with that of the experiment. By correlating the results of the experiment and the simulation, a formation mechanism compatible with ion two-stream instability is proposed.

17:00

ET2 4 Very High Frequency Capacitively Coupled Plasmas of Electronegative Gases SHAHID RAUF, KALLOL BERA, ALEX PATERSON, KEN COLLINS, *Applied Materials, Inc.* Electromagnetic effects play an important role in determining the plasma behavior in large area capacitively coupled plasmas (CCP) generated using very high frequency (VHF) RF sources. A 2-dimensional model is used to elucidate the physics of VHF CCP discharges of electronegative gases. The model includes the full set of Maxwell equations in their potential formulation. The equations governing the vector potential, A , are solved in the frequency domain after every cycle for multiple harmonics of the driving frequency. The coupled set of equations governing the scalar potential, ϕ , and drift-diffusion equations for all charged species are solved implicitly in time. The model also includes the electron temperature equation, Kirchhoff equations for the external circuit, and continuity equations for neutral species. The simulations focus on a 180 MHz CCP discharge, and examine the effect of gas mixture (Ar/CF₄, Ar/SF₆) and inter-electrode spacing on the plasma characteristics. It is found that spatial characteristics of the plasma are determined through a balance of electrostatic and electromagnetic effects.

17:15

ET2 5 Fast silicon etching by plasma-sheath-lens focused negative ions* EUGEN STAMATE, *Risoe National Laboratory, Technical University of Denmark* Plasma processing technologies are based on radical-assisted, ion-induced surface modifications where ions accumulate energy within the sheath then strike the surface with a certain energy and incidence angle. Since reliable information on etching yields and a precise control of reactive species are of critical importance in attaining the desired process the use of plasma-sheath-lens and its discrete and modal focusing effects [1] can bring certain advantages (identical environment with that of real plasma processing; wide range of ion energies at high current densities; the passive surface can be used as a reference or as a collection surface of byproducts). Despite of high etching rates provided by high-density plasmas there are yet unsolved problems which can be avoided by bringing electrons to the bottom of the features, a case in which the etching needs to be performed by negative ions. In this work square, and disk electrodes made of silicon have been exposed to different incident fluxes of negative ions focused by a plasma-sheath-lens. The etching pattern resulted by discrete and modal focusing effect was measured by phase-shift laser interferometry and compared with that from simulation performed for similar parameters. [1] E. Stamate and H. Sugai, *Phys. Rev. Lett.* 94 (2005) 125004.

*Work partially supported by MIRC-CT-2006-046409.

17:30

ET2 6 Plasma Characterization of Electronegatively diluted VHF CCP Plasmas ALEX PATERSON, NED HAMMOND, SHAHID RAUF, *Applied Materials* ED BARNAT, PAUL MILLER, GREG HEBNER, *Sandia National Laboratories* In this study, the plasma characteristics of a VHF capacitively-coupled, 300 mm processing system were investigated. Spatially dependent ion and electron density, as well as electron energy distribution

functions, were measured for frequencies between 27 and 170 MHz and for gas mixtures containing argon, SF₆ and CF₄. In argon plasmas, increasing the frequency above 120 MHz changed the ion and electron density spatial distributions from uniform to center high, producing a convex structure. This suggests that electromagnetic effects become important for this particular chamber geometry as the excitation frequency increases above 120 MHz. However, the addition of electronegative gas reduced the spatial non-uniformities, even at the highest frequencies investigated. For instance, diluting argon with SF₆ resulted in the ion and electron density spatial uniformity changing from convex to uniform to concave. Similar effects were also observed with CF₄ addition, but more dilution was required since it is less electronegative than SF₆. This suggests the increasing negative ion density causes the electron density to reduce below a critical value, which results in the standing wave being "damped," probably due to the increase in the plasma resistance.

17:45

ET2 7 Formation of ion flux in low frequency and low pressure ccrf discharge I.V. SCHWEIGERT, *Institute of Theoretical and Applied Mechanics SBRAS* The formation of ion energy distribution function and ion angular distribution function are studied in 2-13.56 MHz discharge in Ar and BF₃. The results are obtained with self-consistent kinetic simulations with using particle in cell Monte-Carlo collisions algorithm. For low gas pressure and high applied discharge voltages the models of electron and ion motion are modified to take into account the anisotropy of electron and ion scattering.

SESSION FTP1: POSTER SESSION I

Tuesday evening, 2 October 2007

Crystal Ballroom C, Doubletree Crystal City at 19:30

FTP1 1 HIGH PRESSURE GLOW DISCHARGES

FTP1 2 Mechanisms of Atomic Oxygen Generation and Destruction in the Effluent of an RF-Excited Atmospheric Pressure Plasma Jet (APPJ) S. REUTER, *University of Duisburg-Essen* K. NIEMI, V. SCHULZ-VON DER GATHEN, *Ruhr-University Bochum* H.F. DÖBELE, *University of Duisburg-Essen* The aim of this study is to gain a better insight into the mechanisms of atomic oxygen generation and destruction in the effluent of an atmospheric pressure plasma jet (APPJ). The APPJ is a 13.56 MHz RF-excited atmospheric pressure plasma source operated with 2 m³/h helium feed gas plus ~ 1vol% molecular oxygen admixture. The effluent contains very few charged particles and a high oxygen radical density in the order of 10¹⁶ cm⁻³. The space resolved ground state atomic oxygen density is measured with two-photon absorption laser induced fluorescence (TALIF) spectroscopy. Optical emission spectroscopy (OES) measurements reveal the existence of excited atomic oxygen even at 10 cm distance to the jet's nozzle. UV-OES measurements and chemical model calculations are performed to understand energy transport mechanisms into the effluent.

FTP1 3 Study of a 2.45 GHz microwave micro-plasma in air
 J. GREGORIO, *CFP IST 1049-0011 Lisboa / LPGP UPS 91405 Orsay France* P. SYNEK, *DPE Masaryk Univ. 611 37 Brno Czech Rep. / LPGP UPS 91405 Orsay France* L.L. ALVES, *CFP IST 1049-0011 Lisboa Portugal* C. BOISSE-LAPORTE, P. LEP-RINCE, O. LEROY, L. TEULÉ-GAY, *LPGP UPS/CNRS 91405 Orsay France* This paper studies a 2.45 GHz microwave micro-plasma source, working in air at atmospheric pressure. The discharge, similar to the one developed by Kono *et al*[1], is sustained within a slit (50-200 μm wide and 1.4cm width) delimited by two metallic blades placed at one end of a microstrip line. At the other end, a movable short circuit works as an impedance matching unit. The plasma source is placed inside a microwave absorbent box. The power coupling is analyzed theoretically by using the commercial software CST Microwave Studio registered, and experimentally by taking the ratio of the reflected to incident power, with and without plasma and for different slit sizes. A spatially resolved optical emission spectroscopy study was also realized, using the SPECAIR registered software [2] to deduce the gas temperature T_g along the plasma width. In general, T_g is found between 650 and 1650 K, for 60-140W input power and 50-200 μm slit size. [1] A. Kono, T. Sugiyama, T. Goto, H. Furuhashi, Y. Uchida, *Jpn. J. Appl. Phys.* Vol. 40 (2001) pp. L238-L241 [2] <http://www.specair-radiation.net/>

FTP1 4 Electrical and Optical Measurements in an RF-Driven Micro-Discharge Source C.M.O. MAHONY, *University of Ulster* T. GANS, W.G. GRAHAM, *Queen's University Belfast* P.D. MAGUIRE, *University of Ulster* Z.L.J. PETROVIC, *Institute of Physics Belgrade* Microdischarge properties are distinctly different to those of larger sources, leading to potential applications such as: high density tailored plasmas, local heating, fast material processing and scale up to large area sources. Hollow cathode operation is unlikely in micro-hollow cathode devices of diameter $\leq 100 \mu\text{m}$ ^[1] because short mean free paths inhibit pendular electron motion. Thus diameters as small as 10 μm may be required for HC operation, a critical stability challenge. We report radio frequency operation in micro-hollow cathode structures for diameters as small as 25 μm . The sources are operated in argon and helium at pressures of 20 to 600 Torr and ignite readily at ~ 20 W, operating stably at powers < 10 W. Measurements of breakdown characteristics, rf current and voltage and optical emission were recorded. A number of operating modes have been observed in these sub-100 μm dimensions and OES of argon and helium discharges indicates there is less sputtering with helium. Positive dc bias has been observed in the cathode potential under rf operation, similar to that reported by Guo & Hong^[2] at a diameter of 300 μm . [1] Kushner, *J. Phys. D: Appl. Phys.* 38 (2005) 1633 [2] Guo & Hong, *Jpn. J. Appl. Phys.* 42 (2003) 6598

FTP1 5 Study of the transition between MicroHollow Cathode Discharge and MicroCathode Sustained Discharge in a 3-electrode system L.C. PITCHFORD, K. MAKASHEVA, TH. CALLEGARI, J.P. BOEUF, *LAPLACE, CNRS-Universite de Toulouse, 31062 Toulouse, France* J. SANTOS SOUSA, V. PUECH, *LPGP, CNRS-Universite Paris-Sud, 91405 Orsay, France* LAPLACE TEAM, LPGP TEAM, MicroHollow Cathode Discharges (MHCDs) are known to be good sources for production of DC non-thermal plasmas at high gas pressure. Using them as a cathode in a system with third positively biased electrode, placed at distance of about 1 cm from the MHCD, allows the ignition of a stable, larger volume plasma in the MicroCathode Sustained Discharge (MCSD). The aim of our study is to investigate the electrical properties of the discharge when it is sustained in different gases (He, Ne, Ar or O₂). The voltage-current (V-I) characteristics of the MCSD were measured for gas pressures in the range $p = 50 - 200$ Torr, varying gas flow $Q = 50 - 500$ sccm and gas composition. The MHCD is a sandwich type, consisting of 100 μm thick molybdenum electrodes glued on each side of 500 μm thick Al₂O₃ plate, with a 800 μm diameter hole. The transition between the MHCD and MCSD, defined as the point where the third electrode collects all the electron current, is rather abrupt and depends on the operating conditions. Results from model calculations will also be presented to help clarify the phenomena occurring during the transition.

FTP1 6 Reactivity in microplasma operating at medium pressure X. AUBERT, *Ecole Polytechnique* A. PIPA, J. ROPCKE, *INP-Greifswald* D.L. MARINOV, Y. IONIKH, *State University, St Petersburg* A. ROUSSEAU, *LPTP, Ecole Polytechnique, France* IR Tunable Diode Laser Absorption Spectroscopy (TD-LAS) and UV broad band absorption spectroscopy measurements are used to detect O₃, NO and NO₂ produced by a microplasma made of a micro-hollow cathode geometry. The gas flows through the microplasma; an additional plasma plume may be ignited on the microplasma anode region using an auxiliary anode. The microplasma may be operated in continuous or self-pulsing mode [1]. The current density in the microplasma is about 3 orders of magnitude higher than in the plume and may reach 1000 A/cm² in a self pulsing mode. It is shown that NO and NO₂ densities scale as a function of the specific energy (J/l). The effect of the plume ignition is to lower the production of these species. Experimental results are compared with an experimental modeling. [1] A. Rousseau and X. Aubert *J. Phys. D: Appl. Phys.* 39 (2006) 1619-1622.

FTP1 7 Pulsed plasma bubble located in a water capillary P. CECCATO, A. ROUSSEAU, *LPTP, Ecole Polytechnique, France* Several studies have investigated water discharges for hydroxyl radical generation and organic compound removal for water cleaning [1]. We report preliminary results concerning the generation of plasma in a water capillary and the influence of rise time, water conductivity on the plasma injected power, using electric measurement probes and on the plasma propagation, using CCD camera. The plasma may be generated directly in the water after the formation of a gas bubble due to the ohmic heating or, it can be created in an pre-injected bubble. Bubble expansion and plasma current is monitored. The plasma formation occurs at the water/plasma interface where the electric field is higher. Streamer length and initiation time lag have been measured. [1] A. T. Sugiartoa *et al. Journal of Electrostatics* 58 (2003) 135-145.

FTP1 8 Fabrication process and electrical characterization of direct current parallel micro-discharges in helium M. MANDRA, *UT Dallas* R. DUSSART, *U d'Orleans* J.-B. LEE, M. GOECKNER, *UT Dallas* T. DUFOUR, P. LEFAUCHEUX, P. RANSON, *U d'Orleans* L. OVERZET, *UT Dallas* Micro Hollow Cathode Discharges (MHCD) have been fabricated. They are round holes through 250 μm or 500 μm thick Nickel-Alumina-Nickel surfaces. The base surfaces are constructed from 7.5 X 7.5 cm alumina wafers, which are vacuum baked then coated with chromium and copper seed layers and finally patterned. Nickel film, 5-6 μm thick, is then deposited on either side of the alumina wafer using the process of electroplating. Single and multi cavity micro discharges are then laser drilled with diameters ranging from 130 μm to 300 μm and spacing between the cavities ranging from 245 μm to 315 μm . Breakdown vs. pressure measurements show that smaller diameter cavities (130 μm) have higher breakdown voltages than cavities with larger diameter (300 μm). In addition, the difference between the breakdown voltage and the operating voltage is substantially larger. Current-voltage measurements for single hole MHCD devices indicates that they operate in the normal glow regime with decreasing discharge voltage as discharge current is increased.

FTP1 9 Atmospheric-pressure microgap plasma produced by 10-GHz microwave excitation A. KONO, M. KOBAYASHI, M. ARAMAKI, *Nagoya University* Atmospheric pressure high-density glow discharge can be sustained continuously in the microgap (100- μm wide) between two knife-edge electrodes by microwave excitation. Detailed characterizations of a microgap plasma produced by 2.45-GHz microwave excitation were reported previously, including electron density and temperature measurements using laser Thomson scattering, gas temperature measurements under the influence of gas flow, etc. In the present study, we investigate the effect of microwave frequency on the electron density, in view of the analogy with the fact of increasing electron heating efficiency with increasing driving frequency in usual rf low-pressure capacitively coupled discharge. Preliminary studies on three different electrode configurations and microwave driving schemes indicate that the electron density do not reach that in the case of 2.45-GHz excitation, suggesting a large radiation loss of the microwave power in 10-GHz excitation. A discharge structure to reduce the radiation loss is being pursued. (Work supported by Grant-in-aid 15075205 from MEXT Japan.)

FTP1 10 Spatio-temporal development of atmospheric pressure plasma filaments: influence of surface memory effects. S. CELESTIN, O. GUAITELLA, G. CANES-BOUSSARD, A. ROUSSEAU, *LPTP, Ecole polytechnique* A. BOURDON, *EM2C, Ecole Centrale* STREAMERS COLLABORATION, It has been recently shown in a cylindrical DBD that the current amplitude distribution function shows two different peak populations during positive half periods of the 50Hz high voltage (when the metallic inner electrode is positive) [1]. The high current population is caused by the simultaneous propagation of plasma filaments, the so called collective effect. In the present study, CCD imaging is coupled to electrical measurements; we show that, in a pin to plan DBD, the spatial shape of the plasma filaments in the gas gap depends strongly on the "history" of the events. The first peak impacts the dielectric surface close to the center (minimum pathway from the metallic electrode) and then propagates radially on

the surface. The following peaks impact the dielectric with a larger radius. The branching of the plasma filament is also highly dependant on the "history" and increases with the current pulse. [1] O. Guaitella, F. Thevenet, C. Guillard, A. Rousseau *J. Phys. D : appl. Phys* (2006).

FTP1 11 Shock Wave Drag Coefficients in Argon Glow Discharge Plasma* NIRMOL K. PODDER, ANASTASIA V. TARASOVA, RALPH B. WILSON IV, *Troy University, Troy, AL* Mach 2 shock waves are launched into a weakly ionized dc glow discharge plasma. Four pairs of laser beams are setup across the plasma and spaced over the entire positive column. Laser deflections caused by the gradient in the shock wave gas density are recorded on an oscilloscope to obtain the time history of the shock wave propagation through plasma. In this way, multipoint shock wave velocities are measured over a range of operating argon gas pressure from 3-15 Torr and discharge current from 0-70 mA. The shock wave propagation velocity in plasma is seen to increase with increasing discharge current. Shock wave drag coefficients are determined from the functional dependence of the velocity on the position.

*This work is supported by the DOE.

FTP1 12 Modelling gas plasma interactions in driven systems C.S. MACLACHLAN,* D.A. DIVER, H.E. POTTS, *University of Glasgow, Dept. of Physics & Astronomy, Kelvin Building, University of Glasgow, G12 8QQ, UK* We explore numerically the impact of collisions in gas plasma systems and possible ways to exploit plasma chemistry in different experimental contexts. Electron Avalanches: We investigate the early stages of the initiation of a high pressure discharge paying particular attention to the production of excited neutral species. This highly non-equilibrium initiation is a Townsend-like avalanche created by electron impact ionisation and occurs on a sub-nanosecond timescale. Understanding this stage of the discharge could identify a technique for the non-steady production of metastables for high-activation energy chemistry without full plasma ignition. Electronegative Instabilities: Instabilities manifesting as variations in light emission and number density have been reported in electronegative discharges. Here electron attachment and detachment drives a radiative instability in a pre-formed RF discharge. We propose a simple model that captures the physics behind the experimental phenomena.

*c.maclachlan@physics.gla.ac.uk

FTP1 13 DIELECTRIC BARRIER DISCHARGES, DISPLAYS

FTP1 14 Backscattering of secondary electrons to the cathode in the oblique electric field in dielectric barrier discharge systems. VLADIMIR KHUDIK, *University of Toledo* JOEL PENDERY, *Ohio State University* ALEXANDER SHVYDKY, *University of Rochester* CONSTANTINE THEODOSIOU, *University of Toledo* In contrast to electric field lines in gas discharge systems with bare electrodes, electric field lines in dielectric barrier discharge systems, where the cathode is covered with the dielectric layer, may cross the dielectric surface at an oblique

angle. The secondary electrons emitted from this surface either return to the cathode due to collisions with background gas atoms or eventually escape from the region near the cathode. Using the diffusion P1-approximation to the kinetic equation for electrons, we have found analytically the electron escape factor k for different limiting cases. Monte-Carlo simulations of backscattering of electrons have been performed for noble gases and the dependence of the escape factor on the angle between the electric field lines and the dielectric surface have been found. The analytical theory has been used to explain unexpected peculiarities in results of Monte-Carlo simulations.

FTP1 15 Effects of overvolting on direct electron impact and heavy particle excitations of Ar and N₂ electronic states in a pulsed DBD ROBERT LEIWEKE, *UES, Inc.* BISWA GAN-GULY, *Air Force Research Laboratory* The pressure dependence of direct electron impact and heavy particle resonant energy transfer kinetics within a pulsed-excited N₂/Ar DBD have been studied using two different pulsed applied voltage rise times (~ 20 ns and ~ 150 ns) in order to measure the effects of overvolting upon direct electron impact and heavy particle excitation efficiencies. The DBD was operated from 15-500 Torr, up to 8% N₂, 7.75 kV total applied voltage, and 5 kHz repetition rate. Time-resolved emission spectroscopy was used to obtain the relative intensities of the N₂⁺ (B-X), Ar⁺ (4P-4D), Ar (2p₁-1s₂), N₂ (C-B) transitions which have differing excitation thresholds of ~ 19 eV, 19 eV, 13.5 eV, and 11 eV, respectively. Absolute total Ar metastable (Ar^M, 11 eV) column densities were obtained using Diode Laser Spectroscopy. The Ar^M column densities can be used to calibrate the relative emission intensities from the other four excited state species, once the pressure scaling for the pure argon case has been established. These reported results will show that the relative excitation efficiencies peak at different pressures depending upon both the excitation thresholds and overvolting, except for the Ar^M + N₂ \rightarrow Ar + N₂(C-B) excitation.

FTP1 16 ABSTRACT WITHDRAWN

FTP1 17 PLASMA BOUNDARIES: SHEATHS, BOUNDARY, LAYERS, OTHER

FTP1 18 Spatial Plasma Oscillations - Physical Phenomenon or Computational Artefact? RAOUL FRANKLIN, *The Open University, UK* Often when attempting to solve problems involving a bounded active plasma, the expedient is adopted of assuming plausible initial values and then integrating the full fluid equations including generation, collisions, and Poisson's equation, until the wall conditions are met. This procedure generates spatial plasma oscillations of decreasing magnitude. This paper examines a number of different cases and ranges over a wide variation of param-

eters. It seeks to show that such spatial oscillations arise from the approximations made. The oscillations have been the subject of interest in published papers from time to time, and thus we seek to make workers aware of these 'spurious' results in electropositive plasmas. On the other hand we also give results for electronegative plasmas where it is well-established that such oscillations are expected to occur in the vicinity of the core-plasma interface. However there is as yet, so far as I am aware, no experimental evidence for their existence.

FTP1 19 Role of Secondary Electrons in Anode Sheath GILLES CARRY, LOIC SCHIESKO, JEAN-MARC LAYET, MARCEL CARRERE, *CNRS-Universite de Provence* We study electron attracting sheath (anode sheath) both experimentally and theoretically. Experiments are conducted in a low-pressure (0.05 and 0.1 Pa) helicon reactor. A positively biased Cu sample faces a mass and energy analyser. Plasma electrons are accelerated towards sample and ionize background gas creating Ar⁺ ions. These ions in turn are accelerated towards the mass and energy analyser and are detected according to their energy. The energy at which an ion is detected corresponds to local electrical potential at which the ion has been created. Measurements show that no ion is detected with full energy. We explain this considering secondary electrons emitted from surface upon primary electron impacts. These secondary electrons are trapped by potential, accumulate near the sample, and cause a very fast potential variation close to the sample. This fast variation occurs on a too short distance to observe a significant ionization signal and consequently no ion is detected with full energy. Measurements are compared with a numerical model solving Poisson equation including secondary electrons and computing ion energy distribution.

FTP1 20 Neutral energy distribution in the cathode fall of direct-current glow discharges TSUYOHITO ITO, *Osaka University* MARK CAPPELLI, *Stanford University* Energetic neutrals are formed in the cathode fall of dc glow discharges through collisions with accelerated ions. These energetic neutrals contribute to secondary electron emission, electrode erosion, and discharge gas heating. In this study we describe direct measurements and Monte Carlo simulations of the energy distribution of energetic neutrals in an argon dc glow discharge. The measurements are performed by time-of-flight analysis of neutrals escaping through a cathode orifice. The experimental results are found to be in good agreement with the Monte Carlo simulations. A preliminary sensitivity of the MC simulations to angular scattering in ion-neutral collisions suggests that improved agreement can be obtained by including more complex modeling of the charge exchange collision processes. The results also indicate that commonly-used theories for the production of energetic neutrals through charge exchange in the cathode fall do not capture the neutral energy distribution over the range of discharge voltage studied.

FTP1 21 Xenon ion Laser-Induced Fluorescence using a tunable diode laser near 680nm* GREG SEVERN, *Dept. of Physics, University of San Diego* DONGSOO LEE, NOAH HERSHKOWITZ, *University of Wisconsin-Madison* UW-USDCOLLABORATION, Xe ion laser-induced fluorescence (LIF) measurements in low temperature Xe II plasmas ($T_e \sim 1$ eV, $T_i \sim 1/40$ eV, $n_i \sim 10^9$ cm⁻³) have been achieved. The transition studied involves the metastable state (³P₁)5d[3]_{7/2}, at 108423.07 cm⁻¹. The excited states that compose this LIF scheme, which

involve excitation at 680.574nm (air) and fluorescence at 492.15nm (air), have been misidentified in the past. This is due in part to the realization that the energy level structure of Xe II is somewhat better described by jk coupling than by LS coupling. LIF measurements of a room temperature iodine gas cell were used to monitor the wavelength of the laser during the measurements, and these are compared with the molecular iodine absorption spectrum measurements of Gerstenkorn & Luc and of Salami and Ross. These studies have permitted measurements of the ion velocity distribution functions for both ions in a two ion species, Ar+Xe plasma, something never before accomplished, so as to make possible the first experimental test of the Generalized Bohm Criterion.

*Work supported by DOE grant DE-FG02-03ER54728, and NSF grant CHE0321326.

FTP1 22 NEGATIVE ION PLASMAS

FTP1 23 Sheath and presheath in ion-ion plasmas via particle-in-cell simulation ALBERT MEIGE, *LPTP, Ecole Polytechnique* GARY LERAY, JEAN-LUC RAIMBAULT, PASCAL CHABERT, A full particle-in-cell simulation is developed to investigate electron-free plasmas constituted of positive and negative ions under the influence of a DC bias voltage. It is shown that high-voltage sheaths following the classical Child-law sheaths form within a few μs after the DC voltage is applied. Although a characteristic screening length can be defined in the vicinity of the electrodes, the bulk plasma does not appear to be in Boltzmann equilibrium and a Debye length would be more difficult to define. It is also shown that there exists the equivalent of a Bohm criterion with the corresponding presheath accelerating ions collected at one of the electrodes to the sound speed before entering the sheath.

FTP1 24 Production of negative ions at graphite surface in hydrogen plasmas GILLES CARTRY, LOIC SCHIESKO, JEAN-MARC LAYET, MARCEL CARRERE, *CNRS-Universite de Provence* Production of hydrogen negative ions is of great interest for controlled fusion. Indeed neutralized beams of negative ions are used to heat plasma in fusion reactors. Up to now, negative ion sources use cesium surfaces but an important research effort is undertaken to go towards cesium free sources. Dissociative attachment on vibrationally excited hydrogen molecules is known to be the main H^- formation mechanism. Graphite surfaces are expected to give an important vibrational excitation through H recombination. Therefore graphite is a good candidate for next

generation negative ion sources. In this work we show that under positive ion bombardment, a huge number of negative ions are produced on graphite surface. Our goal is to understand this unexpected negative ion production mechanism. In this aim, we put a graphite sample (HOPG) in a helicon reactor, in front of a EQP300 mass spectrometer. The sample is negatively biased with respect to plasma and negative ions energy distribution functions are recorded and analysed versus sample bias, plasma power and pressure, percentage of hydrogen in H_2 -Ar mixtures.

FTP1 25 Numerical investigation on capacitively coupled chlorine discharge. TAESANG LEE, CHOONGSEOCK CHANG, *Korea Advanced Institute of Science and Technology* PIC methods using Monte Carlo collision have been extensively used for the study of chlorine plasma. In our study we introduce a self-consistent particle model for capacitively coupled chlorine discharge which considers motions and collisions of neutral species as well as of charged particles. Chlorine discharge is highly electro-negative which requires long discharge time for steady state where the negative ion population dominates over that of electrons. Multi-scale simulation technique is developed to simulate both plasma steady state and steady state of plasma to neutral gas dynamics. Precise structure of multi-scale simulation method and preliminary results will be shown.

FTP1 26 Investigations of negative oxygen ions in pulsed rf plasmas* MICHAEL KATSCH, ALEXANDER WAGNER, *University of Duisburg-Essen* MICHAEL KRÄMER, *Ruhr-University, Bochum* The spatial and temporal distributions of electrons and ions in ICP GEC reference cell and a large diffusion chamber connected to a helicon plasma source were investigated. The investigations were focussed on the production and loss processes of negative oxygen ions in argon-oxygen mixtures. Laser-induced photodetachment of the negative oxygen ions using of a frequency-doubled Nd:Yag laser along with a Langmuir probe was applied to detect the O^- ions. An increase of the negative ion density in the early afterglow is found at high plasma densities in the GEC cell as well in the diffusion chamber. There is, apparently, a formation channel for negative ions that becomes efficient with reduced electron temperature. Dissociative attachment of electrons to highly excited metastable oxygen molecules are suggested as a negative oxygen ion source. Comparative measurements of the temporal behavior of the negative ions in Ar/O₂, Kr/O₂ and Ne/O₂ mixtures indicate that metastable noble gas atoms do not play an essential role in the formation process of negative ions during the afterglow. A simple global model supports the experimental results.

*This work was supported by the Deutsche Forschungsgemeinschaft through the Sonderforschungsbereich SFB 591 (Project A7).

FTP1 27 Negative Ions and Neutral Beams in Plasma Etching VLADIMIR SAMARA, NICHOLAS BRAITHWAITE, MARK BOWDEN, *Open University* A major problem in etching processes for future nanoscale devices is charge build-up due to the electron shading phenomenon. One possible solution of this problem is to use beams of energetic neutral atoms instead of positive ions in etching. The neutral beam can be produced by generating negative ions which are accelerated toward a substrate and then neutralized¹. This paper presents research aimed at diagnosing and understanding electronegative plasmas. Techniques for measuring negative ion density by laser photodetachment and electrical probes are presented together with preliminary results in SF₆ pulsed rf plasmas. The results will be compared with those from a global model². ¹ S. Samukawa, *Jpn. J. Appl. Phys.* **45**, 2395 (2006). ² Y. T. Lee, M. A. Lieberman, A. J. Lichtenberg, F. Bose, H. Baltes, and R. Patrick, *J. Vac. Sci. & Tech. A* **15**, 113 (1997).

FTP1 28 PLASMA INSTABILITIES

FTP1 29 Influence of the cross field drift on stability of plasma systems: electrostatic and electromagnetic study DRAGANA PETROVIC, ANNEMIE BOGAERTS, *Research group PLASMA-MANT, Dep. of Chemistry, University of Antwerp, Belgium* A general dispersion relation is derived for the coupled electron drift-driven and kinetic Alfvén modes in a strongly collisional, weakly ionized plasma that includes the effects of cross field drift, parallel dynamics and ionisation. It is shown that the kinetic Alfvén mode is totally damped without cross-field electron drift. A finite electron drift decreases the influence of the collisions and results in a weaker damping of the mode, enabling its appearance in the system. However, the kinetic Alfvén mode is still damped and cannot become unstable due to this electron drift. The instability of the system thus originates only from the electron-drift driven mode which is destabilized when the cross-field drift exceeds some critical threshold value. It is shown that the ionisation of neutrals, as the dominant plasma production process, destabilize the plasma system, while the electron parallel dynamics has the opposite effect. The model and equations derived in the study are valid for any partially ionised plasma comprising a substantial amount of neutral atoms.

FTP1 30 DISTRIBUTION FUNCTIONS AND TRANSPORT COEFFICIENTS: ELECTRONS, IONS

FTP1 31 Non-monotonous excitation profiles in positive column of DC nitrogen discharge due to the electron distribution non-locality EUGENE BOGDANOV, ANATOLY KUDRYAVTSEV, SEMEN POPUGAEV, *St. Petersburg State University* LEV TSENDIN, *St. Petersburg State Polytechnic University* Because of the presence of very different energy scales caused by elastic collisions, excitation of vibrational and electronic states, the nonlocal character of the electron distribution function (EDF) manifests itself in various ways in its different parts. As different parts of EDF have different electron energy relaxation lengths, surprising phenomena were revealed in [L. D. Tsendin, E. A. Bogdanov, A. A. Kudryavtsev. *Phys. Rev. Lett.*,

v.94, 015001, 2005] for DC positive column (PC) plasmas in atomic gases: the peaks of the profiles of the excitation rates shift from the discharge axis toward the periphery as the pressure increases. In this report we present the results of kinetic simulations of PC in molecular nitrogen in different pressures and analyze radial distributions of plasma parameters for different conditions. We have found that non-monotonic distributions exist not only for electronic states, but also for vibrational levels. The work was supported by the RFBR grant N.06-02-17317.

FTP1 32 Effect of H₂ and N₂ Impurities in Argon on the Kinetics of Electrons NUNO PINHAO, *Nuclear and Technological Institute, Physics Dept., Sacavem, Portugal* MARIO PINHEIRO, *Lisbon Technical University, Physics Dept., Lisbon, Portugal* ZOLTAN DONKO, *Research Institute for Solid State Physics and Optics, Budapest, Hungary* The presence of small amounts of gas impurities in argon glow discharges used for optical emission spectrometry (GDOES) has strong implications on the accurate calibration of GDOES. To circumvent these difficulties, the intentional admixture of controlled amounts of H₂ or N₂ to argon has been practiced [1]. The understanding of the electron kinetics in these mixtures is valuable for the characterization and calibration of the cell. In this work the electron velocity distribution function, rate coefficients and transport parameters are computed in Ar + xH₂ and Ar + xN₂ mixtures, with 0% ≤ x ≤ 10%, for pulsed Townsend discharge conditions. Different computational techniques are used: a classical two-term expansion, a modified finite elements method applied to the density gradients representation, and a Monte Carlo simulation at the same discharge conditions. Two different set of cross sections for H₂ are used [2,3], allowing a comparison between them. [1] Hodóroaba *et al.* *J. Anal. At. Spectrom.* **18**, 521 (2003) [2] [<http://jilawww.colorado.edu/~avp>] [3] Loureiro *et al.* *J. Phys. D: Appl. Phys.* **22** 1680 (1989)

FTP1 33 HEAVY PARTICLE INTERACTIONS: ION-ATOM, ION-MOLECULE, NEUTRAL-NEUTRAL, OTHER

FTP1 34 Double Ionization of Helium by Fast Proton Impact* MATTHEW FOSTER, JAMES COLGAN, *Los Alamos National Laboratory, Theoretical Division* MITCH PINDZOLA, *Auburn University* We present total cross sections for single and double ionization of helium by various charged ion impact. A non-perturbative time-dependent close-coupling method (TDCC) has been developed to treat the correlated dynamics of ionized electrons by bare-ion impact. The two-electron helium wavefunction is subject to a time-dependent projectile interaction. The projectile-atom interaction is constructed as a multipole expansion that includes monopole, dipole, quadrupole, and octopole terms. For proton, antiproton, and alpha particle impact, good agreement is obtained between our calculations and experimental measurements of total single and double ionization cross sections. We will also report on our progress in using the TDCC method to extract differential cross sections for double ionization by fast protons.

*This work is support by the US Department of Energy through Los Alamos National Laboratory.

FTP1 35 DISSOCIATION, RECOMBINATION, AND ATTACHMENT

FTP1 36 A pulsed nitrogen discharge: A global (volume averaged) model study E.G. THORSTEINSSON, J.T. GUDMUNDSSON, *Science Institute, University of Iceland* A time dependent global (volume averaged) model is applied to study a pulsed low pressure (1 - 100 mTorr) high density nitrogen discharge. The electron density, electron temperature and the density of ions and neutral species is evaluated for various discharge pressures, pulse frequencies and duty cycles. In particular the dissociation of the nitrogen molecule and the role of metastable nitrogen molecules $N_2(A)$ and metastable nitrogen atoms $N(^2D)$ and $N(^2P)$ is explored. The density of the metastable nitrogen atoms $N(^2D)$ and $N(^2P)$ is found to be significant. Furthermore, we explore how the neutral/ion flux ratio Γ_N/Γ_+ varies with duty cycle and pulse frequency.

FTP1 37 COMPUTATIONAL METHODS FOR PLASMAS

FTP1 38 2D Electromagnetic and hydrodynamic models of a microwave plasma torch R. ALVAREZ, *CFP, IST, Lisboa* L. MARQUES, *DF, UM, Braga* L.L. ALVES, *CFP, IST, Lisboa* This work reports simulation results for a microwave (2.45 GHz) plasma reactor, operated by an axial injection torch (TIA). The study is based on a two-dimensional electromagnetic (EM) and hydrodynamic description of the TIA-reactor system. The EM model [1] solves Maxwell's equations, yielding the distribution of the EM fields and the averaged power absorbed, for a given spatial profile of the plasma density (with maximum values in the range $10^{14} - 10^{15} \text{ cm}^{-3}$, according to experimental measurements). Perfect-conductor boundary conditions are satisfied at the reactor walls, and absorbing boundary conditions are used at the open-end of the coaxial waveguide powering the system. The hydrodynamic model solves the Navier-Stokes equations for the flowing neutral gas, yielding the distribution of mass density, pressure and velocities. The input surface (about 1% of the output surface) has a radius of 0,5mm. The boundary conditions impose the input gas flow ($\sim 1000 \text{ sccm}$), the output gas pressure (atmospheric pressure) and no-slip conditions at reactor walls. Simulations are used to provide general guidelines for device optimisation. [1] R. Alvarez, L.L. Alves, *J. Appl. Phys.* 101, 103303 (2007).

FTP1 39 H_α emission in pure hydrogen Townsend discharge obtained by a Monte Carlo simulation VLADIMIR STOJANOVIC, ZELJKA NIKITOVIC, ZORAN PETROVIC, *Institute of Physics* We calculated H_α emission profiles from Townsend discharges in pure hydrogen between two parallel electrodes focusing on details of heavy particle interaction with the cathode surface. The basic data were provided by A. Phelps [1]. Monte Carlo simulation technique employing null collision method was used to follow electrons and heavy particles between collisions with H_2 or with surface for the conditions of a high electric field (E) to gas density (N) ratios E/N . Trajectories of reaction fragments are followed after the collision until their neutralization or thermalization down to the threshold of H_α excitation. For the conditions of Phelps and Petrović's experiment [2], we obtained spatially resolved emission profiles and Doppler broadened line profiles. Intensity of Doppler profile wing showing H_α emission of particles emerging from the cathode direction is obtained assuming that the reflection coefficient of fast H atoms depends on the incident angle and on energy of the incident particle. Some effects of collision dynamic of heavy particles with H_2 on Doppler broadened profile are discussed. [1] A.V. Phelps to be published. [2] Z.Lj. Petrović and A.V. Phelps to be published.

FTP1 40 Computational Methods in Plasma Nanoscience EUGENE TAM, AMANDA RIDER, IGOR LEVCHENKO, KOSTYA (KEN) OSTRIKOV, *Plasma Nanoscience, The University of Sydney* Ion-assisted techniques have been shown in the past to be superior in processing dense arrays of vertically aligned nanostructures to their neutral specie counterparts [1,2]. However, predicting the final outcomes is difficult and requires precise knowledge of the plasma and substrate parameters required. Here, the dynamics of ion-assisted deposition of various ion species onto two-dimensional nanostructure arrays are simulated using a variety of numerical tools including multi-scale hybrid numerical simulations. We have found that important factors in post-processing nanostructures include the plasma sheath width, the aspect ratio of the pre-patterned structures and the density of the array. We also show how increasing the level of complexity of the model, for example, including the effects of multiple species which may exhibit different behaviors, affects the simulation results. The results of this work are generic and can be applied to a broader range of nanostructures and materials. Computational investigations such as these are directly relevant and crucial to the development of deterministic strategies towards precise and cost-efficient plasma-aided nanofabrication. [1] K. Ostrikov, *Rev. Mod. Phys.* 77, 489 (2005) [2] E. Tam et al, *Phys. Plasmas*. 14, 033503 (2007)

FTP1 41 PLASMAKIN: A chemical kinetics library for plasma physics modeling NUNO PINHAO, *Nuclear and Technological Institute, Phys. Dept. Estrada Nacional 10, 2685 Sacavém, Portugal* PLASMAKIN is a package to handle physical and chemical data used in plasma physics modeling and to compute kinetics data from the reactions taking place in the gas or at the surfaces: particle production and loss rates, photon spectra and energy exchange rates. It has no limits on the number of species and reactions that can be handled, is independent of problem dimensions and can be used in both steady-state and time-dependent problems. A broad range of species properties and reaction types are supported: gas or electron temperature dependent rate coefficients, vibrational and cascade levels, branching ratios, superelastic and other reverse processes, three-body collisions, radiation

imprisonment and photoelectric emission. Non-standard rate coefficient functions can be handled by a user-supplied shared library. Reaction data is supplied in text files and is independent of the user's program. Recent additions include the simulation of emission spectra taking line broadening into account; reactions with excited ionic species; 3-body reactions with species with different efficiencies as 3rd body; a species properties database and a Python interface for rapid scripting and debugging.

FTP1 42 CAPACITIVELY COUPLED PLASMAS

FTP1 43 Modes of low-pressure longitudinal combined discharge VALERIY LISOVSKIY, NADIYA KHARCHENKO, VLADIMIR YEGORENKOV, *Kharkov National University, 4 Svobody sq., Kharkov, 61077, Ukraine* RF SYSTEM GROUP TEAM, We studied in experiment the longitudinal combined (RF/DC) discharges. We applied across the electrodes the RF voltage and additionally DC voltage U_{dc} simultaneously. Experiments were performed at the nitrogen pressure of $p=0.01-5$ Torr within the range of amplitude values of the RF voltage $U_{rf} < 2000$ V, DC voltage $U_{dc} < 600$ V and $f=13.56$ MHz. The combined RF/DC discharges might exist in three modes. At low RF voltages the additional DC voltage makes a small contribution to the ionization rate of gas molecules within the plasma volume, and we observe the first mode of the combined RF/DC discharge – “non self-sustained RF discharge perturbed by the DC voltage.” When the RF voltage and the DC voltage are sufficiently large to induce the breakdown of the “cathode” layer, the discharge experiences the transition to the second mode – “combined discharge.” Just this mode is of considerable interest for plasma technology. The third mode may be obtained applying a small RF voltage to the burning DC discharge. We will call it conditionally “non self-sustained DC discharge perturbed by the RF voltage.”

FTP1 44 A global model of a dual frequency capacitive discharge considering the nonlinearity of the sheath and a bulk-chemistry PHILIPP MERTMANN, THOMAS MUSSEN-BROCK, RALF PETER BRINKMANN, PETER AWAKOWICZ, *Ruhr-University-Bochum* INSTITUTE FOR PLASMA TECHNOLOGY TEAM, INSTITUTE FOR THEORETICAL ELECTRICAL ENGINEERING TEAM, A global model of a capacitive coupled low pressure plasma which considers the nonlinear behavior of a boundary sheath and a bulk chemistry, excited by two frequencies is developed. On the basis of certain assumptions the global model for the plasma bulk is derived. The bulk model, which can be solved for its own, is combined with a sheath model to get a self-consistent global model. By that, not the bulk power but the radio frequency voltages over the whole discharge are input parameters of the model, which is close to the experiment. Results for different voltages of the two frequencies and a variation of the pressure are presented.

FTP1 45 Effect of the driving frequency on a VHF capacitively coupled plasma HIROYUKI TAKAHASHI, TAKASHI YAGISAWA, TOSHIKI MAKABE, *Keio University* KEIO UNIVERSITY TEAM, In the next-generation ULSI process, a capacitively coupled VHF (UHF) plasma will be employed in order to obtain higher plasma density with large size of electrodes ($\sim m$).

Then the system will be subject to the strong electromagnetic effect, such as a standing wave and a skin effect. The effect of the standing wave causes nonuniformity along the radial direction to the capacitively coupled plasma (CCP), when the size of the electrode is comparable to the wavelength of the VHF(UHF) voltage source on the electrode. In the present study, nonuniformity of the potential distribution is numerically investigated on a large electrode in the VHF-CCP in Ar in the cylindrical coordinate system (r, z) by using the combination between the transmission line model (TLM) and the relaxation continuum (RCT) model. The influence of potential nonuniformity on the plasma structure will be discussed in detail.

FTP1 46 Analytical Model for Self-Excited Plasma Series Resonances. UWE CZARNETZKI, JULIAN SCHULZE, BRIAN HEIL, DIRK LUGGENHOELSCHER, *Institute for Plasma and Atomic Physics, Ruhr-University Bochum, Germany* Self-excited plasma series resonances are observed in CCP discharges as high frequency oscillations superimposed on the normal RF current. This high-frequency contribution is generated by the interaction between the capacitive sheath and the inductive (due to inertia) and ohmic bulk. The non-linearity of the sheath is essential for the whole effect. In a previous work we have described the effect in the frame of a simple one-dimensional model [1]. It could be shown that at low pressures common in etching applications, PSR can play an important role for both, the actual current waveform and the power transferred to electrons. Here the model is extended to include electron temperature and electrode area ratio effects. Both effects can lead to a reduction of the high-frequency amplitude but have no effect on the frequency itself that is within reasonable limits approximately given by $\omega_{PSR} \approx 2/3 (s/L)^{1/2} \omega_{pe}$, where s is the maximum sheath extension, L the characteristic length of the plasma bulk and ω_{pe} the electron plasma frequency. The derived analytical approximations agree well with numerical solutions of the model. First comparisons with experiment and a fluid-dynamic simulation including an extensive sheath model also show excellent agreement. [1] U. Czarnetzki, T. Mussenbrock, and R.P. Brinkmann, *Phys. Plasmas* 13, 123503 (2006)

FTP1 47 Comparison between measured and simulated breakdown characteristics in micro discharges in argon ZORAN PETROVIC, MARIJA RADMILOVIC-RADJENOVIC, *Institute of Physics* PAUL MAGUIRE, CHARLES MAHONY, *Nanotechnology Research Institute, University of Ulster, Newtownabbey* NIKOLA SKORO, DRAGANA MARIC, *Institute of Physics* Devices with micron and sub-micron gaps can face a serious challenge due to electrical breakdown during manufacturing, handling and operation. Therefore, it is necessary to be aware of the breakdown voltage for different gaps. Gas breakdown and Volt-Ampere characteristics are studied in an atmospheric pressure argon discharges. Experimental results are compared with the results obtained by using PIC/MCC code in order to establish whether the standard micro discharges operate in Townsend regime or in Glow Regime. The code is adjusted to include field emission effect in microgaps. It is applied mainly for the breakdown stage but may also follow the formation of the space charge. The measurements of Volt-Ampere and breakdown characteristics of micro discharges were performed down to $20 \mu m$ gaps at pressures up to 400 Torr. Paschen curves reveal that very tight geometry is required to avoid long path breakdown at the left hand side of the Paschen curve. It is critical to measure width of the discharge to test the scaling and regime of operation of micro discharges.

FTP1 48 Harmonics excitation in capacitive rf discharges: A spatially resolved nonlinear model* DENNIS ZIEGLER, MARTIN LAPKE, THOMAS MUSSENBROCK, RALF PETER BRINKMANN, *Ruhr University Bochum* The excitation of harmonics in capacitively coupled plasmas is a phenomenon that arises from an interaction between the linear behavior of the plasma bulk and the nonlinear behavior of the plasma sheath. Recent research has investigated the phenomenon by studying models which couple either a global or a spatially resolved description of the bulk to sheath models where the charge-voltage relation $V = V(Q)$ was approximated as a quadratic form with constant coefficients.^{1,2} In this contribution, we improve the model by replacing that quadratic form with a more realistic charge voltage relation that is calculated on the basis of a self-consistent sheath model.

*The work is supported by Deutsche Forschungsgemeinschaft in the frame of Graduiertenkolleg 1051 "Non equilibrium phenomena in low temperature plasmas."

¹T. Mussenbrock, D. Ziegler, and R.P. Brinkmann, *Phys. Plasmas* **13**, 083501 (2006).

²T. Mussenbrock and R.P. Brinkmann, *Plasma Sources Sci. Technol.* **16**, 377 (2007).

FTP1 49 Nonlinear electron resonance heating vs. the Herlofson paradox* JENS OBERRATH, MARTIN LAPKE, DENNIS ZIEGLER, THOMAS MUSSENBROCK, RALF PETER BRINKMANN, *Ruhr University Bochum* In the regime of low gas pressure, capacitive rf discharges exhibit resonant behavior which can have a profound impact on the energy budget. This contribution compares two scenarios of resonance-related electron heating known as, respectively, "nonlinear electron resonance heating" (NERH) and "the Herlofson paradox." NERH arises from the self-excitation of the plasma series resonance by harmonics generated via the nonlinearity of the plasma sheath.¹ The Herlofson paradox, on the other hand, is a linear phenomenon that occurs at points where the electron plasma frequency is locally equal to the rf frequency.^{2,3,4} This contribution intended to point out similarities and differences of the two scenarios.¹ T. Mussenbrock and R.P. Brinkmann, *Appl. Phys. Lett.* **88**, 151503 (2006),² F.W. Crawford and K.J. Harker, *J. Plasma Phys.* **8**, 261 (1972),³ V.P.T. Ku, B.M. Annaratone, and J.E. Allen, *J. Appl. Phys.* **84**, 6536 (1998),⁴ V.P.T. Ku, B.M. Annaratone, and J.E. Allen, *J. Appl. Phys.* **84**, 6546 (1998),⁵ F.W. Crawford and K.J. Harker, *J. Plasma Phys.* **8**, 261 (1972).

*The work is supported by Deutsche Forschungsgemeinschaft in the Frame of Graduiertenkolleg 1051 "Non equilibrium phenomena in low temperature plasmas."

FTP1 50 The nonlinear characteristic of the plasma boundary sheath: Results from a self-consistent model* MUSTAFA BAYRAK, DENNIS ZIEGLER, THOMAS MUSSENBROCK, RALF PETER BRINKMANN, *Ruhr University Bochum* The phase-resolved voltage drop across an rf modulated plasma boundary sheath is calculated on the basis of a self-consistent fluid model. The situation is described in terms of a nonlinear charge voltage relation $V(t) = V(Q(t))$, where $Q(t)$ is the instantaneous charge of the sheath. It is found that the form of the curve $V(Q)$

is approximately quadratic. The coefficients of that form, however, are not constant but strongly dependent on the amplitude of the modulation itself. An effective model is constructed which captures this behavior in terms of simple algebraic formulas, and which may be used for a consistent analysis of the nonlinear behavior of capacitively coupled plasmas as a whole.

*The work is supported by Deutsche Forschungsgemeinschaft in the Frame of Graduiertenkolleg 1051 "Non equilibrium phenomena in low temperature plasmas."

FTP1 51 Plasma ionisation in the low pressure operating regime of capacitively coupled radio-frequency plasmas D. O'CONNELL, *Ruhr University Bochum, Germany* A. MEIGE, *Ecole Polytechnique, France* T. GANS, *Queen's University Belfast, Northern Ireland* E. SEMMLER, P. AWAKOWICZ, *Ruhr University Bochum, Germany* R. BOSWELL, *RSPHysSE, ANU, Australia* Fundamental plasma sustaining mechanisms in the low pressure operation regime of a single frequency capacitively coupled plasma are investigated with radio-frequency (rf) excitation at 2 MHz. Both hydrogen and rare gas discharges are explored. The discharge is operated at relatively low voltages to prevent plasma sustainment through secondary electron emission. Two pronounced ionisation mechanisms are observed; one as the retreating sheath approaches the electrode and a second as the advancing sheath expands towards the plasma bulk. The ionisation during the phase of the retreating sheath dominates in the low pressure operation limit (approx. 1 Pa) of all investigated gases. This mechanism is caused by an electric field accelerating electrons towards the electrode. It is believed that the electric field builds up due to inertia preventing electrons following the rapidly retreating sheath over the relatively large sheath width of a few centimetres correlated to the very low plasma density. In the case of rare gases ionisation during the sheath expansion phase becomes more important with increasing pressure and dominates above 5 Pa. Funding: SFB 591, ProInno II, GRK 1051, EPSRC.

FTP1 52 Computational Study of the Dual Frequency Capacitive Discharge* SELMA CETINER, SETH VEITZER, PETER STOLTZ, *Tech-X Corporation* Capacitively coupled radio frequency discharges have many applications including the plasma processing of microelectronic devices, where sputtering, plasma deposition, etching and other surface treatments are utilized. The primary factors that influence many of these processes are the ion energy and flux impinging the target material. Dual frequency discharges generate much interest due to their ability to control these elements independently. The high frequency voltage controls the ion flux through its influence on the electron energy which determines the plasma generation rate by electron impact ionization while the low frequency component determines the average ion impact energy. An investigation of the discharge using kinetic particle-in-cell simulations generated by VORPAL is presented. VORPAL is a plasma simulation framework developed at the University of Colorado at Boulder and Tech-X corporation. Its capabilities include one, two or three dimensions, a choice of kinetic, fluid or hybrid models and the ability to run in serial or parallel.

*This work supported by the Department of Energy, grant #DE-FG02-03ER83797.

FTP1 53 A hybrid, one-dimensional simulation for studying electron kinetics and electron heating by the RF plasma boundary sheath B.G. HELL, J. SCHULZE, D. LUGGENHÖLSCHER, U. CZARNETZKI, T. MUSSENBRÖCK, R.P. BRINKMANN, *Ruhr-University Bochum* A one-dimensional, hybrid, simulation has been developed for investigating electron kinetics and electron heating due to the capacitive sheath of Radio-Frequency (RF) discharges. The simulation calculates the time dependent electric field due to displacement current in the sheath region and the electric field due to conduction current throughout the entire discharge. It includes a simple bulk model and an equivalent electrical model. These elements are combined into a Monte-Carlo simulation which calculates the time resolved Elec-

tron Distribution Function (EDF). The model shows excellent agreement when compared against electric fields measured using Fluorescence Dip Spectroscopy (FDS), and when phase resolved plasma emissions are compared against emissions calculated using EDFs from the Monte-Carlo simulation. The simulation shows beams of electrons that have been accelerated by the plasma sheath travelling through the discharge. This supports the hypothesis that the stochastic heating of electrons is similar to Fermi heating. However this model calculates realistic electric fields instead of using the common step or hard wall model of the sheath. Supported by the DFG through: SFB591 and GK1051, and Andor Technology.

The model shows excellent agreement when compared against electric fields measured using Fluorescence Dip Spectroscopy (FDS), and when phase resolved plasma emissions are compared against emissions calculated using EDFs from the Monte-Carlo simulation. The simulation shows beams of electrons that have been accelerated by the plasma sheath travelling through the discharge. This supports the hypothesis that the stochastic heating of electrons is similar to Fermi heating. However this model calculates realistic electric fields instead of using the common step or hard wall model of the sheath. Supported by the DFG through: SFB591 and GK1051, and Andor Technology.

The model shows excellent agreement when compared against electric fields measured using Fluorescence Dip Spectroscopy (FDS), and when phase resolved plasma emissions are compared against emissions calculated using EDFs from the Monte-Carlo simulation. The simulation shows beams of electrons that have been accelerated by the plasma sheath travelling through the discharge. This supports the hypothesis that the stochastic heating of electrons is similar to Fermi heating. However this model calculates realistic electric fields instead of using the common step or hard wall model of the sheath. Supported by the DFG through: SFB591 and GK1051, and Andor Technology.

The model shows excellent agreement when compared against electric fields measured using Fluorescence Dip Spectroscopy (FDS), and when phase resolved plasma emissions are compared against emissions calculated using EDFs from the Monte-Carlo simulation. The simulation shows beams of electrons that have been accelerated by the plasma sheath travelling through the discharge. This supports the hypothesis that the stochastic heating of electrons is similar to Fermi heating. However this model calculates realistic electric fields instead of using the common step or hard wall model of the sheath. Supported by the DFG through: SFB591 and GK1051, and Andor Technology.

The model shows excellent agreement when compared against electric fields measured using Fluorescence Dip Spectroscopy (FDS), and when phase resolved plasma emissions are compared against emissions calculated using EDFs from the Monte-Carlo simulation. The simulation shows beams of electrons that have been accelerated by the plasma sheath travelling through the discharge. This supports the hypothesis that the stochastic heating of electrons is similar to Fermi heating. However this model calculates realistic electric fields instead of using the common step or hard wall model of the sheath. Supported by the DFG through: SFB591 and GK1051, and Andor Technology.

SESSION GW1: LIGHTING PLASMAS: GLOWS, ARCS, FLAT PANELS, NOVEL SOURCES, OTHER
Wednesday morning, 3 October 2007
Crystal Ballroom A, Doubletree Crystal City at 8:00
John Curry, NIST, presiding

8:00

GW1 1 Propagator Description of Radiation Transport, Applied to Lighting Discharges CHONLARAT WICHADIT, WILLIAM N.G. HITCHON, *Department of Electrical and Computer Engineering, University of Wisconsin, Madison, WI 53706* JAMES E. LAWLER, *Department of Physics, University of Wisconsin, Madison, WI 53706* GRAEME G. LISTER, *OSRAM SYLVANIA INC.* Radiation transport calculations based on the use of propagators (or Green's functions) to describe photon transport are presented for the Hg I resonance at 254 nm in the Complete Frequency Redistribution (CFR) regime. This Hg I resonance dominates the power balance of fluorescent lamp discharges. Recent studies have suggested that transport modes above the fundamental are important in some lamp discharges. The probabilities of photons traveling from one cell of the simulation to another are found by integrating the fluxes due to a point source over the boundaries of each cell volume. Complete hyperfine and isotopic patterns with a Voigt profile for each component are used in our simulations. The Holstein transmittance function $T(R)$ is determined at low opacity using numerical integration across the line profile, and at high opacity using an analytic approximation. A power series expansion of $T(R)$ is then used in geometrical integrals needed to evaluate propagator matrix elements. A time dependent radiation transport equation is solved in a cylindrical geometry and compared to very detailed Monte Carlo simulations of radiation transport in a fluorescent lamp.

8:15

GW1 2 Determination of gas-phase emitter effect in ac operated ceramic metal halide lamps MICHAEL WESTERMEIER, OLIVER LANGENSCHIEDT, JENS REINELT, JUERGEN MENTEL, PETER AWAKOWICZ, *Ruhr-University Bochum, Institute for Electrical Engineering and Plasma Technology* Dydensities and the corresponding electrode tip temperature have been determined by spatially and temporally resolved spectroscopy at and in front of electrodes operated with an ac-current in metal halide lamps. The lamps, made of transparent YAG arc tubes and containing Hg+NaTIDy iodides, were installed in the Bochum model lamp as an outer sleeve. It allows salt pressure depending measurements of the electrode temperature profiles, yielding a global tip temperature and an electrode loss power, and spectroscopic measurements of absolute line intensities to determine the Dy-densities in front of the electrode. It is found that Dy atoms in the gas phase generate a strong gas-phase emitter effect characterized by a clear reduction of the work function. It reduces the electrode temperature, the input power and influences the type of arc attachment. To distinguish between cathodic and anodic effects, phase resolved measurements of the electrode tip temperature will be presented.

8:30

GW1 3 Investigations of HID Lamp Electrodes under HF Operation JENS REINELT, OLIVER LANGENSCHIEDT, MICHAEL WESTERMEIER, JUERGEN MENTEL, PETER AWAKOWICZ, *Ruhr-University Bochum* Low pressure lamps are operated many years at high frequencies to improve the efficiency of these lamps and drivers. For high pressure discharge lamps this operation mode has not been installed yet. Generally it can be assumed that there are changes in the electrode physics which may lead to an undesired lamp behavior if HID lamps are operated at a high frequency. To gain insights into these fundamental changes the so called Bochum Model Lamp is used. It is an easy system which allows a fundamental research on HID electrode behavior and the near electrode region without the occurrence of acoustic resonances. For the investigation phase resolved photography, pyrometry and spectrometry is used. The presented results describe changes in the electrode temperature and changes in the kind of arc attachment on the electrodes (diffuse and spot mode) depending on frequency. Also measurements of the Electrode-Sheath-Voltage (ESV), depending on frequency, are presented.

8:45

GW1 4 Preventing transient spots on thermionic cathodes* MIKHAIL BENOLOV, PEDRO ALMEIDA, MARIO CUNHA, *Departamento de Fisica, Universidade da Madeira, Largo do Municipio, 9000 Funchal, Portugal* Transitions between diffuse and spot modes of attachment of a high-pressure arc to a thermionic cathode, provoked by a current jump, are studied by means of a numerical and physical experiment. The numerical simulation is based on the model of nonlinear surface heating, which has become during the last decade a universally accepted tool for modeling arc-cathode interaction. Experiments were performed on COST-529 standard lamps, which are HID lamps with quartz walls and a quartz envelope. The lamps had pure tungsten cylindrical electrodes and operated at pressures of about 4 bar. The power supply to the lamps was provided by a voltage driven power amplifier FM 1295 DCU/I 750, which functioned as a current source and was controlled by an arbitrary waveform generator Agilent 33220A or by an analogue function generator Leader LFG-1300S. A good agreement between the numerical modeling and experimental results was found. A possibility of prevention of formation of transient spots is demonstrated both numerically and experimentally.

*Work supported by FCT, POCTI-219 and FEDER through projects POCI/FIS/60526/2004 and CCM.

9:00

GW1 5 Mercury-free alternatives for HID lamps RALF METHLING, STEFFEN FRANKE, HELMUT HESS, HARTMUT SCHNEIDENBACH, HEINZ SCHÖPP, *INP Greifswald, Germany* LOTHAR HITZSCHKE, MARKO KÄNING, BERNHARD SCHALK, *OSRAM GmbH, Munich, Germany* Lighting consumes about 20% of the world-wide electrical energy. The development of energy-efficient environmentally friendly lamps proves to be a major task of sustainability research. Up to now most of the highly efficient plasma lamps depend on the unique properties of mercury, which are the high vapor pressure and the large electron momentum-transfer cross section. The replacement of mercury became a challenge and motivation for the development of new high-intensity discharge lamps (HID lamps) in recent years. We introduce a mercury-free high-pressure discharge lamp in quartz technology and compare it with a corresponding mercury-containing lamp. It will be shown that the favorable prop-

erties of mercury are provided in a large extent by a combination of Xe and AlI_3 . The atomic and molecular radiation caused by the admixture of TII and TmI_3 dominates the spectral radiance. For this mercury-free high-pressure discharge a high luminous efficacy of more than 90 lm/W and a good color rendering index of more than 75 are achieved.

9:15

GW1 6 Modeling of dielectric barrier discharge excimer lamp excited by mono polar voltage pulses HARUAKI AKASHI, *Dept. Appl. Phys., National Defense Academy* AKINORI ODA, *Nagoya Institute of Technology* YOSUKE SAKAI, *Hokkaido University* Filamental discharges in Dielectric Barrier Discharge (DBD) excimer lamp excited by mono polar voltage pulses has been simulated using two dimensional fluid model. And the differences of the filament discharges formations between mono po-

lar case and bipolar case [1] have been examined. Xe gas was used and its pressure is 300Torr. Simulated region is 1cm (gap length) x 3cm (radial length). Periodical boundary conditions are assumed for the radial direction boundaries. The both electrodes are covered with dielectrics and their thickness is 0.2cm. Applied voltage is 5kV trapezoid shape with 50% duty ratio waveform and its repetition rate is 200kpps. First a small amount of electron-ion pair is provided in the middle of the gap for initial condition. Then the voltage starts to apply. In the case of bipolar excitation, the discharge starts from one filament (streamer discharge), and finally, 5 filaments are obtained self-consistently. In the case of mono polar case, as first, similar to bipolar case, the discharge starts from one filament, however, only 3 filaments have been obtained. This result is similar to that of 100kHz bipolar voltage case. [1] H. Akashi et al, IEEE Trans. Plasma Science, Vol.33, No.2 (2005) pp.308-309

SESSION GW2: ELECTRONS AND POSITRONS: TRANSPORT AND ANNIHILATION

Wednesday morning, 3 October 2007; Crystal Ballroom B, Doubletree Crystal City at 8:00

Rainer Johnsen, University of Pittsburgh, presiding

8:00

GW2 1 Current Issues in Electron and Positron Transport Theory.*

ROBERT ROBSON, *Australian National University*

In this paper we review the current status of transport theory for low energy electrons or positrons in gases, in the context of both kinetic theory and fluid modelling. In particular, we focus on the following issues: (i) Multiterm vs two-term representation of the velocity distribution function in solution of Boltzmann's equation; (ii) the effect of non-conservative collisions (attachment, ionization, positron annihilation) on transport properties; (iii) the enduring electron-hydrogen vibrational cross section controversy and possible implications for the Boltzmann equation itself; (iv) closure of the fluid equations and the heat flux *ansatz*; and (v) correct use of swarm transport coefficients in fluid modelling of low temperature plasmas. Both hydrodynamic and non-hydrodynamic examples will be given, with attention focussed on the Franck-Hertz experiment, particularly the "window" of fields in which oscillations of transport properties are produced, and the way in which electric and magnetic fields combine to affect transport properties. In collaboration with co-authors Z. L.J. Petrović, Institute of Physics, Belgrade, and R.D. White, James Cook University.

*Supported in part by the Australian Academy of Science.

8:30

GW2 2 Resonances and Bound States in Positron Annihilation on Molecules.*

C.M. SURKO, *Department of Physics, University of California, San Diego*

Positron annihilation is important in such diverse areas as study of metabolic processes in the human brain and the characterization of materials. Annihilation on molecules has been a subject of keen interest for decades. In particular, annihilation rates can be orders of magnitude greater than those expected for simple collisions. Recent results put our understanding of many aspects of this long-standing problem on a firm footing. We now understand that the annihilation proceeds by vibrational Feshbach resonances (VFR). A prerequisite for the existence of these VFR is that the positron binds to the target. The annihilation energy spectra provide the best measures to date of positron binding energies. Predictions of a new theory of VFR-enhanced annihilation in small molecules (methyl halides) [1] show excellent quantitative agreement with experiment. New data and analyses for larger molecules (e.g., hydrocarbons with more than two carbon atoms) show that annihilation rates depend strongly on the number of vibrational degrees of freedom but, surprisingly, only weakly on positron binding energy. This places important constraints on theories of annihilation in these molecules. Results for second bound (i.e., positronically excited) states and overtone and combination-mode VFR, as well as outstanding questions, will also be discussed. This work is done in collaboration with Jason Young. [1] G. F. Gribakin and C. M. R. Lee, Phys. Rev. Lett. 97, 193201 (2006).

*This work is supported by NSF grant PHY 02-44653.

9:00

GW2 3 Theory of Positron Annihilation on Molecules.GLEB GRIBAKIN, *Queen's University Belfast, UK*

Recently there has been a rapid progress in understanding enhanced positron annihilation on polyatomic molecules. Building on the hypothesis about the role of vibrational Feshbach resonances [1] and their first observations in alkanes [2], positron binding energies have been determined for many molecules [3]. Also, first calculations of resonant annihilation have been performed and showed excellent agreement with the measured annihilation rates in methyl halides [4]. I will review the current theoretical understanding of the two annihilation mechanisms, direct and resonant. While the complete problem of positron-molecule annihilation is very complex, its various aspects can be modeled by relatively simple means. Thus, by using zero-range potentials we can study the scaling of the positron binding energy with the size of the molecule. For small polyatomics with infrared active modes (e.g., methyl halides), a complete calculation of resonant annihilation can be done, in good agreement with experiment. Applying this theory to other molecules highlights the role of overtones and combination vibrations, and ultimately, intramolecular vibrational redistribution. [1] G. F. Gribakin, *Phys. Rev. A* **61**, 022720 (2000). [2] S. J. Gilbert *et al.*, *Phys. Rev. Lett.* **88**, 043201 (2002); L. D. Barnes, S. J. Gilbert, and C. M. Surko, *Phys. Rev. A* **67**, 032706 (2003). [3] L. D. Barnes, J. A. Young, and C. M. Surko, *Phys. Rev. A* **74**, 012706 (2006). [4] G. F. Gribakin and C. M. R. Lee, *Phys. Rev. Lett.* **97**, 193201 (2006).

SESSION HW: GEC FOUNDATION TALK

Wednesday morning, 3 October 2007; Crystal Ballroom, Doubletree Crystal City at 10:00

Peter Venzek, Tokyo Electron, presiding

10:00

HW 1 Why Would Anyone be Interested in Charged Particles Ionizing Atoms and Molecules?*DON MADISON, *University of Missouri-Rolla*

In this talk, a general description of Atomic, Molecular and Optical (AMO) collision physics will be given and the objectives of this type of research will be discussed. The primary purpose of the talk will be to demonstrate how the general objectives of AMO research can be achieved using the technique of charged particle impact ionization of atoms and molecules. Several examples will be given showing how this technique can be used to yield different types of information about atoms/molecules and their environment. It will be demonstrated that, through a proper choice of dynamics, the method can be used to directly measure quantum mechanical wavefunctions, to investigate the details of collision dynamics or to directly examine the consequences of the Pauli principle.

*Work supported by NSF grant PHY-0456528.

SESSION JW: BUSINESS MEETING

Wednesday morning, 3 October 2007

Crystal Ballroom A, Doubletree Crystal City at 11:00

SESSION KW: GENERAL COMMITTEE MEETING

Wednesday noon, 3 October 2007

Crystal Ballroom A, Doubletree Crystal City at 12:00

SESSION LW1: PLASMA APPLICATIONS FOR NANOTECHNOLOGY

Wednesday afternoon, 3 October 2007

Crystal Ballroom A, Doubletree Crystal City at 13:30

Uwe Czarnetzki, Ruhr-University Bochum, presiding

Contributed Papers

13:30

LW1 1 Nanoscale particles in reactive RF plasmas: size-dependent dynamics and influence on plasma I.V. SCHWEIGERT, A.L. ALEXANDROV, D.A. ARISKIN, *Institute of Theoretical and Applied Mechanics, 630090 Novosibirsk, Russia* F.M. PEETERS, *University of Antwerpen, B-2020 Antwerpen, Belgium* I.I. STEFANOVIC, E. KOVACEVIC, J. BERND, J. WINTER, *Ruhr-University Bochum, 44780 Bochum, Germany* A CCRF discharge with growing nanoparticles in Ar and C₂H₂ mixture was studied experimentally and with using kinetic PIC-MCC simulations. The dust particle diameter ranged from 0 to 200 nm. It was found that at an initial stage of the growth the nanoparticles are situated near the sheath-plasma boundaries where the ioniza-

tion rate by the electron impact has peaks. The presence of nanoparticles strongly impacts the plasma, and at some critical nanoparticle size the discharge transits from the active sheath regime to the volume dominated mode. Growing further, the dust particles first gradually spread to discharge center and only weakly disturb plasma parameters and then they form the void. The dust particle distribution was measured using Laser Light Scattering technique. In the experiment the nanoparticles are produced and grown by plasma polymerization and we measure their dynamics from early stage until the formation of the void. Calculated and measured properties of discharge, operation modes and nanoparticle distribution agree quantitatively.

13:45

LW1 2 Coagulation in a Nanodusty Plasma* STEVEN GIRSHICK, LAVANYA RAVI, *Dept. of Mechanical Engineering, University of Minnesota* We recently reported [1] a numerical model and simulations for the spatiotemporal evolution of a parallel-plate RF plasma at 100 mTorr, in which nanoparticles were assumed to nucleate in an initial short burst. These simulations predicted that coagulation did not play a significant role, because neutral particles were rapidly either charged by electron attachment or lost by diffusion to the walls. For the remaining negatively charged particles, coagulation was strongly suppressed by the mutual charge repulsion. In the work reported here, we more realistically allow nucleation to continue wherever the local nanoparticle surface area concentration lies below a critical value. In addition, unlike the previous work [1], we account for the enhancement in coagulation caused by the induced dipole in neutral-charged nanoparticle interactions. The new simulations predict that coagulation does indeed play an important role in particle growth. In particular, most coagulation involves very small (approx. 1 nm in diameter) neutral particles that are scavenged by larger charged nanoparticles near the edges of charged particle trapping regions. [1] S. J. Warthesen and S. L. Girshick, *Plasma Chem. Plasma Process.* 27, 292 (2007).

*Partially supported by U.S. Dept. of Energy under grant DE-FG02-00ER54583, and by the Minnesota Supercomputing Institute.

Invited Papers

14:00

LW1 3 Synthesis of Carbon Nanowalls and Challenge for New Functional Devices.MASARU HORI, *Nagoya University*

Carbon nanowalls (CNWs), two-dimensional carbon nanostructures consisting of plane graphene layers, have been synthesized on the substrates without catalyst. The large surface area and thin edges of CNWs may provide us with opportunities for the various applications. In particular, vertically standing CNWs with high surface-to-volume ratio serve as an ideal material for the catalyst support for fuel cells and gas storage. Recently it is reported that one graphene sheet potentially has the high electron mobility and huge sustainable current. Therefore, it is expected that CNWs can be applied for the various kinds of electric devices. Moreover, in the case of application to an efficient emitter for electron field emission, thin edges with moderate spacing and the good uniformity in the height distribution of CNWs are very promising. We have proposed the novel plasma enhanced chemical vapor deposition (PECVD), which is a radical-controlled plasma process using radical injection technique, and demonstrated the fabrication of vertically aligned CNWs using PECVD assisted by H radical injection. By using the radical injection PECVD, we were able to control the CF₃ and H radical density and hereby synthesize the CNWs with a variety of the morphologies and structures. The electric properties of CNWs for advanced nanometer-scaled device were investigated. It was found that the CNWs of n and p-type were successfully formed by radical controlling. In addition, the nano-structure of CNWs indicated the good performance of the electron field emission properties. The surface area with nano-scale high aspect ratio showed the good water repellency, while the surface exposed to O₂ plasma become hydrophilic. These excellent characteristics can be applied for the bio device. On the basis of these results, the potential of CNWs for new functional devices will be introduced.

Contributed Papers

14:30

LW1 4 Growth Process of Carbon Nanowalls Fabricated Using Radical Injection Plasma Enhanced Chemical Vapor Deposition SHINGO KONDO, Nagoya University OLIVERA STEPANOVIC, KOJI YAMAKAWA, MINEO HIRAMATSU, MASARU HORI, Carbon nanowalls (CNWs) consist of two-dimensional graphene sheets standing on the substrate. Due to their unique structures, CNWs have received great attention for various applications. CNWs were fabricated by plasma-enhanced chemical vapor deposition employing C_2F_6 gas with H radical injection. In order to clarify the mechanism of CNWs growth, we have investigated the initial growth process. It was found that a thin film of 10 nm in thickness grew at first 1 minute, and then CNWs grew in the vertical direction from the film. In XPS measurements, C and F were detected in the thin film. The thin film contained neither G-band (1590 cm^{-1}) nor D-band (1350 cm^{-1}) by Raman spectroscopy, on the other hand both bands were clearly detected in CNWs. As a result, the thin film was evaluated to be the amorphous carbon with a little amount of F, and the CNWs were made of graphene sheets. The same results were also obtained by ellipsometry. From these results, it is considered that controlling the structure of thin under layer is very important to synthesize CNWs.

14:45

LW1 5 Fabrication of vertically standing carbon nanowalls by electron beam excited plasma-enhanced CVD MINEO HIRAMATSU, TAKAKERU MORI, Meijo University MASARU HORI, Nagoya University Carbon nanowalls (CNWs), two-dimensional carbon nanostructures, have been grown recently. CNWs are the graphite nanostructure with edges, which comprise the stacks of plane graphene sheets standing almost vertically on the substrate. The large surface area and thin edges of vertically standing CNWs are useful as templates for the fabrication of other types of nanostructured materials as well as an electron field emitter, which have potential applications in energy storage, as electrodes for fuel cells, sensors, and field emission display. In this work, an electron beam excited plasma (EBEP)-enhanced CVD was applied to the synthesis of CNWs. The EBEP is a high-density and low-temperature plasma directly produced by a high-current and low-energy electron beam. Growth experiments were carried out at an electron-beam current of 2A and an electron-acceleration voltage of 60-100 V, a total pressure of 2-4 Pa, and the heater temperature of 550-650°C. Well-defined, vertically standing CNWs were successfully fabricated at growth rate of 32 nm/min by EBEP-CVD employing CH_4/H_2 mixtures. CNWs grown here were very thin, and their thickness was less than 3 nm. The density of CNWs (average distance between adjacent nanowalls) was controllable in the range of 50 to 200 nm by changing the total gas pressure.

15:00

LW1 6 Damage free PECVD based on atmospheric pressure non-thermal plasma and application to high-purity vertically-aligned single-walled carbon nanotube synthesis TOMOHIRO NOZAKI, KUMA OHNISHI, KEN OKAZAKI, Tokyo Institute of Technology We developed atmospheric pressure plasma enhanced chemical vapor deposition for vertically-aligned single-walled carbon nanotubes synthesis, in which both ion-damage and radical-damage are preferentially avoided in atmospheric pressure [1]. In this study, we performed on-line gas analysis using quadrupole mass spectrometer. A metallic capillary tube (O.D. $450\text{ }\mu\text{m}$) was inserted into the cathodic sheath (thickness: $900\text{ }\mu\text{m}$) and reacting gas was extracted for real-time gas analysis. The result revealed the main product was C_2H_6 , but CNTs were missing in the C_2H_6 thermal CVD. Ionic species such as CH_4^+ would have to be abundant reactive species in the plasma sheath. Those species are believed to once absorb on CNT surface and then migrated towards catalyst particles which are anchored on a substrate. We also studied the effect of total pressure. The D/G Raman peak ratios increased as total pressure decreased from 100 kPa to 20 kPa, although ion damage is neglected in this pressure range. Excessive supply of reactive species simultaneously formed amorphous carbon network that ultimately deteriorate CNT quality. [1] T Nozaki et al. *Carbon*, 45, 364-374 (2007)

15:15 Student Excellence Award Finalist

LW1 7 Binary quantum dot arrays: A plasma-based deterministic approach AMANDA RIDER, KOSTYA (KEN) OSTRIKOV, Plasma Nanoscience, The University of Sydney Fabrication of size-uniform, compositionally controlled binary quantum dot (QD) [1] arrays is of great interest to the multidisciplinary research community. The increasing number of QD applications in fields ranging from biology to optoelectronics - each with precise structural requirements, necessitates that a more rigorous approach to fabrication be adopted. Conventional fabrication techniques are unable to cope with the myriad requirements for highly tailored QDs. In this paper, emphasis is placed on plasma-related effects such as substrate heating, surface activation energy and the benefits of low-temperature growth offered by thermally non-equilibrium, low-temperature plasma routes. The competitive edge in using plasmas as versatile nanofabrication tools is examined via a comprehensive analysis of available experimental results and numerical simulation of the deterministic plasma-assisted nanofabrication of compositionally controlled, size-uniform QD arrays. The commercial potential of a plasma-based approach compared to common fabrication techniques such as thermal chemical vapor deposition (CVD) and molecular beam epitaxy (MBE) is explored, as is the application of plasma grown QDs in novel biosensors and third generation solar cells. [1] A. E. Rider et al, *J. Appl. Phys.* 101, 044306 (2007); I. Levchenko, A. E. Rider, K. Ostrikov, *Appl. Phys. Lett.* 90, 193110 (2007).

SESSION LW2: PLASMA PROPULSION

Wednesday afternoon, 3 October 2007; Crystal Ballroom B, Doubletree Crystal City at 13:30
Walter Lempert, Ohio State University, presiding

Invited Papers

13:30

LW2 1 Ion acceleration by beating electrostatic waves: Theory, Experiments and relevance to spacecraft propulsion
EDGAR CHOUERI, *Princeton University*

After a brief overview of electrodeless plasma propulsion concepts, we will focus on a recently discovered ion acceleration mechanism, which appears to occur naturally in Earth's ionosphere, holds promise as an effective means to energize ions for applications in thermonuclear fusion and electrodeless space plasma propulsion. Unlike previously known mechanisms for energizing plasmas with electrostatic (ES) waves, and which accelerate only ions whose initial velocities are above a certain threshold (close to the wave's phase velocity), the new acceleration mechanism, involving pairs of beating ES waves, is non-resonant and can accelerate ions with arbitrarily small initial velocities, thus offering a more effective wave to couple energy to plasmas. We will discuss the fundamentals of the nonlinear dynamics of a single magnetized ion interacting with a pair of beating ES waves and show that there exist necessary and sufficient conditions for the phenomenon to occur. We will see how these fundamental conditions are derived by analyzing the motion's Hamiltonian using a second-order perturbation technique in conjunction with Lie transformations. The analysis shows that when the Hamiltonian lies outside the energy barrier defined by the location of the elliptic and hyperbolic critical points of the motion, the electric field of the beating waves can accelerate ions regularly from low initial velocities, then stochastically, to high energies. We will then illustrate real plasma effects using Monte Carlo numerical simulation and discuss the recent results from a dedicated experiment in my lab in which laser-induced fluorescence (LIF) measurements of ion energies have provided the first laboratory observation of this acceleration mechanism. The talk will conclude with a few ideas on how the fundamental insight can be applied to develop novel plasma propulsion concepts.

Contributed Papers

14:00

LW2 2 Passive optical diagnostic of electric propulsion Xe plasmas: the role of metastable atoms* RAINER A. DRESSLER, YU-HUI CHIU, *Air Force Research Laboratory, Space Vehicles Directorate, Hanscom AFB, MA 01731* LALITA SHARMA, RAJESH SRIVASTAVA, *Department of Physics, Indian Institute of Technology, Roorkee - 247667, India* GEORGE F. KARABADZHAK, *TSNIIMASH, Korolev, Moscow region, 141070, Russia* Metastable Xe atoms play an important role in the radiation of xenon propelled electric thrusters. Experimental and theoretical cross sections for electron-excitation from the $5p^56sJ=2$ metastable level ($1s_5$ state in Paschen notation) to the lowest six $5p^56p$ ($2p$) levels have recently become available, thereby providing important rate coefficients for the depopulation of the $1s_5$ state. Application of a collisional radiative model to near-infrared spectral intensities observed in the plume of a Hall thruster, however, demonstrates that additional depopulation paths are important. Present calculations show that the electron-induced excitation to $5p^56sJ=1$ ($1s_4$) and other $5p^56s$ levels, for which newly calculated cross sections are presented, can account for the additional de-excitation mechanisms in plasma regions with low electron temperatures.

*L. Sharma and R. Srivastava acknowledge support from AOARD (Grant #064029).

14:15

LW2 3 Experimental studies of a Microdischarge Plasma Thruster in a Tri-Electrode Configuration.* UTSAV KC, JOHN BINGAMAN, PHILIP VARGHESE, LAXMINARAYAN RAJA, *University of Texas at Austin* We present results from investigation of a direct-current microdischarge based miniaturized plasma thruster called Micro Plasma Thruster (MPT). The MPT consists of three molybdenum electrodes separated by inter-layer dielectrics, and uses argon at ~ 1 sccm as propellant. The discharge is generated in the hollow fabricated to run through the MPT. The hollow in the upstream part comprising the first two electrodes is sufficiently small (about $100 \mu\text{m}$ dia.) that a pilot microdischarge can be generated. The hollow from the second to third electrode is larger (about $300 \mu\text{m}$ dia.) to allow for expansion of the gas to lower pressure so that an intense secondary discharge, which is stabilized by the pilot discharge, is created in this region. Thrust is generated by the expulsion of ions and neutral species. The MPT is operated with modest voltage (< 1 kV) and low power (~ 1 W). We demonstrate conditions under which a stable microdischarge can be sustained. The voltage-current characteristics from the MPT provide insights into discharge operations. Optical imaging, and spatially resolved optical emission spectroscopy in the plume region are used to characterize the composition of the plume. We also perform electrical probe measurements in the plume to characterize its ion distribution.

*This work was supported by AFOSR under grant FA9550-06-1-0176.

14:30

LW2 4 Simulation Studies of Direct-Current Microdischarges for Electrostatic Mode Microelectric Propulsion THOMAS DECONINCK, SHANKAR MAHADEVAN, LAXMI-NARAYAN RAJA, *The University of Texas at Austin* We are currently developing an electrostatic plasma thruster device based on a direct-current microdischarges. The design uses a dual-stage tri-electrode microdischarge configuration. The pilot stage ($\sim 100 \mu\text{m}$ dia.) provides sufficient constriction to enable low propellant (argon) flow rates ~ 1 sccm, while keeping the pressures high enough (~ 100 Torr) to sustain a pilot microdischarge. A second stage ($\sim 300 \mu\text{m}$ dia.) downstream of the pilot microdischarge expands the flow to near vacuum conditions. In this work we simulate the tri-electrode microdischarge using a coupled plasma-bulk flow computational model. The plasma model provides a self-consistent, multi-species, multi-temperature description of the microdischarge phenomena while the gas dynamics model provides a description of the high-speed low Reynolds viscous compressible flow. A detailed description of the plasma dynamics in the microdischarge including power deposition, ionization, coupling of the plasma phenomena with high-speed flow, and propulsion system performance will be reported. The computational results will be compared to experimental results based on work being done in our group.

14:45

LW2 5 Experimental study of plasma induced flow actuation by direct current discharge. JICHUL SHIN, NOEL CLEMENS, LAXMINARAYAN RAJA, *The University of Texas at Austin* Plasma induced flow actuation using direct-current discharge is conducted at high pressure. The actuator is made of ceramic dielectric plate on which pin-like electrodes (dia. 1/16 inches) are flush mounted. The experiment is conducted in stagnant air at 1 atm. The velocity field of induced flow is acquired at 10 Hz rep. rate using PIV technique with TiO_2 seeding. Under low current DC discharge conditions (~ 10 's mA), a flow is induced by electrohydrodynamic (EHD) forces in the direction from the anode to the cathode. The induced velocity with a continuous 26 mA DC is about 1 m/s with one pair of electrode being turned on. When the DC is pulsed, the flow actuation is improved for pulse frequencies upto about 1 kHz and diminishes for higher frequencies. Also the average discharge power is reduced with pulsed DC. The decrease of pulse duration also improves the actuation down to 50% duty cycle but lower duty cycles reduces the actuation. For larger area actuation such as in airfoils, a linear array of discharges is required to produce an actuation over a finite span-wise length. With an array of discharges, it is expected to reduce the viscous effect of individual actuator pair and hence to improve the actuation performance. The effect of an array of discharges will be presented at various conditions. The performance will be compared with dielectric-barrier discharge (DBD) actuator.

15:00

LW2 6 Simulation of Direct-Current Air Glow Discharge Phenomena SHANKAR MAHADEVAN, LAXMINARAYAN RAJA, *The University of Texas at Austin* Surface plasma discharges are of increasing interest as actuators for flow control. Non-equilibrium glow discharges are particularly attractive for flow actuation since they have significantly lower power requirements compared to other discharges such as thermal arcs. While volumetric heating and electrostatic forcing can be important for flow actuation, the relative importance of each of these mechanisms needs to be understood. In this work develop a 2D compu-

tational model of air glow discharges in parallel-plate DC discharge under conditions similar to plasma flow actuator applications. The model is validated against experimental data and provides a good starting point for plasma flow actuator studies. All important positive and negative ions, radicals, and electrons are included with a finite-rate air chemistry mechanism. Results of model and comparison with experimental data are presented. Characteristics of the air glow discharge in the abnormal and normal glow discharge regime are represented well by the model. Voltage-current characteristics and charged species density profiles in the discharge are compared directly with experimental results and are shown to be in reasonably good agreement.

15:15

LW2 7 Investigation of asymmetric dielectric barrier discharge plasma actuator, driven by repetitive nanosecond pulses. ALEXANDRE LIKHANSKII, DMITRY OPAITS, MIKHAIL SHNEIDER, *Princeton University* SERGEY MACH-ERET, *Skunk Works Lockheed Martin* RICHARD MILES, *Princeton University* DBD plasma actuators are known to be effective for low speed flow control. A comprehensive physically-based numerical model has been developed for explanation of DBD operation. The modeling showed the advantages of using repetitive nanosecond pulses with bias over the sine voltage. If the sine voltage is applied, it carries two functions – plasma generation and producing the body force on the gas. In the pulse case these processes are separated. The plasma is generated using repetitive nanosecond pulses, and the driving of charge particles, which produces the force on the gas, is between the pulses. In pulse configuration the variation of pulse amplitude, sign and the voltage between pulses can produce different force and heating effects on the flow. The verification of the modeling has been done in the experimental investigation of DBD. A new experimental approach for non-intrusive diagnostic of DBD induced flows in quiescent gas was proposed. The schlieren technique, burst mode of plasma actuator operation, and 2D Navier-Stokes numerical model coupled together allowed restoring the entire 2D induced flow and characteristics of the plasma induced force.

SESSION MWPI: POSTER SESSION II

Wednesday afternoon, 3 October 2007

Crystal Ballroom C, Doubletree Crystal City at 16:00

MWPI 1 OPTICAL EMISSION

MWPI 2 Models of $H\alpha$ Doppler profiles from a hydrogen-filled drift tube at high E/N A.V. PHELPS, *JILA, University of Colorado and NIST* Doppler profiles are calculated for the $H\alpha$ line excited in collisions of fast atoms, ions, molecules, and electrons with H_2 in a low-current, uniform-electric-field drift tube at high E/N, where E is the electric field and N is the gas density. Starting with a multi-beam model of the particle fluxes and energy distributions and assumed angular distributions of particles approaching and reflected by the cathode, we calculate the velocity distributions of excited atoms relative to an observer. Spectral profiles are

compared with measurements parallel to the tube axis, e.g., for $E/N = 10$ kTd ($1 \text{ Td} = 10^{-21} \text{ V m}^2$) at 0.15 Torr and 4 cm electrode separation.¹ Spectrally integrated intensity measurements are normalized to electron excitation data at low E/N . Excitation is principally by fast $\text{H} + \text{H}_2 \rightarrow \text{fast H}(n=3) + \text{H}_2$. The calculated magnitude, high degree of profile asymmetry, large change in emission by reflected atoms with cathode material, and change in integrated intensity with E/N agree well with experiment. Predictions are made for observations perpendicular to the tube axis and for a simplified cathode fall model.

¹Z. Lj. Petrović, B. M. Jelenković and A. V. Phelps, *Phys. Rev. Lett.* **68**, 325 (1992).

MWPI 3 Hydrogen Balmer-Line Broadening in a Water-Vapor Microwave Plasma Source ELENA TATAROVA, FRANCISCO DIAS, BORIS GORDIETS, CARLOS FERREIRA, CENTRO DE FISICA DOS PLASMAS, INSTITUTO SUPERIOR TECNICO, 1049-001 LISBOA, PORTUGAL TEAM, Emission spectroscopy was used for the diagnostic of a large-scale, slot-antenna excited microwave (2.45 GHz) plasma source operating in water vapor at low-pressures (1 mbar). The Doppler temperatures corresponding to the broadening of the H_β line at 486.1 nm are in the range 2,500-3,000 K, and much higher than the rotational temperatures (~ 500 K) determined from the Q-branch (in the wavelength range 600-610 nm) of the Fulcher- α band [$d^2\Pi_u(v=0) \rightarrow a^3\Sigma_g^+(v=0)$]. Kinetic considerations demonstrate that the electron-ion and ion-ion recombination processes, respectively $\text{H}_3\text{O}^+ + e \rightarrow \text{H}_2\text{O} + \text{H}_{hot}^* + \Delta E_1$ and $\text{H}_3\text{O}^+ + \text{OH}^- \rightarrow \text{H}_2\text{O} + \text{H}_2 + \text{O}_{hot}^* + \Delta E_2$ can be the source of "hot" hydrogen and oxygen atoms provided H_3O^+ is the main positive ion in the water plasma. "Hot" atoms were also detected in the far remote plasma zone of the source up to 30 cm away from the slot-antennas. Acknowledgment: This study was funded by FCT/FEDER in the framework of the project "Ecological Plasma Engineering Laboratory" POCI/FIS/61679/2004.

MWPI 4 H_α and H_β Line Broadening in Microplasma Jet at Atmospheric Pressure* JAYR AMORIM,†JORGE SOUZA CORREIA, CARLOS OLIVEIRA, BOGOS SISMANOGLU, MARCELO GOMES, Departamento de Física, Instituto Tecnológico de Aeronáutica, Comando-Geral de Tecnologia Aeroespacial, 12228-900, Sao José dos Campos-Brazil Microplasma jets of argon/hydrogen mixture were generated by radio-frequency waves at 144 MHz with powers ranging from 5W to 50W. Microjets with length of 15.0 mm were created at atmospheric pressure. Electrons and ions present in the plasma may induce broadening of Balmer lines due to Stark effect. This effect is the most important one in the H_β line broadening, although contribution from Resonance and Doppler effects should be taken into account. Through the analysis of H_β line the electron density was measured as a function of power and position in the jet. Broadening of H_α line may be mainly due to Doppler, Resonance and Stark effects. Through a careful analysis the influence of each one was evaluated, as a function of electron density and gas temperature in order to estimate the atomic temperature. Analyzing the fine structure splitting of H_α line, the H atom temperature at nozzle jet exit was around 23000 K in the Ar/H₂ micro plasma at atmospheric pressure.

*Work partially supported by CAPES,CNPq and FAPESP

†Membership Pending

MWPI 5 Dependence of the emission intensities with the flow in pulsed N_2 dc discharges LUCIO ISOLA, BERNARDO J.A. GOMEZ, JORGE N. FEUGEAS, Instituto de Física Rosario (CONICET-UNR), Bv. 27 de Febrero 210 Bis., S2000EZF Rosario, Argentina VASCO GUERRA, Centro de Física dos Plasmas Instituto Superior Tecnico 1049-001 Lisboa Portugal +351-21.841.93.22 This work presents an experimental investigation of the behavior of the emission bands of the first negative and second positive systems of nitrogen in the negative glow of a pulsed dc discharge. The discharge current, applied voltage and gas temperature were measured as well. The experiments were carried out at a fixed cathode temperature equal to 705 °K, the pressure was varied between 2.6 and 3.4 Torr, whereas the gas flow was in the range 30-100 ml/min. At constant pressure, the emission intensities pass through a minimum as the gas flow increases. On the other hand, at fixed gas flow all the emissions decrease as the pressure increases. It is shown that the increase in the flow contributes to a departure from quasi-neutrality conditions in the negative glow. Moreover, a decrease in the ionization degree with pressure is observed, as expected.

MWPI 6 Doppler broadening of atomic-hydrogen lines in DC and capacitively coupled RF plasmas KAMRAN AKHTAR, Blacklight Power Inc. J.E. SCHARER, UW-Madison R.L. MILLS, Blacklight Power Inc. The extraordinary broadening of Balmer lines of hydrogen admixed with Ar or He as opposed to Xe in DC glow and capacitively coupled rf discharges is studied over a wide range of pressure and gas compositions. High-resolution optical emission spectroscopy is performed parallel to (end-on) and perpendicular (side-on) to the electrode axis along with Langmuir probe measurements of plasma density and electron temperature for the RF capacitive discharge case. A broad and symmetric (Gaussian) Balmer emission line corresponding to 20-60 eV hydrogen atom temperatures is observed in Ar/H₂ and He/H₂ plasmas. Energy is transferred selectively to hydrogen atoms whereas the atoms of admixed He and Ar gases remain cold (< 0.5 eV). In the field acceleration model [e.g., Cvetanovic et. al. *J. App. Phys.*, Vol. 97, 033302-1, 2005] there apparently is no preferred species to which energy is coupled and according to the model one should observe enhanced temperatures of hydrogen and helium atoms in He/H₂ discharges where the atomic mass is more comparable (4:1). We also briefly examine the experimental results using the Resonance Transfer Model of hydrogen heating [Mills et. al. *IEEE Trans. Plasma Sci.* 31, 338, 2003] as the source of broadening.

MWPI 7 Doppler broadening of atomic-hydrogen lines in low E-field plasmas R.L. MILLS, KAMRAN AKHTAR, J. HE, M. NANSTEEL, B. DHANDAPANI, Z. CHANG, W. GOOD, Y. LU, Blacklight Power Inc. Substantial broadening of the H_α lines of hydrogen admixed with preionized atoms is observed in filament heated and inductively coupled plasmas where the applied electric field is quite low. These filament heated hydrogen plasmas forms at low temperatures (e.g.) and low field strength ($\sim 1-2$ V/cm) when argon and strontium were present with atomic hydrogen, exhibit H_α line broadening (~ 24 eV). H_α line broadening (20-24 eV) is also observed in inductively coupled plasma where the voltage drop across the plasma sheath is small. Moreover, the selective transfer of energy to H atom and the absence of comparable hot helium atoms (< 0.5 eV) where the atomic mass ratio is 4:1 along with the absence of hot H atoms in Xe/H₂ plasmas are also inconsistent with the field acceleration model [e.g., Cvetanovic et. al. *J. App. Phys.*, 97, 033302-1, 2005]. Plasma diagnos-

tics include high-resolution optical emission spectroscopy, Langmuir probe and millimeter wave interferometric measurements. The model of an energetic chemical reaction of hydrogen [Mills et al. *IEEE Trans. Plasma Sci.* 31, 338, 2003] as the source of broadening can explain the observation that certain plasmas exhibit the selective extraordinary broadening.

MWPI 8 Modeling of Electronegative Discharges DEREK D. MONAHAN, MILES M. TURNER, *Dublin City University* Modeling electronegative discharges has been a persistently contentious topic for several years past. In this paper, we show results from an extensive simulation survey of electronegative discharges, spanning a wide range of collisionality, electronegativity and negative ion destruction mechanism. We further consider how these simulation results are best represented by simple zero-dimensional formulations with the character of global models. Various transport models have been proposed for these conditions. We show that one of the simplest such models is mostly adequate, and indeed that considerations such as the form of the electron energy distribution function, and other factors usually neglected, such as the negative ion temperature, are usually more significant than the details of the transport model.

MWPI 9 Modeling and simulation of electromagnetic effects in capacitive discharges MICHAEL LIEBERMAN, *UC Berkeley* We present a self-consistent two-dimensional axisymmetric model and simulation strategy for predicting radial plasma uniformity in large-area high-frequency capacitive discharges. The model couples Maxwell equations, fluid plasma equations and a sheath model with stochastic heating effects taken into account, solving the equation using the finite element method (FEM). Electromagnetic effects (e.g. standing wave and skin effects) as well as the electrostatic edge effect appear in our simulation, whose results are in agreement with recent experiments. The model highlights differences between the edge effect and the skin effect, both of which can cause strong plasma production near the radial reactor edge. At higher frequencies and high pressures, we observed the 'stop band' where waves are highly damped as they propagate from the discharge edge into the center. The model enables an investigation into the transition from global-to-local power deposition as the pressure varies. The use of a FEM-based simulation allows for treatments of irregular geometries, as well as the addition of equations describing fluid flow, heat and mass transfer, and chemical kinetics, although we do not include these effects here.

MWPI 10 Microwave gas breakdown instabilities in the presence of external magnetic field MOHAMMAD GHORBANALILU, *Physic Department of Azarbaijan University of Tarbiat Moallem, Tabriz, Iran* BABAK SHOKRI, *Physics Dept. and Laser-Plasma Research Inst. of Shahid Beheshti University* The electron distribution function (EDF) formed in the interaction of high-frequency microwave (MW) pulsed fields with a rarefied neutral gas is obtained in the presence of the static magnetic field. It is expected that this system undergoes the various instabilities because of the anisotropic structure of the EDF. Making use of the EDF the dielectric permittivity tensor is derived and the general dispersion relation is found in the adiabatic approximation. Analyzing the dispersion relation in the weakly and strongly magnetized regimes for propagation along and across the magnetic field it is shown that the plasma is unstable in the both regimes.

MWPI 11 Low-pressure breakdown in fluorocarbon gases DRAGANA MARIC, NIKOLA ŠKORO, GORDANA MALOVIĆ, MARIJA RADMILOVIĆ-RADJENOVIC, ZORAN PETROVIC, *Institute of Physics Belgrade, Serbia* Fluorocarbon plasmas are typically considered for applications in plasma etching and therefore systems operating in rf fields are studied. However, one needs a lot of information from the basic dc discharges and gas breakdown in order to understand and test the kinetics of secondary electron production at electrodes and to describe the non-local electron kinetics in the cathode fall. We will present experimental and modelling results of breakdown and low current discharge properties obtained for fluorocarbons CHClF_2 , CF_4 and CF_4 -Ar mixtures, in the range of pressures from 100 mTorr to 1 Torr. Experimental measurements in the pulsed mode of operation were used to obtain the basic experimental data especially the spatio-temporal profiles of emission obtained by using ICCD. Particle in cell (PIC) code which includes proper description of secondary electron yield [1] was used to obtain the theoretical data and properties of low current discharges. In addition, we have used a standard Monte Carlo Code [2] to study the non-hydrodynamic region close to the cathode and also the effective electron multiplication coefficients. [1] Radmilović-Radjenović, J. K. Lee, F. Iza and G. Y. Park, *J. Phys. D*, **38** (2005) 950. [2] G. Malović, A. Strinić, S. Živanov, D. Marić and Z. Lj. Petrović, *Plasma Sources Sci. Technol.* **12** (2003) S1.

MWPI 12 PLASMA APPLICATIONS FOR NANOTECHNOLOGY

MWPI 13 Plasma-grown high-surface-coverage nanoislanded Ni Catalyst Films for Dense Nanotube Arrays AMANDA RIDER, KEVIN CHAN, IGOR LEVCHENKO, KOSTYA (KEN) OSTRIKOV, *Plasma Nanoscience, The University of Sydney* Dense carbon nanotube (CNT) arrays are usually grown on surfaces covered with islanded films of Ni, Co or Fe catalyst particles. Adsorbed atoms diffusing about the substrate surface penetrate through the catalyst and form a CNT on the Ni surface. Thus, parameters of the catalyst particles (density and size, distribution function and spatial location) directly determine the characteristics of the final CNT forest. Processes such as self-assembly and island transformations can't be modeled without calculating the real adatom concentration field (ACF). Dissolution of an island can initiate abrupt rearrangement of the ACF resulting in a significant change in rate of growth of the neighboring islands. Displacement of island may lead to the same effect. Some successful attempts at modeling surface phenomena such as island shape transformation are known. In our work we model dissolution, displacement and coalescence of the islands. Our approach is based on direct calculation of the adatom concentration field on the surface. Our simulation results can be used to control and optimize the density, size and distribution of CNT nucleation sites, a critical but yet unresolved issue of nanofabrication [1]. [1] K. Ostrikov, *IEEE Tran. Plasma Sci.* **35**, 127 (2007)

MWPI 14 Effect of Atomic Hydrogen and Ions on Carbon Nanotube Growth in PECVD KOSTYA (KEN) OSTRIKOV, IGOR DENYSENKO, *Plasma Nanoscience, The University of Sydney* A surface diffusion model for multi-wall carbon nanotube (MWCNT) growth in plasma-enhanced chemical vapor deposition (PECVD) is developed. It is assumed that growth is due to deposition of hydrocarbon (HC) molecules, ions and an etching gas (atomic hydrogen) from plasma. The model accounts for reactions of HC neutrals and carbon atoms with an etching gas, decomposition of absorbed particles due to ion bombardment, decomposition of HC ions on MWCNT surface, thermal decomposition of HC neutrals on MWCNT surface, in addition to the film growth between MWCNTs, etching of the film and carbon sputtering. Using the model, MWCNT growth rates are calculated for different substrate temperatures and HC, hydrogen and ion fluxes on the substrate. It is shown that at low substrate temperature the MWCNT growth is mainly due to reactions of ions with HC neutrals and the decomposition of HC ions on the MWCNT surface. Meanwhile, at large ion and low hydrogen fluxes on the substrate the film growth between MWCNTs can dominate over the MWCNT growth. The model reveals that the growth rate is dependant on substrate temperature which has a maximum (T_{max}) that agrees well with experimental data on MWNT growth. T_{max} increases with an increase of the hydrogen atom flux, the ion and HC fluxes. [1] K. Ostrikov, A. B. Murphy, J. Phys. D: Appl. Phys. 40, 2223 (2007)

MWPI 15 Modeling of plasma-assisted fabrication of polymer-nanotube photovoltaic solar cells IGOR LEVCHENKO, KOSTYA (KEN) OSTRIKOV, AMANDA RIDER, EUGENE TAM, *Plasma Nanoscience, The University of Sydney* Given the increasing interest in renewable energy, photovoltaic devices are of great significance. Intensive research efforts are centred on finding a cost-effective, powerful solar cell. One possible solution is polymer/nanotube (CNT)-based solar cells. These devices possess promising characteristics, yet their method of production is intricate and unreliable. Traditionally, CNTs are produced by arc discharges, this is followed by a number of complex manual manipulations to create a dense, perfectly aligned CNT array in a polymer matrix. Here, we present a numerical simulation of polymer/nanotube photovoltaic cell production. Production of a composite nanotube-based solar cell by a single continuous process involving fabrication of ordered arrays of self-assembled single-walled carbon nanotubes, their treatment, activation, functionalization, in addition to construction of the polymer matrix, all via plasma deposition is an excellent example of the versatility of plasmas as nanofabrication tools [1]. [1] K. Ostrikov, Rev. Mod. Phys. 77, 489 (2005)

MWPI 16 Silicon nanocrystal synthesis in microplasma reactor TOMOHIRO NOZAKI, *Tokyo Institute of Technology* TOMOHISA OGINO, TAKASHI NAKAMUTA, KENJI SASAKI, KEN OKAZAKI, Atmospheric-pressure microplasma reactor was developed for the fabrication of tunable photoluminescent silicon nanocrystals. A mixture of Ar, H₂, and SiCl₄ was activated by capacitively-coupled non-equilibrium plasma generated in a capillary glass with a volume less than 1 μ l. The microplasma efficiently realizes supersaturated silicon vapor that leads to gas phase crystal nucleation via three-body collision, followed by rapid termination of crystal growth due to short-residence-time reactor. The room temperature photoluminescence (PL) of as-synthesized material with H₂ = 0.7% exhibited intense visible light emission

with peak intensity around 670 nm. The TEM analysis of the red-luminescent material revealed crystalline particles with sizes around 3 nm and amorphous silicon oxide shell which surrounds the crystalline core. The PL spectrum was blue-shifted to 520 nm with increasing H₂ content. The green-luminescent materials were readily oxidized upon exposure to air, and the PL capability attributing to silicon nanocrystal was extinguished within a few hours. The PL spectrum was well stabilized by adding a trace amount of CH₄. The surface structure of silicon nanocrystals might be modified by inserting hydrocarbon capping.

MWPI 17 Quasi-2D nanostructures: Growth in low-temperature plasmas EUGENE TAM, IGOR LEVCHENKO, KOSTYA (KEN) OSTRIKOV, AMANDA RIDER, SERGEY VLADIMIROV, *Plasma Nanoscience, The University of Sydney* SHUYAN XU, *NIE and Institute of Advanced Studies, Nanyang Technological University* Quasi-two-dimensional nanostructures, such as nanowalls, are currently the subject of enormous research interest. Gas-based synthesis methods follow either a neutral- or ionized gas (plasma)-based route to fabricate structures of reduced dimensionality [1]. Here, we present a multiscale hybrid numerical simulation which demonstrates the superiority of the plasma route in controlling the morphology of quasi-two-dimensional surface nanopatterns. It was found that the nanowall width uniformity was the best in high-density plasmas, becoming more non-uniform in lower-density plasmas. The neutral gas-based process resulted in the worst nanowall width uniformity. This effect is the result of the focusing of ion fluxes by irregular electric fields in the vicinity of the plasma-grown nanostructures on a biased substrate, and the differences in the 2D-atom diffusion fluxes in the ionized gas and neutral gas-based processes. Our simulation results are in good agreement with available experimental results concerning the effect of plasma process parameters on the sizes and shapes of relevant nanostructures. [1] K. Ostrikov, Rev. Mod. Phys. 77, 489 (2005); K. Ostrikov, A. B. Murphy, J. Phys. D: Appl. Phys. 40, 2223 (2007)

MWPI 18 Generation of surface preparation species in an Ar+H₂ plasma discharge KOSTYA (KEN) OSTRIKOV, *Plasma Nanoscience, The University of Sydney* HYUN-JIN YOON, *PDP Technology Research Center, Pusan National University* AMANDA RIDER, *Plasma Nanoscience, The University of Sydney* Deposition surfaces must be carefully prepared before nanoassembly can take place. Therefore, understanding how the surface preparation species or 'working units' (WUs), responsible for surface activation and passivation are generated in a plasma discharge is an important step towards creating reliable and robust plasma-aided nanofabrication methods [1,2]. Here, a two-dimensional fluid simulation of the number densities of WUs in a low-temperature, low-pressure, non-equilibrium Ar+H₂ plasma is conducted. Parameters such as operating pressure, H₂ partial pressure and power were varied in order to observe the effect on production of the argon ion and atomic hydrogen, species responsible for surface activation and passivation respectively. Delicate balances are required between these parameters in order to ensure high number densities of Ar⁺ and H species, and thus to achieve acceptable rates of surface activation and passivation. This paper contributes to the improvement of the controllability and predictability of plasma-based nanoassembly processes. [1] K. Ostrikov et al, Plasma Process. Polym. 4, 27 (2007) [2] K. Ostrikov, Rev. Mod. Phys. 77, 489 (2005)

MWP1 19 A plasma-based pre-treatment for low temperature bonding of silicon wafers* NICHOLAS BRAITHWAITE, JAN KOWAL, *The Open University, UK* TONY ROGERS, *Applied Microengineering Limited* In the fabrication of micro and nano electromechanical systems (MNEMS), there is a demand for adhesive-free, low-temperature wafer bonding. These constraints arise from the need to avoid issues relating to thermal strain and to unacceptability of high temperature processes late in the manufacturing sequence. It has been known for some time that high strength wafer bonding can be achieved by exposure to oxygen plasmas for a few minutes followed by a 200 deg C, 60 minute anneal step. Low pressure and atmospheric pressure routes have been demonstrated commercially. Our studies show that a more effective pre-treatment involves exposure radicals generated in an oxygen plasma, avoiding deleterious effects of excessive ion bombardment and UV flux. In the present configuration the plasma source is an annular arrangement that surrounds a pair of wafers; plasma excitation uses mesh electrodes, and mains frequency voltage. Neutral species diffuse from the source across the surface of the wafer, where they activate the bonding process; the mechanism is yet to be fully elucidated, but has been shown to work effectively.

*Work supported by the Department Trade and Industry, UK.

MWP1 20 Low-temperature Plasma Enhanced Chemical Vapour Deposition of Nanodevice-grade nc-3C-SiC KOSTYA (KEN) OSTRIKOV, *Plasma Nanoscience, The University of Sydney* QIJIN CHENG, SHUYAN XU, JIDONG LONG, *NIE and Institute of Advanced Studies, Nanyang Technological University* The development of robust fabrication techniques that are capable of achieving a synergy of essential structure-, composition-, function/property-, application-, and process-related requirements in the same material is the ultimate goal of Materials Science [1]. Despite the outstanding chemical, mechanical, optical and thermal properties of bulk SiC, applications of nanocrystalline silicon carbide (nc-SiC)[2] in nanodevices are hampered by a substantial lack of such synergy. Here we report on the plasma-based synthesis of nanodevice-grade nc-3C-SiC films, with very high growth rates (7-9 nm/min) at low and ULSI technology-compatible process temperatures (400-550 °C), featuring: high nanocrystalline fraction (67% at 550 °C); good chemical purity; excellent stoichiometry throughout the entire film; wide optical band gap (3.22-3.71 eV); refractive index close to that of single-crystalline 3C-SiC; and clear, uniform, and defect-free Si-SiC interface. The counter-intuitive low SiC hydrogenation in a H₂-rich plasma process is explained by hydrogen atom desorption-mediated crystallization. [1] K. Ostrikov, *Rev. Mod. Phys.* 77, 489 (2007) [2] Q. J. Cheng, S. Xu, J. D. Long, K. Ostrikov, *Appl. Phys. Lett.* 90, 173112 (2007).

MWP1 21 ELECTRON AND PHOTON COLLISIONS WITH ATOMS AND MOLECULES

MWP1 22 Excitation of the 3p⁵5p levels of Argon from the 3p⁵4s metastable levels* RAJESH SRIVASTAVA, LALITA SHARMA, *Physics Department, Indian Institute of Technology Roorkee, Roorkee 247667, India* ALLAN STAUFFER, *Department of Physics and Astronomy, York University, Toronto, Canada*

M3J 1P3 In the light of recent experimental results of Jung et al [1] we have extended our relativistic distorted wave (RDW) calculations [2] to the electron impact excitation of the ten higher-lying fine-structure levels of the 3p⁵5p configuration of argon from the lowest metastable states (the J = 0, 2 levels of the 3p⁵4s configuration). We compare our theoretical results with their experimental results and discuss the differences from the similar excitation to the 3p⁵4p levels from the same metastable states [2]. [1] R. O. Jung, J. B. Boffard, L. W. Anderson and C. C. Lin, *Phys. Rev. A* 75, 052707 (2007). [2] R. Srivastava, A. D. Stauffer and L. Sharma, *Phys. Rev. A* 74, 012715 (2006).

*Supported by the Natural Sciences and Engineering Research Council of Canada and the Asian Office of Aerospace Research and Development (AOARD), Tokyo, Japan (Grant No. 064029)

MWP1 23 Excitation of atomic oxygen by electron impact* RAJESH SRIVASTAVA, LALITA SHARMA, *Physics Department, Indian Institute of Technology Roorkee, Roorkee 247667, India* ALLAN STAUFFER, *Department of Physics and Astronomy, York University, Toronto, Canada* *M3J 1P3* We have carried out relativistic distorted-wave calculations for the excitation of atomic oxygen from its ground (2p)⁴3P state to the excited (2p)³3s ³S, ³P and ³D states and to the (2p)³3d ³D state in the energy range from 15 to 100 eV. We compare our results for the differential cross sections with both experimental measurements and other theoretical calculations for these transitions and find our calculations agree very well with them. We have also compared our integrated cross sections for the excitation of (2p)³3s ³S for which extensive theoretical and experimental data have been reported.

*Supported by the Natural Sciences and Engineering Research Council of Canada, Ministry of Human Resource Development, Government of India.

MWP1 24 Electron impact excitation cross sections into (3p⁵5p levels from the (3p⁵4s metastable level of Ar by the Kim B-E-f Scaling method.* M.A. ALI, P.M. STONE, *National Institute of Standards and Technology, Gaithersburg, MD* We present results for electron impact excitation cross sections from (3p)⁵4s, 1s₅ and 1s₃ metastable states of Ar to (3p)⁵5p, 3p₁ to 3p₁₀ states, which are dipole allowed by the use of the Kim B-E-f Scaling procedure [1]. We use the experimental excitation energy for E-scaling and accurate f values of Zatsarinny and Bartschart [2] for f-scaling. We compare our results with apparent excitation cross sections recently reported by Jung et al. [3]. Our results suggest that cascade contributions for the upper levels are substantial. To gauge the accuracy of B-E-f scaling, we also present similar results for (3p)⁵4s, 1s₅ and 1s₃ metastable states to (3p)⁵4p, 2p₁ to 2p₁₀, dipole allowed states and compare with the distorted wave results of Srivastava et al. [4]. [1] Y-K. Kim, *Phys. Rev. A* 64 032713 (2001). [2] O. Zatsarinny and K. Bartschart *J. Phys. B: At. Mol. Phys.* 39 2145 (2006). [3] R. O. Jung, J. B. Boffard, L. W. Anderson, and C. C. Lin *Phys. Rev. A* 75 052707 (2007). [4] R. Srivastava, A. D. Stauffer, and L. Sharma *Phys. Rev. A* 74 012715 (2006).

*This work was supported in part by the Office of Fusion Energy Sciences, US DOE.

MWP1 25 Electron impact ionization of metastable states of He, Ne, Ar, Kr and Xe.* M.A. ALI, P.M. STONE, *National Institute of Standards and Technology, Gaithersburg, MD* Electron impact ionization cross sections of rare gases are important quantities needed for modeling of rare gas discharges, lighting and plasma displays. We present ionization cross sections of $(np)^5(n+1)s^3P$ ($J=2$ and 0) metastable states calculated within the Binary-Encounter-Bethe (BEB) model of Kim and Rudd [1]. These are compared with very scant experimental data available for He, Ne, and Ar and other theoretical data using advanced methods, where available. Our results compare favorably with results using sophisticated methods but share similar disagreement with experimental data as do results of advanced method calculations. The BEB ionization cross sections of $J=2$ and 0 states for Ne, Ar, Kr and Xe are virtually identical. [1] Y-K. Kim and M. E. Rudd, *Phys. Rev. A* 50 3954 (1994)

*This work was supported in part by the Office of Fusion Energy Sciences, US DOE

MWP1 26 Studies into electron-water scattering and transport phenomena MICHAEL BRUNGER, *ARC Centre for Antimatter-Matter Studies, Flinders University, Australia* WILLIAM MORGAN, *Kinema Research & Software, Monument, Colorado, USA* PENNY THORN, *ARC Centre for Antimatter-Matter Studies, Flinders University, Australia* We have developed an integral cross section data base for electron scattering from water. This data base is self-consistent with available total cross section measurements, as will be demonstrated at the meeting. In addition we have used this data base in conjunction with Boltzmann and Monte Carlo swarm coefficient calculations, in order to further check its self-consistency against measured transport coefficients. Finally, the present cross sections are employed to calculate the atmospherically important quantities: (1) electron energy transfer rates and (2) electron impact excitation rates. All these data will also be presented at the meeting.

MWP1 27 Low energy elastic scattering and vibrational excitation of THF* VIOLAINE VIZCAINO, JAMES SULLIVAN, STEPHEN BUCKMAN, *Centre for Antimatter-Matter Studies, Australian National University* JASON ROBERTS, MICHAEL BRUNGER, *Centre for Antimatter-Matter Studies, Flinders University* Tetrahydrofuran is a reasonable model for the deoxy-ribose part of the DNA backbone and it has attracted much recent attention in the context of electron-induced radiation damage. In this paper we extend recent measurements of absolute elastic electron scattering cross sections to energies below the shape resonance (6.5 eV) and also provide measurements of vibrational excitation for energies below 10 eV.

*Supported by the Australian Research Council

MWP1 28 Near-threshold electronic excitation of N₂* SUBHENDU MONDAL, TYLER RAESIDE, STAN NEWMAN, JULIAN LOWER, STEPHEN BUCKMAN, *Centre for Antimatter-Matter Studies, Australian National University, Canberra, and Flinders University, Adelaide* Absolute cross sections for the electron impact excitation of low lying electronic states of N₂ are measured using a position sensitive, time-of-flight tech-

nique. This technique employs a pulsed, monochromatic electron beam and a large area channelplate detector and delay-line anode which can detect all scattered electrons, elastic and inelastic, over an angular range of $\sim 20^\circ$. The transmission of the detector is uniform in energy and the absolute cross sections for inelastic processes are obtained directly from the measurement of the elastic to inelastic scattering ratio and the well-known absolute elastic scattering cross sections. The incident energy range of interest is 10-15 eV.

*Supported by the Australian Research Council

MWP1 29 Transport Coefficients and Cross Section Set for Electron Scattering in Mixtures CF₄ and CF₂ ZELJKA NIKITOVIC, VLADIMIR STOJANOVIC, ZORAN PETROVIC, *Institute of Physics* We present transport coefficients for electrons in mixtures of CF₄ with CF₂ for conditions such as those found in plasma assisted technologies for semiconductor production. We used a two term numerical solution of the Boltzmann equation and we tested the accuracy of the results by using a Monte Carlo simulation. Mixtures of radicals with CF₄ were constructed by using the cross sections of Tennyson and coworkers [1]. We selected a wide range of abundances of radicals from 0.01% to 10% in the mixture. For low E/N large deviations from values for total electron attachment for pure CF₄ are obtained for mixtures of CF₄ and its radicals if abundances are sufficiently high. The effect of radicals on electron kinetics is relatively small for abundances below 1%. For higher abundances all transport coefficients, mean energies and rate coefficients are affected to a degree which could affect the operating conditions in plasmas. [1] I. Rozum, P. Limaoviera, S. Eden, and J. Tennyson, N.J. Mason, *J. Phys. Chem. Ref. Data*, Vol. 35, No. 1, (2006) 267.

MWP1 30 Electron-impact ionization rates for BF₃ and its fragments* M. RASKOVIC, S. POPOVIC, L. VUSKOVIC, *Old Dominion University* We have calculated the electron-impact ionization rates of BF₃ and its fragments for electron energy distribution present in sheath mode of the repetitively pulsed d.c. diode system. Data are required for BF₃ discharge modeling. BF₃ and its fragments are reactive species used to interact with niobium surface in order to remove oxides and other impurities from the surface in the form of volatile compounds. This cleaning and smoothing treatment of bulk niobium improves the performance of the superconducting radiofrequency cavities used for particle accelerators. In our calculation electronic structures of BF₃ and its fragments were described with several empirical basis sets. After geometry optimization using density functional method B3LYP, MO parameters were calculated with UHF, CCSD(T) and OVG methods. Electron-impact ionization cross-sections were calculated employing the Binary-Encounter-Bethe approximation and results were compared with available experimental data. Relative calculation errors were estimated, which were especially important for the cross-sections obtained with CEP-31G basis set, necessary to describe system containing niobium samples. These cross-sections are used to calculate rates for electron energy distributions of BF₃ plasmas.

*Supported by DOE.

MWP1 31 Theoretical Differential Cross Sections for Transfer-Excitation in Proton-Helium Collisions* A.L. HARRIS, J.L. PEACHER, D.H. MADISON, *University of Missouri-Rolla* Theoretical differential cross sections will be compared with experimental results for transfer-excitation occurring in proton-helium collisions. In the experiment, the incident proton captures one electron from a helium atom, and the remaining electron is left in an excited bound state of the helium ion. These experiments have been performed in Rolla, MO. The theoretical approach we use is a full four-body approach, taking each particle into account. This results in a nine dimensional integral to evaluate the T-matrix. A fully correlated Hylleraas wavefunction is used for the initial state helium atom, and hydrogenic wavefunctions are used for the projectile hydrogen atom and the residual helium ion in the final state.

*Work supported by NSF grant PHY-0456528.

MWP1 32 Total ionization cross sections for Benzene, Furan and Tetrahydro furan on electron impact* C.G. LIMBACHIYA, P.S. Science College, Kadi, INDIA - 382 715 M. VINODKUMAR, V.P. Science College, V.V. Nagar, INDIA - 388 120 S. GANGOPADHYAY, K.N. JOSHIPURA, *Dept. of Physics, S.P. Uni. V.V. Nagar, INDIA - 388 120* Industrial society has increased human exposure to thousands of chemicals in the environment e.g. Benzene (C_6H_6), Furan (C_4H_4O) and Tetrahydrofuran (C_4H_8O). Of particular concern is the potential hazard of these chemicals to produce cancer. The molecules are thus biologically and industrially important. In this paper we have examined scattering of electrons (from threshold to 5 keV) from these targets and calculated the total ionization cross sections. We used complex optical potential formalism (SCOP) [1, 2] to calculate total inelastic cross section Q_{inel} . We have developed a method, Complex Scattering Potential - ionization contribution (CSP-ic) to extract ionization cross sections Q_{ion} from calculated Q_{inel} . [1] M. Vinodkumar, K.N. Joshipura, C.G. Limbachiya & B.K. Antony, *Eur. J. Phys. D* **37** (2006) 67 [2] M. Vinodkumar, K.N. Joshipura, C.G. Limbachiya & B.K. Antony, *Phys. Rev A* **74** 022721 (2006)

*CGL, MVK thank UGC, KNJ thanks ISRO-India for research grants.

MWP1 33 Electron Impact Excitation of Atmospheric Species* C.P. MALONE, P.V. JOHNSON, J.W. MCCONKEY,† J.M. AJELLO, I. KANIK, *Jet Propulsion Laboratory, Caltech, MS 183-601, 4800 Oak Grove Drive, Pasadena, CA 91109, USA* Electron collisions with neutral molecular targets, such as O_2 , H_2 , and N_2 , have been investigated. Resulting fluorescence was probed using various monochromator-detector combinations. Line and band intensities were investigated as a function of wavelength and incident electron energy. The emission cross sections for these atmospheric species will be presented. In the case of O_2 , previous values in the literature, such as [J.M. Ajello and B. Franklin,

J. Chem. Phys. **82**, 2519 (1985); O. Wilhelmi and K.-H. Scharfner, *Eur. Phys. J. D* **11**, 79 (2000)], demonstrated significant discrepancies and provided a strong impetus for this work. The present results are compared to available cross sections.

*This work was performed at JPL, Caltech, under a contract with NASA with support through the PATM program. This research was performed while CPM and JWMcC held NASA Fellowships at JPL.

†Permanent Address: Department of Physics, University of Windsor, Ontario N9B 3P4, Canada.

MWP1 34 Integral Cross Sections for the Electron Impact Excitation of Molecular Nitrogen* C.P. MALONE, P.V. JOHNSON, I. KANIK, *Jet Propulsion Laboratory, Caltech, MS 183-601, 4800 Oak Grove Drive, Pasadena, CA 91109, USA* S. WANG, M.A. KHAKOO, *Department of Physics, California State University, Fullerton, CA 92834, USA* Integral cross sections (ICSS) for the electron impact excitation of the $X^1\Sigma_g^+$ ($v''=0$) ground level to the $a''^1\Sigma_g^+$, $b^1\Pi_u$, $c^1\Pi_u$, $o^1\Pi_u$, $b'^1\Sigma_u^+$, $c'^1\Sigma_u^+$, $G^3\Pi_u$, and $F^3\Pi_u$ states of N_2 are reported at incident energies of 17.5eV, 20eV, 30eV, 50eV, and 100eV. The ICSS were obtained from integrating recent differential cross sections, which were obtained by unfolding new energy-loss spectra taken at electron scattering angles ranging from 2° to 130° . The analysis of the spectra followed a different algorithm from that employed in a previous study of N_2 for the valence states by Khakoo *et al.* [*Physical Review A* **71**, 062703 (2005)], since the $^1\Pi_u$ and $^1\Sigma_u^+$ states form a strongly-interacting Rydberg-valence series. The present results are compared to existing cross sections.

*This work was carried out at JPL, Caltech, under contract with NASA and at CSUF, with support from the NSF-PHY-RUI and NASA OPR programs. This research was performed while CPM held a NASA Fellowship at JPL.

MWP1 35 Electron impact excitation of xenon* OLEG ZATSARINNY, KLAUS BARTSCHAT, *Drake University* We have used the B -spline R -matrix (close-coupling) method with non-orthogonal sets of orbitals [1] to calculate angle-integrated and angle-differential cross sections, as well as spin-polarization and coherence parameters for electron impact excitation of xenon. A total of 31 physical and two pseudo target states were included in the close-coupling expansion, with the latter chosen to account for the dipole polarizability of the ground state. Relativistic effects were accounted for perturbatively through the most important correction terms in the Breit-Pauli Hamiltonian. In light of the very complex structure of xenon, characterized by strong mixing of states with different principal configurations, the use of term-dependent one-electron orbitals was critical for obtaining an acceptable target description, which could still be used in the subsequent collision calculation. We are also in the process of developing a full-relativistic version of the computer code. The progress and the latest results will be reported at the conference. [1] O. Zatsarinny, *Comp. Phys. Commun.* **174** (2006) 273.

*This work is supported by the NSF under PHY-0244470 and PHY-0555226.

MWP1 36 Multiscale analysis in perturbation dynamics for the two-dimensional wake SAU BAL, A three-dimensional initial-value problem to study the linear stability of the two-dimensional wake by means of a multi space and time scale description is presented. The viscous perturbation analysis is carried out so that, by imposing arbitrary three-dimensional perturbations in terms of the vorticity, both the early transient as well as the asymptotic behavior can be considered (Criminale & Drazin 1990, 2000). Analytical Navier-Stokes asymptotic expansions are used to describe the base flow. Non-parallel effects, as non linear convection and both streamwise and transversal diffusion, are directly included (Tordella & Belan 2003). After a Fourier decomposition in the $x - z$ plane, a complex and a real wavenumber in x and z directions are introduced, respectively (Scarsoglio, Tordella & Criminale 2007). The polar wavenumber is the small parameter of the regular perturbation scheme. The limit of small wavenumbers as well as the the more general problem with larger wavenumbers are studied and results are asymptotically compared with spatio-temporal normal mode analyses (Tordella, Scarsoglio & Belan 2006; Belan & Tordella 2006).

MWP1 37 LIGHTING PLASMAS: GLOWS, ARCS, FLAT PANELS, NOVEL SOURCES, OTHERS

MWP1 38 RF Noise Generation in High-Pressure Short-Arc DC Xenon Lamps OLGA MINAYEVA, DOUGLAS DOUGHTY, *PerkinElmer Optoelectronics* Continuous direct current xenon arcs will generate RF noise under certain circumstance, which can lead to excessive electro-magnetic interference in systems that use these arcs as light sources. Phenomenological observations are presented for xenon arcs having arc gaps ~ 1 mm, cold fill pressures of ~ 2.5 MPa, and currents up to 30 amps. Using a loop antenna in the vicinity of an operating lamp, it is observed that as the current to the arc is lowered there is a reproducible threshold at which the RF noise generation begins. This threshold is accompanied by a small abrupt drop in voltage (~ 0.2 volts). The RF emission appears in pulses ~ 150 nsec wide separated by ~ 300 nsec - the pulse interval decreases with decreasing current. The properties of the RF emission as a function of arc parameters (such as pressure, arc gap, electrode design) will be discussed and a semi-quantitative model presented.

MWP1 39 Quantitative X-ray Absorption Imaging of Density Distributions in HID Lamps JOHN J. CURRY, *NIST* Quantitative x-ray absorption imaging of gases is possible with an optical digital array detector, such as a charge-coupled device (CCD), combined with an x-ray phosphor. The linearity and low dark current of a CCD enable the sensitivity needed to image gases quantitatively. X-ray absorption imaging is useful in the high-pressure Hg discharges of HID lamps because Hg has a relatively large x-ray absorption cross-section. However, inversion of a 2-dimensional projected image to obtain a 3-dimensional distribution is not directly solvable when the x-ray source has a broad spectrum and detection is not energy-resolved. Given that the energy-dependent Hg absorption cross-section varies by nearly a factor of 4 over the 15 keV to 25 keV spectral range typical of an

x-ray tube source, as much as a factor of 2 error in the measured Hg density can result. The problem is further complicated by the fact that the x-ray spectrum inevitably varies with position in the image because of spectral filtering by the arc tube. A solution of sufficient accuracy can be obtained by determining, *a priori*, an effective absorption cross-section based on the spectral distribution and energy-dependent response of the CCD/phosphor system. Progress on determining such cross-sections for a range of parameters will be presented.

MWP1 40 Development of light source using micro hollow cathode plasma for monitoring absolute densities of metal atoms in magnetron sputtering TAKAYUKI OHTA, YOSHIHIRO TACHIBANA, MASAFUMI ITO, *Wakayama University* SEIGO TAKASHIMA, *Nagoya University* YASUHIRO HIGASHIJIMA, *NU System Co., Ltd.* HIROYUKI KANO, *NU EcoEngineering Co., Ltd.* SHOJI DEN, *Katagiri Engineering Co., Ltd.* MASARU HORI, *Nagoya University* The quantitative analysis of metal atoms is important for understanding the chemistry and controlling the conditions in sputtering process. The light source, which emits multi-atomic lines simultaneously, is required for diagnostics of behaviors of many kind of metallic atom at the same time. In this study, a multi-micro hollow cathode lamp for simultaneous monitoring of multi-metal atoms in sputtering process was developed. The emissions of Cu, Zn, Fe, and Mo for analysis were simultaneously obtained from 4 hollows. The Cu and Mo densities in the magnetron sputtering were measured using absorption spectroscopy employing the multi-micro hollow cathode lamp. Those densities were measured to be from 10^9 to 10^{10} cm^{-3} in the RF power range from 0 to 100 W at a pressure of 5 Pa. The simultaneous measurement of the atomic densities in the sputtering plasma has been performed.

MWP1 41 A Survey of Infrared Continuum versus Line Radiation from Metal Halide* M. KATO, *University of Wisconsin-Madison* M.T. HERD, J.E. LAWLER, *University of Wisconsin-Madison* Near-infrared radiation (near-IR) losses from the arc of six commercial Metal Halide High Intensity Discharge (MH-HID) lamps with various power levels and with both Na/Sc and rare earth doses were surveyed in this paper. A radiometrically calibrated Fourier transform infrared spectrometer was used. Lamps with rare earth doses have appreciably better Color Rendering Indices (CRI's) than lamps with Na/Sc doses. The ratios of near-IR continuum emission over near-IR line emission from these six lamps were compared. The near-IR continuum dominates near-IR losses from lamps with rare earth doses and the continuum is significant, but not dominant, from lamps with Na/Sc doses. There was no strong dependence of this ratio on input power or Color Temperature (T_c). Total near-IR losses were estimated using absolutely calibrated, horizontal irradiance measurements. Estimated total near-IR losses were correlated with CRI. The lamps with rare earth doses yield the best CRI's, but have appreciably higher near-IR losses due primarily to continuum processes. One of these rare earth MH-HID lamps was used in a more detailed study of the microscopic physics of the continuum mechanism [M. T. Herd & J. E. Lawler, *J. Phys. D* 40, 3386 (2007)].

*Supported in part by NSF CTS 0613277.

**MWPI 42 MAGNETICALLY-ENHANCED PLASMAS:
ECR, HELICON, MAGNETRON, OTHER**

MWPI 43 Effect of the magnetic field divergence on the ion velocity distribution in the expanding region of an argon helicon plasma IOANA A. BILOIU, EARL SCIME, *West Virginia University* COSTEL BILOIU, *Varian Semiconductor Equipment Associates* SAMUEL COHEN, *Princeton Plasma Physics Laboratory* Laser induced fluorescence (LIF) observations downstream from a helicon source-diffusion chamber junction revealed bimodal ion velocity distribution functions (ivdf) along diverging magnetic field lines for 1.5 mTorr argon plasma. By increasing the magnetic field divergence in the expansion region, the speed of the faster component of the distribution function increases, reaching a maximum of ~ 10 km/s. The speed of the slower component is essentially zero. Upstream the junction, i.e., at the end of the helicon source, the distributions are also bimodal but no effect of the magnetic field divergence on fast or slow component is observed. LIF tomography observations of the 2D ivdf in the expansion region show the presence of the fast ion component including slight ion conics with cone angle of $2\theta = 64^\circ$. The strong ion acceleration and the ion conics are strong evidence of weak ion collisionality as the plasma flows out along the diverging magnetic field. The parallel velocity of the fast ions increases as a result of acceleration by the potential drop across the electric double layer at the end of the helicon source and acceleration by the magnetic moment conserving $\mu\nabla B$ force.

MWPI 44 Suppression of High-Energy Backscattered Species in Magnetron Sputter Plasma with Cylindrical Cathode HIROTAKE TOYODA, YUSUKE TAKAGI, *Nagoya University* HIDEO SUGAI, *Chubu University* Recent application of magnetron plasma to nano-scale devices requires high-quality films, e.g., magnetic multilayer films with nano-scale flat interface and with no mixing of atomic components at the interface. In general, surface qualities of sputter deposited films are influenced by incidence of particles with kinetic energies much higher than bond energies of deposited materials. Recently, we have shown abundant flux of high energy (100-200 eV) Ar atom and Ar^+ ion those are produced by backscattering of Ar^+ on the target, i.e., ejection of high-energy Ar atom from target. In this paper, we propose a new magnetron source to suppress high energy Ar and Ar^+ flux using a cylindrical cathode instead of planar cathode. Energy distribution function (EDF) of Ar^+ is measured by a QMA with an energy analyzer. It is shown that a quantity of energetic Ar^+ is much less than that of a conventional plane type cathode. In parallel with the measurement of the Ar^+ EDFs, a Monte Carlo code which simulates Ar and Ar^+ EDFs is developed. The simulation well explains the Ar^+ EDFs and shows that a quantity of the energetic Ar atom is considerably small compared with the plane type cathode. Experimental and simulation results suggest that incidence of energetic particles on the substrate is suppressed in the cylindrical magnetron sputter source.

MWPI 45 Drift Phenomena in an Inductively Coupled Magnetic Neutral Loop Discharge DRAGOS CRINTEA, DIRK LUGGENHOELSCHER, DEBORAH O'CONNELL, *Ruhr-University Bochum, Germany* TIMO GANS, *Queens University Belfast, Northern Ireland* UWE CZARNETZKI, *Ruhr-University Bochum, Germany* The neutral loop discharge is a magnetically enhanced plasma source applicable between 10^{-2} Pa and 10 Pa with electron densities of a few times 10^{10} cm^{-3} to 10^{12} cm^{-3} . A magnetic quadrupole is bent into a torus in which the magnetic field vanishes and is therefore called the neutral loop (NL). The NL is located close to a planar inductive coupling antenna separated from the plasma by a quartz cylinder and operated at 13.56 MHz. The NL confines the electrons and randomizes their trajectories, which leads to an increased heating at low pressures. In addition, the electron pressure gradients in the magnetic field cause a diamagnetic drift. With Thomson scattering the electron velocity distribution is measured and allows the determination of the diamagnetic drift of the electrons along the NL in the range of 10^4 m/s to 10^5 m/s. With an ICCD camera the temporal modulation of the emission is measured and from this the drift velocity is also determined and compared to the laser measurement. Both results agree well over three orders of magnitude in pressure with a simple fluid-dynamic drift-collision model. Drift and confinement are closely related as is also represented by the low transversal electric field measured by a Langmuir probe.

MWPI 46 The plasma parameters in a high power impulse magnetron sputtering discharge (HiPIMS) J.T. GUDMUNDSSON, P. SIGURJONSSON, *Science Institute, University of Iceland* D. LUNDIN, U. HELMERSSON, *IFM Materials Science, Linköping University* The time evolution of the electron density and electron temperature in a high power impulse magnetron sputtering discharge (HiPIMS) are explored with a Langmuir probe. A high-density plasma is created by applying a high power pulse with short duty cycle and low repetition frequency to a planar magnetron discharge [1]. The electron density in a HiPIMS discharge is very high $\sim 10^{19}$ m^{-3} in the substrate vicinity [2,3] and remains high for a while after the pulse is off. The electron energy distribution function (EEDF) in the substrate vicinity during and shortly after the pulse can be represented by a bi-Maxwellian like distribution indicating two energy groups of electrons. Here the time evolution of the two electron groups is monitored. [1] U. Helmersson, M. Lattemann, J. Bohlmark, A.P. Ehasarian, and J.T. Gudmundsson, *Thin Solid Films* 513, 1 (2006) [2] J. T. Gudmundsson, J. Alami, and U. Helmersson, *Appl. Phys. Lett.* 78, 3427 (2001) [3] J. Bohlmark, J. T. Gudmundsson, J. Alami, M. Lattemann, and U. Helmersson, *IEEE Trans. Plasma Sci.* 33, 346 (2005).

**MWPI 47 PLASMA CHEMISTRY: ATMOSPHERIC,
GAS, PHASE, SURFACE**

MWP1 48 Dissociative ionization of JP-10 in a cross-flowing Ar/Xe plasma expansion CHARLES JIAO, *UES, Inc* BISWA GANGULY, ALAN GARSCADDEN, *Air Force Research Laboratory* JP-10 ($C_{10}H_{16}$), a synthetic fuel composed almost exclusively of exo-tetrahydrodicyclopentadiene, has been widely used in missiles, supersonic-combustion ramjets and pulse-detonation engines. Although many combustion research studies have been carried out on JP-10, its detailed combustion mechanism remains to be explored. As plasma-assisted ignition and combustion have been of great interest in recent years, and topics on the roles played by charged species in ignition/combustion are being revisited, it is appropriate to study charged particle collisions with the fuel molecule. Previously we have investigated the electron impact ionization of JP-10. In the current study we examine the formation of ion fragments from JP-10 by adding the fuel to a nozzle-formed expansion of Ar or Xe plasma. Dependences of fragment ion intensities on the rf-power will be presented. Mechanisms for the ion formation will be discussed based on the interpretation of the ion intensity profiles showing both exothermic and endothermic characteristics, and on results from additional measurements including optical emission and plasmas with Ar/N₂ mixtures in the same configuration.

MWP1 49 Measurement of Ground State Oxygen Radical [$O(^3P)$] in Surface Cleaning Process Employing Nonequilibrium Atmospheric-Pressure Pulsed Remote Plasma MASAHIRO IWASAKI, KEIGO TAKEDA, MASARU HORI, *Department of Electrical Engineering, Nagoya University* MASFUMI ITO, *Faculty of Systems Engineering, Wakayama University* EIJI MIYAMOTO, TAKUYA YARA, TSUYOSHI UEHARA, *Sekisui Chemical Co., Ltd.* Plasma surface cleaning technology using the nonequilibrium atmospheric-pressure plasma has the advantages of non-vacuum system, high throughput, and scalability for large area in-line processing. In this study, the surface cleaning on an indium tin oxide film was investigated by using a nonequilibrium atmospheric-pressure pulsed plasma. It was found that a remarkably high cleaning efficiency was realized by plasma treatment with additions from 0.025 to 0.1% O₂ to N₂. The densities of the ground state oxygen radical [$O(^3P)$] and ozone [O₃] were measured using vacuum UV laser absorption spectroscopy and UV absorption spectroscopy, respectively. It was found that the key factor for the surface cleaning was the scission of carbon bonds of organic compounds due to UV emissions, and subsequent oxidation due to $O(^3P)$ and O₃.

MWP1 50 PLASMA-SURFACE INTERACTIONS

MWP1 51 Study of the influence of collisions between physisorbed atoms on the surface recombination probability VASCO GUERRA, *Centro de Física dos Plasmas, Instituto Superior Técnico, 1049-001 Lisboa, Portugal* A dynamical Monte-Carlo method was developed to study the surface kinetics of a simple system. The kinetic scheme comprises physisorption, thermal desorption from physisorption sites, chemisorption, Eley-Rideal recombination, surface diffusion of physisorbed atoms, and Langmuir-Hinshelwood recombination. The model provides the time-evolution of the fractional coverage of both physisorption and chemisorption sites, the recombination probability, and the contribution of each elementary process to recombination. Different grid sizes and averaging procedures were used to optimize the Monte Carlo algorithm. The results were compared with a previously developed mean-field model. The effect of collisions between physisorbed atoms, could not be described within the previous model, was investigated in detail. Evidently, they become important and can change significantly the results in the domain of low surface temperatures, corresponding to a high occupancy of physisorption sites.

MWP1 52 Production and loss of rovibrationally excited H₂ molecules: Expanding Hydrogen plasmas in experiment and model RICHARD ENGELN, ONNO GABRIEL, DAAN SCHRAM, *Eindhoven University of Technology, Eindhoven, The Netherlands*, PETER VANKAN, *Philips Lighting (CDL), Eindhoven, The Netherlands* The rovibrationally resolved density distributions of molecular hydrogen are measured in expanding thermal hydrogen plasmas by means of laser induced fluorescence in the vacuum-UV range (VUV-LIF). The results reveal a non-Boltzmann distributions, where the low rotational states ($J=1-6$) follow a temperature of 700 K, while the higher rotational states are overpopulated compared to these lower states and follow higher temperatures up to 4500 K. Experiments were performed under variation of the surface area in the plasma source by varying the nozzle length. We assume surface association processes of atomic hydrogen at the surface of the nozzle, producing rovibrationally excited H₂ molecules. While the atomic hydrogen flow decreases with increasing surface areas, the H₂^v distribution shows a more pronounced non-Boltzmann behavior. A simple 0D model of (de)excitation processes by collisions with electrons and neutrals results in additional information about the formation of the measured H₂^v distributions.

SESSION PR1: LASER AND AIR PLASMAS

Thursday morning, 4 October 2007; Crystal Ballroom A, Doubletree Crystal City at 8:00

Ed Barnat, Sandia National Laboratories, presiding

Invited Papers**8:00****PR1 1 Transmission line analysis of laser-guided streamers and leaders.***MARTIN LAMPE, *Naval Research Laboratory*

Plasma Physics Division, NRL. We have developed a 1-D transmission-line model for laser-guided discharges, which can be used to analyze both streamers and leaders over the complete length and duration of the discharge, and which facilitates analytic insight as well as providing a simplified, quickly solvable semi-quantitative simulation capability. It is assumed that the laser designates a specified seed electron density within a long thin channel, which is connected directly to a high-voltage source. In this way, the physical situation differs somewhat from natural lightning, which is driven by a uniform electric field, rather than via connection to a voltage source. The mathematics reduces to a 1-D diffusion equation for the electric field $E(z,t)$, with a diffusion coefficient $D(z,t)$ proportional to the channel conductance, very small ahead of the discharge and rapidly increasing at the discharge head. This equation can be solved directly, or the model can be further reduced by requiring that the discharge propagates in a self-similar fashion at a constant propagation speed u ; the diffusion equation then reduces to a first-order O.D.E. in $t' = t - z/u$, which must be solved self-consistently with rate equations that determine $D(t')$. In analyzing streamers (in cold air), we represent the rates as functions of E/n ; this simple model yields immediate insights. In analyzing leaders, where the air is heated and excited, we use a complete air chemistry model. The model provides estimates for the minimum propagation speed of negative waves, the minimum level of pre-ionization required for propagation of positive waves, the electric field in the discharge head and body, and the radius and range of leaders, and is especially useful for understanding the streamer-to-leader transition. Work done in collaboration with R. F. Fernsler, S. P. Slinker, D. F. Gordon, and P. Sprangle.

*Research supported by NAVSEA.

Contributed Papers**8:30****PR1 2 Plasma Excited Chemical-Oxygen-Iodine Lasers: Optimizing Injection and Mixing for Positive Gain***

NATALIA Y. BABAEVA, LUIS A. GARCIA, RAMESH A. ARAKONI, MARK J. KUSHNER, *Iowa State University* Chemical oxygen-iodine lasers achieve oscillation on the ${}^2P_{1/2} \rightarrow {}^2P_{3/2}$ transition of atomic iodine at 1.315 μm by a series of excitation transfers from $\text{O}_2({}^1\Delta)$. In electrically plasma excited devices (eCOILs), $\text{O}_2({}^1\Delta)$ is produced in a flowing plasma, typically He/O_2 , at a few to tens of Torr. The iodine is injected into the flow as a He/I_2 mixture immediately upstream (or in) a supersonic nozzle. A small positive gain with I^* limited to a narrow boundary layer near the wall indicates slow mixing when the I_2 is injected from the wall. This results in low utilization of $\text{O}_2({}^1\Delta)$. In this paper we discuss results from 1- and 2-dimensional computational investigations of means to optimize gain in eCOILs by using different I_2 injection strategies. It was found that due to the plasma generated distribution $\text{O}_2({}^1\Delta)$, placement of injectors closer to the axis significantly increased gain by facilitating complete $\text{O}_2({}^1\Delta)/\text{I}_2$ mixing. This is partly a function of the inlet flow of NO through the discharge which regulates the density of O atoms produced by electron impact dissociation of O_2 . By optimizing the nozzle dimensions, their location, and I_2 and NO flow rates, the yield of $\text{O}_2({}^1\Delta)$ required to achieve positive gain can be minimized.

*Work supported by AFOSR and NSF.

8:45**PR1 3 Kinetics of the Electron Beam Driven Ar-Xe Laser on NRL's Electra Generator***J.P. APRUZESE, J.L. GIULIANI, M.F. WOLFORD, A. DASGUPTA, G.M. PETROV, J.D. SEHIAN, D.D. HINSHELWOOD, M.C. MYERS, *Naval Research Laboratory* F. HEGELER, *Commonwealth Technologies, Inc.* TS. PETROVA, *Berkeley Research Associates*

Due to its efficiency and potentially high power, the Ar-Xe IR laser (1.733 microns) has been the subject of investigation by several groups around the world since the 1980's. Nonetheless, there is still no clear resolution of some of the key physics and kinetics issues that affect its properties. We are addressing these issues in a coordinated program of experiments and modeling at the Naval Research Laboratory. For our experiments we employ NRL's Electra facility, with its extensive suite of diagnostics, developed as a KrF UV laser for the Department of Energy's High Average Laser Power program. We present results showing that Xe_2^+ as well as ArXe^+ significantly contributes to the pumping of the laser, and that dissociation of ArXe^+ accounts for most of the laser's temperature sensitivity. We have also found that for an amplifier with dimensions 30 x 30 x 100 cm, the optimum e-beam power deposition density is 50-100 kW/cc for the 140 nanosecond Electra diode pulse.

*Work supported by the Office of Naval Research.

9:00

PR1 4 Inferring argon plasma properties from optical emission: the role of metastable atoms* R.O. JUNG, JOHN B. BOFFARD, CHUN C. LIN, R. DING, Y.-H. TING, Y. YANG, A.E. WENDT, *University of Wisconsin-Madison* Collisions between electrons and Ar atoms are primarily responsible for the characteristic plasma glow of Ar discharges. The intensity of a given emission line depends upon both the electron energy distribution (EED) and the excitation cross sections for populating the excited levels. Since the EED also drives the plasma chemistry, there is a need for non-invasive diagnostics of the EED in plasmas for industrial processing. One obstacle in using optical emission spectroscopy (OES) of the plasma glow as a diagnostic is that only electrons in the highest energy range of the EED have enough energy to excite atoms directly from the Ar $3p^6$ ground state. Due to the much lower energy threshold, and much larger cross sections, excitation from atoms in $3p^4s$ metastable levels can contribute substantially to plasma emissions. Recent measurements of excitation cross sections into $3p^55p$ levels ($\lambda: 395-470$ nm) from the Ar metastable levels [1] allow us to exploit the role of metastable atoms to probe the low energy range of the EED. Verification of this OES technique with simultaneous Langmuir probe (for the EED) and optical absorption (for the metastable density) measurements is underway. [1] R. O. Jung, et al, *Phys. Rev. A* **75**, 052707 (2007). *-lex

*Supported by the National Science Foundation.

9:15

PR1 5 Electrical and Optical Diagnostics of an Electron-Beam Generated Air Plasma ROBERT VIDMAR, *University of Nevada, Reno* KENNETH STALDER, *Stalder Technologies and Research* A pulsed 1-ms 100-keV 20-mA electron beam injected through a transmission window produces air plasma in a 400-liter test cell filled with laboratory air. The beam current is monitored by a current sensor up-stream to a transmission window and supported against air pressures in the test cell from 1 mTorr to 640 Torr. RF amplitude and phase measurements at 10 GHz quantify electron density. Optical emissions from the plasma are monitored by a diode array spectrometer and quantify nitrogen emissions. Ozone concentration is monitored with a UV absorption system. Concentrations of other species are monitored by tunable diode laser absorption spectroscopy. Representative single-shot data from these diagnostic systems will be discussed. This work is supported by the Air Force Research Laboratory under grant numbers FA9550-04-1-0015 and FA9550-04-1-0444; and State of Nevada matching funds.

SESSION PR2: ELECTRON ATTACHMENT AND RECOMBINATION

Thursday morning, 4 October 2007

Crystal Ballroom B, Doubletree Crystal City at 8:00

Murtadha Khakoo, California State University, Fullerton, presiding

8:00

PR2 1 Collisions of thermal electrons and electron affinities of SF_6 , C_6F_6 and nucleic acids* EDWARD C.M. CHEN, *University of Houston, Clear Lake* EDWARD S. CHEN, *Baylor College of Medicine* New electron affinities of the subject molecule are reported from the temperature dependence of thermal electrons measured with the electron capture detector and negative ion mass

spectra. The electron affinities are compared with values obtained from anion photoelectron spectra. Multiple negative ion potential energy curves are calculated to consolidate all experimental data. The adiabatic electron affinities are: in eV SF_5 , 3.80(12), SF_6 , 2.45(10), C_6F_6 , 1.40(10), Adenine, 1.08(5), Guanine, 1.60(10), Cytosine, 1.04(5), Thymine, 0.93(5), Uracil, 0.96(5). Excited state for all of these except for guanine have been observed in photoelectron spectra. Parent negative ions of the nucleic acids are observed in mass spectra. The gas phase acidities of the deprotonated nucleic acids are reported.

*The Wentworth Foundation.

8:15

PR2 2 Dissociative electron attachment to molecules and unstable species relevant in plasma processing KAROLA GRAUPNER, THOMAS FIELD, *Centre for Plasma Physics, Queens University Belfast* Collisions between low energy electrons (0 to 10 eV) and molecules can lead to formation of negatively charged fragment ions by dissociative electron attachment. Electron attachment to plasma species, such as unstable molecules, formed in 2.45 GHz microwave discharges of CS_2/He [1], C_3F_6/He , SF_6/He , CH_4/He and CCl_4/He has been investigated with ERIC (Electron Radical Interaction Chamber), which includes a trochoidal electron monochromator and time-of-flight mass spectrometer. Knowledge of the spectra of negative ions formed as a function of electron energy for unstable molecules may be useful for understanding chemical processes and negative ion formation in plasmas. It may also be possible to identify unstable molecules in gas sampled from plasmas with these characteristic negative ion spectra. [1] Dissociative electron attachment to the unstable carbon monosulfide molecule CS, K. Graupner, T. A. Field and L. Feketeova, *New J. Phys.* **8** (2006) 314.

8:30

PR2 3 Dissociative Electron Attachment to HCN and HNC* S.T. CHOUROU, A.E. OREL, *University of California, Davis* HCN and its isomer HNC are known to be among the initial species that drive synthesis of amino acid and protein in interstellar media. Dissociative electron attachment (DEA) to those molecules may thus have an impact on these chemical processes of relevance in astrophysics. Previous experimental and theoretical studies have indicated both σ and π low-lying resonances. These resonant states are expected to depend on stretching and bending of the molecule and to lead to competing ($CN^- + H$) and ($CN + H^-$) products. In this work, we present a comparative study of the dissociation mechanism. We carried out electron scattering calculations using the Complex Kohn Variational Method as a function of the three internal degrees of freedom to obtain the resonance energy surface and autoionization widths. We use this as input to a dynamics calculation using the multiconfiguration time-dependant Hartree (MCTDH) approach. We finally compare our DEA cross sections and branching ratios to available findings.

*NSF PHY-05-55401

8:45

PR2 4 Dissociative Electron Attachment to C_2HCl * V. NGAS-SAM, A.E. OREL, *Department of Applied Science, University of California Davis* Studies of dissociative electron attachment (DEA) to acetylene have shown a dramatic effect as a function of bending the molecule. We have begun an investigation of such multidimensional effect on mono-chloro substitute of hydrocarbons. This work concentrates on chloroacetylene. We study the

system in limited dimensionality (*i.e.* as a diatomic) and then contrast this with multidimension studies. We perform electron scattering calculations using the complex Kohn variational method to determine the resonance parameters of this system. The results show a two low lying resonance state of Σ and Π symmetry. Resonant potential energy surfaces are then constructed as a function of the Cl-C and C-C internuclear distances as well as the Cl-C angle. Stretching the C-H distance does not significantly the position and shape of the resonance states, thus the problem is reduced to 3 active degrees of freedom and the DEA dynamics can be study. The time dependent wave packet method is used to solve the one dimension problem and the Multi-Configuration Time-Dependant Hartree method is used for wavepacket propagation on the computed resonant potential energy surfaces in three-dimension. We discuss the mechanisms leading to dissociation into the product channels and report the computed DEA cross sections.

*This work was supported by the U.S. DOE Office of Basic Energy Sciences, Division of Chemical Sciences and the National Science Foundation, PHY-05-55401.

9:00

PR2 5 Branching fraction for radiating products of the dissociative recombination of N_2H^+ , HCO^+ , HOC^+ , and HNC^+ . R. JOHNSEN, M.F. GOLDE, *University of Pittsburgh* R. ROSATI, *Smithsonian Astrophysical Observatory* D. PAPPAS, *Army Research Laboratory* M. SKRZYPKOWSKI, *Prometheus Energy Company* We present the results of a series of flowing-afterglow studies of the emission spectra produced by dissociative electron recombination (DR) of the ions N_2H^+ , HCO^+ , HOC^+ , and HNC^+ . Yields of product states were determined by comparing emission band intensities to model calculations of the afterglow. We find that DR of N_2H^+ results in emission of the $N_2(B-A)$ 1^st positive system (yield of $(19 \pm 8)\%$), but the vibrational distribution indicates that the B-state, in part, is populated by collisional and radiative coupling from other triplet states. DR of HCO^+ forms the long-lived $CO(a^3\Pi)$ state with a yield of $(23 \pm 12)\%$ while DR of HOC^+ populates the triplet states $CO(a^3\Sigma^+)$ and $CO(d^3\Delta)$ with a combined yield of $> 40\%$. Observations of the red and violet CN bands show that DR of HNC^+ results in CN(B) and CN(A) with yields of $(22 \pm 8)\%$ and $(14 \pm 5)\%$, respectively. The vibrational distributions of the product electronic states do not seem to follow a simple pattern: In some cases, a monotonic decline with increasing v' is observed that can be understood on the basis of Bates' impulse model, but other distributions are partially inverted and extend to very high vibrational quantum numbers.

9:15

PR2 6 Four-Particle Dalitz Plots to Visualize Atomic Break-Up Processes* MICHAEL SCHULZ, DANIEL FISCHER, THOMAS FERGER, ROBERT MOSHAMMER, JOACHIM ULLRICH, *University of Missouri-Rolla* We introduce a new method to analyze four-body fragmentation processes, which is basically an extension of Dalitz plots commonly used in particle physics to analyze three-body fragmentation processes. It enables for the first time to present multiple differential cross sections as a function of all four fragments without loss of any part of the total cross section in the integral spectrum. As a first example, the technique is applied to ionization processes in atomic collisions.

*Work supported by NSF.

SESSION QR1: PLASMA SOURCES

Thursday Morning, 4 October 2007

Crystal Ballroom A, Doubletree Crystal City at 10:00

Yohei Yamazawa, Tokyo Electron, presiding

10:00

QR1 1 Two-dimensional Collisionless Weakly-ionized Plasma in Fluid Approximation VALERY GODYAK, *Osram Sylvania* NATALIA STERNBERG, *Clark University* A finite cylinder is a common plasma shape in many research experiments and plasma processing reactors. In the diffusion limit (the Schottky model), the two-dimensional plasma density profile for a finite cylinder of length $2L$ and diameter $2R$ is the product of the corresponding one-dimensional solutions, namely, $n(x,r)/n_0 = \cos(\pi x/2L)J_0(2.4r/R)$. This representation of the plasma spatial distribution is commonly used at low gas pressures, even when the Schottky model is not applicable (such as in the cases of collisionless ions, or variable ion mobility). In this presentation, we will analyze, for a wide range of the aspect ratio L/R , the behavior of the ionization frequency, plasma densities at the radial and axial boundaries, the spatial plasma profile, the plasma flux to the wall, as well as the entering angle of ions at the plasma boundary. We will demonstrate that for cylindrical collisionless plasma, the spatial plasma profile cannot be represented by the product of the corresponding one-dimensional solutions. Moreover, in the limiting cases of small and large aspect ratios, the plasma distribution along the longer length (L or R) approaches the diffusion distribution, which corresponds to the highly collisional ion motion, although the ion motion in this direction is collisionless.

10:15

QR1 2 Capacitive Discharges Driven by Combined DC/RF Sources M.A. LIEBERMAN, EMI KAWAMURA, A.J. LICHTENBERG, *UC Berkeley* E.A. HUDSON, *Lam Research Corporation* The performance of low pressure rf capacitive discharge reactors can be modified by applying an auxiliary dc power source to a reactor electrode. The dc source induces a dc current flow through the plasma and alters the sheath voltages and widths. This can increase the plasma density and etch rate. These effects may be ascribed to an enhanced density of high energy secondary electrons in the discharge due to the alteration of the sheath voltages. We have obtained analytic expressions for the sheath voltages and sheath widths for both collisional and collisionless sheaths driven by a combination of dc and rf voltage sources. The analysis is done for both symmetric (equal area) and asymmetric diode discharges, as well as a triode configuration. The analytical results for the symmetric and asymmetric diode discharges are compared to the results of numerical simulations using plane-parallel and cylindrical 1d3v (one-dimensional displacement, three velocity components) particle-in-cell (PIC) codes over a wide range of pressures and rf frequencies, finding good agreement. Secondary electron dynamics and energy distributions are also examined; these yield increased discharge efficiency. The uniformity of the secondary electron and ion fluxes at the target electrode are also examined with a series of two-dimensional (2D3v) PIC simulations.

10:30

QR1 3 RF discharge under the influence of a magnetic field ED BARNAT, PAUL MILLER, *Sandia National Laboratories* ALEX PATERSON, *Applied Materials* We examined the effects of an externally applied magnetic field (0 to 150 Gauss) on a capacitive 13.56 MHz argon discharge in a Gaseous Electronics Conference (GEC) reference cell. The electrical characteristics of the discharge were measured as functions of applied magnetic field and rf power. At fixed power the rf voltage decreased with increasing magnetic field. The discharge impedance was predominantly capacitive and became more resistive as the electron mobility decreased with increasing magnetic field. We also measured the effect that the magnetic field had on the spatial distribution of the plasma in vertical planes parallel and perpendicular to the direction of the magnetic field using Langmuir probes, optical emission, and laser induced fluorescence. Due to ExB forces, the distribution of excited states in the plasma remained radially symmetric in the plane parallel to the magnetic field and became skewed in the plane perpendicular to the magnetic field. The degree of skew depended on the state probed. Finally, we examined the temporal evolution of the electric fields in the plasma. In the presence of magnetic field, the sheath thickness decreased and most of the voltage drop was contained within the sheath. Consistent with dc voltage trends, there was no significant sheath reversal observed at higher magnetic fields.

10:45

QR1 4 The effect of radio-frequency bias on electron density in an inductively coupled plasma reactor, measured by a wave cutoff probe MARK SOBOLEWSKI, *National Institute of Standards and Technology* JUNG-HYUNG KIM, *Korea Research Institute of Standards and Science* Rf-biased, inductively coupled plasma reactors allow ion energy and ion flux to be varied separately, but it is unlikely that perfectly independent control can be achieved. Although rf bias is intended to only affect ion energies, it may also produce changes in the plasma electron and ion densities and the total ion flux. To provide a better understanding of such changes, we performed a detailed study in Ar, CF₄, and Ar/CF₄ plasmas. We measured the electron density with a wave cutoff probe, which avoids problems with deposition and rf compensation that may affect Langmuir probes. The effect of rf bias on electron density was measured as a function of source power, position, pressure, bias frequency, bias amplitude, and time. Cutoff probe results were also compared to Langmuir probe measurements, and both showed the same effects. Two types of bias-induced changes in electron density were observed. One was a gas composition effect caused by etch or sputter products liberated from the wafer surface. The other was an electron heating effect caused by absorption of bias power by plasma electrons. Simple models of each effect were derived and shown to yield quantitative predictions in agreement with the observations.

11:00

QR1 5 Seasoning of Plasma Reactors: Feedback Control Strategies to Counter Wafer-to-Wafer Drifts* ANKUR AGARWAL, *University of Illinois* MARK J. KUSHNER, *Iowa State University* Seasoning of plasma etching reactors is the deposition of materials on wafers and surfaces of the chamber resulting in process or wafer-to-wafer drift in etch rates or uniformity. Feedback control with *in situ* diagnostics is being investigated to combat this drift. The Virtual Plasma Equipment Model, an implemen-

tation of sensors, actuators and control algorithms in the HPEM, was used to investigate real-time and wafer-to-wafer control strategies. The model system is Ar/Cl₂ etching of Si in an inductively coupled plasma reactor. The passivation of surfaces in contact with the plasma, including the deposition of etch products, change reactive sticking coefficients and produce etch blocks which in turn affect etch rate. Sputtering of dielectrics may introduce additional etch-block capable species. A PID controller was used to vary the bias voltage in response to an etch rate monitor to enable control of etch rate. We found that control is problematic at high bias voltages where the flux of etch products from the wafer is sufficiently large that plasma properties are affected and redeposition increases etch blocks on the wafer. Multiple sensors-and-actuators may be necessary when sputtering of dielectrics produce additional etch-block species.

*Work supported by Semiconductor Research Corp. and the NSF.

11:15

QR1 6 Diagnostics of continuous electron beam-generated plasma for material processing* EVGENIYA LOCK,[†] SCOTT WALTON, RICHARD FERNSLER, *Plasma Physics Division, Naval Research Laboratory, Washington, DC 20375* Electron beam generated plasmas have several unique features that distinguish them from discharges. The latter have electron temperatures in the range of 1-10 eV and a large spread in the electron energy distribution function. The high temperature leads to large plasma potentials and large incident ion energies. The electron beam generated plasma has intrinsically lower electron temperature (< 1 eV), resulting in smaller plasma potentials and in lower incident ion energies. This enables the electron beam generated plasmas to be used in processing of sensitive materials, where excessive ion energies can be problematic. In this work, spatial distributions of electron temperature and plasma density in argon, nitrogen and their mixtures were measured in magnetically confined, continuous electron beam-generated plasmas. The influence of the process parameters including beam energy, magnetic field strength and pressure was analyzed. The only factor that significantly influenced the electron temperature was the gas composition. On the other hand, the plasma density could be adjusted by modifying any of the process variables. Complementary studies on ion energy distributions were performed by Walton, S.G. et al.

*This work was supported by the Office of Naval Research.

[†]NRL/NRC Postdoctoral Research Associate

11:30 *Student Excellence Award Finalist*

QR1 7 Double layers at anode spots in low-pressure plasma* SCOTT BAALRUD, NOAH HERSHKOWITZ, *Engineering Physics Department, University of Wisconsin-Madison* The evolution of the potential profile near an electrode with positive applied potential has three distinct modes. For bias less than the ionization potential of the neutral gas, a monotonic electron sheath is present. When the applied bias is increased beyond the ionization potential, a thin region of increased ionization and a corresponding double layer (DL) form near the electrode. This regime is referred to as anode glow. When the ion density in the anode glow becomes large enough that there are many ions in a Debye sphere, a quasineutral anode spot (AS) forms and the DL moves many Debye lengths away from the electrode. The distance between electrode and DL can be calculated using current balance conditions, Bohm's criterion, and quasineutrality in the AS. For

small electrodes, the AS diameter is typically larger than the electrode and the AS appears approximately spherical. However, for large electrodes the AS diameter can be much shorter than the electrode diameter and the AS is more akin to a cylinder with length longer than diameter. AS and electrode diameters are correlated. Data were taken in a multidipole chamber with mTorr range argon plasma generated by hot filaments.

*Work supported under a National Science Foundation Graduate Research Fellowship and US DOE grant FG02-97ER 54437.

11:45

QR1 8 Study of discharge characteristics on transition from metallic to reactive mode in radio frequency magnetron plasma JOYANTI CHUTIA, HEMEN KAKATI, ARUP RATAN PAL, HEREMBA BAILUNG, *Institute of Advanced Study in Science and Technology* The technique of reactive magnetron sputtering with argon as buffer gas and oxygen as reactive gas is widely used for deposition of different types of metal-oxide films.

SESSION QR2: ELECTRON-ATOM COLLISIONS

Thursday morning, 4 October 2007; Crystal Ballroom B, Doubletree Crystal City at 10:00

Kurt Becker, Polytechnic University, presiding

Invited Papers

10:00

QR2 1 Studies of Electron-Impact Induced Ionization of Atoms and Molecules Using Multi-Particle Imaging Techniques.

ALEXANDER DORN, *Max-Planck-Institute for Nuclear Physics*

Reaction microscopes allow the measurement of the momentum vectors of all fragments produced in ionizing collisions. We have developed such a multi-particle spectrometer for the investigation of electron scattering processes. Here novel studies of fundamental few-body reactions will be presented. For single ionization of helium by fast ($E = 1000$ eV) and by slow ($E = 105$ eV) electron impact the three-dimensional electron emission patterns show structures which, so far, have not been observed in conventional experiments. Kinematically complete experiments for double ionization of helium by electrons with energies close to the threshold enable for the first time a detailed insight into the behaviour of three strongly interacting continuum electrons in the field of the residual ion. Finally, results for ionization of simple molecules as hydrogen or water are discussed where the dependence of the ionization dynamics from the alignment of the molecular axis with respect to the incoming projectile beam can be studied.

Contributed Papers

10:30

QR2 2 Positron scattering from helium CASTEN MAKOCHEKANWA, ADRIC JONES, PETER CARADONNA, STEPHEN BUCKMAN, JAMES SULLIVAN, *Australian National University CENTRE FOR ANTIMATTER MATTER STUDIES COLLABORATION*, The Australian Positron Beamline Facility was built to provide a source of positrons for scattering experiments. Recently, the first high resolution positron beam was produced and has been used to measure positron scattering cross sections from

helium. The beamline is based on techniques developed by Cliff Surko at UCSD and uses a muffer gas trap in a strong magnetic field to trap, cool and form the positrons into a pulsed beam. A beam of 150 meV energy resolution has been obtained and was used to measure the absolute differential positron scattering cross section for helium, below the positronium formation threshold. This is the first time that these measurements have been made and the results will be compared to state of the art theoretical calculations, as a strict test of their validity. Plans for further work using this facility will also be outlined.

10:45

QR2 3 Inner-shell photodetachment of Na^- and electron-impact ionization of auto-ionizing states in Na.* OLEG ZATSARINNY, KLAUS BARTSCHAT, *Drake University* A.A. BOROVNIK, *Institute of Electron Physics, Uzhgorod 88017, Ukraine* We have used the *B*-spline *R*-matrix (close-coupling) method with non-orthogonal sets of orbitals [1] to calculate inner-shell photodetachment of $\text{Na}(3s^2)$ for incident photon energies between 30 and 50 eV. Satisfactory agreement is obtained with the measurements of Covington *et al.* [2]. With the same computational model for the e-Na (half) collision, we can also treat electron impact excitation of the $(2p^5 3s^2)^2P_{3/1,1/2}$ autoionizing states in sodium. Our results for the latter process will be compared with new experimental data, obtained with an energy width (FWHM) of 200 – 250 meV in the incident beam [3]. This improvement in the energy resolution made it possible, for the first time, to resolve the near-threshold excitation of the two fine-structure components $(2p^5 3s^2)^2P_{3/2,1/2}$ separately. [1] O. Zatsarinny, *Comp. Phys. Commun.* **174** (2006) 273. [2] A.M. Covington *et al.*, *J. Phys. B* **34** (2001) L735. [3] A.A. Borovnik, O. Zatsarinny, and K. Bartschat; *Book of Abstracts ICPEAC XXV* (in press).

*Work supported by the NSF under PHY-0244470 and PHY-0555226, and by INTAS under 03-51-4706.

11:00

QR2 4 Projectile Interactions in Simultaneous Excitation-Ionization of Helium* A.L. HARRIS, *University of Missouri-Rolla* M. FOSTER, *Los Alamos National Laboratory* J.L. PEACHER, D.H. MADISON, *University of Missouri-Rolla* The importance of projectile interactions in fully differential cross sections (FDCS) will be explored for the problem of simultaneous

excitation-ionization by electron impact. We will compare the results of two theories- the first Born approximation (FBA) and the four-body distorted wave model (4DW). In the first Born approximation (FBA), the projectile electron is treated as a plane wave, the ejected electron is treated as a Hartree Fock distorted wave, and the final state Coulomb interaction between the two continuum electrons is ignored. In the 4DW model, all continuum electrons are treated as Hartree Fock distorted waves, and a Coulomb distortion factor is included in the final state to account for the interaction between the two outgoing electrons. Results will be presented for an incident electron energy of 500 eV and will be compared to experimental data.

*Work supported by NSF grant PHY-0456528.

11:15

QR2 5 Charged-particle impact of quasi-two electron atoms* KLAUS BARTSCHAT, XIAOXU GUAN, DANIEL WEFLEN, *Drake University* We have applied a hybrid method, combining a second-order distorted-wave method for a fast ionizing projectile with an *R*-matrix (close-coupling) approach for the initial bound state and the ejected electron [1, 2], to calculate electron and positron impact ionization of helium, magnesium, and calcium. Our results will be compared with recent experimental data and predictions from other theoretical approaches. For various kinematical situations, in-plane and out-of-plane, we analyze the sensitivity of the theoretical results to the details of the computational models, as well as the projectile charge. New benchmark experiments to test the various theoretical approaches will be suggested. [1] Y. Fang and K. Bartschat, *J. Phys. B* **34** (2001) L19. [2] K. Bartschat and O. Vorov, *Phys. Rev. A* **72** (2005) 022728.

*Work supported by the NSF under PHY-0244470.

Invited Papers

11:30

QR2 6 Recent Progress in Calculations of Electron-Impact Excitation of Rare Gases and its Impact on Gaseous Electronic Applications.*

ARATI DASGUPTA, *Plasma Physics Division, Naval Research Laboratory, Washington, DC 20375*

In recent years there have been a number of experimental and theoretical investigations of electron-impact excitation (EIE) cross sections with improved measurement techniques and state-of-the-art calculations. These investigations not only reveal many interesting aspects of basic physics of electron collision with neutral atoms, but they are extremely important for many gaseous electronics applications such as lighting, plasma processing, and gas lasers. We will present the current status of many theoretical calculations of EIE cross sections using distorted-wave (DW) and close-coupling *R*-matrix and *B*-spline *R*-matrix methods for several noble gases such as Ar, Kr, and Xe in particular and compare them with recent improved measurements by the University of Wisconsin group using a Fourier-transform spectrometer. Although in some cases there is qualitative agreement between theoretical and experimental results, even with the advancements of both theoretical and experimental techniques and improved data, quantitative discrepancies still exist in most cases. We will present some of the issues regarding the disagreement and also discuss the significant effects of EIE data for various applications. In particular, results from this study have been used to model an electron beam pumped Ar-Xe laser at NRL. We will also comment on the complexity involved in calculating the structure and EIE cross sections of a complex open-shell element such as Mo and its implications for modeling a molybdenum discharge lamp.

*Work supported by the Office of Naval Research and the National Science Foundation.

SESSION RR1: MICRO AND DIELECTRIC BARRIER DISCHARGES

Thursday afternoon, 4 October 2007; Crystal Ballroom A, Doubletree Crystal City at 13:30

Remi Dussart, GREMI - Université d'Orléans, presiding

Invited Papers

13:30

RR1 1 Microcathode Sustained Discharges for the generation of DC, non-thermal plasmas at high gas pressure.*LEANNE PITCHFORD, *LAPLACE, University of Toulouse and CNRS*

It is now well known that non-thermal DC plasmas can be generated and maintained in high pressure gases in small - hundreds of micron-sized - geometries. One such configuration, a MicroHollow Cathode Discharge (MHCD), originally investigated by Schoenbach and colleagues (KH Schoenbach, et al, *Plasma Sources Sci. Technol.* **6**, 468 (1997)), consists of a metal/dielectric/metal sandwich through which a central hole is pierced. The diameter of the hole and the thickness of the sandwich are each some 100's of microns. Larger volume plasmas can be generated by placing a third, positively biased electrode some distance (1 cm) away, in which case the MHCD can act as a plasma cathode. This configuration is called a MicroCathode Sustained Discharge or MCSD (RH Stark and KH Schoenbach *J. Appl. Phys.* **85** 2075 (1999)). This talk will focus on the properties of the MCSD - its initiation and its electrical properties - and on the properties of the plasma generated in the MCSD volume. Experimental and numerical results for discharges in rare gases and in rare gas/oxygen mixtures at pressures up to atmospheric will be used to illustrate that the plasma generated in the MCSD is similar to a positive column plasma, with a low electric field and low to moderate gas temperature. The plasma conditions in the MCSD are suitable for the generation of large densities of radical species, such as oxygen molecules in the singlet delta metastable state (G. Bauville, et al, *Appl. Phys. Lett.* **90**, 031501 (2007)).

*Supported in part by AFOSR through EOARD and by the French ANR. The experimental part of this work was carried out in the groups of V Puech in Orsay, of A. Rousseau in Palaiseau, and of N. Sadeghi and M Touzeau in Grenoble.

14:00

RR1 2 Plasma-Photocatalyst Interaction for VOC Removal: Origin of the Synergy.ANTOINE ROUSSEAU,* *LPTP, Ecole Polytechnique*

It is well known that the coupling of an atmospheric non-thermal plasma with catalytic materials lead to synergetic effects for the abatement of some volatiles organic compounds (VOC). We analyze, here, the mechanisms of such a synergy where the catalyst is a porous semi-conductor (TiO_2). Different porous materials are compared: silica fibers possibly containing SiO_2 and/or TiO_2 nanoparticles. The respective influence of the porosity versus the chemical type of the catalyst is investigated and the oxidizing species are identified using two complementary approaches. 1) Efficiency of the plasma-catalyst coupling in a dielectric barrier discharge (DBD) at atmospheric pressure, 2) Plasma-catalytic surface interaction in a pulsed low pressure discharge. It is shown that the VOC oxidation scales as a function of the specific injected energy and occurs mainly on the porous surface due to short-life species produced the plasma [1-3]; Time resolved and in-situ measurements using laser absorption spectroscopy and emission spectroscopy in a low-pressure experiment have shown that i) plasma- TiO_2 synergy is also evidenced at low pressure[4], ii) O atoms are reversibly adsorbed on porous nanoparticles of TiO_2 ; their desorption occur during the first millisecond of a plasma pulse [5], iii) air-plasma pre-treatment of the porous material leads to an enhancement of VOC adsorption on porous TiO_2 and has no influence on porous silica. [1] U. Roland et al. *Catalysis Today* **73** 315-323 [2] F. Thevenet et al. *Catal. Today* **122** (2007) 186-194 [3] F. Thevenet et al. *International Journal of Plasma Environmental Science and Technology*, **1**, (2007), 52-56 [4] A. Rousseau et al. *Appl. Phys. Lett.* **87**, 221501 (2005) [5] Allegraud et al. *J. Phys. D. : Appl. Phys* submitted.

*In collaboration with O. Guaitella, K. Allegraud, F. Thevenet- Ecole Polytechnique and C. Guillard, U. Lyon 1.

Contributed Papers

14:30

RR1 3 The dynamics of light emission from micro-discharge array devices*

J. WASKÖNIG, D. O'CONNELL, V. SCHULZ-VON DER GATHEN, J. WINTER, *Center for Plasma Science and Technology, Ruhr University Bochum, Germany* Micro-discharges structured in arrays, of up to tens of thousands single devices, are becoming increasingly important with immense application potential. Investigations, in particular experimental, can be challenging on such discharges, however more detailed insight is essential for further development. One such array is investigated

through phase and space resolved optical emission spectroscopy (PROES). Through these investigations insight into ignition and sustaining mechanisms of both the individual discharge devices and the array as a whole are obtained. It can be observed that emission is not continuous over the entire ac period, it occurs only twice in each cycle. The emission in both of these phases exhibits different signatures. Cross-talk between the individual devices can be observed through spatially resolved measurements. Funding: SFB 591, GRK 1051.

*Acknowledgement: J. G. Eden and S.-J. Park, Laboratory for Optical Physics and Engineering, University of Illinois, USA for providing arrays.

14:45

RR1 4 Plasma Confinement in Glass Microcavities: Dependence of Plasma Properties on Microcavity Geometry. S.H. SUNG, A.G. BERGER, J.-Y. KIM, S.-J. PARK, J.G. EDEN, DEPARTMENT OF ELECTRICAL AND COMPUTER ENGINEERING, UNIVERSITY OF ILLINOIS, URBANA, IL USA TEAM, Arrays of glass microcavities having diameters of 50-200 μm and controllable geometries have been successfully fabricated by micropowder blasting techniques. Anisotropic or isotropic microcavities, including cavities with ellipsoidal geometry have been fabricated in large scale arrays with high resolution and various shapes of microcavities were prepared precisely. Arrays having as much as 1000 microcavities were fabricated on 400 μm thick soda lime glasses and a pair of these glasses was aligned and sealed to form a closed microdischarge cell. The cross-sectional microcavity shape in the discharge cell is designed from the calculation of electric field distribution. Powered by electrodes located outside the microcavity with ac frequencies of 20-100 kHz, the stable, uniform discharges and confinement of plasma in entire microcavity was observed at 300-800 Torr of noble gases. From the spatially-resolved measurement of emission from a microcavity, the device has better plasma confinement and increased emission intensity in higher gas pressures. Discharge performance in various gas or gas mixtures and its dependence on microcavity geometry will be discussed.

15:00 Student Excellence Award Finalist

RR1 5 Self organization of streamers in a surface DBD: evidence of collective breakdowns K. ALLEGRAUD, N. LEICK, O. GUAITELLA, A. ROUSSEAU, LPTP, Ecole Polytechnique, France Surface dielectric barrier discharges (DBD) are mainly investigated for airflow control. In this paper, surface processes controlling the filament development are studied. Recent results have shown, that in a cylindrical DBD, most of the energy is transferred via few large amplitude current peaks called collective effects [1]. To get further in the study of this phenomenon, electrical measurements and CCD imaging have been performed on a surface discharge, where the plasma filaments are generated onto

the dielectric surface. The plasma is generated via several nearby (but distinct) filaments occurring simultaneously, the current peak duration being a few tens of nanoseconds. The current peak amplitude is proportional to the number of filaments, with a value of about 40 mA/filament. The filament length depends on the applied and breakdown voltages, independently from the current amplitude. The self-organization of the streamer breakdown in adjacent patterns is due to the simultaneous triggering of individual filaments via a collective effect. We suggest that the origin of such a self triggering is due to the photo-desorption of electrons from the surface by a first filament. These electrons then initiate the neighbouring filaments, and all the filaments contribute to the whole charge transfer. [1] O. Guaitella et.al, Phys. D.: Appl. Phys. 39(2006)

15:15

RR1 6 Experimental observations and simulations of single and double barrier DBD plasma actuators* ALAN HOSKINSON, YOUNG-CHUL KIM, NOAH HERSHKOWITZ, University of Wisconsin - Madison When operated in air, a surface-mounted dielectric barrier discharge (DBD) induces flow in the gas just above its surface. In recent years, interest has grown in using these discharges as aerodynamic actuators. We present the results of our experimental and computational studies of how variations in discharge geometry effect both the plasma and the induced electro-hydrodynamic (EHD) force. Our studies primarily focus on double barrier actuators (both electrodes insulated), but make comparisons to single barrier actuators (one electrode insulated). Pitot tube measurements of the induced air flow show the velocity reaches a plateau several kilovolts above the turn-on voltage, and shows only weak variations with the degree of asymmetry between the two electrodes. To explain this behavior, we present time-resolved optical emission measurements of the plasma volume while varying the diameter of one of the electrodes. We also report the results of fluid simulations of discharges with various electrode sizes.

*Work supported by NASA, under Technical Monitor David E. Ashpis, and AFOSR.

SESSION RR2: ELECTRON-MOLECULE COLLISIONS

Thursday afternoon, 4 October 2007; Crystal Ballroom B, Doubletree Crystal City at 13:30
Rich Fernsler, Naval Research Laboratory, presiding

Invited Papers

13:30

RR2 1 Electron-Driven Ionization of Processing Gases: Status and Perspectives.
KURT BECKER, Polytechnic University

In 1985, experimentally determined absolute partial and total electron-impact ionization cross sections for 31 molecules had been reported in the literature [1]. Today, the number of molecules, for which cross sections have been measured, exceeds 100. Experimental ion formation studies have included work involving free radicals and clusters as targets as well as the study of metastable ionic decay routes. Much effort has been devoted to the study of electron-driven ionization of molecules and free radicals of importance to the plasma processing community. These include many halogen-bearing species, but also molecules such as diborane and silane. While a rigorous, fully quantum mechanical theoretical treatment of molecular ionization processes is still impossible (because of the complexity of the ionization process and the complexity of the targets under study), semi-rigorous approaches such as the method of Khare and co-workers, the Binary Encounter Bethe (BEB) approach of Kim and co-workers, and the Deutsch-Märk (DM) formalism (see Ref. [2] for details of these theoretical approaches) have made [2] significant progress. This talk will review recent progress in the experimental (and to a lesser extent theoretical) progress in the field of electron-induced ionization of processing gases. Special emphasis will be placed on recent studies of the electron-impact ionization of Cl-bearing molecules and radicals and the

respective role direct vs. indirect ionization processes for these targets. This work was supported by the Chemical Sciences, Geosciences, and Biosciences Division, Office of Basic Energy Sciences, US Department of Energy. [1] "Electron Impact ionization," T.D. Märk, G.H. Dunn (editors), Springer Verlag: Vienna (1985) [2] H. Deusch, K. Becker, S. Matt, and T.D. Märk, *Int. J. Mass Spectrom.* **197**, 37 (2000)

14:00

RR2 2 Low Energy Elastic Scattering of Electrons from Polyatomic Molecules.*

MURTADHA A. KHAKOO, *Physics Department, California State University, Fullerton, CA 92834*

Measurements and calculations of the elastic scattering of electrons from "large" polyatomic molecules, e.g. alcohols, CH_3OH and $\text{C}_2\text{H}_5\text{OH}$ are presented. These measurements are made possible by using a modified form of the relative flow method which uses a thin aperture source of target gas, instead of the conventional tube sources used in the past. The aperture source provides an angular distribution of gas which is independent of the pressure behind the source, provided the gas mean-free path does not exceed the aperture thickness. This property has been tested using C_2H_2 , N_2 and He [1]. The experimental data were taken at incident energies of 2eV, 5eV, 10eV, 15eV, 20eV, 30eV, 50eV and 100eV. The theory uses the variational multi-channel Schwinger method with polarization effects [2], and very good agreement between experiment and theory is observed in general. The talk will focus on the experimental implementation of the modified relative flow method and its validity. [1] M. A. Khakoo, K. Keane, C. Campbell, N. Guzman and K. Hazlett, *Low Energy Elastic Electron Scattering from Ethylene*, submitted to *J. Phys. B.* June-2007. [2] C. Winstead and V. McKoy, *Adv. At. Mol. Opt. Phys.* **36**, 183 (1996).

*Funded by the National Science Foundation, Atomic, Molecular and Optical Physics Division under Collaborative Grant Number 0653452 with Drs. B. V. McKoy and C. Winstead, Caltech University, Pasadena, CA 91125.

14:30

RR2 3 Electron Scattering from Molecules.*

MARCO LIMA, *UNICAMP*

Cross sections for low-energy electron-molecule scattering compose a relevant data basis for modeling discharge environments and for understanding important astrophysical and biological phenomena. In this talk I will present our progress with the Schwinger multichannel (SMC) method with pseudopotential (M. H. F. Bettega, L. G. Ferreira, and M. A. P. Lima, *Phys. Rev. A* **47**, 1111 (1993)) recently implemented with a better description of the target (R. F. da Costa, F. J. da Paixão and M. A. P. Lima, *J. Phys. B* **37**, L129 (2004)) to study electronically inelastic processes in electron-molecule scattering. Motivated by the relative success of our applications for H_2 (R. F. da Costa, F. J. da Paixão and M. A. P. Lima, *J. Phys. B* **38**, 4363 (2005)) and N_2 (R. F. da Costa and M. A. P. Lima, *Int. J. Quantum Chem.* **106**, 2664 (2006); *ibid*, *Phys. Rev. A* **75**, 022705 (2007)) molecules, we have obtained inelastic cross sections for few electronic states of CO , C_2H_4 , $\text{C}_4\text{H}_4\text{O}$, and two important alcohols, CH_3OH and $\text{C}_2\text{H}_5\text{OH}$. For e-furan scattering processes (M. H. F. Bettega and M. A. P. Lima, *J. Chem. Phys.* **126**, 194317 (2007)) I will discuss the influence of low-lying electronic states on the elastic cross sections and more important, the influence of polarization effects on the electronic excitation of these states by electron impact. For ethanol and methanol molecules I will show a comparative study for elastic and electronic inelastic processes that is being carried out within an international effort involving three Brazilian and two American groups.

*Brazilian Agencies Fapesp and CNPq.

Contributed Papers

15:00

RR2 4 Electron cooling rates in the atmospheres of Mars and Venus

LAURENCE CAMPBELL, MICHAEL BRUNGER, ARC Centre for Antimatter-Matter Studies, Flinders University THOMAS RESCIGNO, Lawrence Berkeley National Laboratory, Berkeley
Vibrational excitation of molecules by electron impact, followed by radiative decay, is a cooling mechanism in planetary atmospheres. As carbon dioxide is the dominant constituent below 200 and 140 km in the atmospheres of Mars and Venus respectively, the electron cooling rates for CO_2 are required in modeling

the atmospheres of these planets. Such cooling rates were determined many years ago, but new measurements and calculations of the electron impact cross sections have since become available. There have also been new measurements of the atmospheric parameters, such as of the electron density on Mars, that are required in the calculations. Therefore we have assembled a new data base of electron impact cross sections for CO_2 , based on the more recent measurements and calculations, and used it to calculate electron cooling rates for Mars and Venus. One result is that we predict a larger cooling rate for the altitude range 100–150 km in the Martian atmosphere. This may explain why temperatures observed in this region are less than predicted.

15:15

RR2 5 Absolute elastic cross sections for intermediate energy electron scattering from CF_2 radicals* LEIGH HARGREAVES, JESSICA FRANCIS-STAITE, TODD MADDERN, MICHAEL BRUNGER, *Centre for Antimatter-Matter Studies, SoCPES, Flinders University, Adelaide, Australia* STEPHEN BUCKMAN, *Centre for Antimatter-Matter Studies, Australian National University, Canberra* We report on differential and integral elastic cross sections for electron scattering from CF_2 radicals. The energy range of the present measurements is 20-50 eV, while the angular range of the differential cross sections is 20-135°. A full description of the new apparatus, and the techniques that were used to make these measurements, will be given at the meeting.

*Supported by the Australian Research Council.

15:30

RR2 6 Total and total ionization cross sections for NH_x and NF_x ($x = 1, 2$ and 3) on electron impact* C.G. LIMBACHIYA, *P.S. Science College, Kadi, INDIA - 382 715* M. VINODKUMAR, *V.P. Science College, V.V. Nagar, INDIA - 388 120* S. GANGOPADHYAY, K.N. JOSHIPURA, *Dept. of Physics, S.P. Uni. V.V. Nagar, INDIA - 388 120* Electron-impact induced ionization cross-sections for NH_3 and NF_3 and their chemically reactive free radicals, NH_x & NF_x ($x = 1, 2$) are relevant to processes in planetary & cometary atmospheres. In this paper we have reported the total (complete) and total ionization cross sections for molecules NH_x and NF_x ($x = 1, 2$ and 3) on electron impact from threshold to 5 keV. We used complex optical potential formalism (SCOP) [1] to calculate the total inelastic cross sections Q_{inel} and total (complete) cross sections Q_T . Q_{inel} includes Q_{ion} and we have developed a semi-empirical method, Complex Scattering Potential - ionization contribution (CSP-ic) to extract ionization cross sections Q_{ion} from calculated Q_{inel} [2]. [1] M. Vinodkumar, K.N. Joshipura, C.G. Limbachiya & B.K. Antony, *Eur. J. Phys. D.* **37** 67 (2006) [2] M. Vinodkumar, K.N. Joshipura, C.G. Limbachiya & B.K. Antony, *Phys. Rev A* **74** 022721 (2006)

*CGL, MVK thank UGC, KNJ thanks ISRO-India for research grants.

SESSION SRP1: POSTER SESSION III

Thursday afternoon, 4 October 2007

Crystal Ballroom C, Doubletree Crystal City at 16:00

SRP1 1 MATERIALS PROCESSING IN LOW PRESSURE PLASMAS: ETCHING, DEPOSITION, NEW MATERIALS

SRP1 2 Plasma Etching of Extremely High Aspect Ratio Features: Twisting Effects* MINGMEI WANG, ANKUR AGARWAL, YANG YANG, MARK J. KUSHNER, *Iowa State University* Plasma etching of small features having very large aspect ratios allows only a marginal CD variation. Etching extremely high aspect ratios (~ 100) necessitates obtaining a uniform

plasma density with high energy ions to mitigate the effect of energy losses due to sidewall impacts. Undesirable behavior such as tapering and twisting has been observed in etching of such features. Twisting is the sometimes sudden turning of a via or trench from the vertical to a side angle which occurs nearly randomly. For example, of three adjacent features, only one may display the behavior. One theory on the source of twisting is charging within and adjacent to the feature. In this talk, results from a computational investigation of plasma etching of extremely high aspect ratio features will be discussed. The 2-d Hybrid Plasma Equipment Model was linked with the Monte Carlo Feature Profile Model (MCFPM) to assess the effect of charging on the etching of high aspect ratio features. The MCFPM was modified to include the effects of charging by electrons and ions, including solution of Poisson's equation and conduction current through solid materials. Results will be discussed for an electron cyclotron resonance plasma reactor etching of SiO_2 in fluorocarbon plasmas.

*Work supported by Micron Inc. and Semiconductor Research Corp.

SRP1 3 Potential fluctuation induced by discrete particle effect in a nano-scale trench TAESANG LEE, *Korea Advanced Institute of Science and Technology* SEONGSIK KIM, *National Fusion Research Center* CHOONGSEOCK CHANG, *Korea Advanced Institute of Science and Technology* A simplified two-dimensional Monte Carlo simulation is performed to investigate the electric field fluctuations caused by strong Coulomb interactions between discrete particles in nanometer scale trenches. It is found that the discrete particle effect should be an important part of the nano-scale trench physics, raising the ion orbit scatterings in the trench, enhancing the ion deposition on the side walls, and dispersing the material contact energy of the incidence ions.

SRP1 4 Sheath control with plasma wall bias for the collimated ion beam generation SEUNGHOON PARK, TAESANG LEE, HOYUL BAEK, *Department of Physics, KAIST* CHOONGSEOCK CHANG, *Department of Physics, KAIST and Courant Institute, NYU* It is important to find collimated ion beam condition for neutral beam generation. Ion beam quality is dependent of acceleration grid hole geometry and plasma properties. We focus on dependence on plasma properties such as sheath dynamics. In order to form sheath in high density plasma, ICP like heating is modeled and 2D particle in cell (PIC) simulation is performed. It is confirmed that the sheath is deformed by plasma density and Sheath is able to be controlled by plasma wall bias.

SRP1 5 Low-Temperature, Remote Plasma Oxidation of SiC for MOS Device Applications. J.M. WILLIAMSON, B.A. TOLSON, *Innovative Scientific Solutions, Inc., Dayton, OH* S.F. ADAMS, J.D. SCOFIELD, *Air Force Research Laboratory, Wright-Patterson AFB, OH* Silicon carbide is considered a promising semiconductor material for high-frequency, high-power, and high-temperature devices because of its large band gap, high thermal conductivity, high breakdown strength and large saturated electron drift velocity. The performance of SiC metal oxide semiconductor (MOS) devices is limited by the defect density of the semiconductor/oxide interface. High-temperature thermal oxidation leaves carbon impurities at the SiC/SiO₂ interface resulting in high defect state densities with concomitant lower channel conductivity and decreased device efficiency. To circumvent the high

sample temperatures used in thermal oxidation, plasma assisted oxidation of SiC wafers was investigated using O₂/Ar gas mixtures in a remote microwave plasma reactor. Results will be presented for the electrical and material properties of oxide layers as a function of gas mixture, surface temperature, and substrate bias. These results will be correlated with plasma properties determined by in-situ optical diagnostics.

SRP1 6 Modification of Biased Bulk Nb Surface with Ar/Cl₂ Microwave Discharge Plasma* J. UPADHYAY, M. RASKOVIC, S. POPOVIC, L. VUSKOVIC, *Department of Physics, Old Dominion University, Norfolk, VA* Microwave glow discharge in Ar/Cl₂ mixture was used for plasma treatment of bulk niobium surface. The samples were connected to a negative d.c. and radio-frequency bias. This treatment consisted of simultaneous sputtering, favored by sheath formation, and etching, favored by the presence of reactive chlorine atoms. Both of these processes enable the removal of impurities and increase smoothness of the Nb surface [1]. The rate of surface removal was correlated with the concentration of Cl radicals (Cl, Cl⁺, Cl⁻) in the discharge and the temperature of sample. To determine these parameters we developed a set of techniques for a comprehensive plasma characterization. Optical and electrical methods were used to determine plasma parameters. Plasma emission actinometry was used to estimate the absolute densities of Cl, Cl⁺ and Cl₂ under the discharge conditions optimal for the surface treatment. [1] M. Raskovic, et al., Nuclear Instruments and Methods in Physics Research A 569 663-670 (2006).

*Supported by DOE

SRP1 7 Titanium Nitride Coatings Prepared by Reactive Sputtering on Steel SAOULA NADIA, *CDTA, DMIL, PO. Box 17 Baba hassen, Algiers, Algeria* HENDA KARIM, *CDTA KESRI RAFIKA, USTHB, LECTCM, PO. Box 32 El Alia, BabEzzouar, Algiers, Algeria* Titanium nitride is used as coating on cutting tools because of their excellent mechanical properties such as high hardness and high wear resistance. Its chemical inertness gives rise to its application as corrosion protective coating. It's an excellent barrier material with good electrical conductivity in various metallization structures of advanced microelectronic devices. Finally, the golden glance of TiN established its use as decorative coating in the fashion jewellery and in architecture. The deposition process studied, in this work, use RF sputtering of a pure titanium target in a reactive nitrogen/argon gas mixture, at various conditions. The substrates are steel. The main variables investigated are the composition of the Ar/N₂ gas mixture, the total pressure, the deposition time and the discharge power. The aim of this work is to evaluate the performances of a local-made RF plasma reactor. The attention was given to the study of the structure, the composition of titanium nitride deposits, which have a considerable influence on their hardness. The deposited coatings were characterized by X-ray diffraction, energy dispersive spectroscopy (EDS) and micro-indentation.

SRP1 8 Direct liquid droplet injection for PECVD* D. OGAWA, M. GOECKNER, A. SRA, *UT Dallas* R. TIMMONS, *UT Arlington* L. OVERZET, *UT Dallas* Plasma enhanced chemical vapor deposition (PECVD) is a versatile technique for depositing thin films. For common PECVD, vapor phase precursors have been required. This limitation has led to several methods for allowing the use of low-vapor pressure precursors; for example,

entrainment of the precursor vapor in a heated gas flow using bubblers or vaporization sources is common. We are using a new approach, mixing the low vapor pressure precursor into a high vapor pressure solvent and directly injecting the mixture into the low pressure plasma environment as micro-droplets using an automotive fuel injector. We have gone as far as to inject nanoparticles of iron into the plasma by suspending them in hexane (or ethanol). In fact, we believe that metals, dielectrics, superconductors, aromatics, proteins, viruses, etc. could all potentially be injected into low pressure plasma environments using this simple and effective technique. Control over the liquid injection is possible using either the differential pressure across the fuel injector or the time the injector is open. The resulting films formed by the plasma decomposition of the high vapor pressure fluid contain the nanoparticles suspended in the film matrix. We will show that the deposited film depends on the pressure, injection rate and plasma conditions.

*Supported in part through SPRING/AFOSR grant FA9550-05-1-0393.

SRP1 9 Modeling the direct injection of liquid droplets into low-pressure environments and plasmas I. SARAF, M. GOECKNER, L. OVERZET, *UT Dallas* A model for the evaporation of micron-sized liquid droplets injected into low pressures and plasmas is being developed. This model differs from higher pressure models in that it assumes the mean free path is greater than the droplet diameter and therefore allows one to assume that the transport is non-diffusive. The model accounts for both particle and heat flux into and out of the droplet (by collisions with gas molecules, evaporation and the return of molecules {freeze-on}). With the addition of plasma, several other terms are added (ion bombardment, recombination etc.). The model runs in Matlab and indicates that the time required for the droplet to fully evaporate is a function of the background pressure, initial (wall) temperature, the number of droplets inserted simultaneously and initial size. A typical evaporation time for a 50 micron diameter droplet is 7 seconds for hexane and up to 25 seconds for ethanol without plasma. Upon insertion into the low pressure environment, the temperature of the droplet decreases quickly as the first few microns evaporate. The temperature falls to a minimum value, generally below the freezing point where the heat flow balances. This sets the evaporation rate and explains why the evaporation time decreases with increasing the pressure, the number of droplets and the initial droplet temperature. Supported in part by SPRING/AFOSR Grant FA9550-05-1-0393.

SRP1 10 PLASMA DIAGNOSTICS: OPTICAL, ELECTRICAL, OTHER

SRP1 11 Ion Energy Measurements in Continuous Electron Beam-Generated Plasmas* SCOTT WALTON, EVGENIYA LOCK,† RICHARD FERNSLER, *Plasma Physics Division, Naval Research Laboratory, Washington, DC 20375* The US Naval Research Laboratory has developed a plasma processing system that relies on a magnetically collimated, sheet of multi-kilovolt electrons to ionize the background gas and produce a planar plasma. High-energy electron beams are efficient at producing high-

density plasmas ($n_e > 10^{10} \text{ cm}^{-3}$) with low electron temperatures ($T_e < 1.0 \text{ eV}$) over the volume of the beam, resulting in large fluxes of low-energy ions ($< 5 \text{ eV}$) at surfaces located adjacent to the electron beam. In this work we present plasma diagnostic results using a recently developed, continuous electron beam source. In this work, an energy-resolving mass spectrometer is used to determine the ion energies and fluxes at electrodes located adjacent to the electron beam. These measurements are made as a function electron beam intensity and energy, and electrode bias in argon, nitrogen, and their mixtures at various total pressures. We employ both DC and RF biasing schemes in an effort to provide well-controlled incident ion energies for applications requiring both low and high ion energies. The results of this work are related to bulk plasma properties determined using Langmuir probe diagnostics (See paper by E.H. Lock et al. at this conference).

*This work is supported by the Office of Naval Research.

†NRL/NRC Postdoctoral Research Associate

SRP1 12 XUV Spectroscopic Diagnostics for Microplasma Research DAN STUTMAN, MICHAEL FINKENTHAL, *Johns Hopkins University* Microplasmas are high density, dc or pulsed discharges produced in cavities having 10-100 μm typical size. Although spectroscopy is the best tool for their characterization, important plasma parameters such as electron density, temperature, energetic electron fraction and impurity content are difficult to measure using visible light emission. Since the bulk microplasma emission is expected to be in the XUV ($\approx 100\text{-}1500 \text{ \AA}$), we study the possibility of adapting XUV diagnostics developed for magnetically confined plasmas, for use in microplasma research. For instance, a tool that could enable, with appropriate modeling, the characterization of the EEDF in dc microplasmas would be a transmission grating XUV 'radiometer' that measures the spectral distribution of the emitted power. Also a device based on 'multi-energy' filtered photodiodes, similar to that we developed for fast temperature diagnostic in tokamaks, could be used for EEDF characterization in pulsed microplasmas. In addition, the proposed diagnostics will enable new research directions, such as the study of turbulent fluctuations. To benchmark the XUV emission models for microplasma application, we propose to use a scaled-up macroscopic hollow cathode discharge, in which conventional diagnostics can be used for reference measurements of the bulk density, temperature and non-thermal component.

SRP1 13 Electrical diagnostic of a magnetized RF discharge in CH_4 created by a multihole cathode used for a-C:H deposition films. DJEROUROU SAMIRA, OURCHABANE MOHAMED, HENDA KARIM, *Centre de Développement des Techniques Avancées* The present work is carried out in the context of the electrical study of a reactor used for a-C:H deposition. We have studied the influence of the operation system parameters (incident power, pressure and magnetic field) on the self-bias voltage and on the saturation ion current density. These measurements have been made over a wide range of incident power inputs of 50-300 W and pressures of 20-100 mTorr. For electrical diagnostic, the results obtained showed that the energy and ion flow bombarding the substrate presented a maximum values at high incident power and decreased with pressure. A comparative study between confined and unconfined discharges showed that the magnetic field

had a significant influence on the electric parameters of the discharge. The first correlation between electrical parameters and a-C:H deposition was found, polymer-like thin films with high deposition rates can be obtained at low pressure and with grounded substrate holder.

SRP1 14 Density and lifetime evaluation of weakly ionized plasma for laser-triggered lightning by means of laser absorption MICHITERU YAMAURA, *Institute for Laser Technology* The potential ability of lasers to control lightning can be improved by using a train of pulses with sub-millisecond separations [1-2]. Laser-triggered experiments in a small-scale (10 mm gap) atmospheric discharge facility show that the triggering is dramatically enhanced when a five-pulse train of sub-Joule energy is used instead of a single pulse. This effect increases rapidly as the pulse interval is reduced. It appears that at a sub-millisecond pulse interval, sufficient positive and negative ions survive in subsequent pulses, thus enabling easy deionization. Hence, significant plasma build-up occurs from one pulse to the next. However, this persistence of ions would appear to imply that the rate of recombination (effectively a charge transfer between ions) is considerably lower than previously believed. [1] M. Yamaura: *Appl. Phys. Lett.* **88** 251501 (2006). [2] M. Yamaura: *J. Appl. Phys.* **98** 043101 (2005).

SRP1 15 Measuring the Ion Flux to Deposition Substrate in Hollow Cathode Plasma Jet* PETR VIROSTKO, ZDENEK HUBICKA, PETR JELINEK, MARTIN CADA, PETR ADAMEK, *Institute of Physics of the Academy of Sciences of the Czech Republic, v. v. i.* MILAN TICHY, *Charles University in Prague* Different electrical methods of obtaining negative bias of deposition substrate and measuring the resulting positive ion flux in DC and DC pulsed hollow cathode plasma jet deposition system are compared. Ion fluxes are determined for pulse-modulated and continuous RF (13.56 MHz), and for pulsed DC bias of the substrate for different bias and discharge conditions. An electrical model of the feed line to the substrate is proposed to determine RF current and voltage waveforms on the RF biased substrate from the waveforms measured outside of the reactor chamber. The resulting RF current waveforms are compared to a fluid numerical model of an RF biased electrode. The ion fluxes determined from the discharging of capacitor in series with the substrate in pulse-modulated RF bias are comparable with those measured for pulsed DC bias, while ion fluxes determined for continuous RF bias differ significantly. Possible explanations of this discrepancy are discussed.

*Supported by projects KAN400720701 and KJB100100707 of ASCR and by project GA202/06/0776 of GACR.

SRP1 16 Electron-Beam Generated Air Plasma: Electrical and Optical Diagnostic Details ROBERT VIDMAR, *University of Nevada, Reno* KENNETH STALDER, *Stalder Technologies and Research* Diagnostics associated with a pulsed 1-ms 100-keV 20-mA electron beam that generates air plasma are discussed. A mesh sensor measures the beam current up-stream to an electron-beam transmission window. The transmission window separates the electron source from a 400-liter test cell, operated from 1 mTorr to 635 Torr using laboratory air. 10-GHz RF amplitude and phase measurements quantify electron density. A diode array spectrometer is used to measure optical emissions from the plasma typically dominated by neutral and ionic nitrogen emissions. UV absorption at 254 nm is used to detect ozone. Concentrations of

other species such as H_2O , CO_2 , CO , NO , and N_2O are monitored by tunable diode laser absorption spectroscopy. Data from these diagnostic systems, obtained during a single shot, will be discussed and compared. This work is supported by the Air Force Research Laboratory under grant numbers FA9550-04-1-0015 and FA9550-04-1-0444; and State of Nevada matching funds.

SRP1 17 The role of Oxygen triplets in plasma diagnostic
VLADIMIR MILOSAVLJEVIC, ALBERT ELLINGBOE, STEPHEN DANIELS, *NCPST, DCU, Ireland* The oxygen 777nm triplet is very important for the measurement of atomic oxygen in low pressure plasmas, since the 777.42nm spectral line is frequently used for actinometry. Cascade processes from the 6s and 5s energy states to the upper level of the 777nm triplet correlate with errors in the measurement of atomic densities. In this paper we present the intensity dependence of the oxygen 777 (777.19nm, 777.42nm, 777.54nm), 543 (543.69nm, 543.58nm, 543.52nm) and 645 (645.60nm, 645.44nm, 645.36nm) triplets on plasma chemistry. The spectral lines from the 777 triplet belong to the transition $3s-3p$ and multiplet $^5S^0-^5P$. They have same lower energy (E_f) level of 9.15eV, with upper energy (E_i) levels of about 10.74eV. The lines from the 543 and 645 triplets have different E_i levels; for the 543 triplet all spectral lines have $E_i=13.02eV$, while for the spectral lines from the 645 triplet E_i are 12.66eV. The E_f level for spectral lines from the 645 and 543 triplets are E_i level for spectral lines from the 777 triplet. The experiment are performed in a Inductive plasma source operated at 13.56MHz, with 4MHz substrate bias. Working gases are Ar- O_2 - C_4F_8 mixtures, with the addition of helium at the back side of a Oxide coated wafer. Gas pressure is varied from 2 to 6 Pa; flows of 300sccm of Ar and O_2 and C_4F_8 are both varied from 0 to 20 sccm. Source power is varied from 0 to 600 W, and bias power from 0 to 1200 W.

SRP1 18 Comparison of helium two-step plasma emission with that predicted from measured cross sections* C.A. DEJOSEPH, JR., *Air Force Research Laboratory, WPAFB, OH* V.I. DEMIDOV, J.C. BLESSINGTON, *West Virginia University* Plasma emission from the afterglow of a low pressure, 100% modulated, rf discharge, can originate from collisions between metastable atoms and fast electrons. The fast electrons are generated by collisions between pairs of metastables (Penning ionization of one metastable by another) and collisions of metastables with slower electrons (collisions of the second kind). Using time-resolved Langmuir probe data, we have measured the electron energy distribution function (EEDF) containing these fast electrons in a helium afterglow. The EEDF data were used, along with measured excitation cross sections out of the $2s^3S$ metastable level [1], to predict relative intensities of various He emission lines seen in the afterglow. A comparison between the measured and predicted emission will be presented. [1] Boffard, J. B., Lagus, M. E., Anderson, L. W., and Lin, C. C., *Phys Rev. A* **59** (1999) 4079.

*This work supported in part by the Air Force Office of Scientific Research.

SRP1 19 Probe measurements in electronegative plasmas: modeling the perturbative effects of the probe* E.A. BOGDANOV, A.A. KUDRYAVTSEV, K. YU. SERDITOV, *St. Petersburg State University, St. Petersburg, Russia* C.A. DEJOSEPH, JR., *AFRL, Wright-Patterson AFB, OH* V.I. DEMIDOV, *UES, Dayton, OH* A basic property of an electronegative plasma is its separation into two distinct regions: an ion-ion region far from boundaries and a near-boundary electron-ion region, where negative ions have practically negligible density. This is due to the influence of the ambipolar electric field, which depends on electron (not negative ion) plasma parameters. This electric field "holds off" negative ions from the boundary, as the ions have lower mobility and temperature compared to the electrons. Therefore, negative ions will be repelled by any object inserted into the plasma. This can lead to errors in measurements of negative ion parameters by any invasive method. Numerical modeling of electric probes in an argon-oxygen plasma clearly demonstrates possible errors of direct measurements of negative ion current. This can also affect results from the photo-detachment method and direct measurements of negative ion energy distribution.

*This work supported in part by AFOSR and CRDF.

SRP1 20 Electrostatic probe measurement and estimation of the electronegativity for low-pressure inductively coupled SF_6 and O_2 plasmas TAE HUN CHUNG, SUN YOUNG KANG, EUN YOUNG KIM, *Dong-A University* Electrostatic probe measurements for low-pressure inductively coupled SF_6 and O_2 plasmas are performed. From the probe I-V curves, we measure the electron saturation current, the positive ion saturation current, and the electron temperature. By using the ratios of these parameters at three adjacent pressure points, we calculate the electronegativity of the discharges at those pressures. By using the electronegativity and the electron density measured from probe I-V curve, we estimate the negative ion density. The positive ion density is calculated either by the Laframboise OML theory or by the sum of the electron density and the negative ion density. The validity of this approach is discussed and compared to other methods in estimating the negative ion density. The variations of the charged species density with pressure and power are investigated. In addition, mass spectra of SF_6 and O_2 plasmas are obtained to determine the various species in the discharge and the effective mass of the positive ions.

SRP1 21 Behavior of Excited Oxygen Atoms in Rare gas mixture O_2 Surface Wave Excited Plasma KEIGO TAKEDA, SEIGO TAKASHIMA, MASARU HORI, *Nagoya University* Excited oxygen atom ($O(^1D_2)$) has attracted very much on the oxygen-based plasma processes, such as plasma oxidation, surface cleaning, resist ashing, etc. Since it is supposed that the $O(^1D_2)$ atom is the most reactive species in all species in the oxygen-based plasma. Therefore, it is strongly required to investigate the behaviors of $O(^1D_2)$ atom in the oxygen-based plasmas, the quantitative information of $O(^1D_2)$ atom have never been clear, because the convenient light sources for absorption spectroscopic techniques of $O(^1D_2)$ atoms have not developed. The vacuum ultraviolet laser absorption spectroscopy (VUVLAS) has a great potential to measure the atomic radicals in the process plasmas. Therefore, in this study, we have measured the absolute density of $O(^1D_2)$ atom in the rare gas mixture O_2 surface wave excited oxygen plasma (SWP) by using VUVLAS with tunable VUV laser. The absolute densities of $O(^1D_2)$ atom in the O_2/Ar and O_2/Kr SWPs were

evaluated as a function of various plasma conditions. From these results, the O₂/Ar SWP has a potential to realize the high O(¹D₂) atom density compared with the O₂/Kr SWP and the density in the O₂/Ar SWP was the maximum around $2 \times 10^{12} \text{ cm}^{-3}$ at the high Ar flow rate ratio and low pressure.

SRP1 22 Radical density measurement in VHF C₂F₆/H₂ plasma used for carbon nanowall growth MINEO HIRAMATSU, SATORU KATO, *Meijo University* HAJIME SASAKI, WAKANA TAKEUCHI, SHINGO KONDO, *Nagoya University* KOJI YAMAKAWA, *Katagiri Engineering* MASARU HORI, *Nagoya University* Carbon nanowalls (CNWs), two-dimensional carbon nanostructures consisting of plane graphene layers standing on the substrate, have been grown recently. The large surface area and thin edges of CNWs would provide potential applications in energy storage, as electrodes for fuel cells and field emission display. The morphologies and growth rate of CNWs depend on the types of carbon source gases and the amount of H atoms injected. In this work, CNWs were fabricated using VHF C₂F₆ PECVD with H radical injection, which was developed for the large-area growth of CNWs with reasonable growth rate. This system consists of a parallel-plate VHF (100 MHz) capacitively coupled plasma (CCP) region and a surface wave microwave (2.45 GHz) excited H₂ plasma as a radical source. A carbon source gas (C₂F₆) was introduced into the VHF CCP region. By using this system, the heated substrate was showered with fluorocarbon radicals as well as plenty of H atoms in a controlled manner. Absolute H and C atom densities in the plasma were measured by vacuum ultraviolet absorption spectroscopy as functions of input power and pressure in order to investigate the growth mechanism of CNWs. The correlation between CNW growth and radical densities was discussed.

SRP1 23 Measurements of electron temperature and argon metastable density by measuring optical emission in inductively coupled plasma.* YOUNG-KWANG LEE, KWANG-TAE HWANG, MIN-HYONG LEE, CHIN-WOOK CHUNG, *Hanyang University* To obtain electron temperatures and argon metastable number densities at various powers (100 W to 1 kW) and pressures (2 mTorr to 20 mTorr), a spectroscopic method [1] is used. The method is based on the availability of experimental relative emission intensities of only four argon lines that originate from 4p argon levels. Electron temperatures measured by the optical emission lines are compared with those by a Langmuir probe. They were in close agreement. Furthermore, the metastable densities from the model were estimated and presented. [1] D. Mariotti, Y. Shimizu, T. Sasaki, N. Koshizaki, *Appl. Phys. Lett.* 89, 201502 (2006)

*OES diagnostics metastable icp

SRP1 24 Langmuir probe perturbation in plasma distribution measurement in an inductively coupled plasma SUNGHO JANG, JINSUNG KIM, KYEONGHYO LEE, CHINWOOK CHUNG, A single Langmuir probe system [SLP2000TM, Plasmat, INC] was used for the measurement of radial density. The probe was located at 4cm below a dielectric window and the measurement was carried at 25mTorr at various rf powers (13.56MHz). It was found that symmetric radial density distribution becomes asymmetric as rf power increases. To investigate the

cause of this asymmetric density distribution, a wise probe TM(P&A Solutions) that can measure plasma densities and the electron temperatures in real-time was installed on the chamber wall. At high rf powers, as the probe body goes in, the plasma density measured by the wise probe is decreased. This indicates that whole plasma density is affected by the probe intrusion. It appears that the Langmuir probe passes through the skin layer and the probe body impedes electron heating process in the skin layer. The probe measurement method to avoid this perturbation is presented.

SRP1 25 Effect of multiphoton ionization in laser Thomson scattering measurements A. KONO, K. FUKUYAMA, M. ARAMAKI, *Nagoya University* In laser Thomson scattering measurements of electron density and temperature, one should be careful about production of electrons in the scattering volume via laser irradiation. It is generally assumed that Ar plasma is free from such laser perturbations. However, in our measurements for inductively coupled Ar plasma using a frequency-doubled YAG laser (532 nm), Thomson scattering spectra obtained from measurements with different laser energy densities at the focal point differ significantly, when the discharge power is low and hence the ratio of the metastable Ar atom density to the electron density is relatively large. This suggests that multiphoton ionization of metastable Ar atoms may affect the measurement significantly. To clarify the phenomenon, an experiment for determining the ionization yield at the laser focal point in the Ar gas containing a known concentration of metastable Ar atoms is being carried out. The laser beam is focused at the center of a small dc-biased parallel-plate probe and the laser-induced probe current is measured. Preliminary measurements indicate successful detection of the current due to multiphoton ionization of metastable Ar atoms, the efficiency of which is to be quantified. (Work supported by Grant-in-aid 18540491 from MEXT Japan.)

SRP1 26 Electrical characteristics and comparison of two configurations of plasma needle GORDANA MALOVIC, NEVENA PUAC, SASA LAZOVIC, *Institute of Physics, Belgrade, Serbia* ANTONIJE DJORDJEVIC, *School of Electrical Engineering, Belgrade, Serbia* ZORAN PETROVIC, *Institute of Physics, Belgrade, Serbia* Nonequilibrium plasmas is proved to be able to produce chemically reactive species at a low gas temperature while maintaining uniform reaction rates over relatively large areas. Plasma needle is one of the atmospheric pressure sources that can be used for treatment of living matter which is highly sensitive when it comes to low pressure or high temperatures (above 40[r]C). Before any application, it is necessary to examine the properties of such source as well as possible and define the optimum conditions for the specific treatment. For that purpose, it is particularly important to know electrical characteristics of the plasma needle, i.e., the power transmitted to the plasma. In order to achieve that, we have developed derivative probes previously used by Puac *et al.*[1] for measuring transmitted power in low pressure CCP RF discharge. In this paper we will make a comparison between two configurations of plasma needle that we have used in treatment of biological samples. Difference between these two configurations lays in additional copper ring that we have placed around glass tube at the tip of the needle. [1] Puac *et al.*, *Plasma Processes and Polymers*, Eds. R. d'Agostino, P. Favia, C. Oehr and M.R. Wertheimer, (Wiley: (2005) p 193-203.

SRP1 27 Measurement of the electron temperature on microwave surface wave plasmas powered by the radial-line slot antenna MINKYU KIM, LEE CHEN, *Tokyo Electron* A Langmuir probe measurement system was built to study the surface wave plasma produced by radial-line slot antenna (RLSA) [1]. The measurements were performed on the bulk plasma under wide ranges of pressure (50 – 1000 mTorr) and power (1 – 5 kW). General characteristics of surface wave plasma were shown in the measurements through the I-V curve analysis. The electron temperature is low, ~ 1 eV, and the plasma densities is high, $\geq 10^{11}$ cm $^{-3}$. Additional higher electron temperatures were shown in the I-V curves. This second electron temperature shown in the IV curves has different trend from the lower electron temperature. The second temperature is a function of pressure. When the pressure increases, the second electron temperature also increases. EEDF/EPPF analysis is also performed to study the trend of the second electron temperatures. [1] C. Tian, T. Nozawa, K. Ishibasi, H. Kameyama, and T. Morimoto, "Characteristics of large-diameter plasma using a radial-line slot antenna," *J. Vac. Sci. Tech. A24*, Vol. 4, Jul. 2006.

SRP1 28 Langmuir probes in flowing plasmas PETER SHEERIN, MILES M. TURNER, *Dublin City University* Electrostatic probes are a classic method for inferring plasma parameters in many circumstances. Such probes are not easy to interpret when the plasma is flowing with respect to the probe, because there is not a clear theory based on elementary assumptions. Mach probes are a commonly accepted method, but the theory of such probes is not clearly founded on first principles. This paper considers an alternative theory, which is firmly based on first principles. We discuss the basis of this approach, and we present self-consistent particle-in-cell simulations with two space-dimensions as a benchmark for the analytical theory. In particular, we discuss the validity of the theory in the limit of small Mach number, which is the critical case.

SRP1 29 Surface analysis by plasma assisted desorption ionization mass spectrometry (PADI-MS) Y. ARANDA GONZALEVO,¹ T. D. WHITMORE,¹ P. J. HATTON,¹ M. E. BUCKLEY,¹ D. SEYMOUR,¹ C. L. GREENWOOD,¹ J. A. REES,¹ L. V. RATCLIFFE,¹ D. A. BARRETT,² F. J. M. RUTTEN,³ M. R. S. MCCOUSTRA,⁴ ¹Plasma & Surface Analysis Division, Hiden Analytical Ltd., 420 Europa Boulevard, Warrington, UK ²School of Pharmacy, University of Nottingham, University Park, Nottingham, NG7 2RD, UK ³School of Pharmacy and iEPSAM, Keele University, Keele, Staffordshire ST5 5BG, UK ⁴School of EPS-Chemistry, Heriot-Watt University, Edinburgh, EH14 4AS, UK Plasma assisted desorption/ionization mass spectrometry (PADI-MS) is a surface analysis technique that yields sample information under ambient conditions of pressure and humidity without any surface preparation. It is achieved by directing a non-thermal atmospheric plasma onto the surface of interest. Desorption occurs from the surface and the subsequent ionization products are detected in real time by using an atmospheric sampling quadrupole mass spectrometer. We have demonstrated the detection of active ingredients in a range of pharmaceutical and other samples, demonstrating the potential of the technique for high throughput screening in a pharmaceutical or forensics environment.

SRP1 30 IONIZATION OF ATOMS AND MOLECULES

SRP1 31 Comparison of Ion Chemistries in Octafluoro-2-butene (2-C₄F₈) and in Octfluorocyclobutane (c-C₄F₈)* CHARLES JIAO, *ISSI, Dayton, OH* CHARLES DEJOSEPH, ALAN GARSADDEN, *Air Force Research Laboratory, WPAFB, OH* 2-C₄F₈ is one of the promising candidates to replace c-C₄F₈ that has been widely used for dielectric etching but is not environmentally friendly. In this study we have investigated electron impact ionization and ion-molecule reactions of 2-C₄F₈ using Fourier transform mass spectrometry (FTMS), and compared the results with those of c-C₄F₈ we have studied previously. Electron impact ionization of 2-C₄F₈ produces 15 ionic species including C₄F_{7,8}⁺, C₃F_{3,5,6}⁺, C₂F₄⁺ and CF₁₋₃⁺ as the major ions. The total ionization cross section of 2-C₄F₈ reaches a maximum of 1.8x10⁻¹⁵ cm² at 90 eV. The ionization is dominated by the channel forming the parent ion C₄F₈⁺ from 12 to 18 eV, and by the channel forming C₃F₅⁺ from 18 to 70 eV. After 70 eV, CF₃⁺ becomes the dominant product ion. Among the major ions generated from the electron impact ionization of 2-C₄F₈, only CF⁺, CF₂⁺ and CF₃⁺ are found to react with 2-C₄F₈, via F⁻ abstraction or charge transfer mechanism. The charge transfer reaction of Ar⁺ + 2-C₄F₈ produces primarily C₄F₇⁺.

*This work is supported in part by the AFOSR.

SRP1 32 OTHER ATOMIC AND MOLECULAR COLLISION PHENOMENA

SRP1 33 Plasma-Screening Effects on the Electron-Impact Ionization of Atoms / Molecules and Ions Embedded in Weak Plasma BHUSHIT VAISHNAV, *VPMP Polytechnic, Gandhinagar, Gujarat* K.N. JOSHIPURA, S. GANGOPADHYAY, *Dept. of Physics, Sardar Patel University, Vallabh Vidyanagar* Plasma screening effects on electron induced atomic collision properties have attracted considerable research attention, because of applications in inertial confinement fusion and X-ray lasers etc. The theoretical interest is to examine the ionization of atomic/molecular targets by the impact of electrons in plasma. Basically the electron scattering problem is treated in a semi-empirical approach in the complex scattering potential ionization contribution (CSP-ic), to calculate total ionization cross section as a dominant part of total inelastic cross sections. This approach has been successful for number of (free) atomic and molecular targets in [1]. This paper extends the method to the collision processes in plasma and the relative contribution of ionization has been identified. We consider He⁺ ion embedded in weak plasma. The static potential of the e-He⁺ system in plasma environment is derived by us. Results will be discussed in the Conference. [1] K N Joshipura, Bhushit G Vaishnav and Sumona Gangopadhyay, *Int. J. Mass. Spectrom.* **261** (2007) 146.

SRP1 34 Surface catalytic contributions to molecule conversion in plasmas RICHARD ENGELN, RENS ZIJLMANS, ONNO GABRIEL, GÖKSEL YAGCI, DAAN SCHRAM, *Eindhoven University of Technology, Eindhoven, The Netherlands*, STEFAN WELZEL, JURGEN RÖPCKE, FRANK HEMPEL, *Institut für Niedertemperatur Plasmaphysik, Greifswald, German*

The contribution of surface-related processes to the formation of new types of molecules in a recombining plasma with a low electron temperature is investigated. The recombination of a highly dissociated mixture of nitrogen and oxygen is studied with a combination of tuneable diode laser absorption spectroscopy and mass spectrometry. A simulation in CHEMKIN, based on a simplified set of chemical reactions, has been developed to describe the system in detail and to determine the contributions of volume processes and surface-related processes. With sticking coefficient of 0.1 for the radials for all studied conditions, a chance of unity for Eley-Rideal processes to be successful, a desorption energy of 0.7 eV for NO molecules and relatively low activation energies, around 0.5 eV, for the Langmuir-Hinshelwood processes gives a good agreement with the measurements. We show that NO₂ can only be formed at surfaces in our system, whereas NO and N₂O are at least for a significant fraction formed at the surfaces of the reactor. Especially at low pressure conditions and at low oxygen admixture, the role of the surfaces is pronounced.

SRP1 35 OTHER PLASMA TOPICS

SRP1 36 Spectroscopic investigations into extraordinary phenomena in hydrogen plasmas with certain catalysts SANDER NIJDAM, ANDREAS VAN DEN BRINK, NIELS DRIESSEN, PETER VAN NOORDEN, RUUD DE REGT, TIM RIGHART, GERRIT SITTERS, EDDIE VAN VELDHUIZEN, RUUD WIJTVLIET, GERRIT KROESEN, *Technische Universiteit Eindhoven*

In recent years hydrogen plasmas have been created that display extraordinary behavior, like breakdown at low electric fields, anomalous plasma afterglow, excessive hydrogen Balmer- α spectral line broadening and EUV and VUV emission. Experiments have been done on three types of hydrogen discharges in order to reproduce the extraordinary plasma behavior observed. We have investigated these hydrogen discharges with different spectroscopic measuring devices. We focused on broadening of the hydrogen Balmer- α line and the emission of EUV and VUV radiation. The measurements in the visible part of the spectrum have been performed using a B&M100 type (1000 mm) Czerny-Turner monochromator attached to a CCD camera or a photomultiplier. For the VUV and EUV measurements we have used three different monochromators: a Jobin Yvon LHT 30 (320 mm, near grazing incidence), a Jobin Yvon HR 1500 (1500 mm, normal incidence) and a McPherson Model 234/302 vacuum monochromator (200 mm, normal incidence). In all cases a scintillator plate has been used to convert the diffracted UV radiation into visible light which was quantified by a CCD camera or a photomultiplier.

SRP1 37 Deterministic Plasma-aided Nanofabrication research within the International Plasma Nanoscience Network IGOR LEVCHENKO, KOSTYA (KEN) OSTRIKOV, SHUYAN XU, *Plasma Nanoscience Network*

Plasma Nanoscience is a sub-field at the cross-roads of cutting-edge nanoscience, plasma and gas discharge physics, materials and surface science, engineering,

astrophysics and bionanotechnology. Understanding how plasma-based nanoassembly works in natural environments and translating this knowledge to laboratory and industrial nanofabrication, eventually finding better, cheaper and industrially-viable ways of fabricating nanoscale objects and nanodevices is the main aim of the International Plasma Nanoscience Network. The concept of (plasma-controlled) determinism is central to our research endeavors. Here, we present the latest advances in experimental and computational research on deterministic plasma-aided nanofabrication and processing of various nanoscale objects of different dimensionality, sizes, shapes, crystalline structure, elemental composition, arrangement and ordering in nanoarrays, etc. [1]. The benefits and advantages of using low-temperature (non-equilibrium and thermal) plasma environments are revealed and the relevant processes optimized to meet the continuously rising demands of nanotechnology [1]. [1] K. Ostrikov, *IEEE Tran. Plasma Sci.* 35, 127 (2007); K. Ostrikov, A. B. Murphy, *J. Phys D.: Appl. Phys.* 40, 2223 (2007)

SRP1 38 PLASMA PROPULSION AND AERODYNAMICS

SRP1 39 Structure of stationary shock waves in weakly ionized gas D.J. DRAKE, B. RODGERS, S. POPOVIC, L. VUSKOVIC, *Department of Physics, Old Dominion University*

We performed detailed laboratory measurements of the excited-species population distributions across stationary shock waves in weakly ionized gas. Ionized gas was sustained in a cylindrical cavity integrated in the supersonic microwave flowing afterglow apparatus. An oblique solid body was suppressing the flow to generate a stationary acoustic shock wave. A cylindrical cavity was used to sustain a discharge in air, argon, and Martian air in the pressure range of 100-600 Pa. Argon is also a significant constituent of terrestrial and Martian air. Excited state populations of argon were measured using emission and absorption spectroscopy for the absolute intensities of the (4p-4s) spectral lines. Comparison was made between the populations in a model free flow and across the shock front. Oblique shock parameters were evaluated exactly for the given model geometry. Obtained data on the shock wave structure were compared with available shock-wave computational models.

SRP1 40 Schlieren observation of vortex flow structures in asymmetric dielectric barrier discharges DMITRY OPAITS, ALEXANDRE LIKHANSKII, GABRIELE NERETTI,*SOHAIL ZAIDI, MIKHAIL SHNEIDER, *Princeton University* SERGEY MACHERET, *Skunk Works, Lockheed Martin* RICHARD MILES, *Princeton University* PRINCETON UNIVERSITY TEAM, SKUNK WORKS, LOCKHEED MARTIN TEAM,

Asymmetric DBD plasma actuator for flow control has been studied both numerically and experimentally. A comprehensive kinetic model for asymmetric DBD actuators in air has been developed. A new approach for non-intrusive diagnostic of plasma actuator induced flows in quiescent gas was proposed. The schlieren technique, burst mode of plasma actuator operation, and 2-D fluid

numerical model coupled together allowed us to restore the entire two-dimensional unsteady plasma induced flow pattern as well as characteristics of the plasma induced force. A new voltage profile, consisted of nanosecond repetitive pulses added to low-frequency sinusoidal bias voltage, is proposed. Advantages of the new voltage profile have been demonstrated experimentally. Dependences of the DBD operation on bias voltage, pulse voltage and repetition rate have been investigated for both polarities of the pulses. Significance of the surface charge has been demonstrated.

*Visiting student from the University of Bologna.

SRP1 41 LASER MEDIA, KINETICS, PROCESSES

SRP1 42 X-ray laser spectroscopy of heavy ions at the GSI, Darmstadt, Germany ALEXANDER MAYR, RUSTAM BER-EZOV, JOACHIM JACOBY, J.W. Goethe-University, Frankfurt THOMAS KUEHL, OLGA ROSMEJ, GSI, Darmstadt BERND SICHERL, J.W. Goethe-University, Frankfurt DANIEL URESCU, GSI, Darmstadt BERNHARD ZIELBAUER, MBI, Berlin DANIEL ZIMMER, J. Gutenberg-University, Mainz As a branch of the PHELIX laser project at GSI, a 13.9 nm x-ray laser is developed. Using this x-ray laser, spectroscopic measurements on highly-charged heavy ions will be made. At GSI, ions up to uranium can be provided in specific charge states by the fragment separator FRS and then stored and cooled in the experimental storage ring ESR. The upcoming FAIR facility will also produce many radioactive nuclei. The unique combination of heavy-ion beam and x-ray laser allows the accurate spectroscopic rating of quantum-mechanical states of atomic nuclei and the comparison of this information with theoretical predictions. This will be achieved by the use of lithium-like heavy ions because for these four-body systems the models of quantum electrodynamics give results which are precise enough. The paper will give information about the realisation of the experimental concept, the current state of the x-ray laser setup and the development of the corresponding detection systems.

SRP1 43 KrF Laser Amplification in the Multi-Staged Electra Facility* J. GIULIANI, M. WOLFORD, M. MYERS, J. SEHIAN, Naval Research Laboratory F. HEGELER, CTI P. BURNS, RSI R. JAYNES, SAIC Electra is a rep-rated, e-beam pumped KrF laser system at the Naval Research Laboratory investigating the physics and technology required for inertial fusion energy. To date the main cell has operated as an oscillator and achieved ~ 1.5 kW at 5 Hz for 2000 shots and at 2.5 Hz for over 22,000 shots. The next step is to convert Electra into an amplifier system. A commercial KrF discharge oscillator will provide the initiating laser pulse. This pulse is then sequentially amplified through a preamp in a single pass, followed by a double pass through the main amp. The final system output laser energy depends upon the e-beam pumping power in each amp. To examine this dependency the KrF kinetics/laser simulation code Orestes has been used to follow the growth of the low energy oscillator pulse as it sequentially propagates through the two amplifiers. In addition to the energy, the final output laser pulse shape is a complex

product of the amplification and timing between the multiplexed laser pulses and the e-beam pulsed power. Simulations for the preamp have demonstrated partial agreement with the profiles and provide a test of the molecular/plasma kinetic processes used in Orestes.

*Supported by DOE/NNSA.

SRP1 44 INDUCTIVELY COUPLED PLASMAS

SRP1 45 Measurement of radial density of Ar metastables in an inductively coupled plasma in Ar/O₂ YUICHIRO HAYASHI, SATOSHI HIRAO, TOSHIKI MAKABE, Keio University O₂ plasma is used for ashing and trimming of the resist in semiconductor production processes, and for the surface modification of metals and polymers. In these processes atomic O radicals play important roles. It is reported that the density of atomic metastables increase in Ar/O₂ mixture as compared with that in pure O₂ in CCP [1]. We measured the radial profile of the density of Ar metastables (1s₃, 1s₅) and the temperature in an inductively coupled plasma at 13.56 MHz in Ar/O₂ as a function of admixture O₂ by using laser absorption spectroscopy. The average densities of metastable Ar are $2 \times 10^{10} \text{ cm}^{-3}$ (1s₃) and 10^{11} cm^{-3} (1s₅) for 0-20% O₂ fraction, and have the peak at 5-10%. The temperatures are 2000 K (1s₃) and 1600 K (1s₅) and are highest at 10%. [1] T. Kitajima, T. Nakano, and T. Makabe, Appl. Phys. Lett., **88**, 091501 (2006).

SRP1 46 Space- and Time-Resolved E-H Transition by using ICCD Camera in an Inductively Coupled Plasma in Ar SATOSHI HIRAO, YUICHIRO HAYASHI, TOSHIKI MAKABE, Keio University Inductively coupled plasma (ICP) has been widely used as a high density plasma source in various applications. ICP has two operating modes. One is a low density (capacitively coupled) E-mode sustained by the static electric field between terminals of the induction coil. The other is a high-density (inductively coupled) H-mode sustained by the induced electromagnetic field. It is well known that there is an E-H transition in ICP, however the details of this phenomenon are not well-known. In our previous work, we experimentally studied the ICP in Ar by using ICCD camera located at the side of the reactor, and observed the E-H transition by the line-integrated time-resolved emission images. In the present study, we set the ICCD camera on the top of the reactor to measure the 2D-t plasma structure at the coil plane. We mainly focus on the emission from Ar(2p₁) as a probe of high energy electrons, and discuss the behavior of plasma during E-H transition.

SRP1 47 Kinetics of charged particles and nonlocal control of plasma properties in a pulsed rf icp in argon-oxygen mixtures* J.C. BLESSINGTON, V.I. DEMIDOV, M.E. KOEPKE, WVU, Morgantown, WV C.A. DEJOSEPH, JR., Air Force Research Laboratory, WPAFB, OH Previously [1], we showed that a simple, three-level model could explain the rapid growth of charge particles following application of rf power to a noble gas. In this work we show experimentally that addition of a small amount of oxygen can significantly reduce the rate of growth

of charged particle density, indicating the simple three-level model is no longer applicable. Even in this case, the positive ion density (measured by probes) reaches a stationary value much faster than the atomic oxygen density (estimated from plasma emission). Thus, by changing the duration of the rf pulse, the ratio of fast electron production, by the reaction $O + O^- \rightarrow O_2 + e$ (3.6 eV), compared to the ambipolar flux of positive ions to the discharge walls, can be controlled. This effect can be used for nonlocal regulation of plasma properties [2]. [1] V. I. Demidov, C. A. DeJoseph, Jr. et al, PSST, 2004, 13, 600. [2] C. A. DeJoseph, Jr. et al, Phys. Plasmas, 2007, 14, 057101.

*This work supported in part by AFOSR. The work of VID supported by AF Summer Fellowship.

SRP1 48 Fluid model for a Cl_2/Ar inductively coupled discharge EMILIE DESPIAU-PUJO, PASCAL CHABERT, *LPTP, Ecole polytechnique, France* DAVID B. GRAVES, *Dept of Chemical Engineering, University of California, Berkeley, USA* III-V compounds such as GaAs, InP or GaN-based materials are widely used for photonics and optoelectronic applications, especially in the telecommunications and light detection industries. Although many problems remain to be understood, inductively coupled discharges seem to be very promising to etch such materials, using Cl_2/Ar , Cl_2/N_2 and Cl_2/H_2 gas chemistries. Hsu et al. [1] developed a 2D-fluid model to calculate the plasma parameters along with the neutral radical densities and profiles for purely inductive discharges in Ar/O_2 and $Ar/O_2/Cl_2$ mixtures. The model couples plasma electrodynamics to neutral chemistry and transport, under the assumption of quasi-neutrality. Power deposited into electrons comes from inductive coupling from an external coil. We have used this model to investigate Cl_2/Ar chemistries and get information about the electron density and temperature, composition of the ion wall flux and radical densities. Some comparisons with experimental measurements are reported. The addition of capacitive coupling and the study, in the presence of negative ions, of the transitions from E to H modes are under investigation. [1] Hsu et al, J. Phys. D: Appl. Phys. 39 (2006) 3272-3284

SRP1 49 The effect of a planar antenna on a ferromagnetic core ICP JIN YOUNG BANG, SUNG WON CHO, CHIN WOOK CHUNG, PNA TEAM, A side type ferrite inductively coupled plasmas (ICPs) with high efficiency and low voltage suitable for next generation processing was recently developed [1]. In this ICP, the plasma density at edge of the chamber is higher than center of the chamber because the region where the plasma generation is localized at the edge of the chamber. To control plasma uniformity in various environments, an additional planar antenna on the top of the chamber was installed at the center to increase the center density and the effect of the additional antenna was analyzed. [1] K. H. Lee, Y. K. Lee, S. W. Lee, C.W. Chung, Gases Electron Conference 2006.

SRP1 50 Development of a novel Inductive coupled plasma source* HYONG-HO NAM, HYO-CHANG LEE, CHIN-WOOK CHUNG, To improve plasma uniformity, a three-turn cross antenna was developed. The three-turn cross antenna has low inductance and low antenna voltage. The antenna voltage is 227V at 100W(13.56MHz) and at argon 10 mTorr while it is 1200 V at a single turn antenna. Plasma density is $10^{11} \sim 10^{12} cm^{-3}$ in the range of 5mTorr to 20mTorr and 100W to 600W. Plasma azimuthal asymmetry is below 5%. This antenna is expected to be suitable for next generation plasma processing.

*ICP three-turn antenna

SRP1 51 Investigation of an RF ICP J. WIECHULA, M. IBERLER, J. JACOBY, C. TESKE, *University of Frankfurt, Institute for Applied Physics* In the present study, an experiment with an electrode less inductively coupled plasma (ICP) is under investigation. The main section of the experimental setup is a discharge tube of glass wrapped with a cylindrical induction coil. The RF power is coupled into the plasma by transformer action. Driven at a fixed frequency of 13.56MHz the generator used in this experiment can deliver up to 10kW of RF power. For diagnostic purposes Ar and He is used as a working gas. A main interest of this experiment is the influence of the coil geometry on the coupling efficiency between the external circuitry and the plasma. Therefore, measurements of the electrical parameters are performed to determine the coupling efficiency and monitor the capacitive-to-inductive transition, which occurs at higher power levels. The electron temperature of the discharge plasma is measured by spectroscopic means where else the electron density is determined using a langmuir probe. Comparing these results with the electrical measurements will enable us to achieve further insights into the relation between plasma parameters and the electrical characteristics of the driving circuitry.

SRP1 52 BIOLOGICAL AND EMERGING APPLICATIONS OF PLASMAS

SRP1 53 Chemical modification and its evaluation of CNT-based bio-nanosensor by plasma activation technique T. HIRATA, S. AMIYA, M. AKIYA, *Dept. of Biomed. Eng., Musashi Inst. of Technol.* O. TAKEI, *Saitama Small Enterprise Prom. Corp.* T. SAKAI, *Saitama Univ.* T. NAKAMURA, J. TOTAKE, T. YAMAMOTO, *Univ. of Tokyo* R. HATAKEYAMA, *Tohoku Univ.* In order to chemically modify single-walled carbon nanotubes (SWCNTs), plasma ion irradiation (plasma activation) is demonstrated on a bio-nanosensor based on poly[ethylene glycol]-grafted SWCNTs (PEG-SWCNTs) network. The PEG-SWCNTs network is placed between the electrodes in the sensor-chip using a micropipet. The experimental apparatus for the plasma-activation is a magnetron-type plasma generator. The gas used for the production of carboxyl (COOH) groups in order to the immobilization of living body materials such as antibody or DNA is atmospheric air. PEG-SWCNTs are synthesized by azo-PEG (initiators). According to the XPS analysis, peaks which correspond to COOH groups are observed, the ratio of the COOH peak to all peak areas has increased to 34 times that before ion irradiation. In addition, evaluation of the bio-nanosensor for a characteristic response to bovine serum albumin (BSA) [or oligonucleotides] revealed an increase in impedance between the electrodes due to BSA/anti-BSA binding (or oligonucleotides hybridization) after injection. The results of this study indicate that this bio-nanosensor reacts with a quick response time (ca. 60 s).

SRP1 54 ENVIRONMENTAL APPLICATIONS

SRP1 55 Evaluation of Decomposition Treatment for Halogenized Compounds by Acceleration of Electrons from Carbon Nanotubes* MICHITERU YAMAURA, *Institute for Laser Technology SHIGEAKI UCHIDA, Tokyo Institute of Technology MASAYUKI FUJITA, MASAHIRO NAKATSUKA, CHIYOE YAMANAKA, Institute for Laser Technology* A novel decomposition treatment for halogenized compounds using a carbon nanotube (CNT) electron source is proposed [1]. It is observed that high concentrations of chlorophenols can be significantly decreased by using a CNT electron source. The concentration is reduced to a maximum level of less than 1/1000 after only a few minutes of treatment. The input energy required for 1 g of chlorophenol is 46 J when the injection power is 0.5 W. The input energy is only 1/161 times lesser than that required for the treatment using barrier discharge. The proposed treatment using CNTs has a high efficiency because the input energy is provided only by the accelerated electrons. A harmless and high-efficiency decomposition treatment for halogenized compounds using an electron source with carbon nanotubes is discussed. [1] M.Yamaura, et al. *Chem. Phys. Lett* **435**, 148 (2007).

*A part of this work is supported by a Grant-in-Aid for Young Scientists (B) Research from Japan.

SRP1 56 Development of simultaneous decomposition technique of diesel particulate materials and nitric oxides using dielectric barrier discharge* YUKIHIKO YAMAGATA, YOZO KAWAGASHIRA, *Kyushu Univ.* KATSUNORI MURAOKA, *Chubu Univ.* Recently, we have proposed a new decomposition technique for environmentally hazardous materials with very low concentration, and successfully decomposed volatile organic compounds. This is based on the combination of dielectric barrier discharge (DBD) with condensation/localization technique. In order to apply this technique to an after treatment of diesel exhaust gas, simultaneous decomposition of diesel particulate materials (DPMs) and nitric oxides was demonstrated. DPMs were collected in a reactor using an electrostatic precipitation operated by a negative corona discharge. At DC 5 kV more than 95% of DPMs were continuously collected for 60 min. Subsequently, the collected DPMs were decomposed in a model gas including NO molecules by a DBD. In the presence of DPMs, a large amount of NO was decomposed compared with that in the absence of DPMs. It is suggested that actual DPMs and NO which acts as the oxidant and reductant, respectively, are decomposed simultaneously and effectively by DBD.

*This work has been partially supported by Grant-in-Aid for Scientific Research from the Ministry of Education, Science, Sports, Culture and Technology of Japan.

SESSION VF1: MATERIALS PROCESSING IN LOW PRESSURE PLASMAS II: ETCHING, DEPOSITION, NEW MATERIALS

Friday morning, 5 October 2007; Crystal Ballroom A, Doubletree Crystal City at 8:00
Evgeniya Lock, Naval Research Laboratory, presiding

Invited Papers
8:00
VF1 1 Reaction of Fluorocarbon Species with Si and SiO₂ Surfaces.*

 HIROTAKA TOYODA, *Nagoya University*

Highly-selective high-aspect-ratio etching of SiO₂/Si is an indispensable key issue in the ULSI manufacturing processes. Furthermore, recent etching technology utilizes high density plasmas and requires complex fluorocarbon molecules such as C₄F₆ or C₅F₈ to achieve high etching speed and high etching selectivity. To improve etching performance, precise control of fluorocarbon plasmas based on deep understanding of radical reactions on SiO₂ and Si surfaces is required. Well-defined beam experiments in ultra-high vacuum are powerful for basic study of surface reactions. This paper shows elementary surface processes of fluorocarbon etching process, especially focused on the unique chemical reactivity of C₅F₈ molecule under co-incident of Ar ion. The device was specially designed so as to enable *in situ* measurements of etching yield and etched surfaces. Namely, Ar⁺ beam at energies from 50 to 400 eV and various kinds of fluorocarbon neutral species (C₅F₈, C₄F₈, CF₂) are co-incident on a clean SiO₂ surface at a controlled flux. Etching yield of beam-incident surface is measured by profilometer while *in-vacuo* X-ray photoelectron spectroscopy (XPS) analysis reveals a time evolution of atomic composition of surface layer during the etching. In the case of C₄F₈/Ar⁺, surface atomic composition after SiO₂ etching was almost similar to that of pure Ar⁺ sputtering except for a small amount of F component. In the case of C₅F₈/Ar⁺, however, formation of fluorocarbon layer after SiO₂ removal was observed as in the case of CF₂/Ar⁺. The SiO₂ etching yield monotonically increased with the Ar⁺ incident energy above 400 eV, and the etching yield of 2.4 was obtained at an Ar⁺ incident energy of 900 eV with C₅F₈ co-incident, which was about 3 and 1.5 times larger compared with pure Ar⁺ sputtering and CF₂/Ar⁺ co-incident, respectively. These results suggest that fluorocarbon molecules themselves are important species in fluorocarbon etching plasma.

*The author would like to thank Prof. H. Sugai and Dr. N. Takada for their supporting this work.

Contributed Papers
8:30

VF1 2 Modeling high aspect ratio contact etch of SiO₂ PHILIP STOUT, *Applied Materials* A Monte Carlo based feature scale model has been applied to the high aspect ratio contact etch of a dielectric stack. The model includes physical effects of transport to surface, specular and diffusive reflection within the feature, adsorption, surface diffusion, deposition and etching. Discussed will be 3D feature modeling of an etch sequence through an anti reflective coating / amorphous carbon / SiO₂ / SiN material stack. The effect of passivation, off normal ion angular distributions, and feature opening geometry on the etched profile will be discussed. The etch rate decreases as the aspect ratio of the contact increases due to the shadowing of etchant reactants from the etch front. The passivant buildup at the contact opening over the course of the etch also plays a role in the reduced etch rate with time. The passivant buildup can also reflect incident ions off normal into the feature contributing to a bowed etch profile. The amount of polymer (i.e. passivant) in the etch chemistry can transition profiles from bowed to tapered to etch stop. Off normal ion incidence can increase the etch rate due to off angle yield peaks and cause tilting of the etched profile.

8:45

VF1 3 Time dependence analysis of the 3D profile charging during SiO₂ etching in Ar⁺/CF₄ plasma BRANISLAV RADJENOVIC, *Vinca Institute of Nuclear Science* MARIJA RADMILOVIC-RADJENOVIC, ZORAN PETROVIC, *Institute of Physics* Damage to integrated circuits (ICs) during manufacturing as a result of charging of the dielectrics during finalization of interconnects is both reducing the profitability and reducing the ability to reach large sizes of microchips and make complex system integration on a single chip. The ability to simulate feature charging was added to the 3D level set profile evolution simulator. The ion and electron fluxes were computed along the feature using a Monte Carlo method. The surface potential profiles and electric field for the entire feature were generated by solving Laplace equation using finite elements method. Calculations were performed in the case of simplified model of Ar⁺/CF₄ non-equilibrium plasma etching of SiO₂. The time necessary for the electric field in the feature to reach its steady-state value is potentially very important for the orderliness of the whole simulation cycle. Since the calculations show that this time is about several milliseconds, which is very short comparing to the etching time step (during which we assume that the etching rate is constant), it is reasonable to calculate steady-state values of the electric field in the beginning of every Monte-Carlo step and use this field subsequently, instead of devising a complex and computationally costly scheme for the recalculation of the field during particle fluxes calculations.

9:00

VF1 4 Plasma Modeling for Cu barrier/seed applications
 PRASHANTH KOTHNUR, ANANTH BHOJ, RON KINDER, *Novellus Systems, Inc.* Ionized Metal Physical Vapor Deposition (IMPVD) enables barrier/seed layer deposition in high aspect ratio trenches and vias for microelectronics fabrication. As device sizes continue to shrink, the capability to predict bulk plasma dynamics coupled with feature-scale evolution on the surface of the trench or via is becoming increasingly important. The focus of this talk is to describe a methodology for modeling IMPVD Cu deposition using a combination of reactor scale and feature scale modeling. The Hybrid Plasma Equipment Model (HPEM) is used to simulate the bulk plasma in the chamber and compute the flux and energy distributions of species at the wafer. The Monte Carlo Feature Profile Model (MCFPM) predicts trench profiles using the species fluxes and energies obtained from the HPEM and a detailed set of surface sticking coefficients and sputtering yield curves. The choice of input parameters to the MCFPM is guided by a fast string-based feature evolution algorithm (Feature 2D). Surface properties on the trench such as neutral and ion sticking coefficients, and sputtering yield curves are deduced by comparing Feature 2D results with experimental profiles. The overall procedure provides a method to predict the Cu seed layer profile on the trench as a function of chamber operating conditions. Results are presented for typical processing conditions (argon plasma sputtering a Cu target at 1 -15 mTorr) and varying source power and rf bias.

9:15

VF1 5 Spatial distributions of Cu particulates in high-pressure magnetron sputtering plasmas studied by laser light scattering
 N. NAFARIZAL, *Nagoya University, University Tun Hussein Onn Malaysia* N. TAKADA, K. SASAKI, *Nagoya University* M. IKEDA, Y. SAGO, *Canon ANELVA Corporation* Ionized physical vapor deposition (IPVD) is a new technique to deposit barrier and seed layers on the surface of narrow trenches and holes. In our previous works, we have found that the ionization ratio of metal atoms in a conventional magnetron sputtering plasma increased with the discharge pressure. However, the high-pressure plasmas may have a risk of the formation of particulates. In the present work, we detected Cu particulates produced in high-pressure magnetron sputtering plasmas by laser light scattering. We observed the scattered laser light in the gas phase of the sputtering plasma when the discharge pressure was higher than 200 mTorr. Typically, particulates were concentrated at the boundary between the bright plasma and the dark region. The peak of the scattered intensity was located adjacent to the ring anode of the magnetron sputtering source. The scattered intensity varied with time after the initiation of the discharge. Since the intensity of the scattered laser light is dependent on the mean size and the density of particulates, this result indicates the temporal variations of the size and the density of particulates. In addition, it was found that the scattered intensity was very sensitive to the discharge power and the gas pressure.

9:30

VF1 6 Multi-hollow discharge plasma CVD reactor with magnets for highly stable a-Si:H film deposition KAZUNORI KOGA, WILLIAM M. NAKAMURA, HIROSHI SATOU, HIROOMI MIYAHARA, MASAHARU SHIRATANI, *Kyushu University* Incorporation of amorphous silicon nanoparticles (clusters) has been related to a-Si:H films' light induced degradation [1]. In the present work, we have developed a multi-hollow discharge plasma CVD reactor in which we introduced magnets into the electrode to produce a magnetic field (400 G) along the holes' axis to increase the confinement of electrons of low kinetic energy < 10eV. Due to such selective confinement of electrons, the generation rate of SiH₃ radicals, which is the main precursor of good films, increases; while the generation rate of SiH₂, which forms clusters, is reduced. By applying the magnetic field, we have obtained a deposition rate 20-100% higher than that without the magnetic field. Moreover, the volume fraction of clusters in films deposited in the downstream region is 14-80% lower when applying the magnetic field. These results indicate that a-Si:H of high stability can be deposited at high rate by applying the magnetic field to the electrodes. [1] M. Shiratani, K. Koga, N. Kaguchi, K. Bando, and Y. Watanabe, *Thin Solid Films*, **506-507**, 17 (2006).

9:45

VF1 7 Control of structures of Carbon Nanowalls in plasma enhanced CVD WAKANA TAKEUCHI, *Nagoya Univ.* YUTAKA TOKUDA, *Aichi Inst. Tech.* MINEO HIRAMATSU, *Meijo Univ.* HIROYUKI KANO, *NU-Eco Eng* MASARU HORI, *Nagoya Univ.* Carbon nanowalls (CNWs), two-dimensional carbon nanostructures consisting of graphite sheets standing vertically on the substrate, have attracted much attention for several applications. In view of the practical application of CNWs, it is necessary to control their structure and electronic properties. In this study, we focused on the control of CNW structures. CNWs were fabricated on the Si substrate by the fluorocarbon plasma-enhanced CVD with H radical injection. We investigated the influence of O₂ addition to the mixture of C₂F₆/H₂ on the morphology and structure of CNWs. Raman spectroscopy was used to evaluate the structure of CNWs. The morphology and crystallinity of CNWs were found to be controlled by the O₂ addition. Raman spectra for all samples have a strong peak at 1590 cm⁻¹ (G-band) indicating the formation of a graphitized structure and another peak at 1350 cm⁻¹ (D-band) corresponding to the disorder-induced phonon mode. As a result of O₂ addition, width and peak intensity ratio of D/G bands of CNWs decreased. Oxygen atom would play a role of etching of disorder carbon phase and contribute to the higher graphitization.

SESSION VF2: PLASMA DIAGNOSTICS I

Friday morning, 5 October 2007; Crystal Ballroom B, Doubletree Crystal City at 8:00

Alex Paterson, Applied Materials, presiding

Invited Papers**8:00****VF2 1 Reflections on Electric Probes.**NICHOLAS BRAITHWAITE, *The Open University*

One of the more immediate temptations for an experimental plasma physicist is to insert some kind of refractory, conducting material into a plasma, as a simple means of probing its charge composition. Irvine Langmuir tried it in the 1920s and was one of the first to develop an electrical probe method in his early work on electrical discharge plasmas. There are now numerous variations on the theme including planar, cylindrical and spherical geometry with single, double and triple probes. There are also probes that resonate, propagate and reciprocate. Some probes are electrostatic and others are electromagnetic; some are effectively wireless; most absorb but some emit. All types can be used in steady and transient plasmas, while special schemes have been devised for RF plasmas, using passive and active compensation. Magnetised plasmas pose further challenges. Each configuration is accompanied by assumptions that constrain both their applicability and the analytical methods that translate the measured currents and voltages variously into charge densities, space potentials, particle fluxes, energy distributions and measures of collisionality. This talk will take a broad look at the options and opportunities for electric probes, principally in the environment of non-equilibrium plasma.

Contributed Papers**8:30****VF2 2 Xenon operation of the Non-ambipolar Electron Source***

NOAH HERSHKOWITZ, BEN LONGMIER, *Engineering Physics Department, University of Wisconsin-Madison* The Non-ambipolar Electron Source (NES) is an RF plasma-based electron source that does not rely on electron emission at a cathode. All of the random electron flux in NES is extracted through an electron sheath resulting in total non-ambipolar flow when the ratio of the ion loss area to the electron loss area is approximately equal to the square root of the ratio of the ion mass to the electron mass, and the ion sheath potential drop at the chamber walls is much larger than T_e/e . Operation with Xe has increased the output current (from previous results with Ar at 15 A) to 30 A when using 2.2 sccm Xe, and 1.2 kW RF power at 13.56 MHz and increased the gas utilization, the ratio of extracted electron current to neutral supply current, to 180. Operation with a graphite ion collector/Faraday shield has significantly reduced sputtering. NES could replace hollow cathode electron sources in a wide variety of applications. The physics behind the improved Xe operation compared to Ar is described.

*Work supported by US DOE grant FG02-97ER 54437.

8:45**VF2 3 Nanoparticle charging in weakly ionized gases***

MARCO FRANCESCO GATTI, UWE KORTSHAGEN, *University of Minnesota* Charging dominates the behavior of nanoparticles immersed in weakly ionized gases. The nanoparticle charge is virtually always modeled through the Orbital Motion Limited (OML) theory, even though serious doubts exist about its validity. The approach adopted in this study allows one to overcome most of the simplifying assumptions of the OML theory, providing in-

sight into the behavior of nanoparticles in real laboratory plasmas. The method adopted is a self-consistent molecular dynamic-Monte Carlo simulation in which the ion motion is tracked, and the collisions between ions and background gas are treated statistically, while electrons are modeled through an analytical expression. This method allows for the investigation of the effects of ion-neutral collisions (elastic scattering and charge exchange) and of high particle density. Simulations are performed over a wide range of particle concentration, gas pressure, particle size, and electron temperature. The results show a strong dependence of the nanoparticle charge on the particle density, and a non monotonic dependence on gas pressure. Furthermore, the role of particle size and electron to ion temperature ratio is highlighted. An analytical model capable of predicting the dependence of the nanoparticle charge upon all the aforementioned parameters is derived.

*This work is supported by NSF under grant CBET-0500332, and the Minnesota Supercomputing Institute

9:00**VF2 4 Electric probes for characterization of microwave produced plasma.**

VIPIN K. YADAV, *Centre for Space Physics, Kolkata, India* Electric probes namely Langmuir and capacitive probes are designed to characterize microwave produced plasma. In microwave or electron cyclotron resonance (ECR) produced plasmas, the simple Langmuir probe gives error in the measurement of plasma parameters due to the presence of a steady magnetic field. To eliminate these errors along with the already existing sheath effects, some modifications are mandatory to be incorporated in the design of a Langmuir probe. Two such probes, a Langmuir probe to measure plasma parameters and a capacitive probe to detect plasma oscillations are designed. The plasma parameters measured by the designed probe matches well with the theoretically estimated values.

9:15

VF2 5 The Bohm Criterion Revisited NATALIA STERNBERG, *Clark University* VALERY GODYAK, *Osram Sylvania* The plasma-sheath model and the Bohm criterion introduced by Bohm is one of the earliest attempts to model the plasma and the sheath separately, and to find a way to join the plasma and the sheath solutions. Although there is hardly a paper on plasma-sheath modelling that does not quote the Bohm criterion, Bohm's paper and his results are widely misunderstood. The reason for this is that in his paper, Bohm himself misinterpreted his result by concluding that the sheath edge coincides with the reference point of his plasma-sheath model. As a result, the criterion for the reference point obtained by Bohm to ensure monotonicity of his sheath solution (i.e., the Bohm criterion) was erroneously applied to the sheath edge and used in the literature as a criterion for sheath formation. We show that the Bohm criterion when applied to the sheath edge contradicts Bohm's own definition of the sheath, and cannot be obtained from Bohm's plasma-sheath model.

9:30

VF2 6 First experimental test of the generalized Bohm criterion using Ar⁺ and Xe⁺ LIF in Ar-Xe plasmas* DONGSOO LEE, NOAH HERSHKOWITZ, *University of Wisconsin-Madison* GREG SEVERN, *University of San Diego* The Bohm sheath criterion in single- and two-ion species plasmas is studied with laser-induced fluorescence (LIF) using two diode lasers in Xe and Ar-Xe plasmas. The plasmas are generated in a weakly-collisional (< 1 mTorr) unmagnetized dc hot filament discharge confined by multipole magnetic fields. Two LIF schemes are employed to measure the argon and xenon ion velocity distribution functions (ivdfs) near a negatively biased boundary plate. The Ar II transition sequence at 668.614 nm and Xe II at 680.574 nm are adopted to detect each ion's fluorescence. The results show that

the argon and xenon ion velocities appear to approach the ion sound speed of the system near the sheath-presheath boundary, which excludes the possibility that both the ions will have their own Bohm velocities. In addition, the generalized Bohm criterion is also satisfied with the measured data. This is the first experimental test of the generalized Bohm criterion.

*Work supported by DoE Grant No DE-FG02-97ER54437.

9:45

VF2 7 Numerical Solutions for Langmuir Probes* RICHARD FERNSLER, *Plasma Physics Division, Naval Research Laboratory* A simple numerical technique is presented for computing the electrostatic potential around spherical and cylindrical Langmuir probes residing in plasmas consisting of hot electrons and cold, collisionless, positive ions. Rather than solving Poisson's equation directly, its derivative is solved instead using a "shooting" method. The new equation is one order higher, but it is linear in the field and can thus be solved implicitly. The scheme is therefore stable numerically, but it requires initial values for the potential, electric field, and derivative of the field at some starting location. Fortunately, these parameters are all easy to obtain in the bulk plasma. The numerical results show that the sheath around the probe can be surprisingly wide, and as a result the ion saturation current has a more complicated dependence on probe voltage than is commonly assumed. (That dependence is related to but separate from the variation seen with probes smaller than a Debye length.) The numerical technique presented can in principle be used with any nonlinear, ordinary differential equation (including with multipoint boundary conditions or unknown eigenvalues), provided a suitable set of initial values can be obtained.

*This work was supported by the Office of Naval Research

SESSION WF1: BIOLOGICAL AND EMERGING APPLICATIONS OF PLASMAS

Friday morning, 5 October 2007; Crystal Ballroom A, Doubletree Crystal City at 10:30

Scott Walton, Naval Research Laboratory, presiding

Invited Papers

10:30

WF1 1 Low-energy electron interactions with hydrated DNA and complex biological targets.*

THOMAS M. ORLANDO, *Georgia Institute of Technology*

We have theoretically and experimentally examined low-energy (5-50 eV) electron induced damage of hydrated DNA targets. In particular, we have modified a multiple scattering "path approach" to theoretically calculate low-energy (5-50 eV) electron diffraction and incident electron intensity at particular sites within a hydrated DNA double-strand. Constructive interference associated with water in the DNA major grooves occurs and can enhance the experimentally observed DNA damage probability. We associate the observed enhancements in the break probability as a function of incident electron energy with diffraction and decay of compound core-excited Feshbach resonances. These excitations are localized at the hydrated DNA interface but can decay by autoionization and lead to damage at sites spatially removed from the initial excitation. Diffraction can enhance damage but the inherent spatial specificity is not preserved. We have also begun studies to examine spatially and chemically resolved plasma mediated desorption of small molecules from complex targets such as cell membranes.

*This work was supported by the U. S. Dept. of Energy, Office of Science, Contract DE-FG02-02ER15337.

Contributed Papers

11:00

WF1 2 Nanostructured heterolayers for biosensor and photovoltaic nanodevices: A plasma technique AMANDA RIDER, IGOR LEVCHENKO, KOSTYA (KEN) OSTRIKOV, *Plasma Nanoscience, The University of Sydney* Novel structures incorporating heterolayers of buried quantum dots (QDs) have been proposed for biosensors and solar cells, in some cases there is an additional layer of unburied, surface QDs or larger nanostructured islands, the signal from which is reported to be enhanced due to correlation with the buried QDs. Such devices are particularly alluring due to the current research focus on nanobiotechnology and renewable energy. For satisfactory device performance, care must be taken to ensure a high level of control over the composition, size, morphology and positioning of these QDs, both buried and on the surface. Such considerations are crucial for, amongst other things, band-gap engineering efforts, device efficiency and bio-functionalization. The distinct advantages of the low-temperature growth afforded by plasmas are particularly notable when considering biological and photovoltaic applications. The utilization of plasma-based methods is a promising way to ensure all these requirements are met. We demonstrate through hybrid numerical simulation, the plasma-assisted fabrication of both buried and surface quantum dots with precise control over composition [1], size-uniformity [2], morphology, crystallinity and positioning. [1] A. E. Rider, *J. Appl. Phys.* 101, 044306 (2007); [2] A. E. Rider et al, *Plasma. Process. Polym.*, article accepted (2007).

11:15

WF1 3 Molded Microcavity Plasma Arrays And Channels In Polymer Structures: UV Lighting Sources For Biophotonic Applications J. ZHENG, T.S. ANDERSON, J.H. MA, M. LU, B.T. CUNNINGHAM, S.-J. PARK, J.G. EDEN, DEPARTMENT OF ELECTRICAL AND COMPUTER ENGINEERING, UNIVERSITY OF ILLINOIS, URBANA, IL USA COLLABORATION, Arrays of microcavity plasma devices, transparent in the ultraviolet(UV) have been fabricated in multilayer polymer structures by replica molding process. Microscale, on-chip UV-emitting light sources integrated into plastic substrate are an attractive tool for biomedical diagnostics such as cell detection or radiation treatments. In this presentation, arrays of microchannels with cross-sectional dimensions as small as $100 \times 100 \mu\text{m}^2$ and lengths up to 2 inches (aspect ratio of 500:1) are described. Each channel is hermetically sealed and contains mixtures of UV emitting gas such as Ar/N₂, Ar/D₂, and Ar/H₂O at atmospheric pressures. Channels are fabricated adjacent to one or more microfluidic channels containing a liquid dye solution which is photoexcited by the microplasma. Driven by an ac voltage source, the microchannel plasmas are observed to be stable glows and the microplasma emission is found to be dependent upon the electrode geometry. The characteristics of the UV emission produced by the microplasmas, and the selective detection of dye samples in the fluidic channel will be discussed.

Invited Papers

11:30

WF1 4 Cold plasma treatment in wound care: efficacy and risk assessment.

EVA STOFFELS, *Eindhoven University of Technology*

Cold atmospheric plasma is an ideal medium for non-destructive modification of vulnerable surfaces. One of the most promising medical applications of cold plasma treatment is wound healing. Potential advantages in wound healing have been demonstrated in vitro: the plasma does not necrotize the cells and does not affect the extracellular matrix [1], has clear bactericidal or bacteriostatic effects [2], and stimulates fibroblast cells towards faster attachment and proliferation [3]. However, safety issues, such as the potential cytotoxicity of the plasma must be clarified prior to clinical implementation. This work comprises the recent facts on sub-lethal plasma effects on mammalian cells, as well as studies on apoptosis induction and quantitative assessment of DNA damage. Fibroblast, smooth muscle and endothelial cells were treated using the standard cold plasma needle [1,2]; intra- and extracellular oxidant levels as well as the influence of the plasma on intracellular antioxidant balance were monitored using appropriate fluorescent markers [1]. We have studied long-term cellular damage was monitored using flow cytometry to determine the DNA profiles in treated cells. Dose-response curves were obtained: increased proliferation as well as apoptosis were visualized under different treatment conditions. The results from the in vitro studies are satisfying. [1] I.E. Kieft, "Plasma needle: exploring biomedical applications of non-thermal plasmas," PhD Thesis, Eindhoven University of Technology (2005). [2] R.E.J. Sladek, "Plasma needle: non-thermal atmospheric plasmas in dentistry" PhD Thesis, Eindhoven University of Technology (2006). [3] I.E. Kieft, D. Darios, A.J.M. Roks, E. Stoffels, *IEEE Trans. Plasma Sci.* 34(4), 2006, pp. 1331-1336.

12:00

WF1 5 Modeling atmospheric pressure plasmas for biomedical applications.DAVID GRAVES, *University of California*

The use of cold, atmospheric pressure plasmas for biomedical treatments is an exciting new application in gaseous electronics. Investigations to date include various tissue treatments and surgery, bacterial destruction, and the promotion of wound healing, among others. In this talk, I will present results from modeling the 'plasma needle,' an atmospheric pressure plasma configuration that has been explored by several groups around the world. The biomedical efficacy of the plasma needle has been demonstrated but the mechanisms of cell and tissue modification or bacterial destruction are only just being established. One motivation for developing models is to help interpret experiments and evaluate postulated mechanisms. The model reveals important elements of the plasma needle sustaining mechanisms and operating modes. However, the extraordinary complexity of plasma-tissue interactions represents a long-term challenge for this burgeoning field.

SESSION WF2: PLASMA DIAGNOSTICS II

Friday morning, 5 October 2007; Crystal Ballroom B, Doubletree Crystal City at 10:30

Timo Gans, *Queen's University - Belfast*, presiding*Invited Papers*

10:30

WF2 1 Laser-aided diagnostics of reactive plasmas for better understanding of material processing.KOICHI SASAKI, *Plasma Nanotechnology Research Center, Nagoya University*

The roles of plasma diagnostics in the development of plasma-aided material processing are classified into two categories. One is to provide deep understanding of reactive plasmas, which is indispensable for the efficient development of new processing technologies via laboratory experiments. The other role is to monitor the operation conditions of plasma processing tools in factories in order to realize efficient mass production. Laser-aided diagnostics have mainly played the former role in the last two decades, but they have potential applications in plasma monitoring tools which are required strongly from the industrial point of view. In this talk, we will show two examples of laser-aided precise diagnostics for laboratory experiments and an example of laser-aided monitoring of reactive plasmas. The first diagnostics is the measurement of sheath electric field in an electronegative Ar/SF₆ plasma by laser-induced fluorescence-dip spectroscopy. We observed a stepwise electric field distribution which was induced by the localized reflection of negative ions. The second diagnostics is laser-induced fluorescence imaging spectroscopy. We visualized two-dimensional distributions of radical densities and the velocity distribution function of Fe atoms in magnetron sputtering plasmas. The final one is a method for estimating electron density and electron temperature of a processing plasma based on diode laser absorption spectroscopy. This method would be utilized as a plasma monitoring tool because of the low cost and the maintenance-free operation of the diode laser.

Contributed Papers

11:00

WF2 2 Measurement of Absolute Carbon Atom Density in Reactive Plasmas using Vacuum Ultraviolet Absorption Spectroscopy with Microdischarge Hollow Cathode Lamp HAJIME SASAKI, SEIGO TAKASHIMA, MASARU HORI, *Nagoya University* Carbon atoms play an important role in the reactive plasma processes such as carbon nanostructure formation, etching and so on. In order to realize the smart plasma processing, it is very important to measure the absolute C atom density in the process plasma using carbon based gasses, because the C atoms have a high sticking coefficient. We have developed a measurement technique for absolute C atom densities using a vacuum ultraviolet absorption spectroscopy (VUVAS) employing a microdischarge hollow cathode lamp (MHCL). Helium gas containing a small amount of CO₂ gas was used as the gas of the MHCL. The transition lines 2p3s³p₂-2p²3P₂ at 165.7 nm were used for C atom measurements. By using VUVAS system, we measured the abso-

lute C atom density in the CO-ICP at the pressure of 8.0 Pa. The densities increased from 1.7x10¹¹ to 9.5x10¹³ cm⁻³ when the RF power increased from 10 to 1000 W. his measurement method will be useful for the plasma processing for synthesize a diamond like carbon, carbon nanotube and so on.

11:15

WF2 3 Optical probe for space resolved measurement of atom densities in reactive plasmas SHUNJI TAKAHASHI, SEIGO TAKASHIMA, *Nagoya Univ.* KOJI YAMAKAWA, SHOJI DEN, *Katagiri Engineering* HIROYUKI KANO, *NU Eco-Engineering* MASARU HORI, *Nagoya Univ.* Atomic radicals such as H, N, O, and C play important roles in process plasmas. We have developed a compact measurement system of these atom densities in the reactive plasmas using a vacuum ultraviolet absorption spectroscopy (VUVAS) with a microdischarge hollow cathode lamp (MHCL). However, the two opposite ports are basically necessary to measure the densities using the system. Moreover, it is difficult to measure the spatial distribution of the densities. In this study,

the monitoring probe for the atomic radicals has been developed. The probe installed to the plasma was 2.7 mm in diameter. The port for the measurements was one. It enables us to measure the spatial distribution of the atom densities by moving the probe along the chamber radius. Using the probe, the spatial distribution of the H atom densities in the remote H₂ plasmas was successfully measured at the pressure of 1.33 Pa, the RF power of 300 W. The densities decreased drastically from $1.2 \times 10^{12} \text{ cm}^{-3}$ to $4.4 \times 10^{11} \text{ cm}^{-3}$ near the chamber wall.

11:30

WF2 4 Direct measurements of neutral density depletion by two-photon absorption laser-induced fluorescence spectroscopy (TALIF) LAURENT LIARD, ANE AANESLAND, GARY LERAY, JACQUES JOLLY, PASCAL CHABERT, *LPTP - CNRS PRAGM TEAM*, The neutral ground state density of xenon is measured by spatially resolved laser-induced fluorescence spectroscopy with two-photon excitation (TALIF) giving direct access to the neutral density depletion in high density plasmas. Significant neutral depletion is measured in the diffusion chamber of a magnetized, high density helicon reactor operated in xenon. The depletion at the centre of the core increases with increasing magnetic field, increasing rf power and decreasing fill pressure. The neutral depletion is due to the high electron pressure in the centre of the discharge which has been measured by Langmuir probe techniques. Temporal behaviour has also been studied both at ignition and extinction of the plasma.

11:45

WF2 5 Plasma induced by Resonance Enhanced Multi-Photon Ionization (REMPI) in Inert Gas MIKHAIL SHNEIDER, ZHILI ZHANG, RICHARD MILES, *Princeton University* We present a model for REMPI plasma evolution in the neutral inert gas (argon) during and after the ionizing laser pulse. The theory of REMPI breakdown is considered in 1D cylindrical geometry and includes time dependent continuity equations in the diffusion-drift approximation for plasma components: Rydberg atom states excited in 3 photon process, electrons, Ar⁺ and Ar²⁺ ions. The

Poisson equation for potential and the electron heat transfer equation together with 1D gasdynamic Navier-Stokes equations are also included. Both ionization by REMPI and by collisions of bulk electrons with atoms are taken into account. Our study demonstrates the complete process of REMPI plasma generation and decay in the inert gas together with the gas dynamic equations. Plasma expansion represents a classical ambipolar diffusion. It is shown that gas becomes involved in the motion not only by the pressure gradient due to the heating, but also because of momentum transfer from the charged particles to gas atoms. Gas heating and momentum transfer from charged particles result in a weak shock or acoustic wave. The time dependence of the total number of electrons computed in the theory is in agreement with the results of the coherent microwave scattering experiment.

12:00

WF2 6 Coherent Microwave Rayleigh Scattering from Resonance Enhanced Multiphoton ionization in argon* ZHILI ZHANG, MIKHAIL SHNEIDER, RICHARD MILES, *Princeton University* APPLIED PHYSICS GROUP, MECHANICAL AND AEROSPACE ENGINEERING TEAM, Microwave scattering from a resonance enhanced multi-photon ionization (REMPI) produced plasma provides a new means for the direct, time accurate observation of the free electrons and thus a new method for high sensitivity REMPI spectroscopy of a gas and a new method for the measurement of electron formation and loss processes. The REMPI plasma acts as a coherent microwave scatterer, with the scattering electric field amplitude proportional to the number of electrons. Since the size of the REMPI plasma is small compared to the microwave wavelength, the scattering falls into the Rayleigh regime. Multiphoton ionization and electron recombination processes are studied in argon using this method. A time dependent one dimensional plasma dynamic model is developed to predict the time evolution of the microwave scattering from the plasma. Experimental results of the argon ionization spectrum and electron recombination rates are in good agreement with the model predictions.

*Supported by AFOSR under Dr. John Schmisser.

Author Index

A

Aanesland, Ane WF2 4
 Adamek, Petr SRP1 15
 Adamovich, Igor BT1 2,
 BT1 4
 Adams, S.F. SRP1 5
 Agarwal, Ankur QR1 5,
 SRP1 2
 Ajello, J.M. MWP1 33
 Akashi, Haruaki GW1 6
 Akhtar, Kamran MWP1 6,
 MWP1 7
 Akishev, Yuri ET1 3
 Akiya, M. SRP1 53
 Al-Hagan, Ola BT2 4
 Alexander, Jason BT2 3
 Alexandrov, A.L. LW1 1
 Ali, M.A. MWP1 24,
 MWP1 25
 Allegraud, K. RR1 5
 Almeida, Pedro GW1 4
 Alvarez, R. FTP1 38
 Alves, L.L. FTP1 3,
 FTP1 38
 Amiya, S. SRP1 53
 Amorim, Jayr MWP1 4
 Anderson, T.S. WF1 3
 Angot, Thierry ET1 4
 Apruzese, J.P. PR1 3
 Arakoni, Ramesh A. PR1 2
 Aramaki, M. FTP1 9,
 SRP1 25
 Ariskin, D.A. LW1 1
 Aubert, X. FTP1 6
 Awakowicz, Peter CT1 2,
 CT1 4, FTP1 44,
 FTP1 51, GW1 2,
 GW1 3

B

Baalrud, Scott QR1 7
 Baba, Kazuhiko CT2 1
 Babaeva, Natalia Y. PR1 2
 Baby, A. DT1 7
 Baek, Hoyul FTP1 16,
 SRP1 4
 Bailing, Heremba QR1 8
 Bal, Sau MWP1 36
 Bang, Jin Young SRP1 49
 Bao, Ainan BT1 4
 Barnat, Ed ET2 6, QR1 3
 Barrett, D.A. SRP1 29
 Bartlett, Philip BT2 1
 Bartschat, Klaus MWP1 35,
 QR2 3, QR2 5
 Bayrak, Mustafa FTP1 50
 Becker, Kurt RR2 1
 Benilov, Mikhail GW1 4

Bera, Kallol ET2 4
 Berezov, Rustam SRP1 42
 Berger, A.G. RR1 4
 Bernd, J. LW1 1
 Bhoj, Ananth VF1 4
 Biloiu, Costel MWP1 43
 Biloiu, Ioana A. MWP1 43
 Bingaman, John LW2 3
 Blessington, J.C. SRP1 18,
 SRP1 47
 Boeuf, J.P. FTP1 5
 Boeuf, Jean-Pierre ET2 3
 Boffard, John B. BT2 2,
 PR1 4
 Bogaerts, Annemie
 FTP1 29
 Bogdanov, E.A. FTP1 31,
 SRP1 19
 Boisse-Laporte, C. FTP1 3
 Borovik, A.A. QR2 3
 Boswell, R. FTP1 51
 Boswell, Rod ET2 3
 Bourdon, A. FTP1 10
 Bowden, Mark FTP1 27
 Braithwaite, Nicholas
 FTP1 27, MWP1 19,
 VF2 1
 Brinkmann, R.P. CT1 5,
 FTP1 44, FTP1 48,
 FTP1 49, FTP1 50,
 FTP1 53
 Brunger, Michael
 MWP1 26, MWP1 27,
 RR2 4, RR2 5
 Buckley, M.E. SRP1 29
 Buckman, Stephen
 MWP1 27, MWP1 28,
 QR2 2, RR2 5
 Burns, P. SRP1 43

C

Cada, Martin SRP1 15
 Callegari, Th. FTP1 5
 Campbell, Laurencé RR2 4
 Canes-Boussard, G.
 FTP1 10
 Cappelli, Mark FTP1 20
 Caradonna, Peter QR2 2
 Carrere, Marcel FTP1 19,
 FTP1 24
 Cartry, Gilles ET1 4,
 FTP1 19, FTP1 24
 Ceccato, P. FTP1 7
 Celestin, S. FTP1 10
 Cetiner, Selma FTP1 52
 Chabert, Pascal ET2 2,
 ET2 3, FTP1 23,
 SRP1 48, WF2 4

Chan, Kevin MWP1 13
 Chang, Choongseock
 FTP1 16, FTP1 25,
 SRP1 3, SRP1 4
 Chang, Z. MWP1 7
 Chen, Edward C.M. PR2 1
 Chen, Edward S. PR2 1
 Chen, Lee SRP1 27
 Cheng, Qijin MWP1 20
 Chiu, Yu-hui LW2 2
 Cho, Sung Won SRP1 49
 Choueiri, Edgar LW2 1
 Chourou, S.T. PR2 3
 Chung, Chin-Wook
 SRP1 23, SRP1 24,
 SRP1 49, SRP1 50
 Chung, Tae Hun SRP1 20
 Chutia, Joyanti QR1 8
 Clemens, Noel LW2 5
 Cohen, Samuel MWP1 43
 Colgan, James FTP1 34
 Collins, Ken ET2 4
 Critea, Dragos MWP1 45
 Cunha, Mario GW1 4
 Cunningham, B.T. WF1 3
 Curry, John J. MWP1 39
 Czarnetzki, Uwe CT1 3,
 CT1 5, CT1 7, FTP1 46,
 FTP1 53, MWP1 45

D

Daniels, Stephen SRP1 17
 Dasgupta, Arati PR1 3,
 QR2 6
 de Regt, Ruud SRP1 36
 Deconinck, Thomas LW2 4
 DeJoseph, Charles
 SRP1 18, SRP1 19,
 SRP1 31, SRP1 47
 Demidov, V.I. SRP1 18,
 SRP1 19, SRP1 47
 Den, Shoji MWP1 40,
 WF2 3
 Denysenko, Igor MWP1 14
 Despiau-Pujo, Emilie
 SRP1 48
 Dhandapani, B. MWP1 7
 Dias, Francisco CT2 3,
 MWP1 3
 Ding, R. PR1 4
 Diver, D.A. FTP1 12
 Djordjevic, Antonije
 SRP1 26
 Doebele, H.F. CT2 4,
 FTP1 2
 Donko, Zoltan FTP1 32
 Donnelly, Vincent M.
 ET1 1

Dorn, Alexander QR2 1
 Doughty, Douglas
 MWP1 38
 Drake, D.J. SRP1 39
 Dressler, Rainer A. LW2 2
 Driessen, Niels SRP1 36
 Duc, Tran ET1 3
 Dufour, T. FTP1 8
 Duluard, C. DT1 3
 Dussart, R. DT1 1, DT1 3,
 FTP1 8
 Dyatko, Nikolay ET1 3

E

Eden, J.G. RR1 4, WF1 3
 Ellingboe, Albert CT1 2,
 CT1 7, SRP1 17
 Engeln, Richard
 MWP1 52, SRP1 34
 Eriguchi, Koji DT1 4,
 ET1 2

F

Fedjuschenko, A. CT2 5
 Felizardo, Edgar CT2 3
 Fenger, Thomas PR2 6
 Fernsler, Richard QR1 6,
 SRP1 11, VF2 7
 Ferreira, Carlos CT2 3,
 MWP1 3
 Feugeas, Jorge N. MWP1 5
 Field, Thomas PR2 2
 Finkenthal, Michael
 SRP1 12
 Fischer, Daniel PR2 6
 Foster, M. FTP1 34,
 QR2 4
 Francis-Staite, Jessica
 RR2 5
 Franke, Steffen GW1 5
 Franklin, Raoul FTP1 18
 Fujita, Masayuki SRP1 55
 Fukuyama, K. SRP1 25

G

Gabriel, Onno MWP1 52,
 SRP1 34
 Gangopadhyay, S.
 MWP1 32, RR2 6,
 SRP1 33
 Ganguly, Biswa CT2 2,
 FTP1 15, MWP1 48
 Gans, T. CT1 2, CT2 7,
 FTP1 4, FTP1 51
 Gans, Timo CT1 4,
 MWP1 45
 Garcia, Luis A. PR1 2

- Garscadden, Alan
MWP1 48, SRP1 31
- Gatti, Marco Francesco
VF2 3
- Ghorbanalilu, Mohammad
MWP1 10
- Girshick, Steven LW1 2
- Giuliani, J. PR1 3,
SRP1 43
- Gocic, S. BT1 5
- Godet, Ludovic ET2 1
- Godyak, Valery QR1 1,
VF2 5
- Goekner, M. ET1 6,
FTP1 8, SRP1 8, SRP1 9
- Golde, M.F. PR2 5
- Gomes, Marcelo MWP1 4
- Gomez, Bernardo J.A.
MWP1 5
- Gonzalvo, Y.A. SRP1 29
- Good, W. MWP1 7
- Gordiets, Boris MWP1 3
- Graham, W.G. FTP1 4
- Graupner, Karola PR2 2
- Graves, David SRP1 48,
WF1 5
- Greenwood, C.L. SRP1 29
- Gregorio, J. FTP1 3
- Gribakin, Gleb GW2 3
- Grushin, Mikhail ET1 3
- Guaitella, O. FTP1 10,
RR1 5
- Guan, Xiaoxu QR2 5
- Gudmundsson, J.T.
FTP1 36, MWP1 46
- Guerra, Vasco BT1 5,
MWP1 5, MWP1 51
- Guha, Joydeep ET1 1
- H**
- Hagelaar, Gerjan ET2 3
- Hamaoka, Fukutaro DT1 2
- Hammond, Ned ET2 6
- Hargreaves, Leigh RR2 5
- Harris, A.L. MWP1 31,
QR2 4
- Hatakeyama, R. CT2 1,
SRP1 53
- Hatton, P.J. SRP1 29
- Hayashi, Yuichiro
SRP1 45, SRP1 46
- He, J. MWP1 7
- Heberlein, Joachim CT2 6,
CT2 8
- Hebner, Greg ET2 6
- Hegeler, F. PR1 3,
SRP1 43
- Heil, Brian CT1 3, CT1 5,
CT1 7, FTP1 46,
FTP1 53
- Helmersson, U. MWP1 46
- Hempel, Frank SRP1 34
- Henriques, Julio CT2 3
- Herd, M.T. MWP1 41
- Hershkowitz, Noah
FTP1 21, QR1 7, RR1 6,
VF2 2, VF2 6
- Hess, Helmut GW1 5
- Higashijima, Yasuhiro
MWP1 40
- Hinshelwood, D.D. PR1 3
- Hiramatsu, Mineo LW1 4,
LW1 5, SRP1 22, VF1 7
- Hirao, Satoshi SRP1 45,
SRP1 46
- Hirata, T. SRP1 53
- Hitchon, William N.G.
GW1 1
- Hitzschke, Lothar GW1 5
- Hori, Masaru LW1 3,
LW1 4, LW1 5,
MWP1 40, MWP1 49,
SRP1 21, SRP1 22,
VF1 7, WF2 2, WF2 3
- Hoskinson, Alan RR1 6
- Hu, W. ET1 6
- Hubicka, Zdenek SRP1 15
- Hudson, E.A. QR1 2
- Hwang, Kwang-Tae
SRP1 23
- I**
- Iberler, M. CT2 5,
SRP1 51
- Ikeda, M. VF1 5
- Ionikh, Y. FTP1 6
- Irie, Shoki DT1 4
- Isola, Lucio MWP1 5
- Ito, Masafumi MWP1 40,
MWP1 49
- Ito, Tsuyohito FTP1 20
- Iwasaki, Masahiro
MWP1 49
- J**
- Jacoby, J. CT2 5, SRP1 51
- Jacoby, Joachim SRP1 42
- Jang, SungHo SRP1 24
- Jaynes, R. SRP1 43
- Jelinek, Petr SRP1 15
- Jiang, Naibo BT1 2
- Jiao, Charles MWP1 48,
SRP1 31
- Johnsen, R. PR2 5
- Johnson, P.V. MWP1 33,
MWP1 34
- Jolly, Jacques WF2 4
- Jones, Adric QR2 2
- Joshiyura, K.N. MWP1 32,
RR2 6, SRP1 33
- Jung, R.O. PR1 4
- K**
- Kaening, Marko GW1 5
- Kaiser, Christian BT2 4
- Kakati, Hemen QR1 8
- Kaneko, Toshiro CT2 1
- Kang, Sun Young SRP1 20
- Kanik, I. MWP1 33,
MWP1 34
- Kano, Hiroyuki MWP1 40,
VF1 7, WF2 3
- Karabadzhak, George F.
LW2 2
- Karim, Henda SRP1 7,
SRP1 13
- Kato, M. MWP1 41
- Kato, Satoru SRP1 22
- Katsch, Michael FTP1 26
- Kawagashira, Yozo
SRP1 56
- Kawamura, Emi QR1 2
- KC, Utsav LW2 3
- Khakoo, M.A. MWP1 34,
RR2 2
- Kharchenko, Nadiia
FTP1 43
- Khudik, Vladimir FTP1 14
- Kim, Eun Young SRP1 20
- Kim, J.Y. RR1 4
- Kim, JinSung SRP1 24
- Kim, Jung-Hyung QR1 4
- Kim, Minkyu SRP1 27
- Kim, Seongsik SRP1 3
- Kim, Young-Chul RR1 6
- Kinder, Ron VF1 4
- Kirk, Seth DT1 5
- Knake, N. CT2 7
- Kobayashi, M. FTP1 9
- Kochetov, Igor BT1 3,
ET1 3
- Koepke, M.E. SRP1 47
- Koga, Kazunori VF1 6
- Kondo, Shingo LW1 4,
SRP1 22
- Kono, A. FTP1 9,
SRP1 25
- Kortshagen, Uwe VF2 3
- Kothnur, Prashanth VF1 4
- Kovacevic, E. LW1 1
- Kowal, Jan MWP1 19
- Kraemer, Michael FTP1 26
- Kroesen, Gerrit SRP1 36
- Kudryavtsev, A.A.
FTP1 31, SRP1 19
- Kuehl, Thomas SRP1 42
- Kushner, Mark J. DT1 5,
PR1 2, QR1 5, SRP1 2
- L**
- LaForge, Aaron BT2 3
- Lampe, Martin PR1 1
- Langenscheidt, Oliver
GW1 2, GW1 3
- Lapke, Martin FTP1 48,
FTP1 49
- Laux, Christophe BT1 1
- Lawler, J.E. GW1 1,
MWP1 41
- Layet, Jean-Marc ET1 4,
FTP1 19, FTP1 24
- Lazovic, Sasa SRP1 26
- Lee, Dongsoo FTP1 21,
VF2 6
- Lee, G.S. ET1 6
- Lee, Hyo-chang SRP1 50
- Lee, J.B. FTP1 8
- Lee, KyeongHyo SRP1 24
- Lee, Min-Hyong SRP1 23
- Lee, Taesang FTP1 16,
FTP1 25, SRP1 3,
SRP1 4
- Lee, Young-Kwang
SRP1 23
- Lefauchaux, P. DT1 3,
FTP1 8
- Leick, N. RR1 5
- Leiweke, Robert FTP1 15
- Lempert, Walter BT1 2,
BT1 4
- Leprince, P. FTP1 3
- Leray, Gary ET2 2,
FTP1 23, WF2 4
- Leroy, O. FTP1 3
- Levchenko, Igor FTP1 40,
MWP1 13, MWP1 15,
MWP1 17, SRP1 37,
WF1 2
- Liard, Laurent WF2 4
- Lichtenberg, A.J. QR1 2
- Lieberman, Michael
MWP1 9, QR1 2
- Likhanskii, Alexandre
LW2 7, SRP1 40
- Lima, Marco RR2 3
- Limbachiya, C.G.
MWP1 32, RR2 6
- Lin, Chun C. PR1 4
- Lino da Silva, M. BT1 5

- Lisovskiy, Valeriy
FTP1 43
- Lister, Graeme G. **GW1 1**
- Lock, Evgeniya **QR1 6**,
SRP1 11
- Long, Jidong **MWP1 20**
- Longmier, Ben **VF2 2**
- Loureiro, J. **BT1 5**
- Lower, Julian **MWP1 28**
- Lu, M. **WF1 3**
- Lu, Y. **MWP1 7**
- Luggenhoelscher, Dirk
CT1 3, CT1 5, CT1 7,
FTP1 46, FTP1 53,
MWP1 45
- Lundin, D. **MWP1 46**
- M**
- Ma, J.H. **WF1 3**
- Macheret, Sergey **LW2 7**,
SRP1 40
- MacLachlan, C.S. **FTP1 12**
- Maddern, Todd **RR2 5**
- Madison, D.H. **MWP1 31**,
QR2 4
- Madison, Don **BT2 4**,
HW 1
- Maguire, P.D. **DT1 7**,
FTP1 4
- Maguire, Paul **FTP1 47**
- Mahadevan, Shankar
LW2 4, LW2 6
- Mahony, C.M.O. **DT1 7**,
FTP1 4
- Mahony, Charles **FTP1 47**
- Makabe, Toshiaki **DT1 2**,
DT1 6, FTP1 45,
SRP1 45, SRP1 46
- Makasheva, K. **FTP1 5**
- Makochekanwa, Casten
QR2 2
- Malone, C.P. **MWP1 33**,
MWP1 34
- Malovic, Gordana
MWP1 11, SRP1 26
- Mandra, M. **FTP1 8**
- Maric, Dragana **FTP1 47**,
MWP1 11
- Marinov, D.L. **FTP1 6**
- Marques, L. **FTP1 38**
- Mayr, Alexander **SRP1 42**
- McConkey, J.W. **MWP1 33**
- McCoustra, M.R.S.
SRP1 29
- Meige, A. **ET2 2, ET2 3**,
FTP1 23, FTP1 51
- Mentel, Juergen **GW1 2**,
GW1 3
- Mertmann, Philipp
FTP1 44
- Methling, Ralf **GW1 5**
- Miles, Richard **LW2 7**,
SRP1 40, WF2 5, WF2 6
- Miller, Paul **ET2 6, QR1 3**
- Mills, R.L. **MWP1 6**,
MWP1 7
- Milosavljevic, Vladimir
SRP1 17
- Minayeva, Olga **MWP1 38**
- Mintousov, Evgeny **BT1 4**
- Mintusov, Eugene **BT1 2**
- Miyahara, Hiroomi **VF1 6**
- Miyamoto, Eiji **MWP1 49**
- Mohemed, Ourchabane
SRP1 13
- Monahan, Derek D.
MWP1 8
- Mondal, Subhendu
MWP1 28
- Morgan, William
MWP1 26
- Mori, Masahito **DT1 4**
- Mori, Takakeru **LW1 5**
- Moshammer, Robert **PR2 6**
- Muraoka, Katsunori
SRP1 56
- Murray, Andrew **BT2 4**
- Mussenbrock, T. **CT1 5**,
FTP1 44, FTP1 48,
FTP1 49, FTP1 50,
FTP1 53
- Myers, M. **PR1 3**,
SRP1 43
- N**
- Nadia, Saoula **SRP1 7**
- Nafarizal, N. **VF1 5**
- Nakamura, T. **SRP1 53**
- Nakamura, William M.
VF1 6
- Nakamuta, Takashi
MWP1 16
- Nakatsuka, Masahiro
SRP1 55
- Nam, Hyong-ho **SRP1 50**
- Nansteel, M. **MWP1 7**
- Napartovich, Anatoly
BT1 3, ET1 3
- Nelson, C. **ET1 6**
- Neretti, Gabriele **SRP1 40**
- Newman, Stan **MWP1 28**
- Ngassam, V. **PR2 4**
- Niemi, K. **CT2 7, FTP1 2**
- Nijdam, Sander **SRP1 36**
- Nikitovic, Zeljka **FTP1 39**,
MWP1 29
- Nozaki, Tomohiro **LW1 6**,
MWP1 16
- O**
- O'Connell, D. **CT1 2**,
CT1 4, FTP1 51,
MWP1 45, RR1 3
- Oberrath, Jens **FTP1 49**
- Oda, Akinori **GW1 6**
- Oehrlein, Gottlieb **ET1 5**
- Ogawa, D. **SRP1 8**
- Ogino, Tomohisa
MWP1 16
- Ohnishi, Kuma **LW1 6**
- Ohta, Takayuki **MWP1 40**
- Okazaki, Ken **LW1 6**,
MWP1 16
- Oliveira, Carlos **MWP1 4**
- Ono, Kouichi **DT1 4**,
ET1 2
- Opaits, Dmitry **LW2 7**,
SRP1 40
- Orel, A.E. **PR2 3, PR2 4**
- Orlando, Thomas M.
WF1 1
- Osano, Yugo **DT1 4**
- Ostrikov, Kostya (Ken)
FTP1 40, LW1 7,
MWP1 13, MWP1 14,
MWP1 15, MWP1 17,
MWP1 18, MWP1 20,
SRP1 37, WF1 2
- Otto, J. **CT2 5**
- Oubensaid, E.H. **DT1 3**
- Overzet, L. **ET1 6**,
FTP1 8, SRP1 8, SRP1 9
- P**
- Pal, Arup Ratan **QR1 8**
- Pappas, D. **PR2 5**
- Park, S.J. **RR1 4, WF1 3**
- Park, Seunghoon **SRP1 4**
- Paterson, Alex **ET2 4**,
ET2 6, QR1 3
- Peachar, J.L. **MWP1 31**,
QR2 4
- Peeters, F.M. **LW1 1**
- Pendery, Joel **FTP1 14**
- Petrov, G.M. **PR1 3**
- Petrova, Ts. **PR1 3**
- Petrovic, Dragana **FTP1 29**
- Petrovic, Z.Lj. **FTP1 4**
- Petrovic, Zoran **FTP1 39**,
FTP1 47, MWP1 11,
MWP1 29, SRP1 26,
VF1 3
- Pfender, Emil **CT2 8**
- Phelps, A.V. **MWP1 2**
- Pichon, L.E. **DT1 3**
- Pindzola, Mitch **FTP1 34**
- Pinhao, Nuno **FTP1 32**,
FTP1 41
- Pinheiro, Mario **FTP1 32**
- Pipa, A. **FTP1 6**
- Pitchford, Leanne **FTP1 5**,
RR1 1
- Plihon, Nicolas **ET2 3**
- Podder, Nirmol K.
FTP1 11
- Popovic, S. **MWP1 30**,
SRP1 6, SRP1 39
- Popugaev, Semen **FTP1 31**
- Potts, H.E. **FTP1 12**
- Puac, Nevena **SRP1 26**
- Puech, M. **DT1 3**
- Puech, V. **FTP1 5**
- R**
- Radjenovic, Branislav
VF1 3
- Radmilovic-Radjenovic,
Marija **FTP1 47**,
MWP1 11, VF1 3
- Raeside, Tyler **MWP1 28**
- Rafika, Kesri **SRP1 7**
- Raimbault, Jean-Luc
ET2 2, FTP1 23
- Raja, Laxminarayan
LW2 3, LW2 4, LW2 5,
LW2 6
- Ramachandran, S. **ET1 6**
- Ranson, P. **DT1 3, FTP1 8**
- Raskovic, M. **MWP1 30**,
SRP1 6
- Ratcliffe, L.V. **SRP1 29**
- Rauf, Shahid **ET2 4**,
ET2 6
- Ravi, Lavanya **LW1 2**
- Rees, J.A. **SRP1 29**
- Reinelt, Jens **GW1 2**,
GW1 3
- Rescigno, Thomas **RR2 4**
- Reuter, S. **CT2 4, FTP1 2**
- Rider, Amanda **FTP1 40**,
LW1 7, MWP1 13,
MWP1 15, MWP1 17,
MWP1 18, WF1 2
- Rienecker, T. **CT2 5**
- Righart, Tim **SRP1 36**
- Roberts, Jason **MWP1 27**
- Robson, Robert **GW2 1**
- Rodgers, B. **SRP1 39**
- Roepcke, Juergen **SRP1 34**
- Rogers, Tony **MWP1 19**
- Ropcke, J. **FTP1 6**
- Rosati, R. **PR2 5**

- Rosmej, Olga SRP1 42
 Rousseau, A. FTP1 6, FTP1 7, FTP1 10, RR1 5
 Rousseau, Antoine RR1 2
 Rutten, F.J.M. SRP1 29
- S**
 Sago, Y. VF1 5
 Sakai, T. SRP1 53
 Sakai, Yosuke GW1 6
 Samara, Vladimir FTP1 27
 Samira, Djerourou SRP1 13
 Sands, Brian CT2 2
 Santos Sousa, J. FTP1 5
 Saraf, I. SRP1 9
 Sasaki, Hajime SRP1 22, WF2 2
 Sasaki, K. VF1 5
 Sasaki, Kenji MWP1 16
 Sasaki, Koichi WF2 1
 Sato, Toshikazu DT1 6
 Satou, Hiroshi VF1 6
 Schalk, Bernhard GW1 5
 Schaper, L. CT2 7
 Scharer, J.E. MWP1 6
 Schiesko, Loic FTP1 19, FTP1 24
 Schneidenbach, Hartmut GW1 5
 Schoepp, Heinz GW1 5
 Schram, Daan MWP1 52, SRP1 34
 Schulz, Michael BT2 3, PR2 6
 Schulz-von der Gathen, V. CT2 4, CT2 7, FTP1 2, RR1 3
 Schulze, J. CT1 5, FTP1 53
 Schulze, Julian CT1 3, CT1 7, FTP1 46
 Schweigert, I.V. ET2 7, LW1 1
 Scime, Earl MWP1 43
 Scofield, J.D. SRP1 5
 Semmler, E. CT1 2, FTP1 51
 Semmler, Egmont CT1 4
 Serditov, K. Yu. SRP1 19
 Sethian, J. SRP1 43
 Sethian, J.D. PR1 3
 Severn, Greg FTP1 21, VF2 6
 Seymour, D. SRP1 29
 Sharma, Lalita LW2 2, MWP1 22, MWP1 23
 Sheerin, Peter SRP1 28
 Shin, Jichul LW2 5
 Shiratani, Masaharu VF1 6
 Shneider, Mikhail LW2 7, SRP1 40, WF2 5, WF2 6
 Shokri, Babak MWP1 10
 Shvydky, Alexander FTP1 14
 Sicherl, Bernd SRP1 42
 Sigurjonsson, P. MWP1 46
 Sismanoglu, Bogos MWP1 4
 Sitters, Gerrit SRP1 36
 Skoro, Nikola FTP1 47, MWP1 11
 Skrzypkowski, M. PR2 5
 Sobolewski, Mark QR1 4
 Sommer, Francoise ET1 3
 Souza Correa, Jorge MWP1 4
 Sra, A. SRP1 8
 Srivastava, Rajesh LW2 2, MWP1 22, MWP1 23
 Stalder, Kenneth PR1 5, SRP1 16
 Stamate, Eugen ET2 5
 Stauffer, Allan MWP1 22, MWP1 23
 Stefanovic, I.I. LW1 1
 Stepanovic, Olivera LW1 4
 Sternberg, Natalia QR1 1, VF2 5
 Stoffers, Eva WF1 4
 Stojanovic, Vladimir FTP1 39, MWP1 29
 Stoltz, Peter FTP1 52
 Stone, P.M. MWP1 24, MWP1 25
 Stout, Phillip VF1 2
 Strobel, Mark DT1 5
 Stutman, Dan SRP1 12
 Sugai, Hideo MWP1 44
 Sullivan, James MWP1 27, QR2 2
 Sung, S.H. RR1 4
 Surko, C.M. GW2 2
 Synek, P. FTP1 3
- T**
 Tachibana, Kunihide CT2 2
 Tachibana, Yoshihiro MWP1 40
 Takada, N. VF1 5
 Takagi, Yusuke MWP1 44
 Takahashi, Hiroyuki FTP1 45
 Takahashi, Shunji WF2 3
 Takashima, Seigo MWP1 40, SRP1 21, WF2 2, WF2 3
 Takeda, Keigo MWP1 49, SRP1 21
 Takei, O. SRP1 53
 Takeuchi, Wakana SRP1 22, VF1 7
 Tam, Eugene FTP1 40, MWP1 15, MWP1 17
 Tao, L.S.N. ET1 6
 Tarasova, Anastasia V. FTP1 11
 Tatarova, Elena CT2 3, MWP1 3
 Teske, Ch. CT2 5, SRP1 51
 Teule-Gay, L. FTP1 3
 Theodosiou, Constantine FTP1 14
 Thomas, Cedric ET1 4
 Thorn, Penny MWP1 26
 Thorsteinsson, E.G. MWP1 36
 Tichy, Milan SRP1 15
 Timmons, R. SRP1 8
 Ting, Y.H. PR1 4
 Tokuda, Yutaka VF1 7
 Tolson, B.A. SRP1 5
 Totake, J. SRP1 53
 Toyoda, Hirotaka MWP1 44, VF1 1
 Trelles, Juan CT2 8
 Trushkin, Nikolay ET1 3
 Tsendin, Lev FTP1 31
 Turner, Miles CT1 1, CT1 2, MWP1 8, SRP1 28
- U**
 Uchida, Shigeaki SRP1 55
 Uddi, Mruthunjaya BT1 2
 Ueda, Yoshinori ET1 2
 Uehara, Tsuyoshi MWP1 49
 Ullrich, Joachim PR2 6
 Upadhyay, J. SRP1 6
 Urescu, Daniel SRP1 42
- V**
 Vagin, Nikolay BT1 3
 Vaishnav, Bhushit SRP1 33
 van den Brink, Andreas SRP1 36
 van Noorden, Peter SRP1 36
 van Veldhuizen, Eddie SRP1 36
 Vankan, Peter MWP1 52
 Varghese, Philip LW2 3
 Veitzer, Seth FTP1 52
 Vidmar, Robert PR1 5, SRP1 16
 Vinodkumar, M. MWP1 32, RR2 6
 Virostko, Petr SRP1 15
 Vizcaino, Violaine MWP1 27
 Vladimirov, Sergey MWP1 17
 von Keudell, Achim CT1 4
 Vuskovic, L. MWP1 30, SRP1 6, SRP1 39
- W**
 Wagner, Alexander FTP1 26
 Walton, Scott QR1 6, SRP1 11
 Wang, Mingmei SRP1 2
 Wang, S. MWP1 34
 Waskoenig, J. RR1 3
 Weflen, Daniel QR2 5
 Welzel, Stefan SRP1 34
 Wendt, A.E. PR1 4
 Westermeyer, Michael GW1 2, GW1 3
 Whitmore, T.D. SRP1 29
 Wichaidit, Chonlarat GW1 1
 Wiechula, J. SRP1 51
 Wijtvlit, Ruud SRP1 36
 Williamson, J.M. SRP1 5
 Wilson IV, Ralph B. FTP1 11
 Winter, J. CT2 7, LW1 1, RR1 3
 Wolford, M. PR1 3, SRP1 43
- X**
 Xu, Shuyan MWP1 17, MWP1 20, SRP1 37
- Y**
 Yadav, Vipin K. VF2 4
 Yagci, Goeksel SRP1 34
 Yagisawa, Takashi DT1 2, FTP1 45
 Yamagata, Yukihiko SRP1 56
 Yamakawa, Koji LW1 4, SRP1 22, WF2 3
 Yamamoto, T. SRP1 53
 Yamanaka, Chiyo SRP1 55

Yamaura, Michiteru
SRP1 14, SRP1 55
Yamazawa, Yohei CT1 6
Yang, Guang CT2 6
Yang, Y. PR1 4
Yang, Yang DT1 5,
SRP1 2

Yara, Takuya MWP1 49
Yegorenkov, Vladimir
FTP1 43
Yoon, Hyun-Jin MWP1 18
Yoshida, Masahiro ET1 2
Yuryshev, Nikolay BT1 3

Z
Zaidi, Sohail SRP1 40
Zatsarinny, Oleg
MWP1 35, QR2 3
Zhang, Zhili WF2 5,
WF2 6

Zheng, J. WF1 3
Ziegler, Dennis FTP1 48,
FTP1 49, FTP1 50
Zielbauer, Bernhard
SRP1 42
Zijlmans, Rens SRP1 34
Zimmer, Daniel SRP1 42

NOTES

Restaurant Guide Crystal City/Pentagon City

Pentagon City Mall/Shopping Center

- Three blocks from the DoubleTree Hotel (about a 10 minute walk)
- Complimentary shuttle service from DoubleTree to Pentagon City Mall/Fashion Center every 30 minutes from 6 a.m. – 10 p.m., Monday-Friday. On Saturday and Sunday: 7 a.m. – 10 p.m.

Mall Hours:

Monday-Saturday, 10 a.m. – 9:30 p.m.
Sunday, 11 a.m. – 6 p.m.

Food Court/Eateries

Au Bon Pain; Bain's Deli; Boardwalk Fries; Desert Moon Café; Frank & Stein; Great Steak & Potato Company; Kabuki Sushi; Kelly's Cajun Grill; McDonalds; Panda Express; Pik-A-Pita; Pop's Chicken & Sea; US Bistro; Villa Pizza

Restaurants (Pentagon City Mall)

Johnny Rockets Restaurant — on Metro level of the Mall (near food court); This 1940's style corner malt shop offers hamburgers, fries and malts.
Hours: Monday-Saturday: 10:00 a.m. – 10:00 p.m.; Sunday: 10 a.m. – 9 p.m.

L&N Seafood Grill Restaurant — 3rd Level of Mall: Seafood, pasta, delicious and freshly expertly prepared shrimp, lobster and fish. Served in a variety of ways at reasonable prices, great atmosphere.

Hours: Monday: 11:00 a.m. – 10:00 p.m., Friday-Saturday: 11:00 a.m. – 11:00 p.m., Sunday, 11:00 a.m. – 8:00 p.m.

Mozzarella's American Café Restaurant — Second level of the mall by the elevator and escalator. Good old American food! Anything from chicken pot pie, pastas to gourmet pizzas.

Hours: Monday-Thursday: 11:00 a.m. – 10:00 p.m.; Friday-Saturday: 11:00 a.m. – 11:00 p.m.; Sunday: 11:30 a.m. – 8 p.m.

Pentagon Centre (Directly across from the Pentagon City Mall on S. Hayes Street)

California Pizza Kitchen — Hearth Baked pizzas, creative pastas, incredible salads, delicious desserts and more.

Hours: Monday-Thursday: 11:30 a.m. – 10:00 p.m. Friday/Saturday: 11:30 a.m. – 11:00 p.m.; Sunday: 11:30 a.m. – 8:30 p.m.

Chevy's Mexican Restaurant — South of the Border Fresh Mex Food and festive atmosphere; mesquite grilled chicken, beef, shrimp and vegetable fajitas and home made tortillas.

Hours: daily: 11:00 a.m. – 11:00 p.m.

Starbucks Coffee — Pentagon Centre: street level—Hayes Street; open daily.

23rd Street Restaurant Row Crystal City (about a 15 minute walk from the DoubleTree Hotel)

Afghan/Pakistani

Kabob Palacei

2315 South Eads Street

703 486-3535

Lunch and Dinner Entrees

\$4.50 - \$5.75. Most popular dishes are chicken kabob (boneless and bone in) and chicken curry. Open every day except Monday. Hours: 24 hours

American

McDonalds

2620 Jefferson Davis Highway

(703) 683-2107

Open 24 Hours

Crystal City Sports Pub

529 23RD ST S,
(703) 521-8215

Open till 2am

Ruth Chris Steakhouse

2231 Crystal Drive
703 979-7275

Entrees from \$22.95 - \$31.95

Most popular dishes are Filet Mignon, New York Strip, T-bone Steaks, and fresh lobster. Recently renovated. Open Monday-Friday, 11:30 a.m. - 10:30 p.m.; Saturday 5-11 p.m.; Sunday 5 p.m. - 10 p.m.

Stars and Stripes

567 South 23rd Street
703-979-IUSA

Lunch entrees from \$7.95 - \$9.95; dinner entrees from \$11.95 - \$16.95. Most popular dishes are Maryland backfin crabs, St. Louis barbecue backribs, New York steak and New Orleans cajun penne. Open Monday-Thursday, 11:00 a.m. - 10 p.m., Friday - 11 a.m. - 11 p.m., Saturday: 5 p.m. - 11 p.m.; Sunday 5 p.m. - 10 p.m.

Wild Azalea

(Southern Style cooking)

1648 Crystal Square Arcade
703 413-2250

Entrees for lunch and dinner; \$7.95 - \$12.95. Most popular dishes are Sheveport fish and grits, southern fried chicken breast, and Mama's meat loaf. Open Monday-Friday; 11 a.m. - 10 p.m.; Saturday 12 - 9 p.m.

Hamburger Hamlet

1601 Crystal Drive (Crystal City Underground)
703 413-0422

Open Everyday; Sunday 11:30 a.m. - 9 p.m.; Saturday: 11:30 p.m. - 10 p.m.; Monday-Friday 11 a.m. - 10 p.m. Variety of entrees (hamburgers, sandwiches, salads, lunch/dinner entrees); reasonably priced.

King Street Blues

1648 Crystal Square
Crystal City Shops North (near Starbucks Coffee)
703 415-BLUE

Contemporary, southern roadhouse restaurant. Designed to seat 150 with separate "neighborhood" bar featuring the restaurant's own "Roadhouse Red": microbrew and live blues; concentrates on smoked meats,

barbecue, made-from-scratch soups and daily specials that have won acclaim in the Washington area. Open 11 a.m. - 10 p.m. daily.

Morton's Steakhouse

16th & Crystal Drive
Crystal City
703 418-1444

Hours: Monday-Sunday. Bar opens 5:00 p.m. Dinner is served from 5:30 p.m. - 11:00 p.m. Sunday dinner is served from 5:00 p.m. - 10:00 p.m. Menu is a la carte, and our prices vary slightly by market. The average check for a full dinner for two is about \$145.00 not including tax and gratuity, and that would depend on the beverages ordered with the meal. Dress code: business attire/smart casual wear (jacket and tie are not necessary).

Chinese**Young Chow**

420 South 23rd Street
703 892-2566

Szechuan and Hunan Cooking. Prices Range \$6.00-\$10.00. Most popular dishes are General Tso's chicken, shrimp and broccoli with garlic sauce, and triple delight. Open Sunday-Thursday, 11 a.m. - 10 p.m., Friday and Saturday, 11 a.m. - 11 p.m.

Ethiopian**Demera**

2325 South Eads Street
703 271-8663

Entrees for lunch and dinner \$6.75 - \$13.95. Most popular dishes are doro wat (chicken marinated in lemon), yebeg alitchka (lamb), and yebeg tips (cubed lamb marinated in spices). Latin bands perform late night. Open Monday-Thursday. 11 a.m. - 12 p.m.; Friday, Saturday and Sunday: 10 a.m. - 2 p.m.

Greek**Athena Pallas (formerly Crystal Pallas)**

550 South 22nd Street
703 521-3870

Greek Cuisine Seafood & Mediterranean Dishes! All Freshly Prepared on the Premises, along with our Homemade Breads. Hours: Monday - Friday: 11 a.m. - 10 p.m.; Saturday 5 p.m. - 11 p.m.

Italian

Café Italia

519 South 23rd Street
703 521-2565

Lunch entrees \$6.95 - \$9.95, dinner entrees, \$9.95 - \$15.95. Most popular dishes are veal parmigiana, baked fish of the day, and prime rib with pasta. Open Monday-Thursday, 11 a.m. - 10 p.m.; Friday, 11:00 a.m. - 11:00 p.m., Saturday, 5 p.m. - 11 p.m., Sunday, 5 p.m. - 10 p.m.

Portofino Restaurant

526 South 23rd Street
703 979-8200

Lunch entrees from \$8.50 - \$14.95; dinner entrees from \$14.95 - \$19.95. Most popular dishes are chicken portofino, cannelloni al gratin, and omaggi di nettuno. Open for lunch Monday-Friday - 11 a.m. - 2 p.m. Dinner daily: 5 - 10 p.m.

Japanese

Bonsai Grill

553 S. 23rd Street
703 553-7723

Lunch entrees from \$5.95 - \$9.95; dinner entrees from \$9.95 - \$17.95. Most popular dishes are sushi combinations, tempura, and teriyaki dishes. Open Monday-Saturday, 11:30 a.m. - 2:30 p.m., Monday-Thursday, 5 - 10 p.m., Friday and Saturday, 5 p.m. - 10:30 p.m., Sunday, 4:00 p.m. - 9:30 p.m.

Mediterranean

Cha Cha's

509 South 23rd Street
703 979-7676

Fish with Mediterranean flavors (Portugal, Spain, Italy and Greece) is the predominant theme. Entrees \$9.99 - \$16.95. The most popular dishes include zazueta Valenciana, shrimp Estoril, and melitzana Santorini. Open Monday-Saturday, 5 - 10 p.m., closed Sunday.

Mexican

San Antonio Bar and Grill

1664-A Crystal Square Arcade
703 415-0126

Entrees: \$6.95 - \$9.95. Most popular dishes are house specialties, pollo asado, arroz con pollo, lomo

saltado and Tex Mex brochettes. Open Monday-Thursday, 11 a.m. - 10 p.m., Friday and Saturday, 11 a.m. - 10:30 p.m.; Mariachi music Friday 4-7 p.m.

Taco House

515 South 23rd Street
703 979-7033

Entrees: \$5.25 - \$9.95. Most popular dishes are chimichangas, chilles rellenos and fajitas. Open Monday-Saturday: 11 a.m. - 10 p.m., Sunday 12 - 9 p.m.

Seafood

Legal Seafoods

2301 Jefferson Davis Highway
703 415-1200

This lobby-level restaurant welcomes a regular neighborhood clientele of residents and business people from the vibrant Crystal City complex. Convenient garage parking is adjacent, and free validation is available during certain hours. Full take-out services are offered, and smoking is permitted in the bar area. The entire facility is handicapped-accessible. No reservations are accepted. Hours: Monday-Thursday: 11:00 a.m. - 10:00 p.m., Friday and Saturday: 11:00 a.m. - 11:00 p.m., Sunday, Noon - 9:00 p.m.

Thai

Top Thai

523 South 23rd Street
703 521-1305

Regular entrees \$7.95-\$17.95. Most popular dishes are pad Thai, chicken or beef with basil leaves and chicken with cashew nuts. Open Monday-Friday, 11 a.m. - 3 p.m.; 5 p.m. - 10 p.m., Saturday 12 noon - 10 p.m., Sunday, 5 p.m. - 10 p.m.

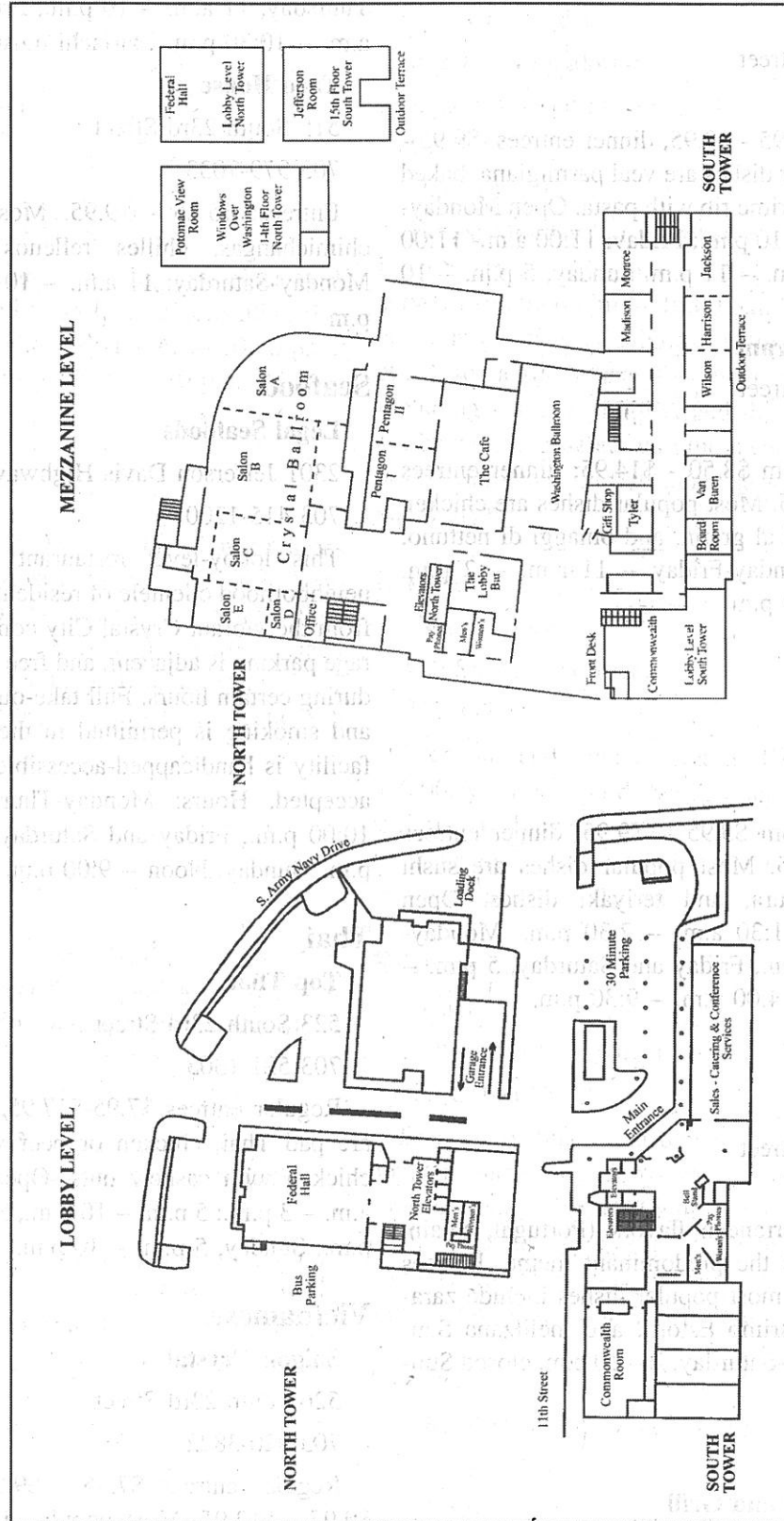
Vietnamese

Saigon Crystal

526 South 23rd Street
703 920-3822

Regular entrees \$7.95 - \$9.95. Chief specialties, \$9.95 - \$12.95. Most popular dishes are red snapper with ginger sauce; soft shell crabs, and fisherman clay pot. Enlarged patio for outside dining. Open Sunday-Thursday, 11 a.m. - 10 p.m., Friday and Saturday, 11 a.m. - 11 p.m.

**DOUBLE TREE[®]
HOTEL**
CRYSTAL CITY



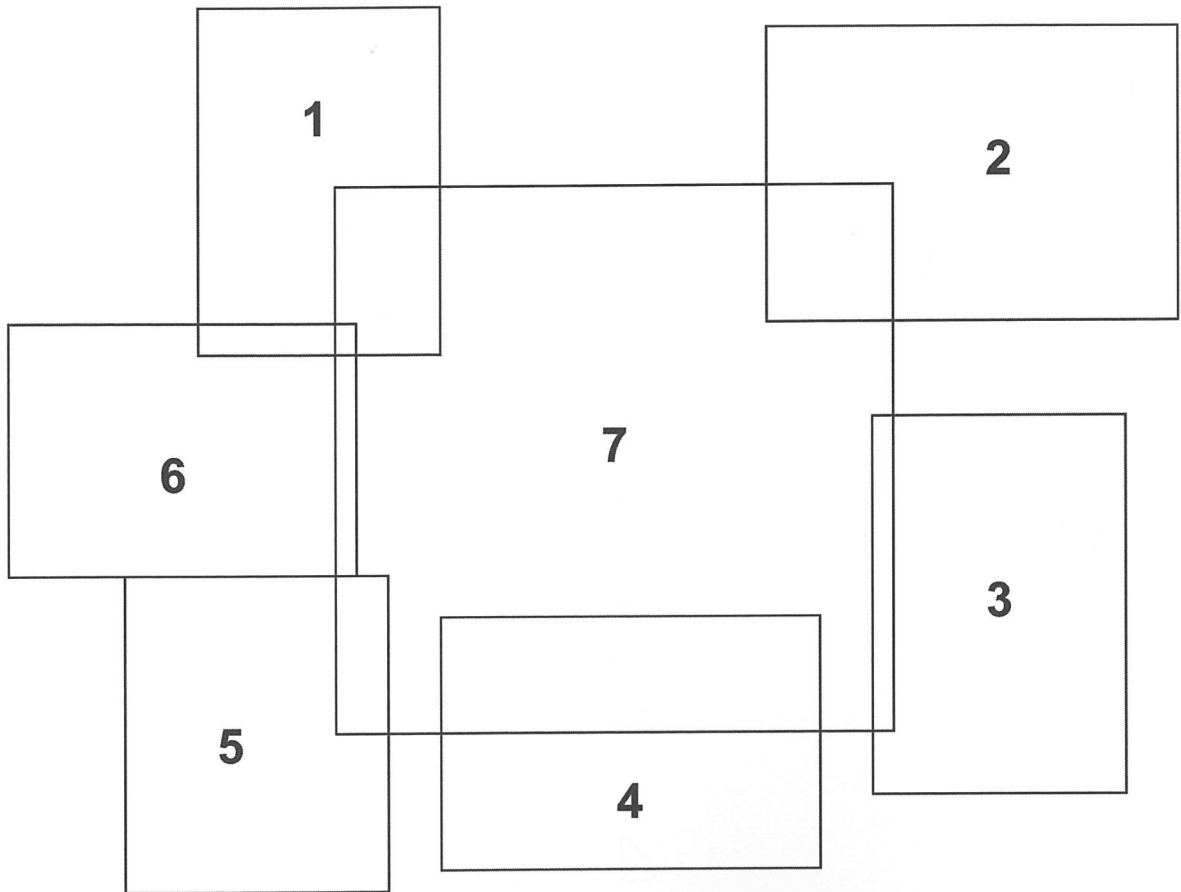
Windows Over Washington
Potomac View Room
Pool

Skydome
14th Floor
North Tower

SD Floor
North Tower

Jefferson
15th Floor
South Tower

On the Cover



Key:

- 1 - Jefferson Memorial (foreground) and Washington Monument (Courtesy of www.washington.org)
- 2 - Electron beam produced plasma (Courtesy S.G. Walton, Naval Research Laboratory)
- 3 - Washington Monument from across Potomac (Courtesy S.G. Walton)
- 4 - US Capitol Dome (Courtesy of www.washington.org)
- 5 - Magnetron (Courtesy S.G. Walton, Naval Research Laboratory)
- 6 - White House (Courtesy S.G. Walton)
- 7 - Electron beam generated plasma (Courtesy S.G. Walton, Naval Research Laboratory)

Epitome of the 60th Gaseous Electronics Conference of the American Physical Society

18:00 MONDAY EVENING
1 OCTOBER 2007

AS **Reception**
Windows Over Washington
Doubletree Crystal City

8:00 TUESDAY MORNING
2 OCTOBER 2007

BT1 **Plasma Combustion and Chemistry**
Christophe Laux
Crystal Ballroom A,
Doubletree Crystal City

BT2 **Electron Impact Ionization**
Philip Bartlett, John B. Boffard
Crystal Ballroom B,
Doubletree Crystal City

10:00 TUESDAY MORNING
2 OCTOBER 2007

CT1 **Capacity Coupled Plasmas**
Miles Turner
Crystal Ballroom A,
Doubletree Crystal City

CT2 **High Pressure Arcs**
Crystal Ballroom B,
Doubletree Crystal City

13:30 TUESDAY AFTERNOON
2 OCTOBER 2007

DT1 **Materials Processing in Low Pressure Plasmas I: Etching, Deposition, New Materials**
Remi Dussart
Crystal Ballroom A,
Doubletree Crystal City

16:00 TUESDAY AFTERNOON
2 OCTOBER 2007

ET1 **Plasma-Surface Interactions**
Gottlieb Oehrlein
Crystal Ballroom A,
Doubletree Crystal City

ET2 **Electronegative Plasmas**
Ludovic Godet
Crystal Ballroom B,
Doubletree Crystal City

19:30 TUESDAY EVENING
2 OCTOBER 2007

FTP1 **Poster Session I**
Crystal Ballroom C,
Doubletree Crystal City

8:00 WEDNESDAY MORNING
3 OCTOBER 2007

GW1 **Lighting Plasmas**
Crystal Ballroom A,
Doubletree Crystal City

GW2 **Electrons and Positrons: Transport and Annihilation**
Robert Robson, C.M. Surko, Gleb Gribakin
Crystal Ballroom B,
Doubletree Crystal City

10:00 WEDNESDAY MORNING
3 OCTOBER 2007

HW **GEC Foundation Talk**
Don Madison
Crystal Ballrooms A/B,
Doubletree Crystal City

11:00 WEDNESDAY MORNING
3 OCTOBER 2007

JW **Business Meeting**
Crystal Ballroom A,
Doubletree Crystal City

12:00 WEDNESDAY NOON
3 OCTOBER 2007

KW **General Committee Meeting**
Crystal Ballroom A,
Doubletree Crystal City

13:30 WEDNESDAY AFTERNOON
3 OCTOBER 2007

LW1 **Plasma Applications for Nanotechnology**
Masaru Hori
Crystal Ballroom A,
Doubletree Crystal City

LW2 **Plasma Propulsion**
Edgar Choueir
Crystal Ballroom B,
Doubletree Crystal City

16:00 WEDNESDAY AFTERNOON
3 OCTOBER 2007

MWP1 **Poster Session II**
Crystal Ballroom C,
Doubletree Crystal City

8:00 THURSDAY MORNING
4 OCTOBER 2007

PR1 **Laser and Air Plasmas**
Martin Lampe
Crystal Ballroom A,
Doubletree Crystal City

PR2 **Electron Attachment and Recombination**
Crystal Ballroom B,
Doubletree Crystal City

10:00 THURSDAY MORNING
4 OCTOBER 2007

QR1 **Plasma Sources**
Crystal Ballroom A,
Doubletree Crystal City

QR2 **Electron-Atom Collisions**
Alexander Dorn, Arati Dasgupta
Crystal Ballroom B,
Doubletree Crystal City

13:30 THURSDAY AFTERNOON
4 OCTOBER 2007

RR1 **Micro and Dielectric Barrier Discharges**
Leanne Pitchford, Antoine Rousseau
Crystal Ballroom A,
Doubletree Crystal City

RR2 **Electron-Molecule Collisions**
Kurt Becker, Murtadha A. Khakoo, Marco Lima
Crystal Ballroom B,
Doubletree Crystal City

16:00 THURSDAY AFTERNOON
4 OCTOBER 2007

SRP1 **Poster Session III**
Crystal Ballroom C,
Doubletree Crystal City

19:00 THURSDAY EVENING
4 OCTOBER 2007

TR **Banquet**
Crystal Ballroom,
Doubletree Crystal City

8:00 FRIDAY MORNING
5 OCTOBER 2007

VF1 **Materials Processing in Low Pressure Plasmas II: Etching, Deposition, New Materials**
Hirotsuka Toyoda
Crystal Ballroom A,
Doubletree Crystal City

VF2 **Plasma Diagnostics I**
Nicholas Braithwaite
Crystal Ballroom B,
Doubletree Crystal City

10:30 FRIDAY MORNING
5 OCTOBER 2007

WF1 **Biological and Emerging Applications of Plasmas**
Thomas M. Orlando, Eva Stoffels, David Graves
Crystal Ballroom A,
Doubletree Crystal City

WF2 **Plasma Diagnostics II**
Koichi Sasaki
Crystal Ballroom B,
Doubletree Crystal City



0003-0503(200710)52:8:1-L